Formal Syntheses of Eribulin and Synthesis of Biologically-active Small Molecules

by

Anissa Kaghad

M.Sc., Ecole Nationale Supérieure de Chimie de Montpellier, 2017

B.Sc., Ecole Nationale Supérieure de Chimie de Montpellier, 2015

Thesis Submitted in Partial Fulfillment of the
Requirements for the Degree of
Doctor of Philosophy

in the
Department of Chemistry
Faculty of Science

SIMON FRASER UNIVERSITY

Spring 2022

Declaration of Committee

Name:	**Anissa Kaghad**
Degree:	**Doctor of Philosophy**
Title:	**Formal Syntheses of Eribulin and Synthesis of Biologically-active Small Molecules**
Committee:	Chair: **Paul Li** Professor, Chemistry
	Robert Britton Supervisor Professor, Chemistry
	Roger Linington Committee Member Associate professor, Chemistry
	Peter Wilson Committee Member Associate professor, Chemistry
	Robert Young Examiner Professor, Chemistry
	Andrew Evans External Examiner Professor, Chemistry Queen's University

Abstract

Natural products have been used as medicines since the dawn of recorded history and, today, continue to be an integral part of the drug discovery process. Yet, their impact has decreased significantly over the past two decades following the advent of high-throughput screening (HTS) and the post-genomic era. In this regard, total synthesis has served as a powerful tool to address some of the challenges associated with natural product drug discovery. A noticeable example is the discovery and development of the natural product analogue, eribulin mesylate, the most complex, fully synthetic drug on the market. Albeit impressive, the commercial process of eribulin involves a total of 67 steps from which, 45 are used to construct the C14-C35 fragment of the macrocyclic lactone. To improve upon this process, we exploited methodology developed in the Britton group for tetrahydrofuran synthesis. Most notably, we anticipated that the application of our expertise in the stereoselective synthesis of hydroxytetrahydrofurans would allow us to considerably reduce the overall length of the synthesis and consequently the cost of producing eribulin. Following this strategy, we have developed concise and stereoselective syntheses of two C14-C35 key fragments and also, a scalable synthesis of the C14-C26 building block.

Nucleoside analogues have largely been used as anticancer drugs or for the treatment of infectious diseases. Among them, immucillin H was approved in Japan in 2017 to treat peripheral T-cell lymphoma and immucillin A was found active against a broad range of viruses. Driven by the concept of “step economy”, we have developed a concise and stereoselective formal synthesis of these two nucleoside analogues.

Moreover, a collaboration between the Britton group, the Structural Genomics Consortium, and Bayer has led to the design and synthesis of inhibitors selective against PRMT4, an enzyme overexpressed in several cancers.

Keywords: natural product; total synthesis; α-chloroaldehyde; stereoselective; step economy

Table of Contents

List of Tables

List of Figures

List of Schemes

List of Acronyms

°C	Celsius degrees
δ	Chemical shift in ppm from tetramethylsilane
$[\alpha]_D$	Specific rotation at the sodium D line (589 nm)
Ac	Acetyl
acac	Acetylacetonate
ACTs	Artemisinin-based combination therapies
API	Active pharmaceutical ingredient
aq	Aqueous
BAIB	[*Bis*(acetoxy)iodo]benzene
BDP	1,2-*Bis*(diphenylphosphino)benzene
Bn	Benzyl
br.	Broad
Bu	Butyl
Bz	Benzoyl
cat.	Catalytic amount
COSY	Correlation spectroscopy
DBU	1,8-Diazabicyclo[5.4.0]undec-7-ene
DCE	Dichloroethane
DEAD	Diethyl azodicarboxylate
DIPA	Diisopropylethylamine
DIBALH	Diisobutylaluminium hydride
DMAP	*N,N*-Dimethylaminopyridine
DMF	*N,N*-Dimethylformamide
DMSO	Dimethylsulfoxide
DNA	Deoxyribonucleic acid
dpm	Dipivaloylmethanato
d.r.	Diastereoisomeric ratio
E	Entgegen (trans)
e.e.	Enantiomeric excess
equiv.	Equivalents
Et	Ethyl
Et_2O	Diethyl ether

FDA	Federal Drug Administration
hex	Hexyl
HMDS	Hexamethyldisilazane
HPLC	High-performance liquid chromatography
HRMS	High-resolution mass spectrometry
HWE	Horner–Wadsworth–Emmons
Hz	Hertz
HTS	High-throughput screening
i	Iso-
IC_{50}	Half maximal inhibitory concentration
IPA	Isopropyl alcohol
LDA	Lithium diisopropylamide
LAH	Lithium aluminium hydride
M	Molar
MCPBA	*meta*-Chloroperoxybenzoic acid
Me	Methyl
Mes	Mesityl
MeCN	Acetonitrile
MeOH	Methanol
mmol	Millimole(s)
MMTr	Monomethoxytrityl
mol	Mole(s)
MOM	Methoxymethyl ether
Ms	Methanesulfonate
MS	Molecular sieves
NCS	*N*-chlorosuccinimide
NIS	*N*-iodosuccinimide
NMR	Nuclear magnetic resonance
NP	Natural product
nOe	Nuclear overhauser effect
Nu	Nucleophile
p	Para
PCC	Pyridinium chlorochromate
pH	$-\log_{10}[H^+]$

Ph	Phenyl
PMB	*para*-Methoxybenzyl
PNB	*para*-Nitrobenzyl
ppm	parts-per-million
Piv	Pivaloyl
PPTS	Pyridinium *para*-toluenesulfonate
Pr	Propyl
ProA	Prolinamide
r.t.	Room temperature
RCM	Ring closing metathesis
Red-Al	Sodium dihydrido-*bis*(2-methoxyethoxy)aluminate
RNA	Ribonucleic acid
SAR	Structure-activity relationship
SOMO	Single occupied molecular orbital
subt	Substrate
t	*tert*-
TBDPS	*tert*-butyldiphenylsilyl
TBS	*tert*-butyldimethylsilyl
temp	Temperature
Tf	Trifluoromethanesulfonate
THF	Tetrahydrofuran
TIPS	Triisopropylsilyl
TLC	Thin layer chromatography
TMDS	1,1,3,3-Tetramethyldisiloxane
TMEDA	*N,N,N′,N′*-Tetramethylethylenediamine
TMP	Tetramethylpiperidine
TMS	Trimethylsilyl
Ts	Toluenesulfonate
TSA	Transition state analogue
WHO	World health organization
Z	Zusammen (*cis*)

Chapter 1.

Introduction

1.1. Natural products in drug discovery

Natural products (NPs) refer to any compound produced by a living organism. These include animals, plants, fungi, and bacteria. NPs are generally organic (comprised mostly of carbon, hydrogen, oxygen, nitrogen, sulphur, phosphorus, and halogen atoms), but occasionally incorporate other atoms including common metals (e.g. copper, iron, cobalt, zinc). Today, about 1 million natural products have been discovered and are classified into categories that include DNA, RNA, proteins, carbohydrates, structural polymers (lignins and polysaccharides), and small molecules (hormones, primary metabolites, and secondary metabolites).[1]

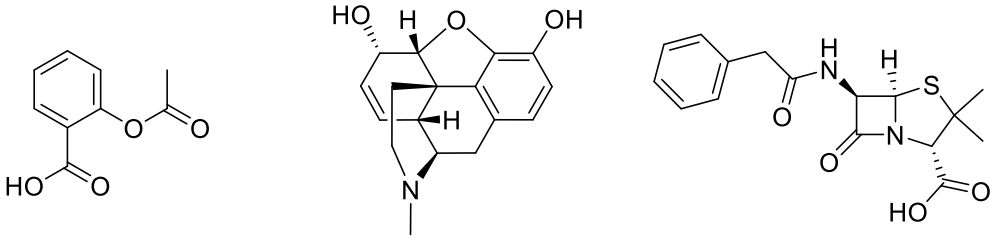

aspirin (1) **morphine (2)** **penicillin (3)**

Figure 1.1. Groundbreaking natural product medicines throughout HISTORY.

Historically, natural products have played a key role in drug discovery, especially as analgesics and treatments for cancer and infectious diseases.[2] Indeed, the widely used pain reliever acetylsalicylic acid (**1**) (Figure 1.1), better known as aspirin, was originally derived from the natural product salicin, extracted from the bark of the willow tree. Here, the pain-relieving properties of this tree were known since antiquity, and Amerindians had relied on tea made from willow bark for many centuries. Another notable example is opium, which was originally extracted from the latex from *Papaver somniferous* (a flowering poppy plant). While opium-based elixir was used in Byzantine times, the most potent narcotic component of opium, morphine (**2**) (Figure 1.1), was discovered by the German

pharmacist Friedrich Sertürner in 1804 and commercialized by Merck in 1827.[3] Today, this opioid receptor agonist is still widely used with more than 400 tons produced annually. The first antibiotic, penicillin (**3**) (Figure 1.1), was also isolated from a naturally occurring *Penicillium* mold.[4] For the discovery of penicillin, Sir Alexander Fleming, Ernst B. Chain, and Sir Howard Florey were awarded the Nobel Prize in 1945. A few years later, the Nobel Prize was given to Selman A. Waksman for the discovery of streptomycin, which represented a new class of antibiotic natural product.[5] Building on these key findings, sustained efforts in natural product discovery over the following decade (i.e., 1950-1960), led to a wide array of new medicines, and currently, ~50% of approved drug substances are natural products or derived/inspired from natural products.[6]

Despite the clear importance of natural products to human health, their impact has decreased significantly over the past two decades following the advent of high-throughput screening (HTS) and the post-genomic era. Today, less than one-quarter of drug approvals are natural products or related/inspired by natural products. Indeed, many pharmaceutical companies reduced or abandoned their natural product discovery programs following the significant progress in combinatorial synthesis and HTS, which has the combined potential to rapidly and cost-effectively construct and test massive libraries of small molecules. These processes compare favorably to natural product drug discovery, which involves many steps and special know-how.[7] For example, the processes involved in natural product drug discovery are depicted in Figure 1.2 and start with the extraction of natural products from organisms such as bacteria or plants. To maximize the diversity of the extracted NPs, the crude material is often extracted with several solvents employed in order of increasing polarity. To isolate a bioactive compound, the extracts are then subjected to a bioactivity-guided purification process that requires a highly specific and sensitive screening system. Moreover, some source organisms cannot be cultured or stop the production of relevant NPs when taken out of their natural habitat. Thus, new methods for culturing and *in* situ analysis are often required for replication purposes. At the extraction step, difficulties that include the presence of known or nuisance NPs and insufficient amounts of NPs for characterization or testing can further slow down the use of NPs in drug discovery.[8]

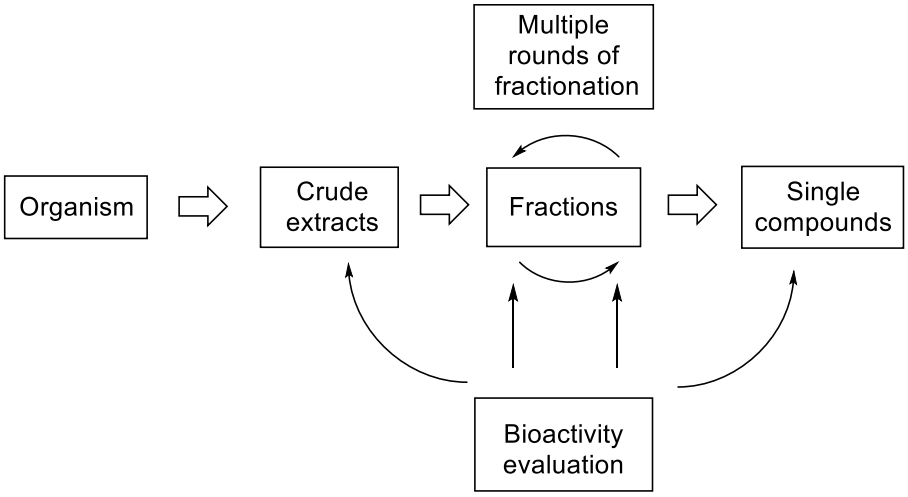

Figure 1.2. Outline of the bioactivity-guided isolation steps in natural product drug discovery.

While the percentage of natural product-related drugs may be decreasing, they remain important sources of inspiration for drug discovery. In fact, five out of the thirteen natural-product-related drugs approved between 2005 and 2007 represented the first members of new classes of drugs: the peptides exenatide and ziconotide and the small molecules ixabepilone (**4**), retapamulin (**5**) and trabectedin (**6**) (Figure 1.3).[9] The unique and diverse biological activities displayed by NPs are often related to their vast structural diversity and complexity, which samples a much broader region of chemical space than libraries of small molecules produced by chemical synthesis.[10,11] NPs are also differentiated from their synthetic contemporaries by virtue of their generally higher molecular masses, increased number of H-bond acceptors and donors, and lower calculated octanol-water partition coefficients (cLogP). Additionally, NPs are naturally "optimized" by evolution to serve specific biological functions and many serve as endogenous defence mechanisms for the producing organism, which explains the high relevance of NPs for treating infectious diseases. Thus, despite the challenges associated with their isolation, their unique structural features have contributed to the long-standing attraction of NPs for drug discovery.

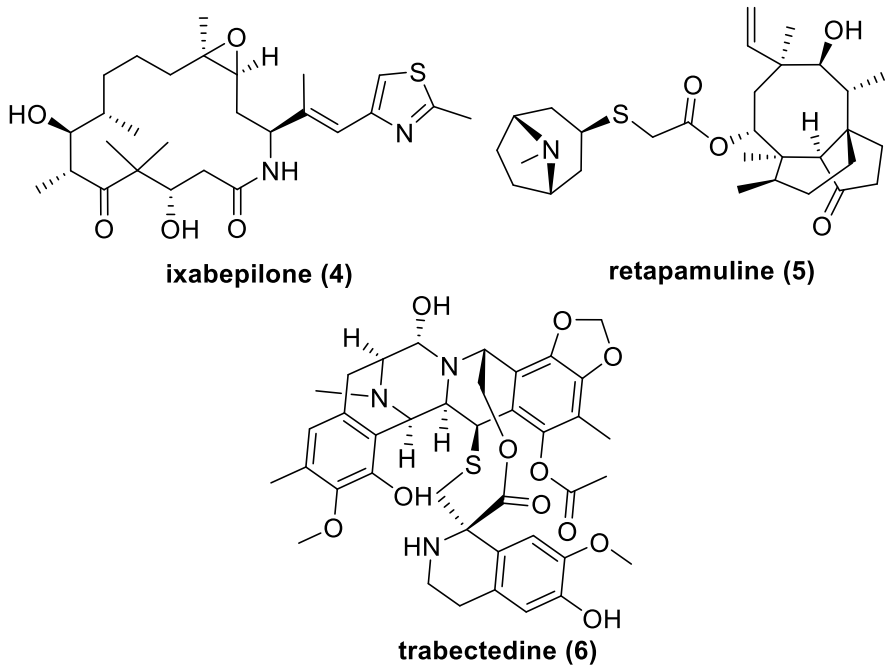

Figure 1.3. First members of new classes of drugs approved between 2005 and 2007.

1.2. Total synthesis in drug discovery

1.2.1. A powerful tool for structure elucidation and confirmation

Total synthesis refers to the complete synthetic preparation of a given compound from more simple, commercially available precursors.[12] This branch of chemistry along with the broader field of organic chemistry traces its origins to 1828 when Friedrich Wöhler prepared urea, an organic compound, from inorganic materials. Indeed, urea was formed from the reaction of silver cyanate with ammonium chloride. Despite its apparent simplicity, this work demonstrated that a substance that had previously only been available from living organisms could be made in a laboratory, a milestone in the history of chemistry.[13] Since this time, the practice of total synthesis has been driven in part by an increasing complexity and diversity of natural product targets and has brought many achievements and benefits to science and society.[14]

In the early 20th century, a major focus of total synthesis was the confirmation of the structure of a natural product.[13] Indeed, before the emergence of total synthesis, the

process of assigning molecular structure to naturally occurring compounds was extremely challenging and relied on primitive instruments and techniques. As the ultimate confirmation of structure often required degradation and comparison to known compounds, total synthesis provided a complementary approach that instead relied on converting known compounds into NPs using well-established reactions. While the development of enabling analytical, spectroscopic, and X-ray crystallographic methods and techniques has simplified the task of structure elucidation, total synthesis still provides unequivocal proof of structure for a significant number of natural products.[15] In this regard, 19 examples of structural re-assignment have been disclosed by the Nicolaou group alone during their total synthesis endeavours of the last four decades. The two natural products palmerolide A (**7**), in which three stereogenic centres were misassigned, and viridicatumtoxin B (**8**), that originally incorporated an α-hydroxy epoxide, are examples of these achievements (Figure 1.4).[14]

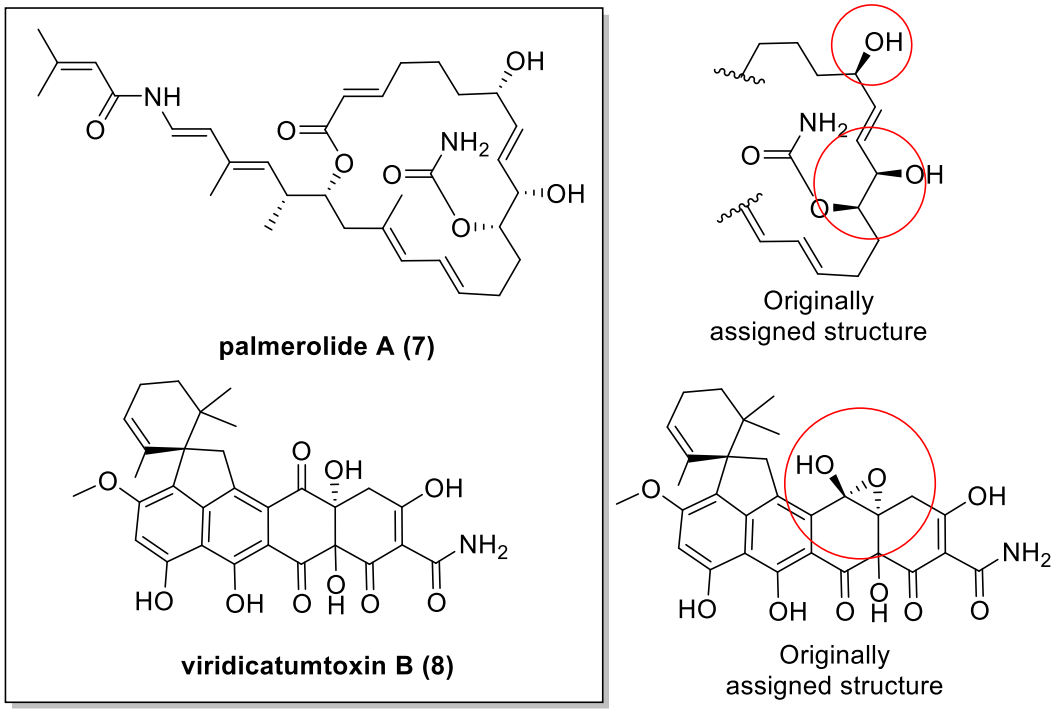

Figure 1.4. Nicolaou structure reassignments of palmerolide A (7) and viridicatumtoxin B (8).

1.2.2. Supply of natural products for biological evaluation

Total synthesis is not only restricted to the structure elucidation of natural products but it is also well-integrated in the drug discovery process. Indeed, many promising natural product leads are available only in minute quantities from natural resources and, therefore, the lack of supply can preclude further biological evaluation and clinical development.[16,17] A noticeable example is the potent antitumor polyketide natural product, (+)-discodermolide (**9**) (Figure 1.5), isolated from the Caribbean marine sponge *Discodermia dissoluta* in 1990.[18] In this case, total synthesis served to confirm the assigned structure and absolute stereochemistry and also provided sufficient material to support preclinical studies.

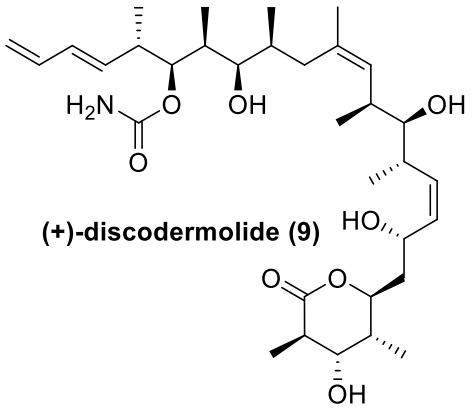

(+)-discodermolide (9)

Figure 1.5. The antitumour polyketide natural product (+)-discodermolide (9).

Due to the promising antiproliferative activity of (+)-discodermolide against a panel of cancer cell lines (including the NCI-60 panel),[19] and the extreme scarcity of the drug from natural sources (0.002% w/w from frozen marine sponge), intense efforts focused on its total synthesis. In fact, a total of 13 syntheses were disclosed between 1993 and 2008.[20] Notably, the gram-scale synthesis reported by Smith in 1999[21] and the Paterson 1st generation synthesis reported the following year[22] became the foundation for a 60 g total synthesis disclosed in 2004 by researchers at Novartis.[23] Noteworthy, while Smith and Paterson's syntheses provided the polyketide natural product in 6 and 10.3% overall yield and 21 and 23 steps (longest linear sequence), respectively, the overall yield of Novartis 26-step process was only 0.65%. Nevertheless, the Novartis campaign was able

to overcome the discodermolide supply issue and provided sufficient material to start a Phase I clinical trial.

Likewise, during the development of the chemotherapeutic agent trabectedin (**6**) (Figure 1.3), total synthesis was also contemplated as a means to supply the drug for clinical evaluation. In this case, after isolation of the highly-cytotoxic natural product from the tunicate *Ecteinascidia turbinate* in 1984,[24] attempts to farm the sea squirt showed limited success and yields were extremely low (1 tonne of tunicate was required to isolate 1 gram of trabectedin). As only 5 grams of the highly potent drug were deemed necessary to support a clinical trial, a group at Harvard headed by Corey was tasked with identifying a synthetic route to solve the supply challenge. In two years, a total synthesis of trabectedin was successfully developed that supported a human trial in 1996.[25] Further clinical development, supported by a more viable semi-synthetic route developed at PharmaMar, has led to the approval of trabectedin in 2015 to treat soft-tissue sarcomas and ovarian cancer.[26]

1.2.3. Discovery of natural product analogue drug candidates

Beyond providing material for biological evaluation or clinical studies, total synthesis can also serve as a means to discover more potent or better-tolerated analogues of a natural product. Indeed, while natural products continue to serve as a major source of new pharmaceuticals, the total fraction of unmodified natural products approved annually by the FDA has diminished since the 1930s. In their place, semisynthetic and synthetic natural product analogues are becoming increasingly common.[6] Thus, analogues of a natural product that can only be accessed through total synthesis allow for modulation of key drug characteristics such as toxicity, selectivity and bioavailability. Furthermore, while semi-synthesis has provided access to important natural product analogues including the well-known chemotherapeutic agent docetaxel (analogue of Taxol), others, like the tetracycline-related antibiotic eravacycline, were only accessible through total synthetic efforts.[27]

First generation tetracyclines

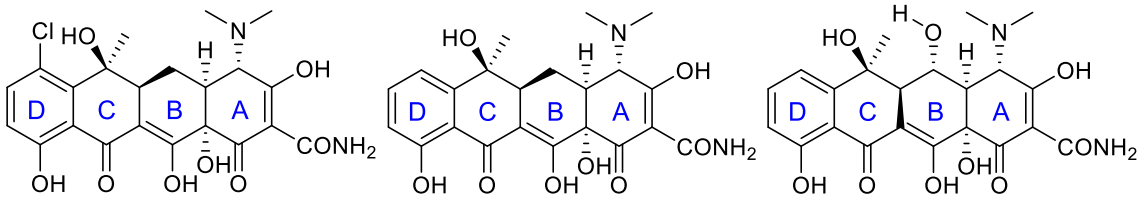

chlorotetracycline (10) **tetracycline (11)** **oxytetracycline (12)**

Second generation tetracyclines

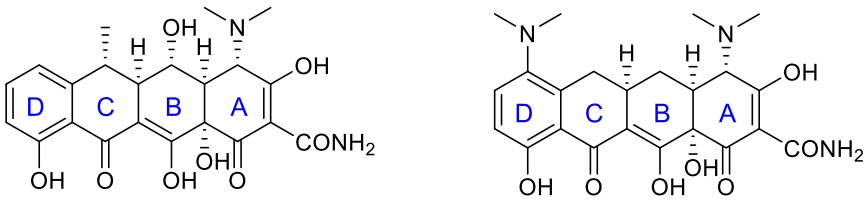

doxycycline (13) **minocycline (14)**

Third generation tetracyclines

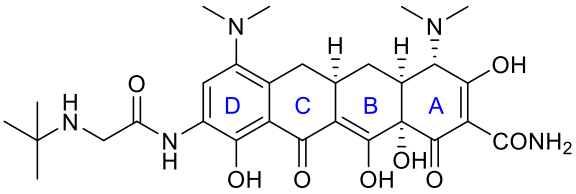

tigecycline (15)

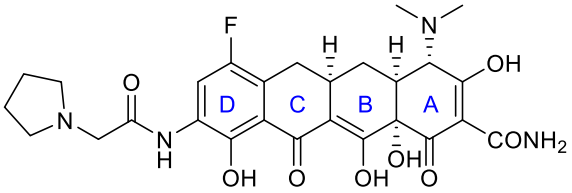

eravacycline (16)

Figure 1.6. Key members of the tetracycline antibiotic family.

The tetracycline family of natural products is characterized by a linear arrangement of four fused 6-membered carbocycles (labeled A through D, Figure 1.6) and has played a key role in the treatment of Gram-positive and Gram-negative bacterial infections for more than 60 years. The first member of this family to be identified was chlorotetracycline **10** (Figure 1.6), which was discovered in 1945. This discovery was quickly followed by a series of other closely related compounds isolated from different *Streptomyces* strains

such as tetracycline **11** (Achromycin) and oxytetracycline **12** (Terramycin) (Figure 1.6).[28] These compounds belong to the family of so-called “first generation” tetracyclines, which include unmodified natural products or compounds resulting from simple synthetic modifications. For example, tetracycline **11** was obtained via catalytic hydrogenation of chlorotetracycline **10**. The “second generation” family of tetracycline analogs (**13** and **14**) were then accessed through semi-synthesis campaigns starting with natural product building blocks. Notably, the antibiotics doxycycline **13** (Vibramycin) and minocycline **14** (Minocin) were discovered during this work (Figure 1.6). Unfortunately, widespread use of tetracyclines led to the development of antibiotic resistance and new analogs became necessary to overcome resistance. While other semi-synthetic derivatives, such as the glycil-substituted tetracycline **15** (Figure 1.6)[29] were discovered during this phase of tetracycline development, the structural diversity of new compounds was limited by the accessible natural product building blocks. Given the high degree of structural complexity and functional density of the tetracyclines, these molecules stimulated interest from synthetic chemists. Notably, the first total synthesis of a tetracycline-like derivative was developed by the Woodward group in 1962.[30] Their linear strategy, in which the construction of the ring system is performed in the D/A direction, inspired most of the following total and semi-synthetic endeavours.[31,32] Unfortunately, while an incredible accomplishment, Woodward-like synthetic strategies were found to be too inefficient to support clinical evaluation and thus, until recently, semi-synthesis was the only practical approach to generate derivatives with improved antimicrobial and pharmacokinetic profiles. Moreover, X-ray crystal structures of tetracycline bound to its bacterial ribosome target suggested that modifications on the D ring would be most interesting.[33] Unfortunately, such modifications were not possible using the Woodward strategy or semi-synthesis.

The tetracycline situation dramatically changed with Myers’ unique synthetic approach that was first reported in 2005. Notably, this breakthrough synthesis gave access to numerous structurally-diverse tetracycline analogs[34,35] and relied on the late-stage union of the D ring moiety **17** and the AB fragment **18**, along with the formation of the central C ring (Scheme 1.1).

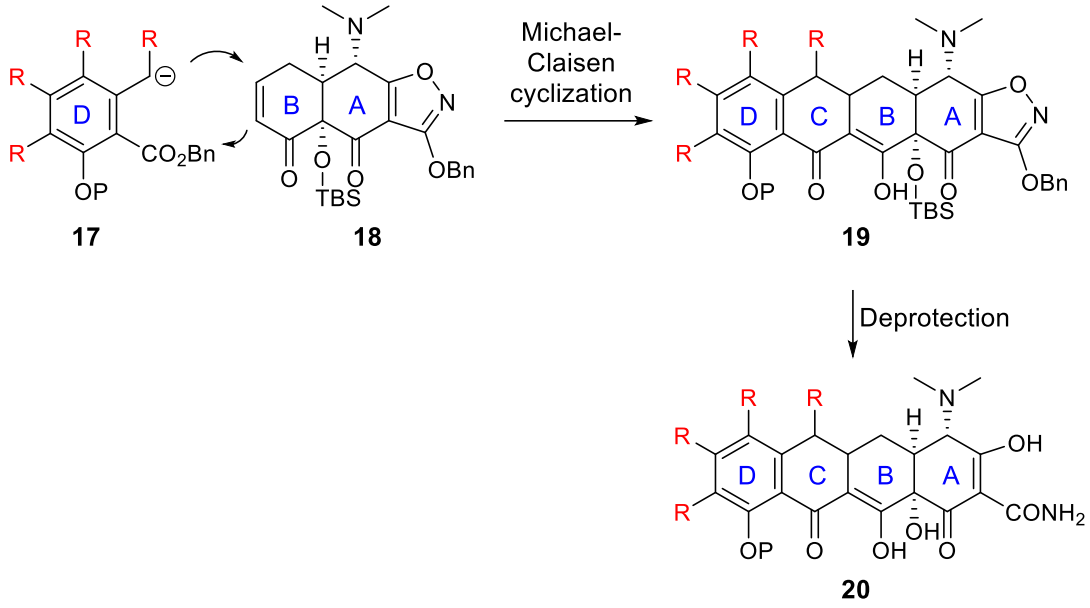

Scheme 1.1. Myers's New Approach Toward Tetracycline-like Derivatives.

This key step involves a tandem Michael-Claisen cyclization reaction, which after further refinement, turned out to be highly efficient and stereoselective with a broad range of substrates.[36,37] Not only is this approach considerably more efficient than classic strategies (about 10 steps shorter) and more practical for large-scale synthesis but also highly flexible. Consequently, Myers's synthesis paved the way for the production of numerous structurally diverse tetracycline analogs not available by semi-synthesis. In fact, more than 3000 compounds, many of which retained activity against tetracycline-resistant bacteria, were produced.[38] Notably, systemic variation of the D ring of the molecule led to the identification of eravacycline **16** (TP-434, Figure 1.6), the first member of a new subclass of tetracyclines that are fluoro-substituted.[39,40] This new antibiotic is active against many multi-drug resistant strains of bacteria and was approved by the FDA on August 27, 2018.[41] Importantly, eravacycline **16** has superior potency to that of currently marketed antibiotics for intraabdominal infections.[27] Thus, total synthesis provided an avenue to uniquely expand the structural diversity among the tetracyclines and has proven to be a game-changer for antibiotic drug discovery. Moreover, this work also provided a cost-effective manufacturing process capable of supplying the drug on an industrial scale.

1.3. The story of eribulin mesylate: The beauty and limitation of fully synthetic processes

1.3.1. Introduction

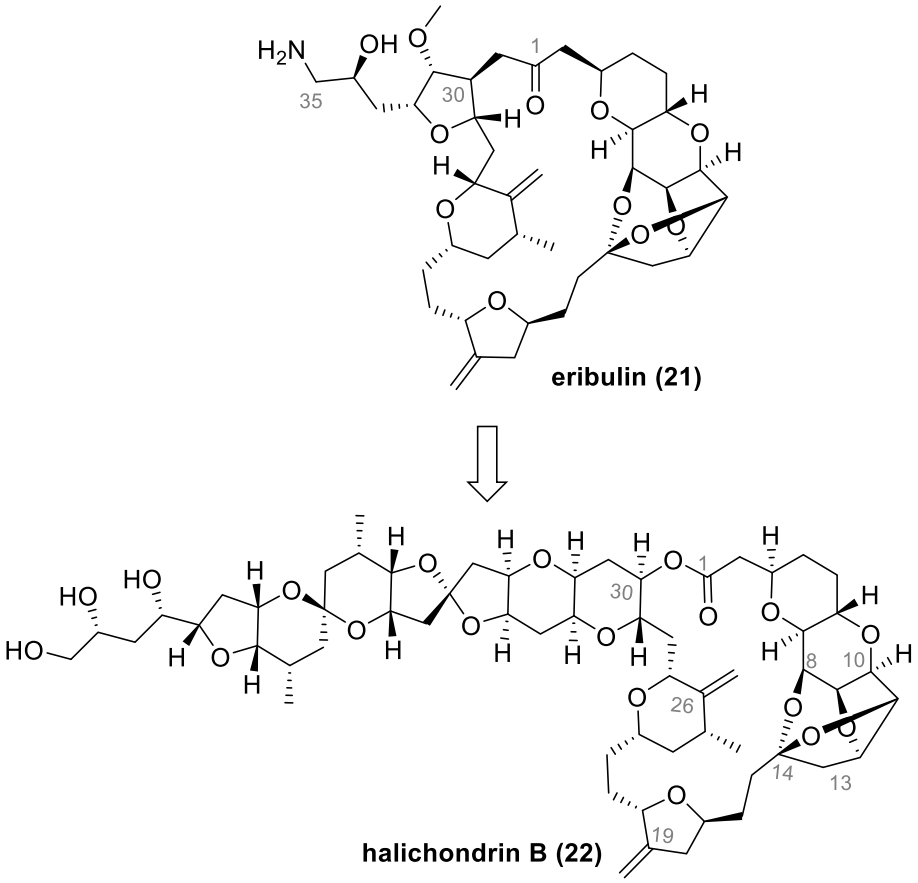

Figure 1.7. Eribulin (21), analogue of the marine natural product halichondrin B (22).

When a natural product is too structurally complex for the development of a scalable synthetic route, and extraction from the natural organism is too low-yielding, simpler analogues can be identified that provide opportunities for drug discovery. In this regard, the story of the anticancer drug eribulin mesylate, an analogue of the marine natural product halichondrin B (see **21** and **22**, Figure 1.7), is an excellent illustration. Here, total synthesis solved the initial supply issue and enabled the discovery of a new, structurally simpler, and more potent analogue. It is noteworthy that the industrial production of an active pharmaceutical ingredient of such structural and stereochemical

complexity was unprecedented.[42] As a result, the discovery of eribulin beautifully illustrates the intrinsic powers of total synthesis, but also, its limitations when it comes to scaling-up synthetic routes.

1.3.2. Isolation and biological activities of the halichondrin family

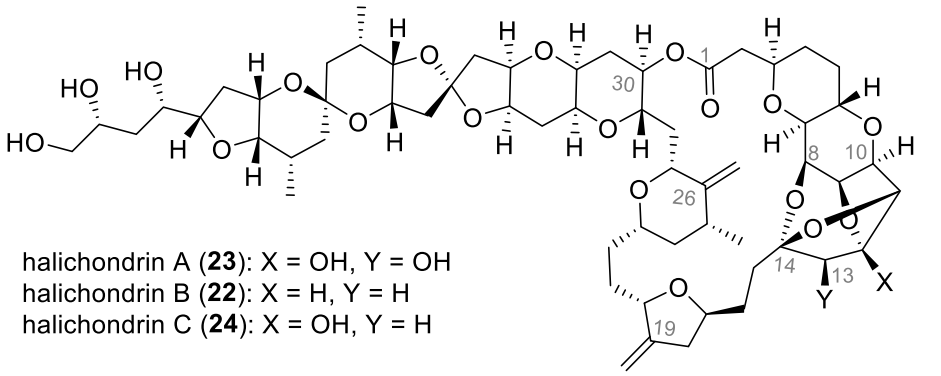

halichondrin A (**23**): X = OH, Y = OH
halichondrin B (**22**): X = H, Y = H
halichondrin C (**24**): X = OH, Y = H

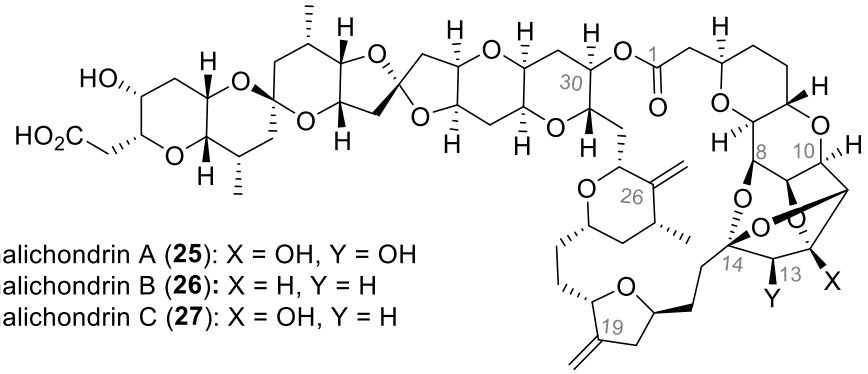

norhalichondrin A (**25**): X = OH, Y = OH
norhalichondrin B (**26**)**:** X = H, Y = H
norhalichondrin C (**27**): X = OH, Y = H

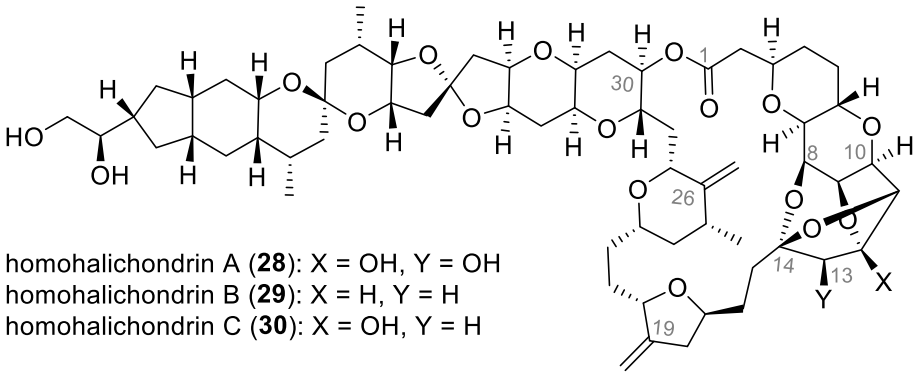

homohalichondrin A (**28**): X = OH, Y = OH
homohalichondrin B (**29**): X = H, Y = H
homohalichondrin C (**30**): X = OH, Y = H

Figure 1.8. The halichondrin family.

The halichondrins are a family of natural products that feature an unusual 2,6,9-trioxatricyclo[3.3.2.0]decane ring system. Following the isolation of the first member of this

family, norhalichondrin A (**28**), in 1985 from the marine sponge *Halichondria okadai*, many scientists became interested in this class of highly complex polyether macrolides. In fact, seven other members were isolated from a 600 kg harvest of *Halichondria okadai* and divided into 3 subgroups based on the length of the carbon backbone and the oxidation state at C12 and C13 (e.g., compounds **22**–**30**, Figure 1.8). Among these compounds, halichondrin B turned out to be the most potent compound, featuring an IC_{50} of 0.0093 ng/mL against B-16 melanoma cell cytotoxicity assay. Subsequent in-depth profiling revealed nanomolar growth-inhibition activity against various cancer cell lines and considerable increased survival times in mouse models of melanoma and leukemia. Mechanistically, halichondrin B (**22**) was shown to interact with tubulin and create nonproductive tubulin aggregates, resulting in the suppression of microtubule assembly and apoptosis. Interestingly, further investigations revealed that the activity was maintained when tested against taxane-resistant cancer cell lines and thus, halichondrin B (**22**) was suggested for preclinical trials by the US National Cancer Institute (NCI). However, given the low material supply available through the extraction of the marine sponge, it became obvious that total synthesis would be the only viable alternative able to match the future commercial demand (estimated at 1-5 kg/year).

1.3.3. Total synthesis of Halichondrin B

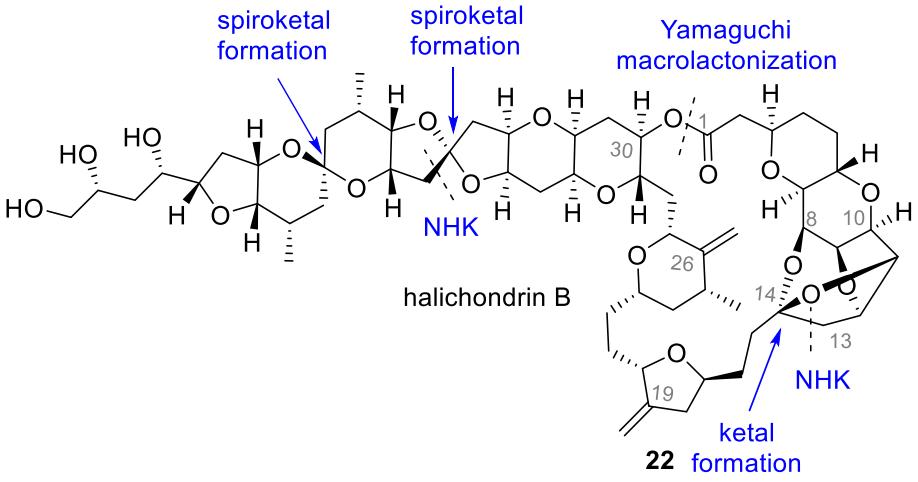

Figure 1.9. Kishi retrosynthetic approach toward halichondrin B (22).

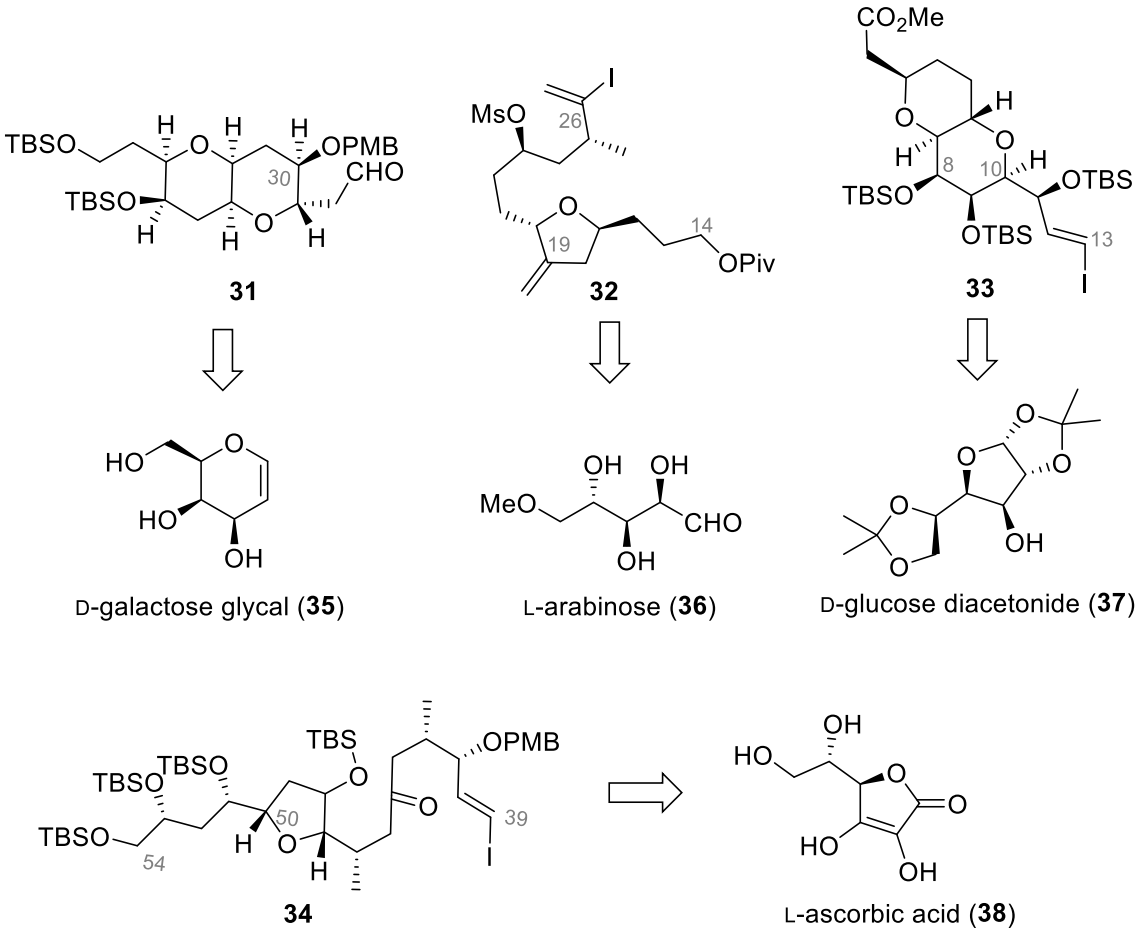

Scheme 1.2. Chiral Pool Starting Materials to Access Key Building Blocks 31, 32, 33 and 34.

Many groups reported synthetic studies toward the halichondrin members. Among these, the Kishi group was the first to succeed in developing a total synthesis of halichondrin B in 1992. Their highly convergent approach connects four subunits corresponding to the C27-C38 fragment **31**, C14-C26 fragment **32**, C1-C13 fragment **33**, and the C39–C54 fragment **34**, all of which were prepared from readily available carbohydrate-based starting materials (Scheme 1.2). Importantly, independent modifications were possible in each module and, therefore, paved the way for the synthesis of simpler analogues. In this regard, it was shown that the right-half macrolactone fragment **39** (Figure 1.10) was solely responsible for the observed growth inhibitory activity, suggesting that further simplification of the eastern region could be performed without dramatic loss of the activity.

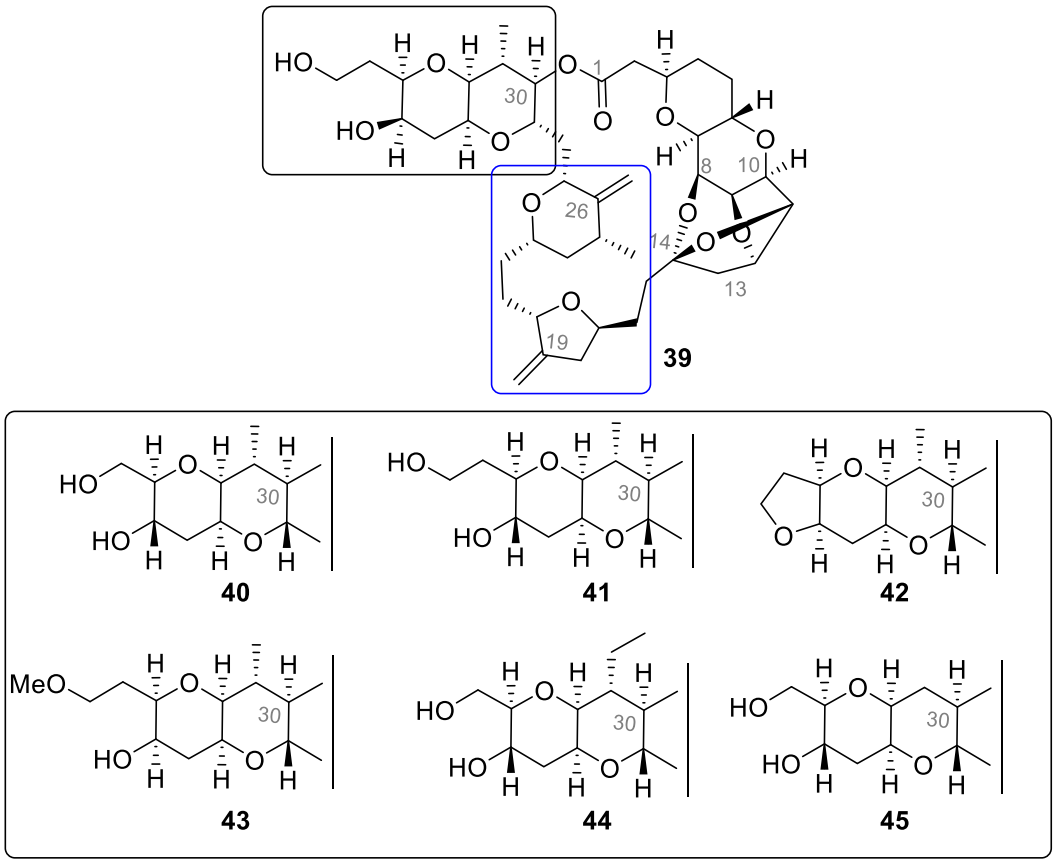

Figure 1.10. Structure-activity relationships in the C30-C38 and C19-C26 regions.

As the macrolactone **39** (Figure 1.10) was not active in human xenograft models, the C35-C38-modified analogs **40** to **45** (Figure 1.10) were subsequently synthesized and tested. Among this series, compound **40** induced an acceptable level of irreversible mitotic block and exhibited excellent antitumor activity in the LOX human melanoma xenograft model. To further simplify the structure, a series of C27-C38 pyrano-pyran modified analogues were synthesized and tested (not depicted). Most notably, it was discovered that the western-fused pyran moiety could be replaced by simple tetrahydrofuran or tetrahydropyran fragments. Further refinement in the tetrahydrofuran subseries led to the identification of compound **46** (Figure1.11), which displayed better *in vitro* activity and irreversible mitotic block, but unfortunately, was not stable in the serum used for LOX human melanoma xenograft experiments. Specifically, nonspecific mouse serum esterases were thought to be responsible for the lack of stability. To remedy this situation, bioisosteres of the C1 ester function were explored. Most notably, the ketone analogue **47** (Figure 1.11) was found to be very potent against four human xenografts. Subsequent

derivatization at C34 and C35 led to the discovery of the amine **21** (eribulin, E7389, Figure 1.11), which was selected for preclinical development at Eisai.

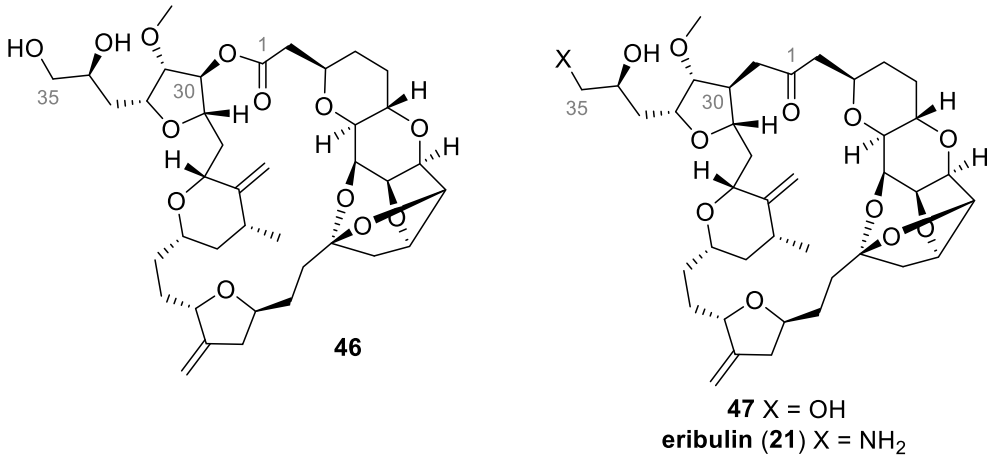

Figure 1.11. Structure of lead compounds 46, 47 and eribulin (21).

Based on these results, the Kishi group in collaboration with Eisai started a 6-year journey to transform the 62-step synthesis of eribulin into an economically feasible process. The success of this campaign culminated in 2010 with the FDA approval of eribulin to treat metastatic breast cancer. Here, total synthesis provided both the only means to access halichondrin B and led to the discovery and approval of a novel antimitotic drug that displays a unique mechanism of action. Noteworthy, from the Kishi total synthesis of halichondrin B to its transformation into eribulin and to the elaboration of an industrial process, 20 years of intense research were required. While the successful launch of eribulin demonstrates the state of the art in total synthesis, due to the numerous challenges in scaling up such a process, such achievements are rare. In fact, eribulin is still considered the most structurally complex, non-peptidic, fully synthetic drug on the market.

1.4. The limits of total synthesis in drug production

During scale-up campaigns, numerous factors must be considered. First, a process must be safe and minimize the use of hazardous materials. Physicochemical parameters such as reaction kinetics, solubility, temperature and dilution become major concerns on an industrial scale. Impurities resulting from side reactions must also be

identified and quantified. While the reactions themselves are often considered straightforward, work-up and isolation can be very challenging. Sometimes, multiple aqueous or organic solvent washes are necessary and result in the production of large volumes of waste that must be appropriately disposed of. Thick slurries can be generated during the isolation process that translate into difficult separations and extractions. Routine benchtop solvent removal techniques become much more challenging and time-consuming. Indeed, conventional benchtop purification methods, such as column chromatography, generate extraordinary solvent waste and are avoided whenever possible in favor of recrystallization. Even the cleaning of a reaction vessel after completion of a given process is a major operation. Thus, intermediates are used without purification, or several steps are performed in the same vessel (telescoping processes) or even the same solvent to avoid such manipulations.[43]

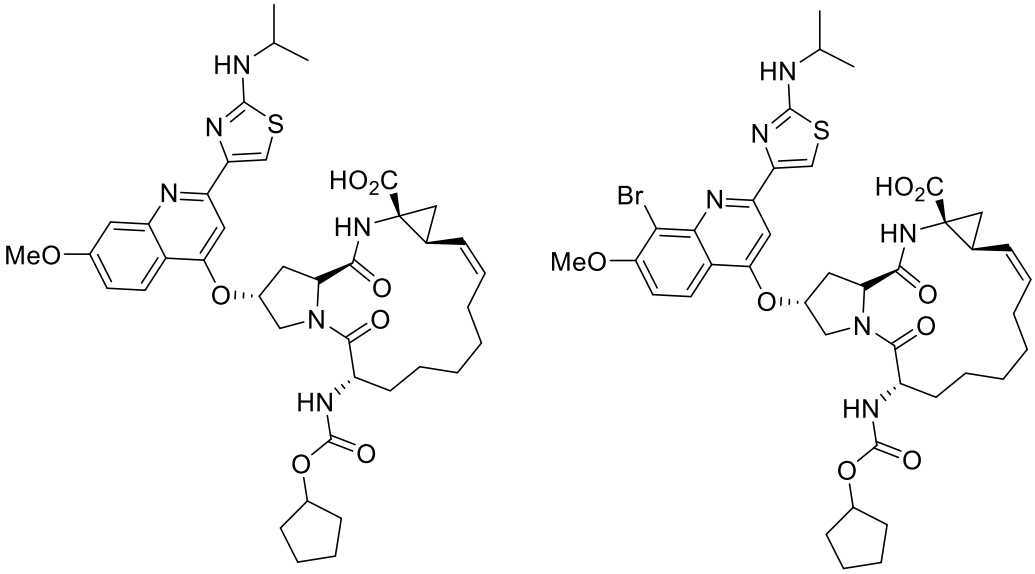

Figure 1.12. NS3 protease inhibitors BILN 2061 (48) and BI 201302 (49).

A good example to illustrate the unique challenges faced by process chemists is the development of novel NS3 protease inhibitors designed to treat Hepatitis C patients. Here, the process chemistry team at Boehringer Ingelheim (BI) was tasked with developing a less expensive and more efficient route to the active NS3 inhibitor BI 201302 **49**, a close analogue of BILN 2061 **48** (Figure 1.12). A major complication in the initial

scale-up route to BILN 2061[44] was a ring closing metathesis macrocyclization (e.g., **50** and **51**, Scheme 1.3).

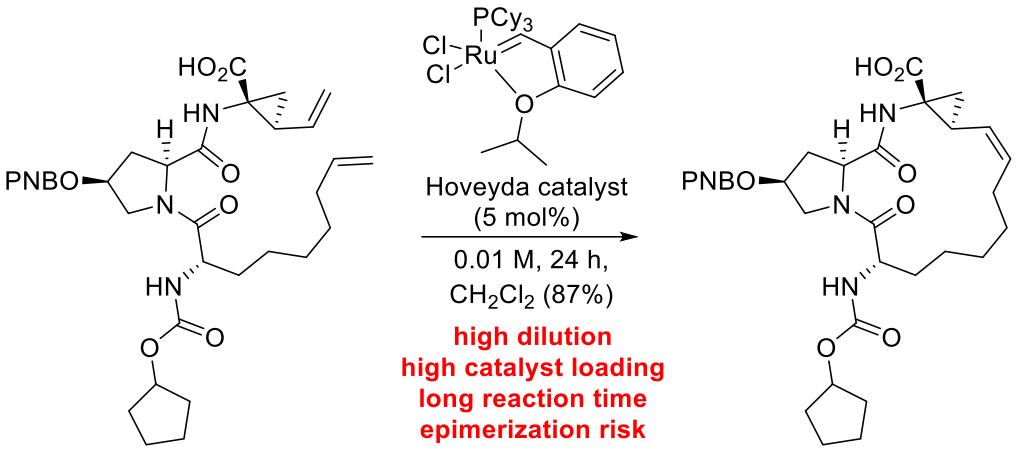

50 **51**

Scheme 1.3. Challenging Ring Closing Metathesis in the Synthetic Route to BILN 2061 (48).

The process team identified several key shortcomings with the initial ring closing metathesis conditions. First, high dilution was necessary to avoid undesired dimerization of the diene starting material, which on large scale resulted in lower throughput and higher solvent and waste disposal costs. Moreover, high catalyst loadings (5 mol%) and extensive reaction times (24 hours) were found essential to drive the reaction to full completion and, thus, rendered this process financially unreasonable. To address these issues, a thorough analysis of the cross-metathesis reaction was undertaken that revealed the impact of conformation on the formation of undesired dimers. Most notably, it was found that the use of a Boc-protected amide analogue **52** (Scheme 1.4) shifted the site of the metathesis initiation and improved the rate of the desired intramolecular reaction.[45] Having reduced the rate of competing dimerization, the catalyst could be switched to the more reactive and less expensive Grela catalyst. Eventually, it was found that the reaction could be run at a standard reaction dilution of 0.1-0.2 M and the catalyst loading could be decreased to 0.1 mol%. Therefore, despite the high yielding nature of the initial ring-closing metathesis reaction conditions, significant effort and innovation were required to identify an acceptable scale-up process for this one step.

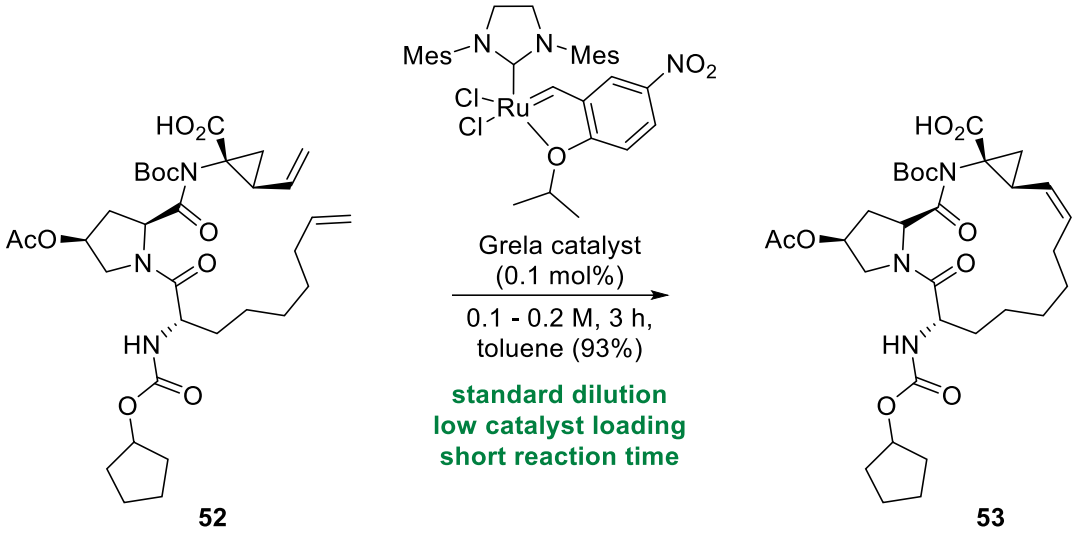

52 53

Scheme 1.4. Optimized RCM for the Scale-up Route to BI 201302 (49).

The antimalarial medication artemisinin (**54**) (Scheme 1.5) provides an additional excellent example of process optimization. In 1970, extracts of *Artemisia Annua,* which had been used for over two millennia in Chinese herbal medicine, were found to possess antimalarial properties and lead to the discovery of artemisinin. Artemisinin-based combination therapies (ACTs) were eventually designated by the World Health Organization (WHO) as the front-line treatment for uncomplicated malaria caused by the parasite *P. falciparum*.[46] As the drug was produced by isolation from the natural source, availability and price fluctuated annually based on plant production, temperature, humidity, and soil quality. In addition, crop disruption caused by natural disasters and geopolitical events represented a serious concern. Consequently, the market price for artemisinin varied between US$120 and $1,200 per kilogram from 2005 to 2008.[47] To combat these fluctuations in supply and cost, a global effort was focused on identifying alternative means of production, with total synthesis at the forefront.

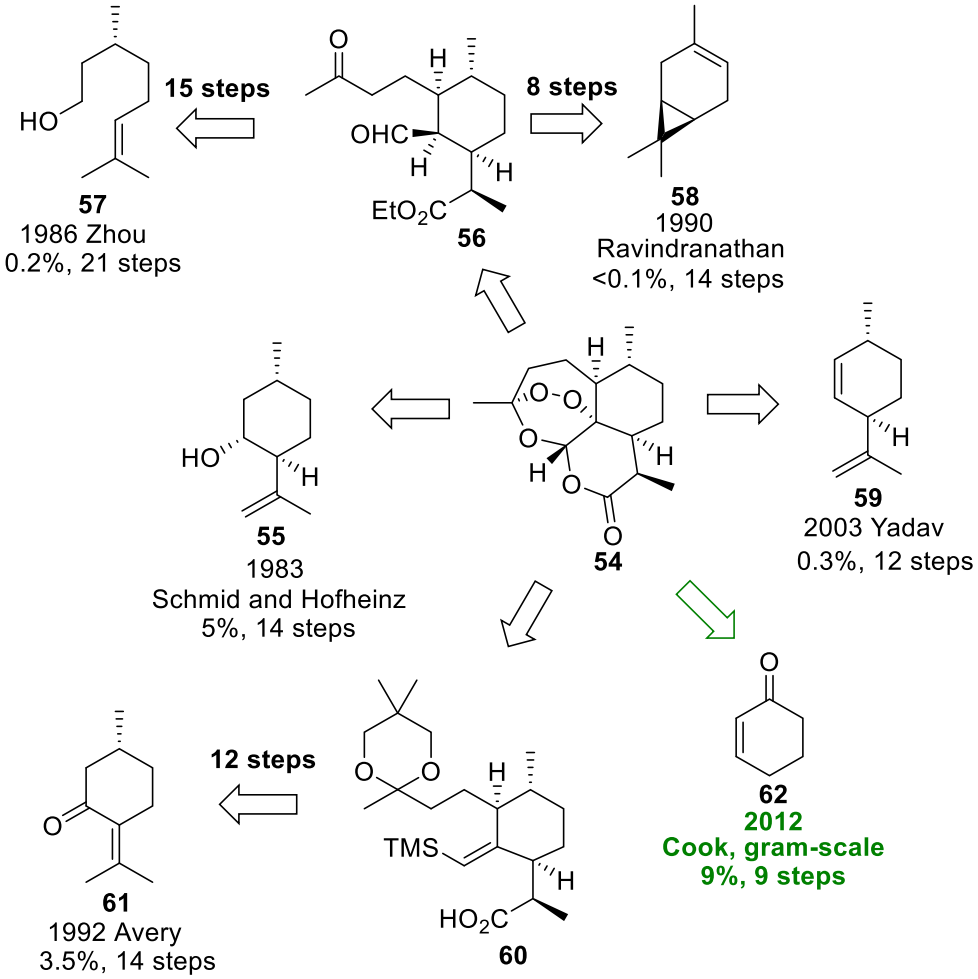

Scheme 1.5. Total Syntheses of Artemisinin (54).

As depicted in Scheme 1.5, numerous artemisinin total syntheses were developed, most of which relied on a chiral pool starting material (e.g., compounds **55**, **57**, **58**, **59** and **61**, Scheme 1.5). This task was first achieved by Schmid and Hofheinz in 1983, using the commercially available (-)-isopulegol **55** (Scheme 1.5). The route provided the antimalarial drug in fourteen steps (longest linear sequence) with an overall yield of 5%.[48]

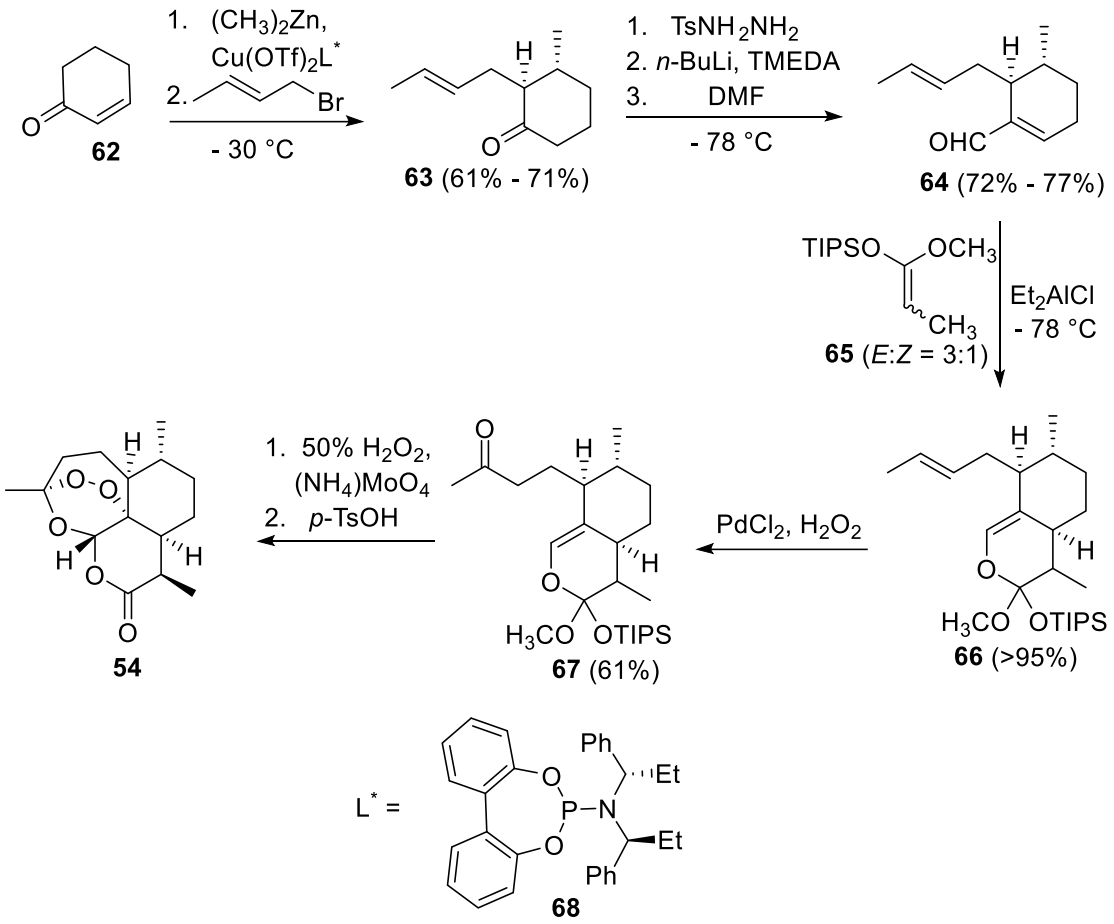

Scheme 1.6. Cook's Total Synthesis of Artemisinin (54).

In 2012, a scalable, cost-effective synthesis was developed by Cook that provided 1.26 g of artemisinin.[49] As shown in Scheme 1.6, the synthesis starts with a one-pot conjugate addition/alkylation sequence of the inexpensive, widely available cyclohexanone **62**. The resulting ketone **63** then reacts with $TsNH_2NH_2$ to provide a hydrazone intermediate, which is subsequently treated with *n*-butyllithium and quenched with DMF. The α,β-unsaturated aldehyde **64** then engages in a [4+2] reaction with the silyl ketene acetal **65** to furnish the ortho ester **66** in 95% yield. A simple treatment with aqueous H_2O_2 and palladium dichloride selectively oxidizes the less-hindered olefin function delivering the corresponding ketone **67** in 61% yield. Finally, the reaction of compound **67** with singlet oxygen, generated from the decomposition of H_2O_2 by ammonium molybdate, and subsequent treatment with *p*-TsOH achieved a 9-step synthesis to artemisinin (**54**). Importantly, this synthesis is concise, initiates with a cheap,

widely available starting material, and several steps are performed in the same vessel, thus, reducing the total number of operations to five. Nonetheless, despite these appealing features, Cook's synthetic process remains less viable than direct extraction from the plant and in 2013 Sanofi reported a semi-synthetic route that is now undoubtedly the cheapest and most reliable production method. [50]

In the Sanofi process, the sequence initiates with the stereoselective reduction of the naturally occurring artemisinic acid (**69**) (Scheme 1.7). Ethyl chloroformate activation of the resulting acid **70**, is followed by a Schenck ene reaction to provide an allyl peroxide intermediate **72**. A subsequent cascade of reactions, which includes a Hock cleavage, an oxygenation and a ring closure, delivers the drug in 54% overall yield.

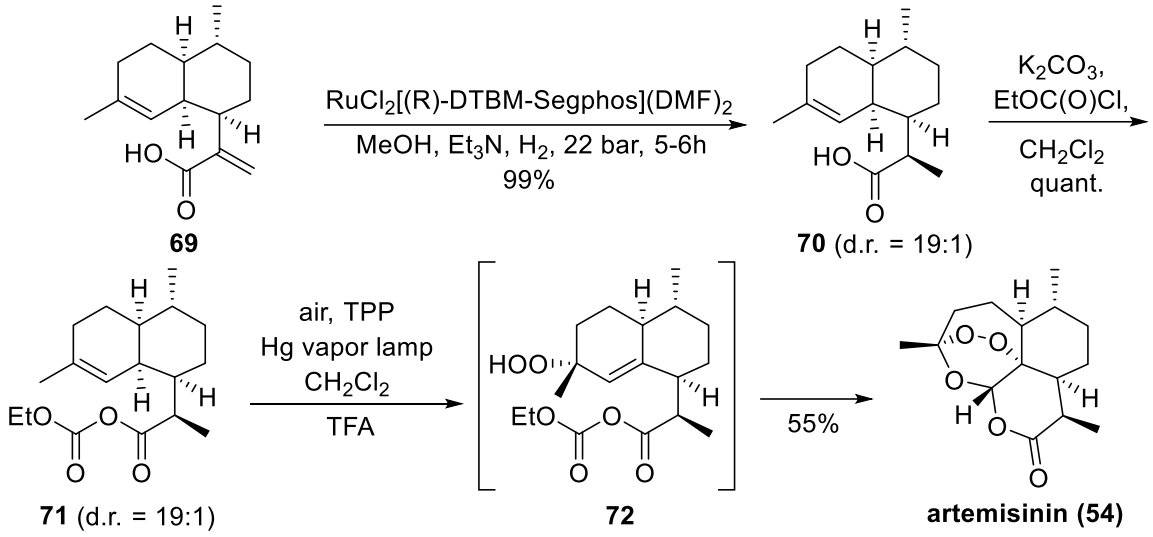

Scheme 1.7. Sanofi Semi-synthetic Process of Artemisinin (54).

More recently, a very efficient and cost-effective process was developed to produce large quantities of artemisinic acid **69**. This technology, first engineered in the Keasling group, relies on the use of a genetically modified bacteria in which the biosynthesis machinery of a plant was cloned.[46] Thus, cheap and scalable production of the key precursor **69**, combined with the Sanofi 3-step sequence, led to the delivery of ~55 tonnes of artemisinin in 2014. Most notably, this material was sold for $350-400 per kilogram, roughly the same price as the botanical source. Consequently, this highly efficient semi-synthetic process is the first reliable supply chain for artemisinin.

1.5. Conclusion

Whether for their structural complexity, their naturally optimized scaffolds, or their phenomenal diversity, natural products continue to inspire the field of drug discovery.[2] Yet, since the late 20th century the number of approved natural products and natural product analogues has declined steadily.[6] A combination of factors that include challenges in isolation, the advent of high-throughput screening and synthetic library production, and the scarcity of the active ingredients from natural sources have all contributed to this trend.[9] However, total synthesis can serve as a powerful tool to address some of the challenges associated with natural product drug discovery, continues to play an important role in structure elucidation,[15] and is often the only means to provide sufficient material for clinical development.[23] Moreover, total synthesis has proven extremely valuable in the synthesis of natural product analogs and the establishment of structure-activity relationships. Indeed, the flexibility offered by total synthesis provides avenues to expand chemical space in ways otherwise not possible.[51] The first fully synthetic epothilone B analogue in clinical development, sagopilone,[52] and the discovery of the new broad-spectrum antibiotic eravacycline (Figure 1.6) are excellent examples of the importance of total synthesis to drug discovery.[27] The power of total synthesis is well demonstrated in the discovery and development of the chemotherapeutic drug eribulin mesylate. Here, total synthesis of halichondrin B led to the synthesis of new, structurally simpler analogs, and ultimately to the production of a new anticancer drug. Nonetheless, the production of highly complex molecules often relies on direct extraction from the natural organism or semi-synthetic processes. Thus, in the case of the antimalarial drug artemisinin, a large-scale semi-synthetic route was developed to solve the long-standing supply issue. Finally, factors such as dose, treatment regimen, and targeted disease all greatly impact the economical feasibility of a synthetic process.[53,54] Thus successful launch of eribulin produced via total synthesis was only possible due to the nanomolar potency, treatment regimen (1.4 mg/m² on day 1 and day 8 every 3 weeks)[55] and disease targeted (cancer).

1.6. Thesis overview

This thesis is focused on the development of concise synthetic routes towards valuable natural product analogs.

In Chapter 2, the development of a novel synthetic approach to the Eisai C14-C35 fragment of eribulin is presented. Eribulin belongs to a family of natural and synthetic compounds that disturb microtubule dynamics and are among the most effective and widely used cancer chemotherapeutic drugs. With 19 stereogenic centres, this macrocyclic ketone is the most complex, fully synthetic drug on the market. Therefore, tremendous effort was required to adapt the 62-step synthesis to an economically feasible process. Most notably, the synthetic route currently used to produce the C14-C35 fragment of this drug involves a total of 43 steps. To improve upon this process, we exploited methodology developed in the Britton group for tetrahydrofuran synthesis. Most notably, we anticipated that the application of our expertise in the stereoselective synthesis of hydroxytetrahydrofurans would allow us to considerably reduce the overall length of the synthesis and consequently the cost of producing eribulin.

In Chapter 3, the result of a collaboration with Eurofins Alphora, an FDA-approved contract development and manufacturing organization focused on process chemistry, is described. Notably, Eurofins Alphora has spent several years developing a cost-effective synthetic route to eribulin mesylate. Our cooperation led to the development of scalable synthesis of Alphora C14-C26 fragment of eribulin. Subsequently, based on synthetic work developed in Chapter 2, a stereoselective synthesis of the Alphora C14-C35 building block was elaborated.

In Chapter 4, a short formal synthesis of the two nucleoside analogues, immucillin A and H, is reported. Notably, the tandem α-chlorination/aldol reaction developed in the Britton group was successfully used to rapidly construct the iminosugar moiety. However, the limitations of this strategy were also identified as early introduction of the heteroaromatic function proved not possible.

Finally, the thesis concludes with one appendix which relates the design, synthesis and evaluation of a new series of indole-based PRMT4 inhibitors that represent potential biological probes or therapeutics. While no on-target effect in cells was achieved, these inhibitors represent a new chemotype for further development of cell-active PRMT4 inhibitors.

Chapter 2.

Development of a Concise Synthesis of Eisai C14-C35 Fragment of Eribulin

2.1. Introduction

2.1.1. First-generation synthesis of eribulin

As detailed in Chapter 1, eribulin was identified by Eisai during the synthesis of simpler analogues of the marine natural product halichondrin B.[56] At the time, a milligram scale synthesis of eribulin was developed based on Kishi's total synthesis of halichondrin B.[57] This first-generation synthesis hinged upon a late-stage halogen-metal exchange coupling to connect the fragments **73** and **74**, prior to an intramolecular Nozaki-Hiyama-Kishi (NHK) macrocyclization (Scheme 2.1). In turn, a Nozaki-Hiyama-Kishi coupling of aldehyde **75** and vinyl iodide **32** led to the key precursor **73** (Scheme 2.1).[58]

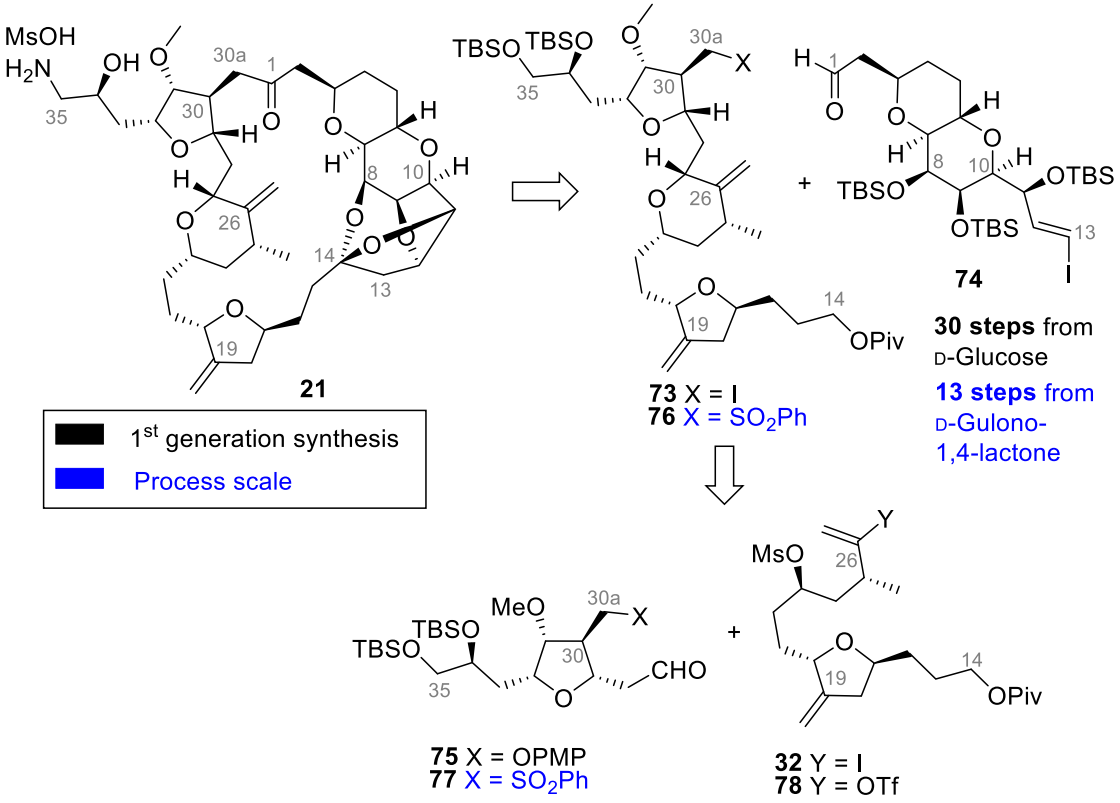

Scheme 2.1. Eisai's Retrosynthesis of Eribulin (21).

Structurally, a key difference between eribulin and halichondrin B is the C30-C1 junction, which incorporates a ketone function in eribulin and an ester function in the natural product. To construct the ketone, a new C27-C35 fragment **75** was elaborated from the stock intermediate **79** that was used to support the preparation of halichondrin B analogues (Scheme 2.2). Overall, aldehyde **75** was prepared in 24 steps from L-arabinose (**80**) (Scheme 2.2).[59]

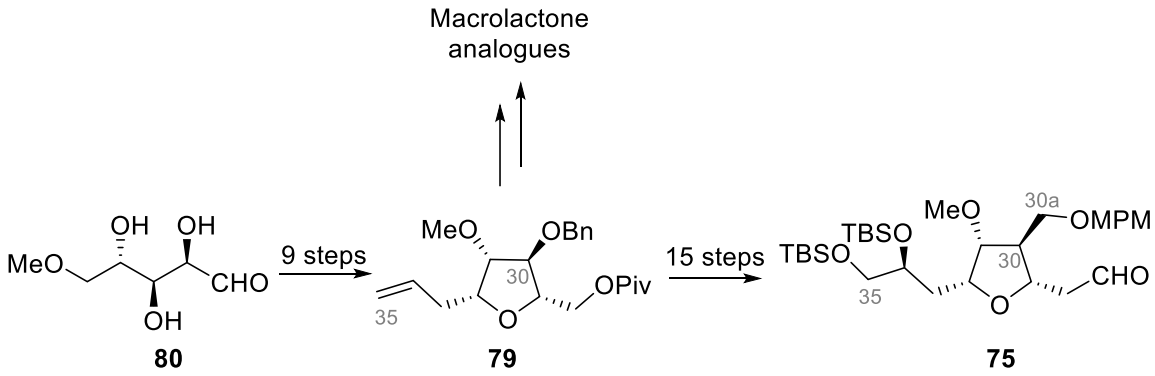

80 **79** **75**

Scheme 2.2. First-generation Synthesis of the C27-C35 Fragment 75 from L-Arabinose.

As shown in Scheme 2.3, Ni/Cr-mediated coupling of aldehyde **75** with vinyl iodide **32** and subsequent formation of the tetrahydropyran ring under basic conditions (Williamson ether cyclization) delivered compound **81** that was further elaborated into the iodide **73** through a four-step sequence. Lithium–iodide exchange provides the corresponding organolithium species that underwent reaction with the aldehyde **74**. Based on the routes established in the total synthesis of halichondrin B, the resulting alcohol **82** was further elaborated into eribulin in 9 additional steps (Scheme 2.3).

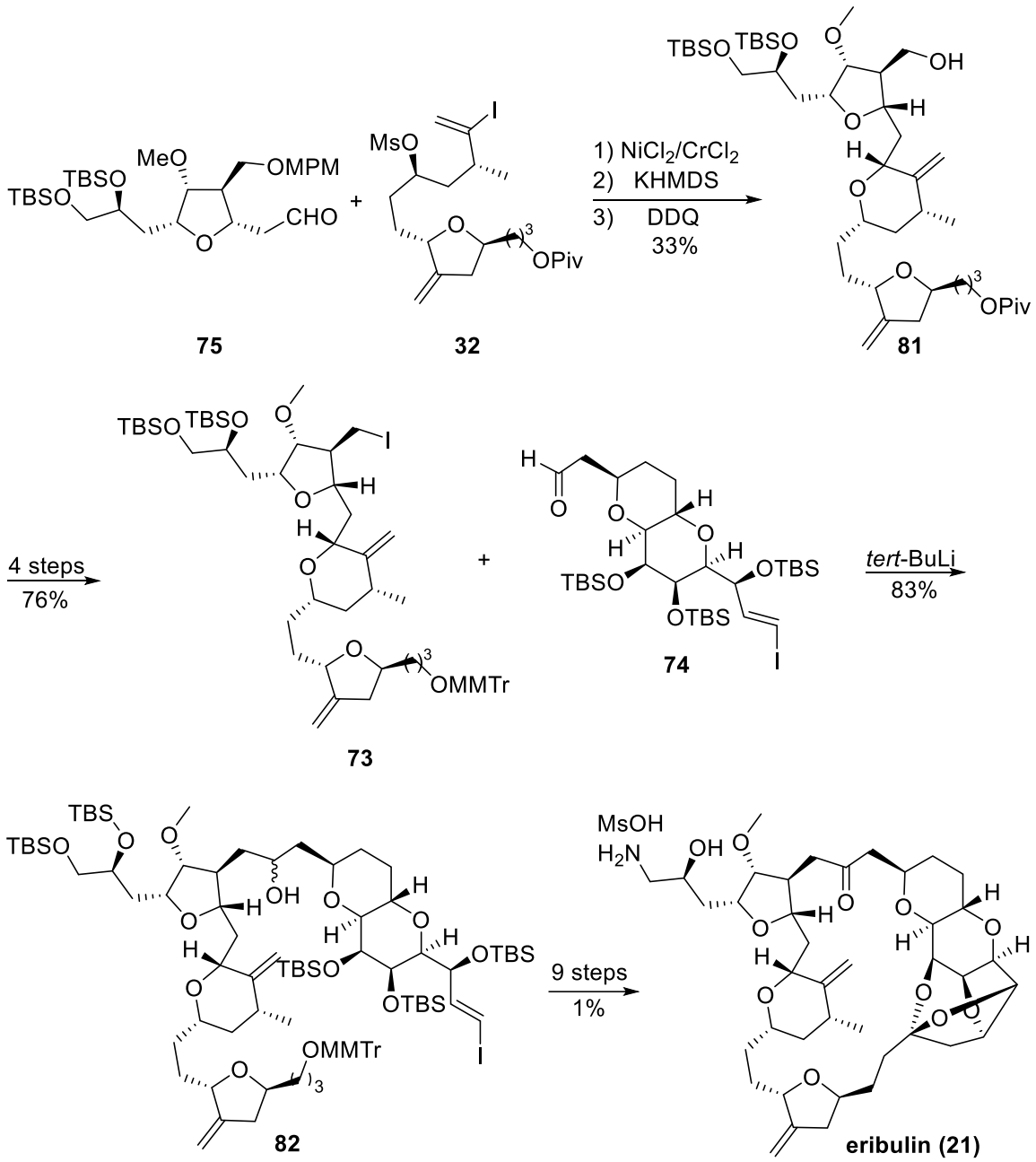

Scheme 2.3. First-generation Synthesis of Eribulin (21).

2.1.2. Process-scale synthesis of eribulin

The first-generation, 62-step synthesis of eribulin produced 0.6 mg of material that was used for analytical characterization and supported initial *in vitro* biological profiling.[42] However, this extremely long process was not designed to provide the large quantity of

drug necessary for development. Therefore, due to increased needs, a major scale-up campaign was initiated by researchers at Eisai. Here, it was discovered that the key coupling reaction between iodide **73** and aldehyde **74** (Scheme 2.1) was low yielding when conducted at a larger scale. Instead, the reaction of an α-lithiated sulfone **76** with the aldehyde **73** (Scheme 2.4) was found to be more reproducible than the initial halogen-metal exchange methodology. In fact, solvent screening for this key coupling led to an optimized process that delivered 86% of the desired addition product **83** (Scheme 2.4).[42,59]

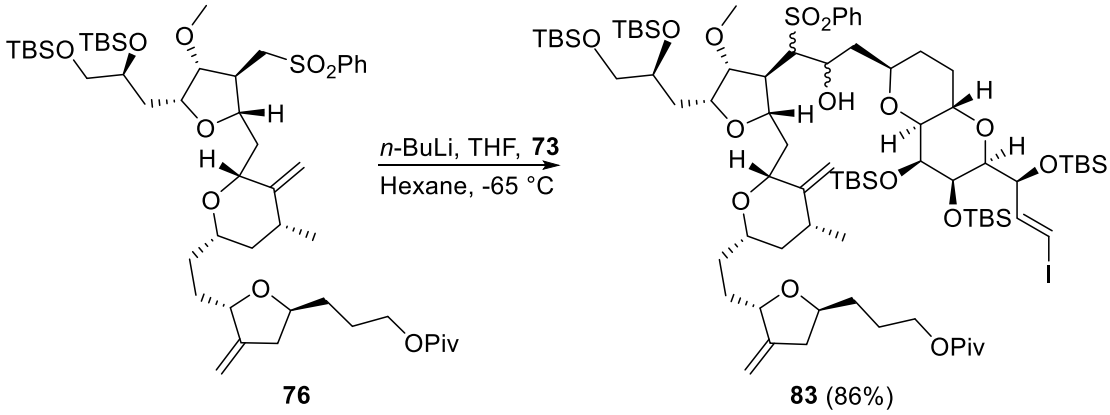

76 **83** (86%)

Scheme 2.4. Large-scale Coupling of Sulfone 76 and Aldehyde 73.

To produce the C14-C35 sulfone **76**, a process-scale synthesis of compound **77**, a sulfone analogue of the initial C27-C35 fragment **75** (e.g., **75** and **77**, Scheme 2.1), was developed (Scheme 2.5).[60] This synthesis initiates with acetonide protection of the commercially available D-glucurono-3,6-lactone **84**. A subsequent deoxygenation reaction provided the crystalline lactone **85** in 60% overall yield, which was then converted in the β-hydroxysilane **86** by diisobutylaluminum hydride reduction and the subsequent addition of trimethylsilylmagnesium chloride. Peterson elimination of **86**, followed by treatment with benzyl bromide and potassium *tert*-butoxide then furnished the ether **87** in 88% yield over two steps. Asymmetric dihydroxylation of the alkene function in **87** under modified Sharpless conditions,[61] was followed by protection of the resulting diol to provide the di-benzoate **88** in excellent yield (d.r. = 3:1). C-glycosylation of **88** with allyl trimethylsilane and subsequent recrystallization from isopropanol and *n*-heptane, resulted in production of the desired diastereoisomer **89** in 59% yield. Oxidation of the alcohol function in **89** and condensation with the lithium anion of methyl phenyl sulfone then delivered a mixture of *E* and *Z* vinyl sulfones **90**. Compound **90** was then further elaborated into the crystalline

triol **91** via a selective benzyl deprotection and a hydroxy-directed conjugate reduction of the olefin moiety. Subsequent hydrolysis of the benzoate esters, using sodium carbonate in methanol, provided compound **91** in 57% yield over five steps. The latter material **91** was then converted to tetrahydrofuran **92** in a 4-step sequence that includes, a series of protections and deprotections of the diol moiety and selective methylation of the C31-alcohol. Finally, ozonolysis of the olefin function in **92**, and a subsequent reductive work-up in the presence of the Lindlar catalyst, afforded the key C27-C35 aldehyde **77** in 68% yield from **91**.

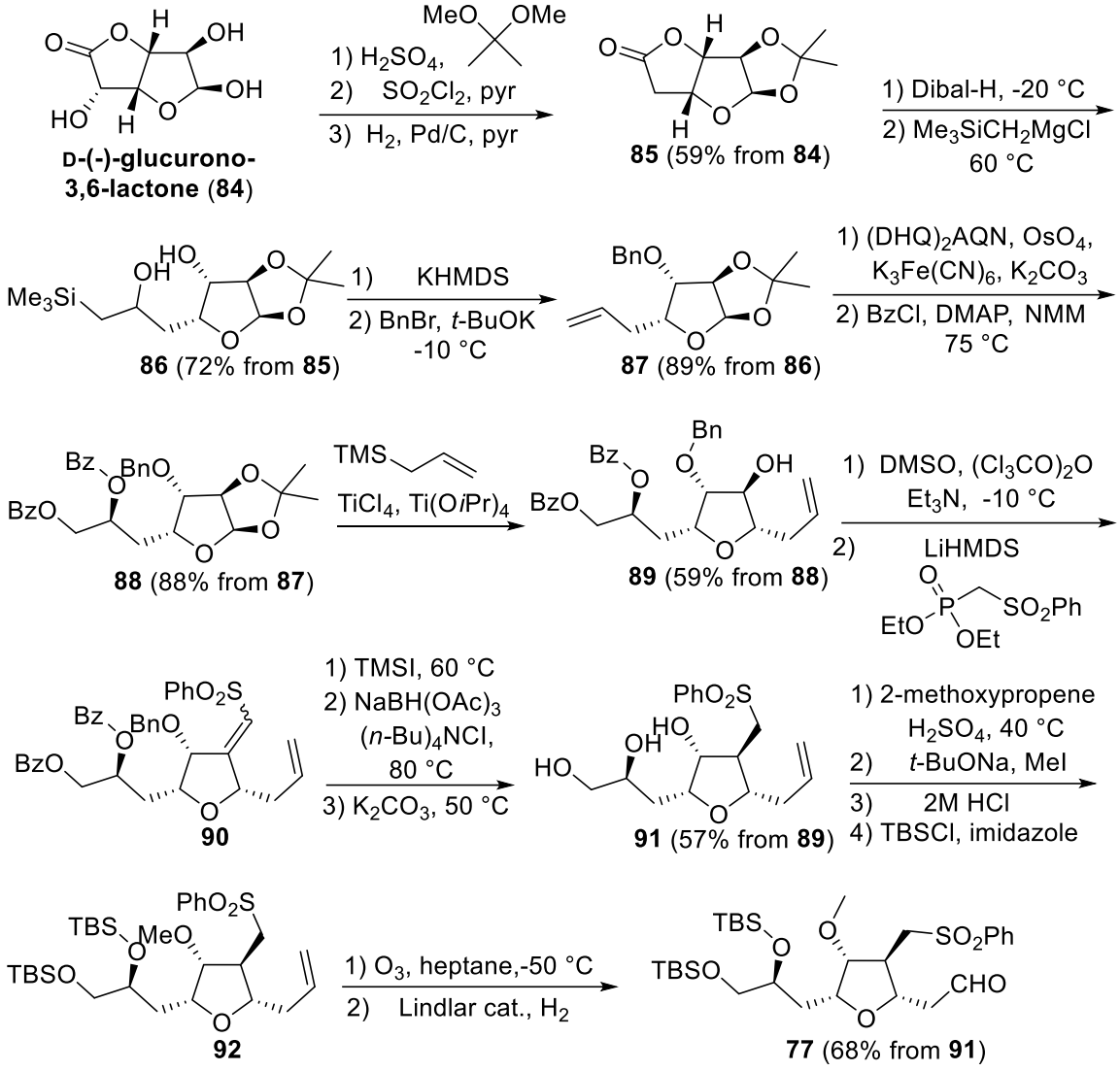

Scheme 2.5. Process-scale of the C27-C35 Fragment 77.

Considerable improvements were also made to the synthesis of the C1-C13 building block **74**. In fact, the initial route used in halichondrin B total synthesis (30 steps from D-glucose) was replaced by a 13-step process from D-manno-γ-lactone.[62] More recently, as the stereogenic centre corresponding to C11 (eribulin numbering) is ultimately destroyed, a more viable route was developed from the widely available epimeric sugar D-gulonolactone and is now used to produce the C1-C13 fragment of eribulin.[63]

As depicted in Scheme 2.6, treatment of D-gulonolactone **93** with cyclohexanone provided the protected tetraol **94** in 60% yield as a pure crystalline material. Diisobutylaluminium hydride reduction of **94** and subsequent Wittig reaction furnished the olefin **95**, which could be used in the next step without further purification. Compound **65** was then transformed into the lactol **96** via a stereoselective osmylation and a deprotection/protection sequence. C-glycosylation of **96** with commercially available methyl 3-trimethylsilyl-4-pentanoate **97** was followed by a sodium methoxide-promoted diacylation/olefin conjugation/oxy-Michael cascade reaction. Subsequent cleavage of the resulting diol **98** provided the corresponding aldehyde **99** in quantitative yield. Ni(II)/Cr(II)-mediated coupling of **99** and 1-bromo-2-trimethylsilylethylene **100** was followed by acidic treatment and TBS protection to provide compound **101**. This latter material was then further converted to the corresponding iodide using NIS and catalytic amount of TBSCl. Finally, careful diisobutylaluminum hydride reduction of the ester moiety completed a 13-step synthesis of the key building block **74**.

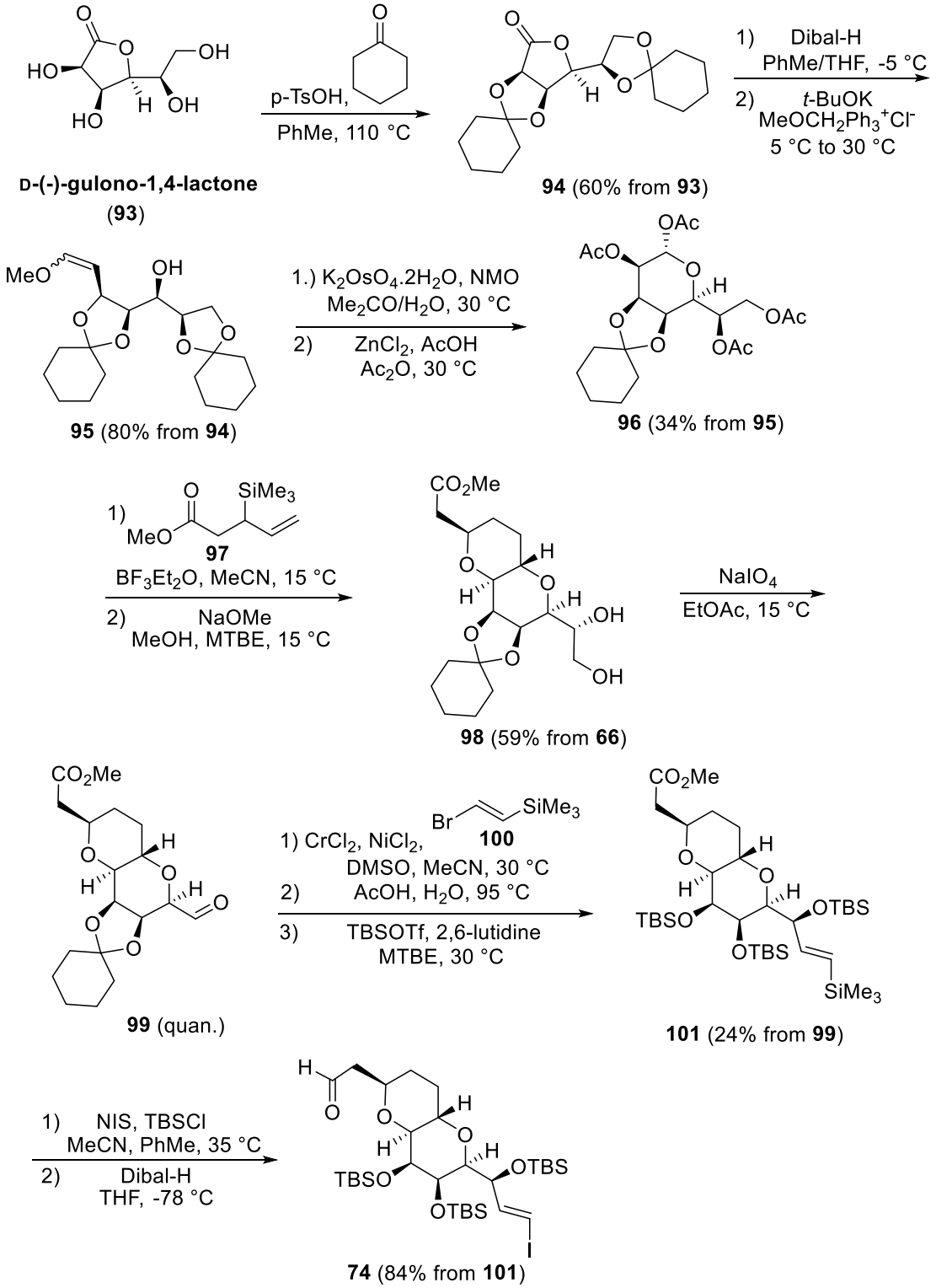

Scheme 2.6. Process-scale Synthesis of the C1-C13 Building Block 74 from D-(-)-Gulono-1,4-lactone (63).

During the development of eribulin, a new synthesis of the C14-C26 building block **78** was investigated. Most notably, the total number of steps required to access the key intermediate was significantly reduced (from 30 steps to 20 steps). As shown in Scheme 2.7, this approach is based on a late-stage NHK-coupling of the two intermediates **102** and **103**.

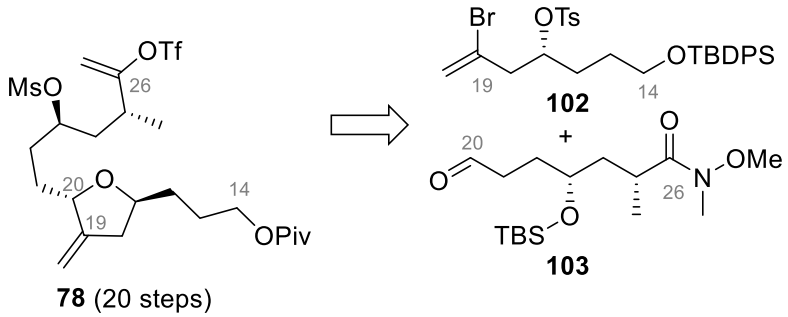

Scheme 2.7. Retrosynthesis of the C14-C26 Fragment 78.

The synthesis of the vinyl bromide **102** starts with an acid-catalyzed hydration of commercially available 2,3-dihydrofuran **104** and is followed by a tin-mediated addition of 2,3-dibromopropene (Scheme 2.8). A subsequent TBDPS-protection provides a racemic mixture of alcohols **105**. After chiral separation, and Mitsonobu reaction of the undesired enantiomer **105b**, the alcohol **105a** is formed in 20% overall yield. Tosylation of **105a** completed the 6-step process to the coupling partner **102**.[64]

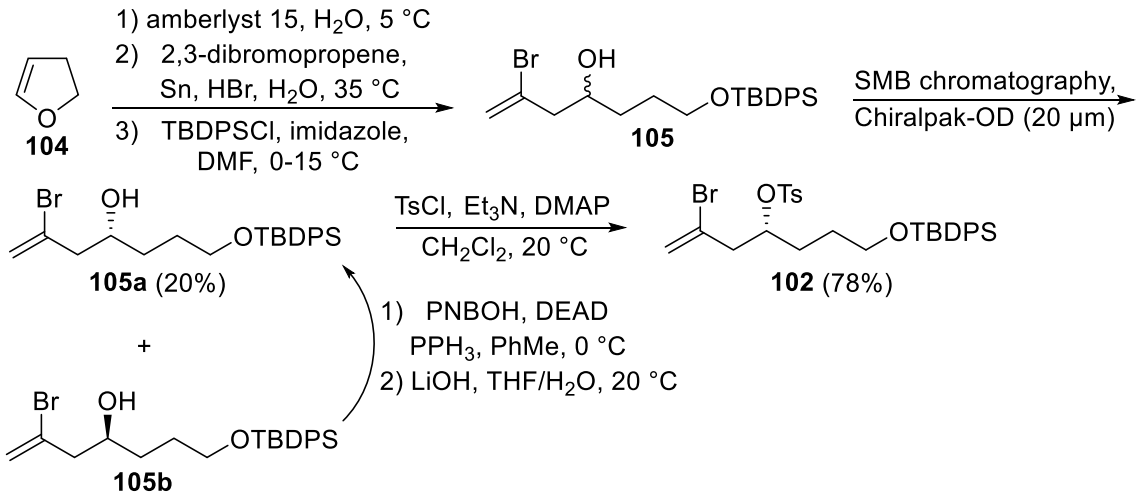

Scheme 2.8. Synthesis of the C14-C19 Fragment 102.

The synthesis of **103** is initiated with the addition of diethyl malonate **106** to the optically pure epoxide **107** (Scheme 2.9), previously synthesized via a Jacobsen hydrolytic kinetic resolution of the corresponding racemic oxirane.[65] Subsequent decarboxylation of the resulting lactone was followed by a diastereoselective methylation to provide the α-methyl lactone **109** (d.r. = 6:1) in 49% overall yield. Successive ring-opening and TBS-protection of **109** followed by oxidative cleavage delivered the C20-C26 fragment **103**. NHK coupling of intermediates **102** and **103**, and a subsequent silica-mediated cyclization, then provided the tetrahydrofuran **111** as a mixture of diastereoisomers (C20 d.r. = 8:1 and C25 d.r. = 6:1). The latter material **111** was then converted into the corresponding vinyl triflate through a 3-step sequence, after which, HPLC purification furnished the desired configurational isomer **112** (42% overall yield). Finally, a selective protection of the primary alcohol in **112**, and a subsequent mesylation achieved the process-scale synthesis of the C14-C26 building block **78**.[66]

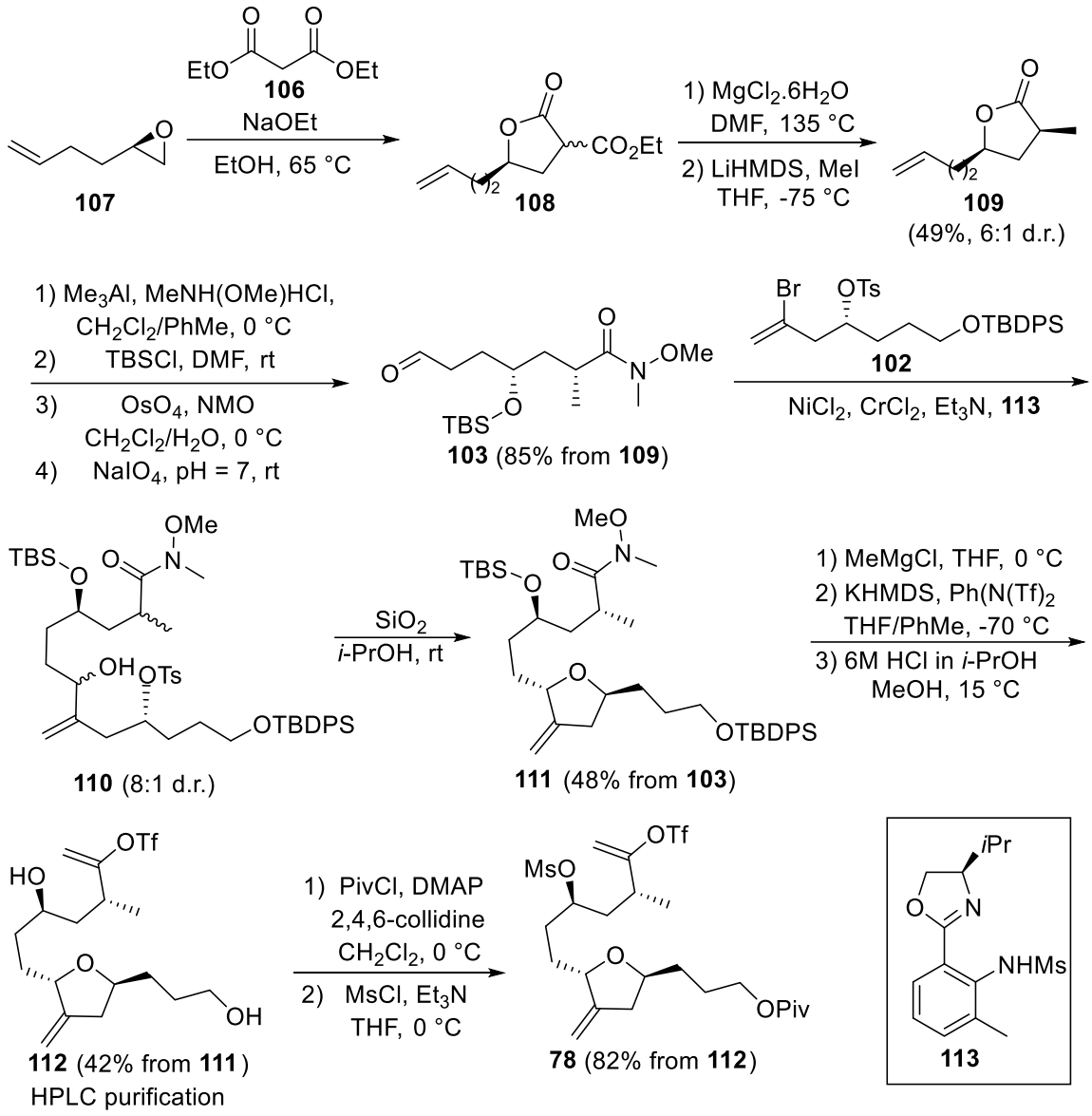

Scheme 2.9. Process-scale Synthesis of the C14-C26 Fragment 78.

To summarize, many improvements were made during the scale-up synthesis of eribulin and today the commercial route provides a viable supply of the drug. However, while the current process to access the C1-C13 fragment **74** is concise (13 steps) and efficient (Scheme 2.5), the route to the C14-C35 subunit **76** (Scheme 2.5, 2.8 and 2.9) still involves several challenges. Most notably, the industrial process accounts for a total of 44 synthetic steps and non-commercially available, stoichiometric chiral ligands (see **113**, Scheme 2.9) are required in key Nozaki-Hiyama-Kishi couplings. The route to access the

vinyl triflate **78** (Scheme 2.9) also suffers from a non-stereoselective step that leads to a mixture of configurational isomers (e.g., **105a** and **105b**, Scheme 2.8). Finally, in addition to several chromatography separations, the process scale of the C14-C35 fragment **76** includes two HPLC purifications.

2.1.3. Recent progress

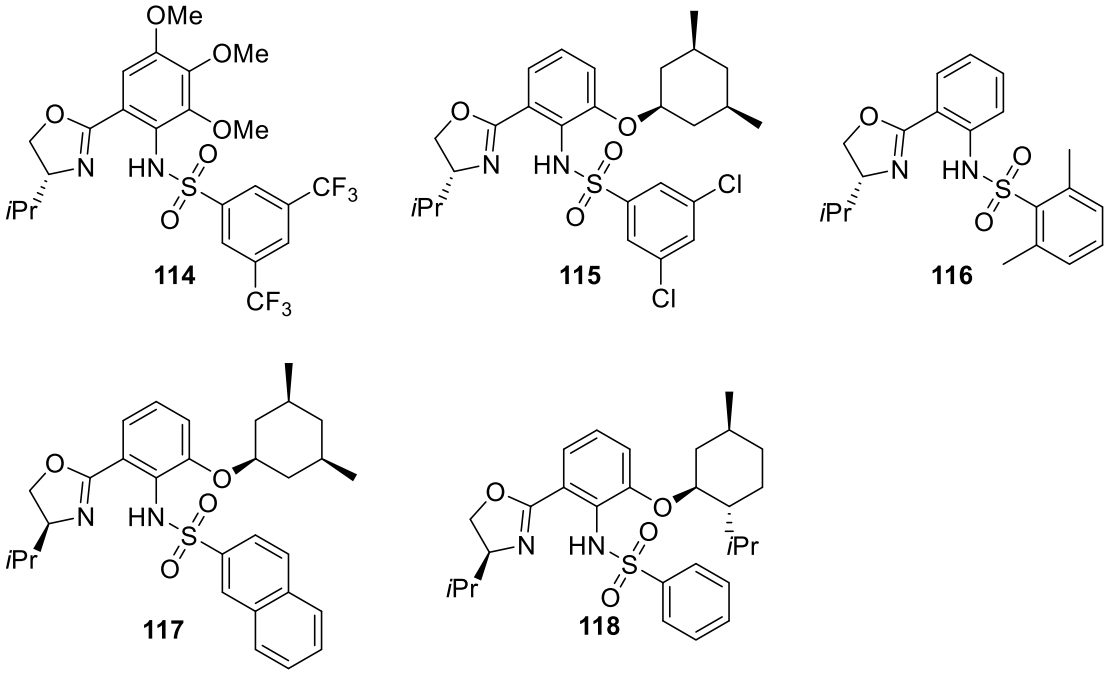

Figure 2.1. Ligands developed by the Kishi group for catalytic asymmetric Cr-mediated NHK couplings.

During the last decade, many efforts directed toward the synthesis of Eisai C14-C35 fragment of eribulin **76** have led to the development of further improved sequences. Most notably, Kishi's impressive work on catalytic asymmetric Cr-mediated coupling reactions resulted in the development of a "toolbox" of ligands (e.g., **114** to **118**, Figure 2.1) that was systematically applied to the various C–C bond-forming reactions in the synthesis of eribulin.[67–70] Moreover, as an alternative to the Williamson ether cyclization (e.g., KHMDS, Scheme 2.3), new methods to construct the tetrahydropyran in **76** were explored. In this regard, a silver-mediated approach provided the tetrahydropyran **120** in excellent yield and diastereoselectivity from the chlorohydrin derivative **119** (Scheme 2.10, 84% yield, >28:1 d.r.).[70] Importantly, the cyclization was found to follow a double inversion

mechanism that involves formation of an oxonium ion intermediate such as **121** (Scheme 2.10). Interestingly, this approach avoids the formation of the olefin side-product resulting from elimination of the mesylate observed in previous cyclizations using basic conditions (KHMDS or *t*BuOK).

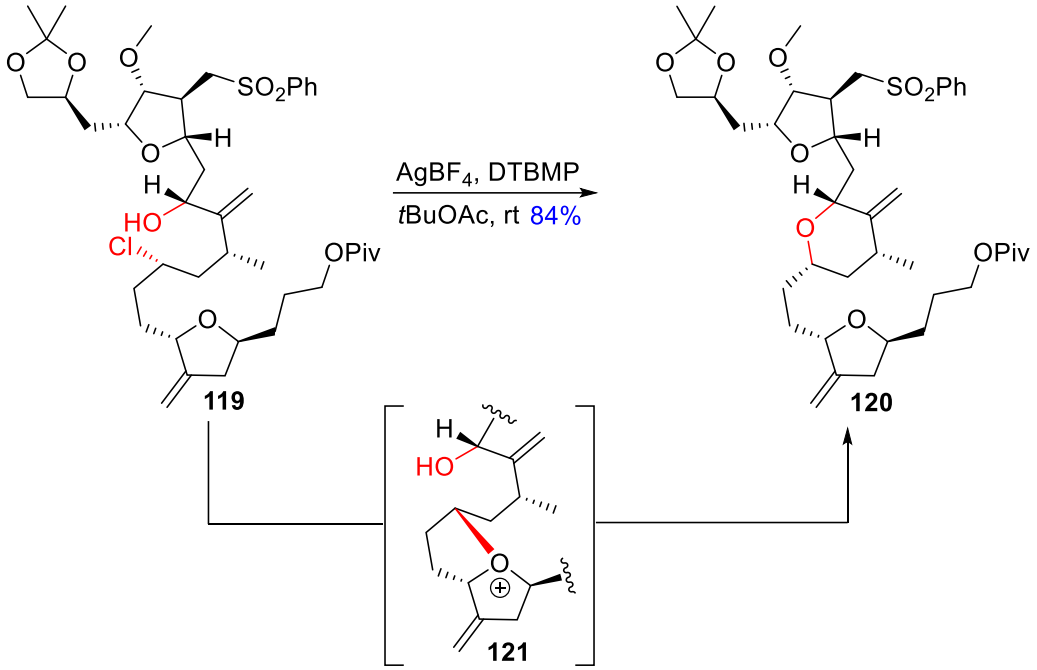

Scheme 2.10. Kishi Silver Acid-mediated Cyclization of Chlorohydrin 119.

In 2015, Eisai reported a crystallization-based route for the C14-C26 building block **78**. Unlike the previous syntheses of the C1-C13 and C27-C35 fragments that relied on cyclic carbohydrate templates, obtaining crystalline intermediates during the synthesis of the C14–C26 building block proved to be more challenging. Exploiting a rigid, bicyclic template, researchers at Eisai were able to correctly establish the non-contiguous stereogenic centres in **78** and develop a scalable route to the C14-C26 fragment.[71]

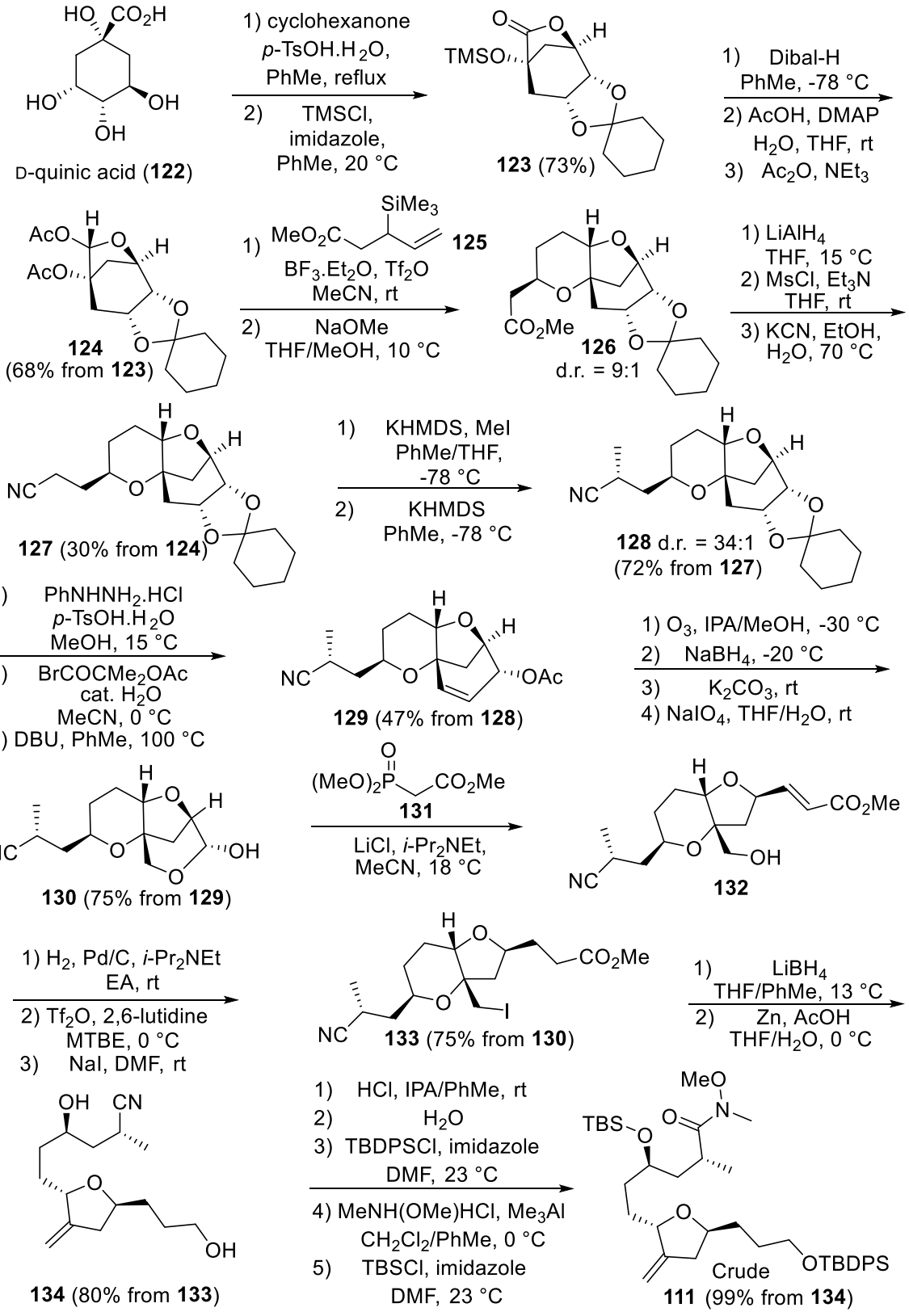

Scheme 2.11. Synthesis of Weinreb Amide 111 from D-Quinic acid.

As depicted in Scheme 2.11, the reaction of D-quinic acid (**122**) with cyclohexanone *p*-TsOH and a subsequent silylation furnished the protected bicyclic lactone **123** in 73% yield. Diisobutylaluminum hydride reduction of the ester moiety in **123** was then followed by a one-pot TMS removal/*bis*-acetate protection to provide crystalline ether **124** in 65% yield. Lewis acid-mediated C-glycosylation of **124** with allyl silane **125** and acetate deprotection resulted in the formation of tricyclic compound **126** (d.r. = 9:1 at C23). Ester **126** was then converted into the nitrile derivative **127** upon successive LAH reduction, mesylation and nucleophilic substitution with cyanide. After recrystallization, the nitrile **127** was obtained in high stereochemical purity with regard to the C23 stereogenic centre (d.r. > 100:1). Alkylation of **127** with KHMDS and methyl iodide followed by treatment of the resulting mixture with catalytic amounts of KHMDS, produced the desired configurational isomer **128** in excellent diastereoselectivity (d.r. = 34:1). The diol, resulting from hydrolysis of the ketal function in **128**, was further transformed into the corresponding bromoacetate (not depicted). Dehydrobromination then provided the crystalline allylic acetate **129** in 45% yield over 3 steps. Ozonolysis of the cyclohexene ring in **129** followed by reductive work-up and acetate removal, produced a triol that upon treatment with $NaIO_4$ afforded the cyclic hemiacetal **130**. Horner–Wadsworth–Emmons (HWE) reaction of **130** with phosphonate **131** under Masamune–Roush conditions[72] then provided the olefin **132** that can be further elaborated into the iodoester **133** through a 3-step sequence. Reduction of the ester in **133** and a zinc-induced Vasella fragmentation[73] smoothly delivered the correctly configured tetrahydrofuran **134**. Compound **134** was then converted into the known Weinreb intermediate **111** in a highly efficient 5-step sequence (99% yield from **134**).

2.1.4. General synthetic strategy to Eisai fragment

2.1.4.1. Late-stage Corey-Chaykovsky reaction

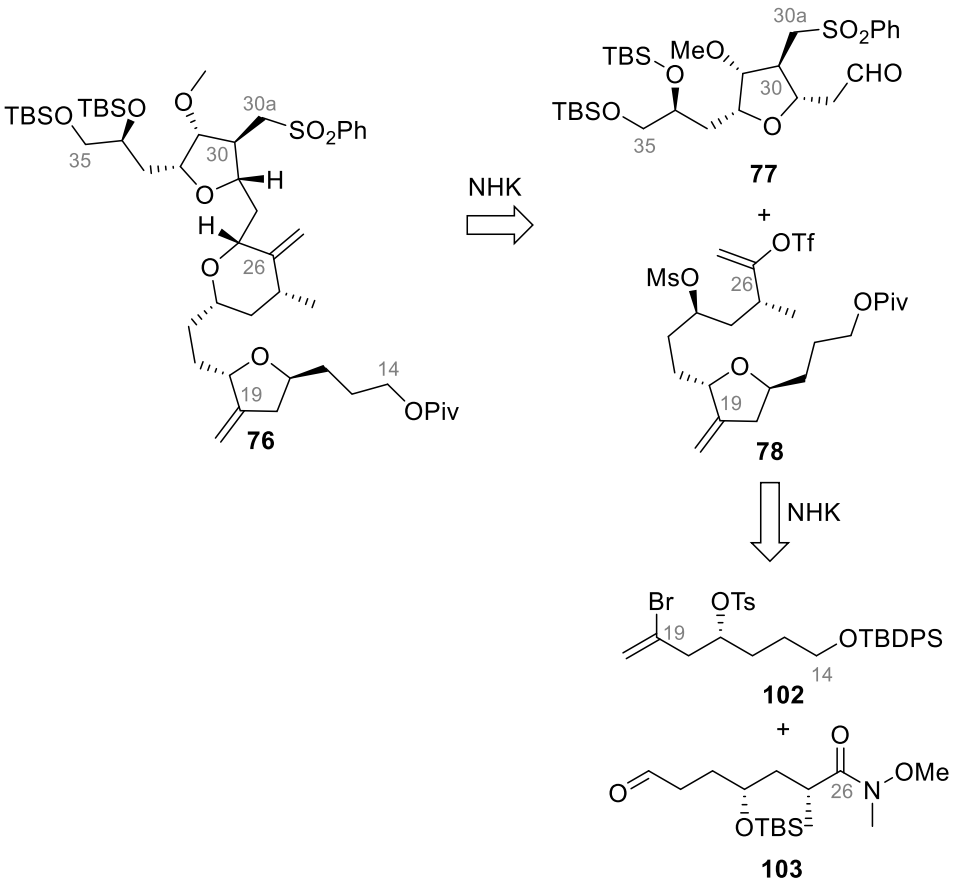

Scheme 2.12. Eisai's Retrosynthesis of the C14-C35 Fragment 76.

As shown in Scheme 2.12, the Eisai process-scale synthesis of the C14-C35 building block **76** involves several Nozaki-Hiyama-Kishi (NHK) couplings. Despite being highly convergent, this approach accounts for a total of 43 synthetic steps. As a result, many academic and industry groups are currently working on improved or alternative syntheses of the C14-C35 fragment **76**.

As shown in Scheme 2.13, we envisioned that a late-stage Corey-Chaykovsky reaction between a sulfur ylide derived from sulfonium salt **136** and a ketone **137**, could provide a potential precursor **135** for the C14-C35 fragment **76**.

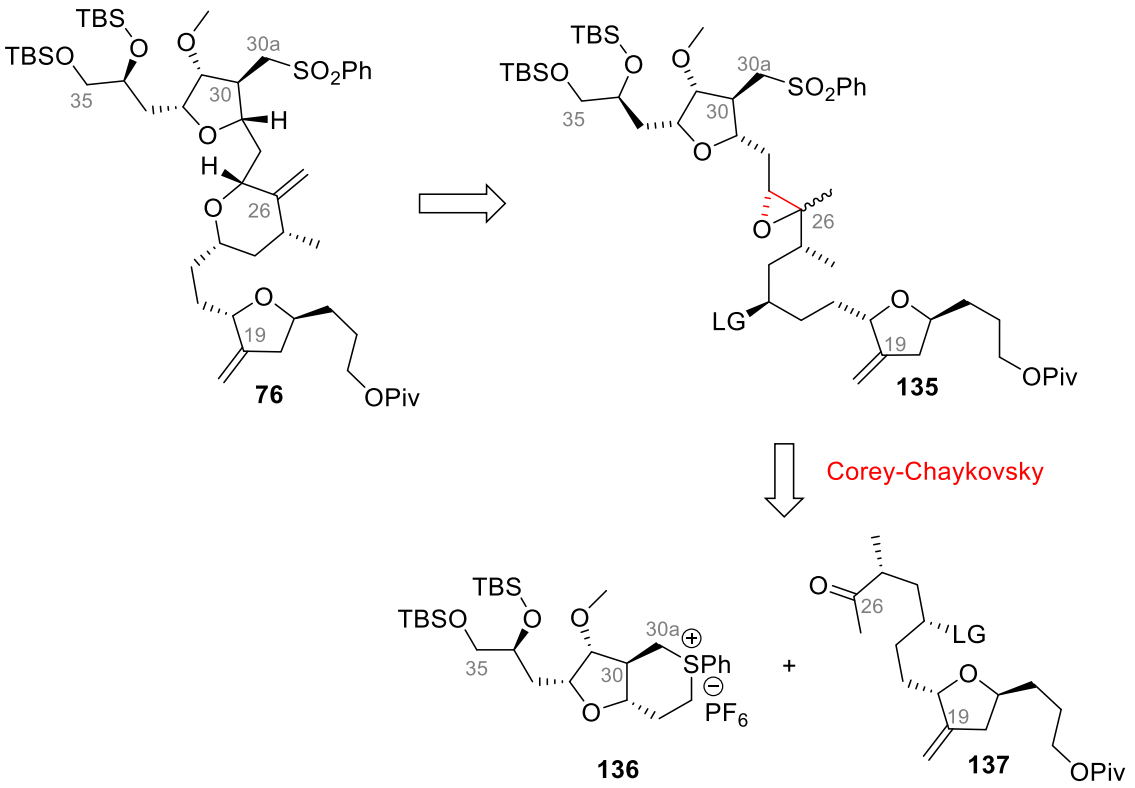

Scheme 2.13. Retrosynthesis of Eisai C14-C35 Fragment 76.

In fact, we anticipated that the tetrahydropyran motif in **76** could result from the isomerization of the epoxide function in **135** and a subsequent cyclization. The execution of this new synthetic strategy toward Eisai C14-C35 fragment of eribulin is described later in this chapter (section 2.4). Below are two sections that provide background about the key Corey-Chaykovsky reaction and the use of α-chloroaldehydes in stereoselective synthesis of polyketides.

2.1.4.2. The Corey-Chaykovsky reaction

The Corey-Chaykovsky reaction, sometimes referred to as the Johnson-Corey-Chaykovsky, was first reported in 1961 by Johnson but, then, significantly improved by Corey and Chaykovsky.[74,75] As shown in Scheme 2.14, the reaction is initiated by the addition of a sulfur ylide **138** to a ketone or an aldehyde **139**. Subsequent expulsion of the sulfonium cation, promoted by an intramolecular attack of the newly formed negative charge, releases the corresponding oxirane **141**.

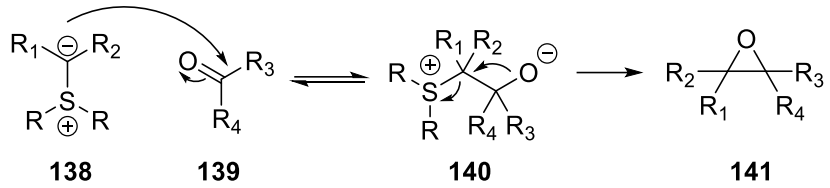

Scheme 2.14. Mechanism of the Corey-Chaykovsky Reaction.

While the reaction scope has been extended to the synthesis of cyclopentanes and aziridines,[76] the Corey-Chaykovsky has often been used as an alternative to the more conventional peroxide-epoxidation methods, to access oxirane derivatives. The Corey-Chaykovsky reaction has also been exploited in several total syntheses. Most notably, the ylide resulting from deprotonation of trimethylsulfonium iodide was used by Danishefsky in the total synthesis of the widely used antimitotic agent Taxol (**144**) (Scheme 2.15).[77]

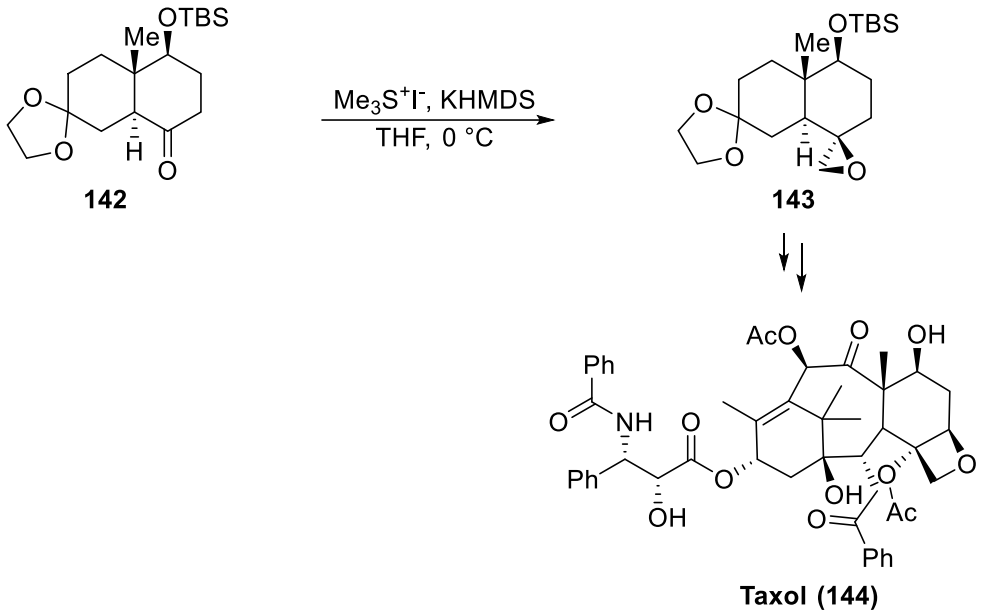

Scheme 2.15. Corey-Chaykovsky Reaction in Danishefsky's Taxol Total Synthesis.

While rare, a few enantioselective variations of this reaction have been developed that rely on the use of expensive chiral thiol derivatives. The most successful reagents are shown below. In both cases, the enantioselectivity results from steric interactions that control the approach of the carbonyl or the facial selectivity of the ylide (see **145** and **147**, Scheme 2.16).[76,78]

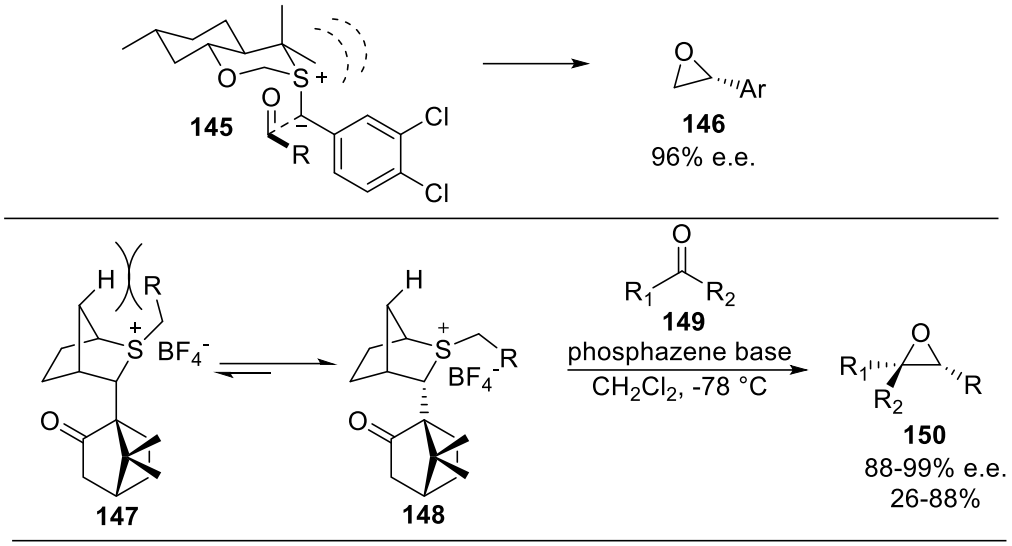

Scheme 2.16. Enantioselective Corey-Chaykovsky Reactions.

In 2002, the reactivity of 5- and 6-membered ring sulfonium ylides toward aldehydes and ketones was studied extensively in the Yamamoto group.[79] For example, they reported that deprotonation of a six-membered ring sulfonium salt **151** with sodium *bis*(trimethylsilyl)amide and a subsequent nucleophilic attack on a series of aldehydes and ketones afforded the corresponding oxirane derivatives in excellent yields (entries 1-4, Table 2.1).

Table 2.1. Reported Corey-Chaykovsky using Cyclic Sulfonium Salt 151.

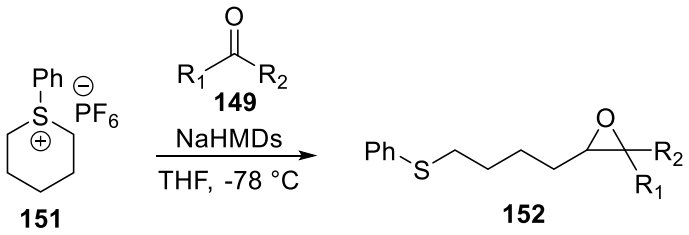

entry	R_1	R_2	yield[a]
1	Ph	H	96%[b]
2	Ph	Me	96%[c]
3	*n*-Pr	H	97%[c]
4	Me	Me	95%[c]

[a] As mixtures of cis:trans isomers. [b] cis:trans = 4:6. [c] cis:trans ratio not determined.

2.1.4.3. Enantiopure α-chloroaldehydes to access optically enriched, multifunctional building blocks

Over the past two decades, α-chloroaldehydes have been increasingly exploited as building blocks for the synthesis of stereochemically rich heterocycles. Importantly, their bifunctional nature, availability from feedstock chemicals and inherent chirality have made them ideal starting materials for stereoselective syntheses.[80] In the following section, common methods to synthesize optically pure α-chloroaldehydes will be summarized and the use of α-chloroaldehydes in natural product synthesis will be demonstrated.

Enantioselective methods to access α-chloroaldehydes

In 1871, Schröder reported the first preparation of an α-chloroaldehyde. Here, upon treatment of 3-methylbutanal with chlorine gas, a racemic mixture of the corresponding α-chloroaldehyde was formed (Scheme 2.17).[81]

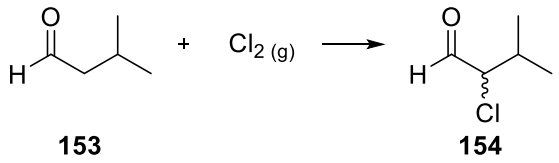

Scheme 2.17. First Synthesis of an α-Chloroaldehyde by Schroder.

It was not until 1992 that the first synthesis of a highly optically enriched α-chloroaldehyde was described. At this time, Martin and Palazon were particularly

interested in the synthesis of marine natural compounds containing halo-substituted tetrahydropyrans. During this investigation, an enantiomerically enriched epoxide **155** was converted into the corresponding chlorohydrin **156**. A subsequent reaction with sodium periodate provided a highly enantioenriched α-chloroaldehyde **157** (Scheme 2.18).[82]

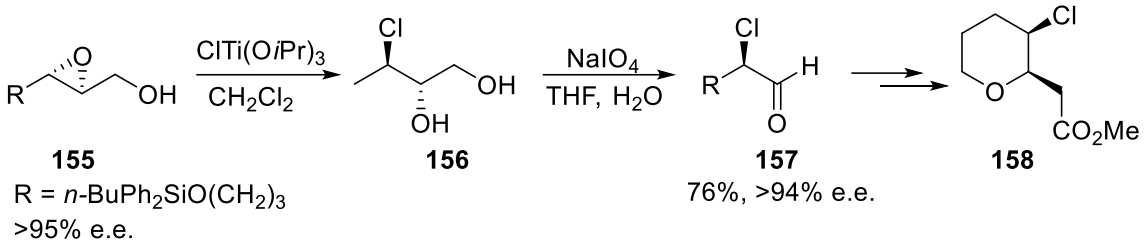

155 **156** **157** **158**

R = *n*-$BuPh_2SiO(CH_2)_3$

>95% e.e.

76%, >94% e.e.

Scheme 2.18. First Synthesis of a Highly Optically Enriched α-Chloroaldehyde.

The first example of direct organocatalytic enantioselective α-chlorination of aldehydes was reported by McMillan in 2004.[83] In this work, a series of aldehydes **159** were treated with Lectka's quinone **160** and imidazolidinone **161** (Scheme 2.19). The enantioselective step was proposed to involve a Zimmerman-Traxler type transition state **162**, resulting from a carbonyl-proton association and a concomitant chlorine activation between an enamine nucleophile and an electrophilic chlorine source (Scheme 2.19). Using this process, the corresponding α-chloroaldehydes **163** were obtained in excellent yields and enantiopurities (71-94%, 80-95% e.e.). Moreover, the reaction was compatible with a variety of functional groups and substrates with an alkene, an ester, or an acetal were smoothly converted to the corresponding α-chloroaldehydes.

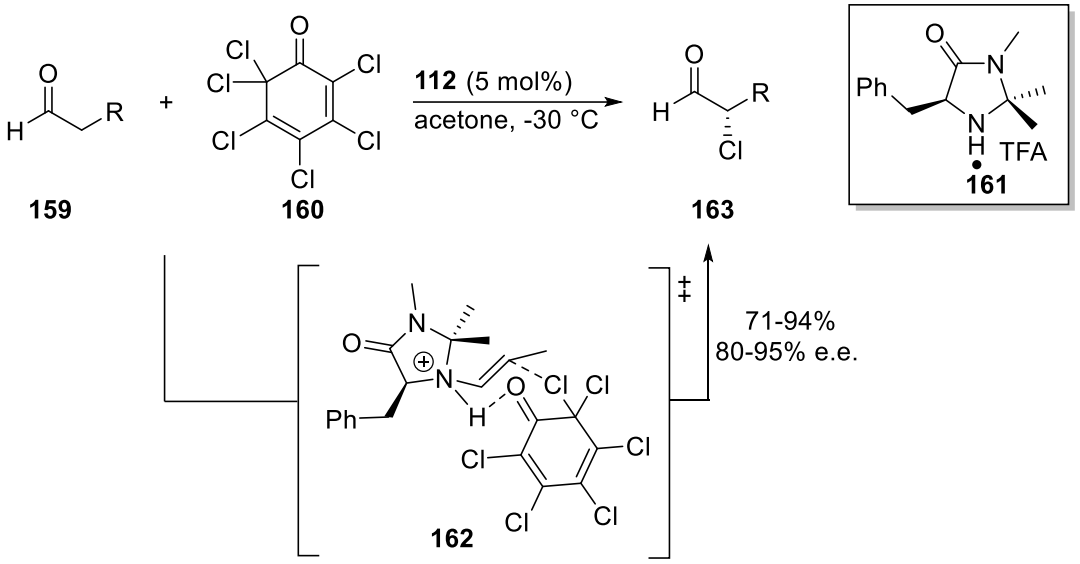

Scheme 2.19. Seminal Work of MacMillan on Organocatalytic Enantioselective α-Chlorination of Aldehydes.

In the same year, Jørgensen reported the use of several distinct chiral amine catalysts for the direct α-chlorination of 3-methylbutanal.[84] Notably, the two pyrrolidines **164** and **165** (Scheme 2.20), in the presence of *N*-chlorosuccinimide (NCS), provided the corresponding α-chloroaldehydes **163** in high yield and enantioselectivity. In the case of L-prolinamide **164**, hydrogen-bonding interactions between the amide protons and the carbonyl of the incoming chlorine source direct the electrophile's approach toward the *Re*-face of the enamine nucleophile (see **166**, Scheme 2.20). As for 2,5-diphenylpyrrolidine **165**, experimental and computational studies suggested that the electrophilic chlorine atom of NCS was first trapped by the nucleophilic enamine nitrogen atom (see **167**, Scheme 2.20). Subsequent iminium ion formation, prior to hydrolysis, was thought to occur via an intramolecular 1,3-sigmatropic shift. In total, 8 aldehydes were subjected to Jørgensen's α-chlorination procedure using both catalysts **164** and **165**. The corresponding α-chloroaldehydes **163** were delivered in good yields and enantioselectivity (Scheme 2.20).

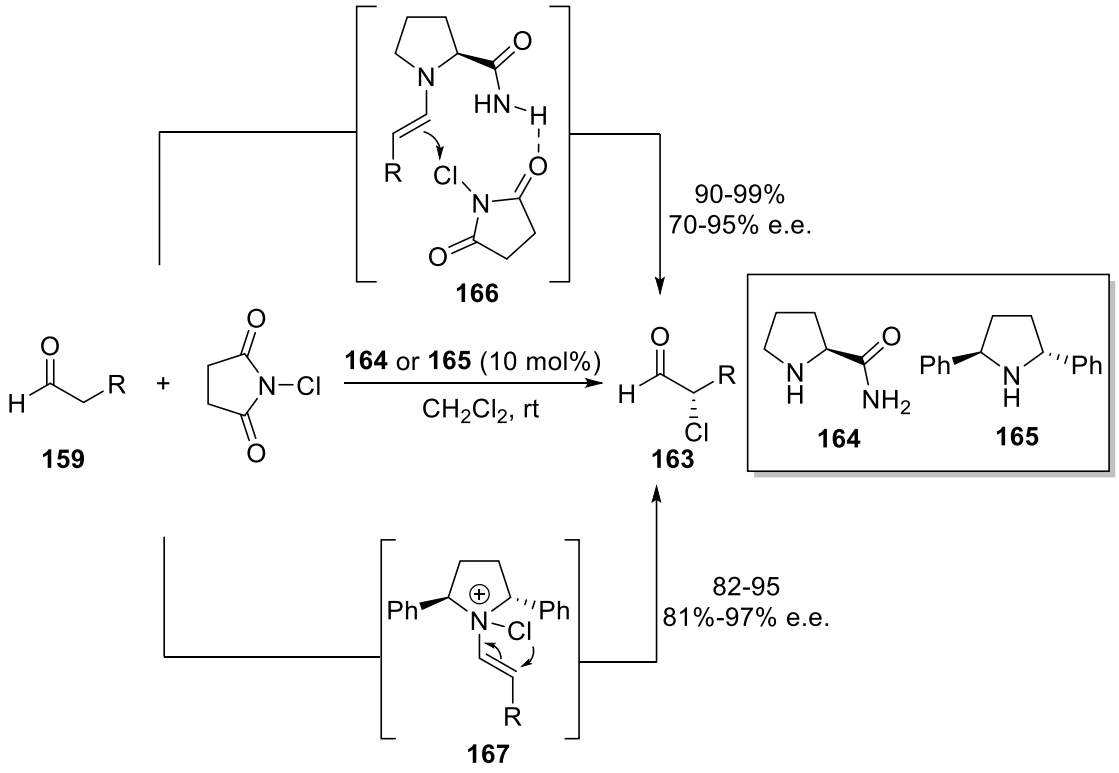

Scheme 2.20. Jørgensen Direct Organocatalytic Enantioselective α-Chlorination of Aldehydes Catalyzed by Pyrrolidines164 and 165.

A few years later, a new mechanistic approach for the direct α-chlorination of aldehydes was reported by the MacMillan group.[85] Here, an iminium ion is activated to a singly occupied molecular orbital (SOMO) state by the action of an oxidant. The radical **168** (Scheme 2.21), which projects the 3π-electron system away from the bulky *tert*-butyl group, is then trapped by a chlorine nucleophile. As shown in Scheme 2.21, a series of aldehydes were subjected to the MacMillan SOMO-catalysis reaction conditions and provided the corresponding α-chloroaldehydes **163** in high yields and optical purity (75-95%, 91-96% e.e.). Interestingly, the resulting α-chloroaldehydes were further converted into epoxides **170** upon successive treatment with sodium borohydride and potassium hydroxide (Scheme 2.21).

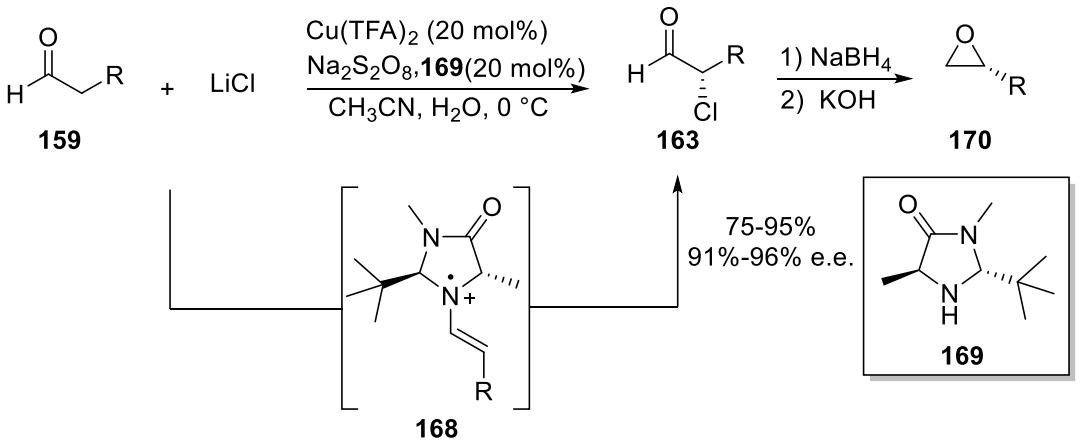

Scheme 2.21. MacMillan SOMO-catalyzed α-Chlorination of Aldehydes.

α-Chloroaldehydes in natural product synthesis

One of the most powerful carbon-carbon bond-forming strategies in the synthesis of natural products is the 1,2-addition of nucleophiles to aldehydes. Interestingly, in the context of 1,2-nucleophilic additions to α-chloroaldehydes **170**, the *anti*-chlorohydrin **174** is selectively formed over the *syn*-product **173**. Both the Felkin-Anh and Cornforth models have been used to rationalize this stereochemical outcome.[86,87] However, Evan's study on the addition of enolborane nucleophiles to chiral heteroatom-substituted aldehydes revealed that the relative energy of the transition-state structures in each model depends on the nature of the heteroatom substituent.[88] Most notably, electronegative substituents (F, OMe, Cl) were shown to favour Cornforth structures and thus, the Cornforth model has become the generally accepted model to rationalize the 1,2-asymmetric induction in additions to α-chloroaldehydes. Here, the need for a sufficient overlap between the highest occupied molecular orbital (HOMO) of the nucleophile and the lowest unoccupied molecular orbital (LUMO) of the carbonyl bond, sets the approach of the nucleophile at the Bürgi-Dunitz trajectory (105° ± 5°).[89] Moreover, in the transition state, electrostatic dipole effects are minimized and, consequently, the C-Cl bond and adjacent carbonyl group are aligned in an opposite orientation (see **171** and **172**, Scheme 2.22). As a result, the approach along the Burgi-Dunitz angle shown in transition state **171** (Scheme 2.22) is disfavoured due to steric hindrance (see)(in **171**) and, thus, **174** is formed predominantly.

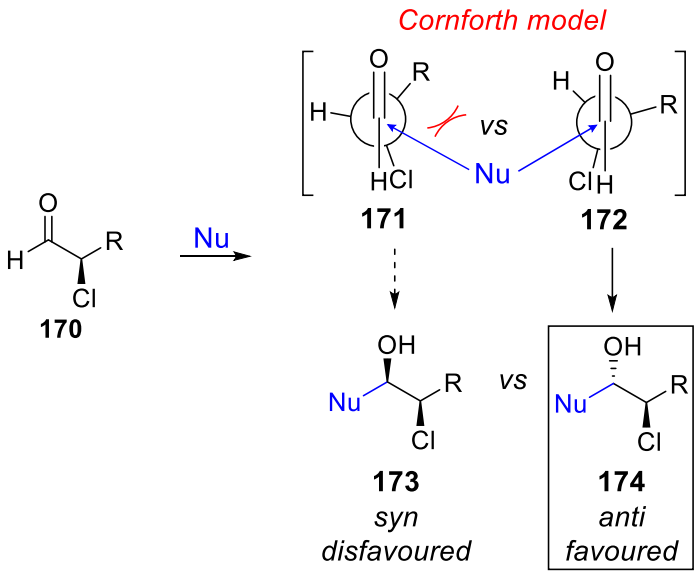

Scheme 2.22. The Cornforth Model to Rationalize the Selectivity of the 1,2-Nucleophilic Addition to α-Chloroaldehydes.

Numerous stereoselective transformations starting from α-chloroaldehydes have been developed and used in the synthesis of natural products.[80] [80] For example, Christmann exploited the organocatalyst used in MacMillan's linchpin protocol (see **169**, Scheme 2.21) for the *in situ* conversion of aldehydes into enantioenriched terminal epoxides. Notably, this methodology was used in the total synthesis of (-)-*cis*-aerangis lactone, a pleasant fragrance.[90] As depicted in Scheme 2.22, α-chlorination of (+)-citronellal **175** and subsequent treatment with sodium borohydride and potassium hydroxide, provides the terminal epoxide **176** in good yield and excellent diastereoselectivity (>99:1 d.r.). Copper(I)-catalyzed nucleophilic epoxide opening of **176** with *n*-butyllithium affords the alcohol **177** in 72% yield. A subsequent ozonolysis delivers a lactol intermediate which is readily oxidized to provide the fragrant natural product **178**.

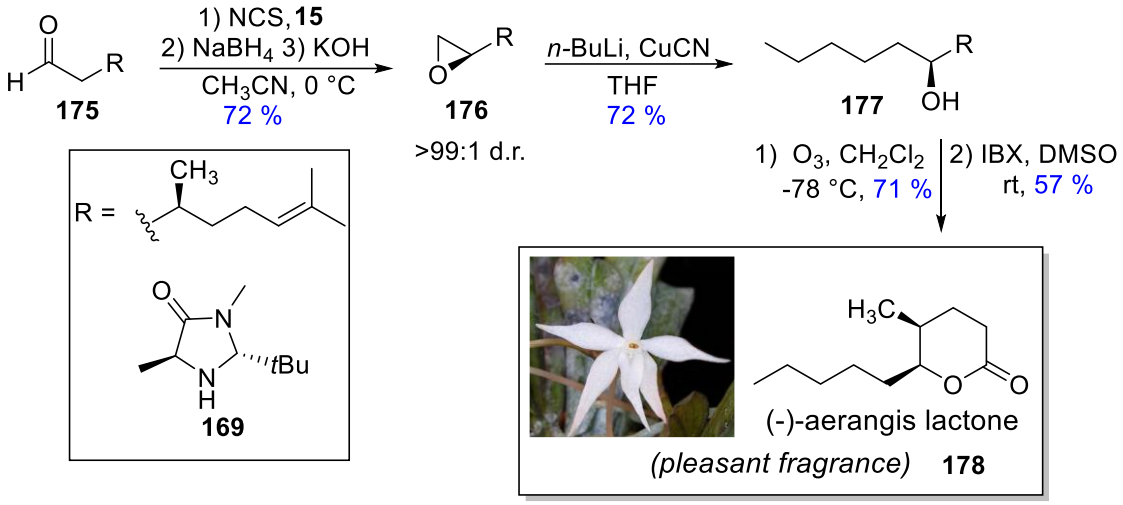

Scheme 2.23. Total Synthesis of (-)-Aerangis Lactone (178) via Reduction and Cyclization of an *in situ* Formed α-Chloroaldehyde.

The Britton group has also developed several strategies to transform enantioenriched α-chloroaldehydes into 2,5-disubstituted tetrahydrofuranols, a common scaffold in natural products.[91] Here, a 6-step synthesis of the anthelmintic oxylipid **133** (Scheme 2.24) was developed.[92] This synthesis initiates with the 1,2-nucleophilic addition of the enolate derived from carbonyl **180** to the α-chloroaldehyde **179** to provide the anti-aldol adduct **181** in excellent diastereoselectivity. Subsequent stereocontrolled reduction of compound **181** and cyclization furnishes the tetrahydrofuranol **182** (10:1 d.r.). Ozonolysis of the olefin function in **182** and Grignard addition completed the stereoselective synthesis of oxylipid **183**.

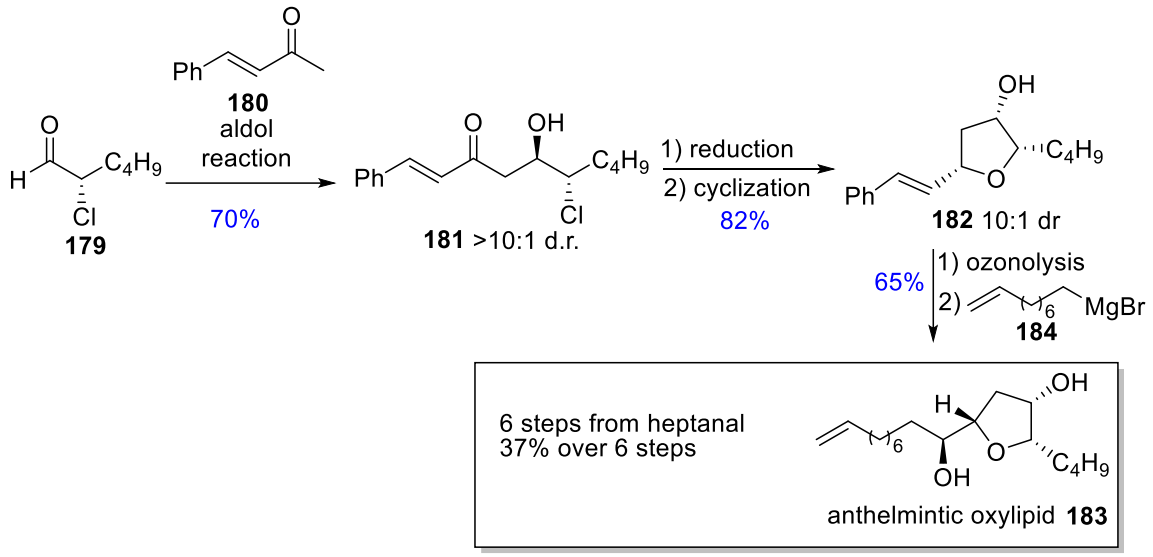

Scheme 2.24. Rapid Access to Anthelmintic 183 via an Asymmetric Aldol Reaction with α-Chloroaldehyde 179.

2.2. Synthesis of the C14-C26 fragment of eribulin

As depicted in Scheme 2.13 (section 2.1.4), our retrosynthetic strategy relies on the synthesis of two key building blocks: the C14-C26 fragment **137** and the C27-C35 fragment **136**. In this section, the various synthetic approaches explored during the preparation of ketone **137** will be described. It is noteworthy that enantiopurity and absolute stereochemistry of the various compounds synthesized during this work were not determined (unless indicated). As a result, compounds were carried out throughout the different sequences investigated assuming the stereogenic centres were set as anticipated by the chemistry used and formation of products was confirmed by ^{1}H NMR spectroscopy and mass spectrometric analysis. Ultimately, these findings led to the development of a viable route in which all compounds were fully characterized.

2.2.1. Construction of the THF ring

2.2.1.1. Gold-catalyzed synthesis of dihydrofuran-3-one from homo-propargylic alkynes

Our first approach to the C14-C26 fragment **137** relied on a gold-catalyzed oxidation of propargylic alkynes into dihydrofuran-3-ones.[93] As depicted in Scheme 2.25,

this method involves the formation of a reactive α-oxo gold carbene **187** generated from the 1,2-addition of a pyridine *N*-oxide **184** to a propargylic alcohol **185**. Subsequent intramolecular O-H insertion into the gold carbene moiety in **187** and hydrolysis generates dihydrofuran-3-one **188**.

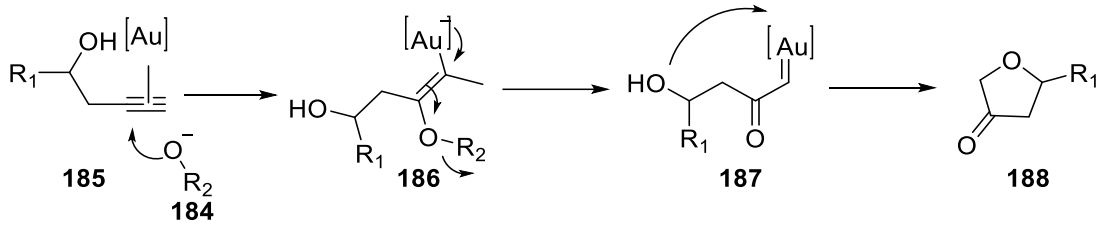

Scheme 2.25. Proposed Mechanism for the Gold-catalyzed Transformation of Propargylic Alcohols 185 into Dihydrofuranones 188.

As detailed in Scheme 2.26, retrosynthetic disconnection of the indicated bond in the C14-C26 fragment **137** provides the epoxide **189** as a potential precursor. In the synthetic direction, nucleophilic epoxide-opening of **189** could achieve the formation of the C25-C24 bond. A few straightforward functional group modifications would then complete the assembly of **137**. Cleavage of the indicated bond in **189** would then lead to the dihydrofuranone **190** and the tosylate **191** as potential precursors. Synthetically, reaction of an enolate derived from **190** with **191** could achieve the formation of the C20-C21 bond. A Wittig olefination reaction would then complete the assembly of **189**. The dihydrofuranone **190** could be elaborated through a gold-catalyzed oxidation (Scheme 2.25) of a homo-propargylic alcohol **192** that, in turn, could result from a ring-opening reaction of an optically pure epoxide **193**. We envisioned that the epoxide precursors **193** and **191** could be easily traced back to α-chloroaldehydes such as **194** and **195**.

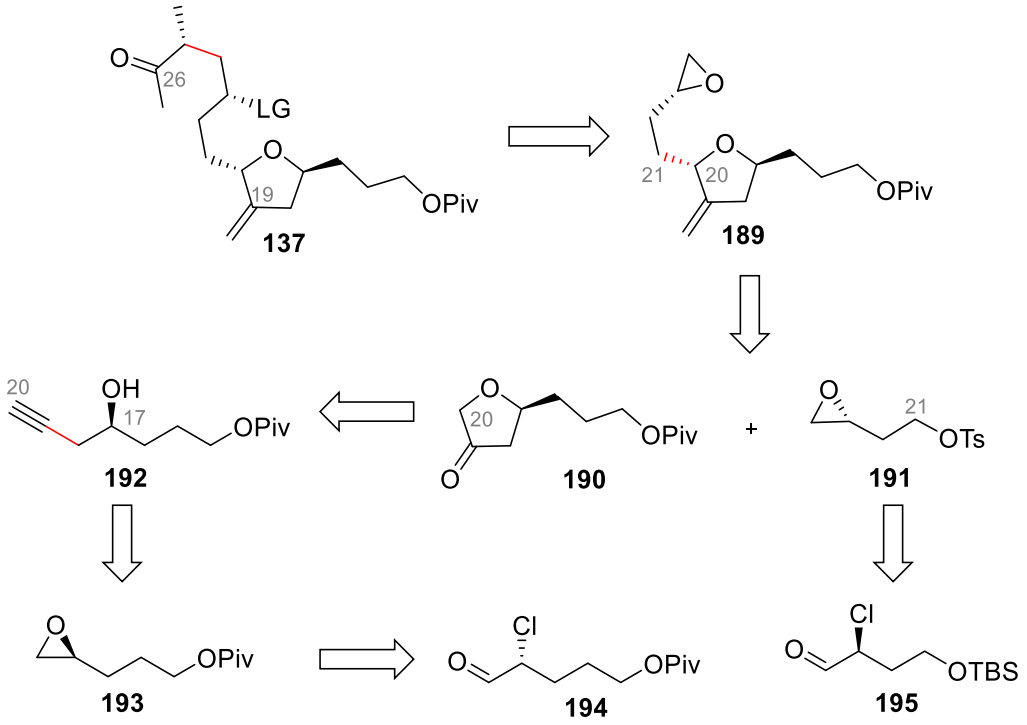

Scheme 2.26. Retrosynthetic Analysis of the C14-C26 Fragment 137.

Following this strategy, a concise and stereoselective synthesis of dihydrofuran-3-one **190** (Scheme 2.26) was developed. As described in Scheme 2.27, the synthesis of **190** initiated with the mono protection of 1,5-pentanediol **196** using pivaloyl chloride followed by a pyridinium chlorochromate (PCC) oxidation to produce the aldehyde **198** in 63% yield. α-Chlorination of **198** using Jørgensen's prolinamide reaction conditions[94] and subsequent treatment with sodium borohydride, resulted in the production of the α-chloroalcohol **199** in 70% yield. The latter material was then smoothly converted to the corresponding epoxide **193** upon reaction with sodium hydroxide in a mixture of tetrahydrofuran and water at 45 °C. Nucleophilic epoxide-opening of compound **193** with lithium (trimethylsilyl)acetylide **200** followed by treatment with potassium carbonate, then furnished the homo-propargylic alcohol **192** in 75% overall yield. Gratifyingly, the proposed gold-catalyzed oxidation methodology successfully transformed the alcohol **192** into the corresponding dihydrofuran-3-one **190**.

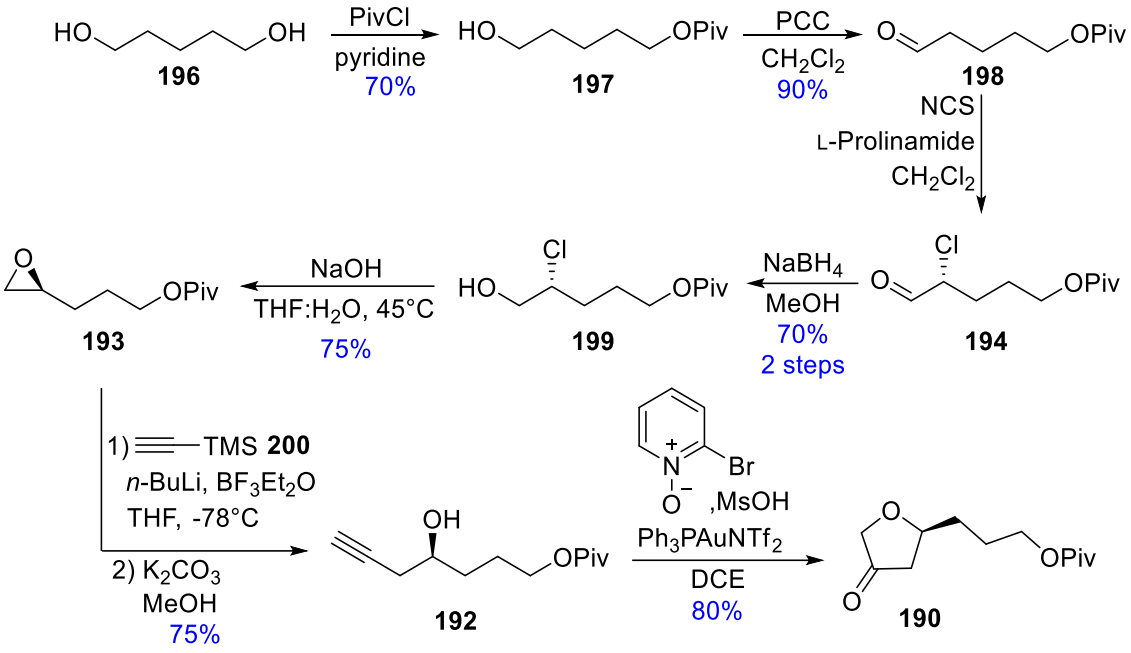

Scheme 2.27. Synthesis of Dihydrofuran-3-one 190.

In turn, synthetic studies toward the tosylate precursor **191** are summarized in Scheme 2.28. Ring-opening of the commercially available γ-butyrolactone **201** with *N*,*O*-dimethylhydroxylamine and dimethylaluminum chloride followed by TBS-protection of the resulting alcohol, furnished the Weinreb amide[95] **202** in 92% yield. The latter material was then reduced to the corresponding aldehyde **203** using lithium aluminum hydride. Subsequent α-chlorination with *N*-chlorosuccinimide and D-prolinamide afforded the enantioenriched α-chloroaldehyde **195** (not depicted), which was reduced to the corresponding alcohol **204** in 70% yield from **203**. Cyclization of chlorohydrin **204** was then successfully conducted using NaOH in THF and water (Scheme 2.28).

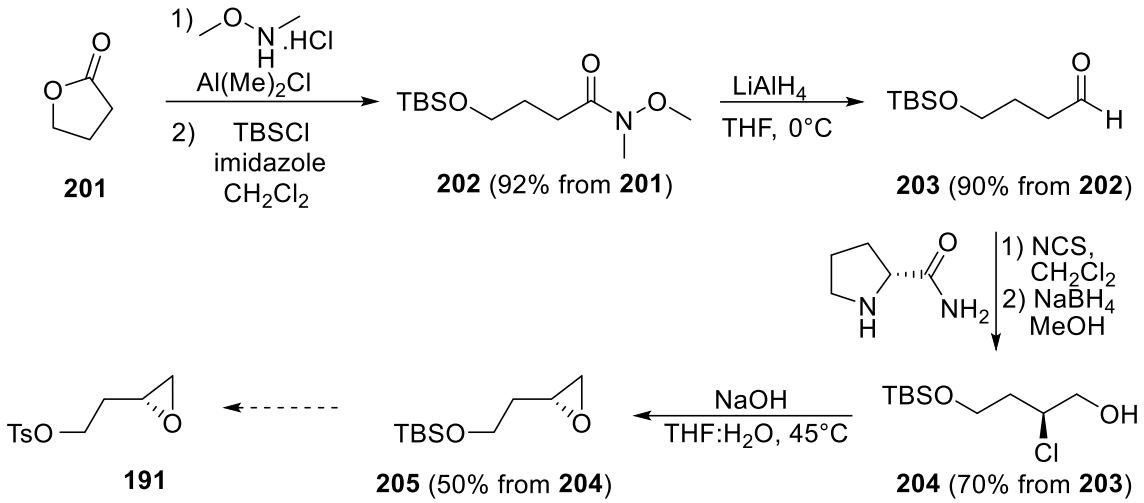

Scheme 2.28. Synthetic Studies Toward the Synthesis of Epoxide 191.

In parallel, the synthetic feasibility of the envisioned α-alkylation reaction was assessed (Scheme 2.29). Here, commercially available 4-bromobut-1-ene **206** was selected as a model alkylating agent.

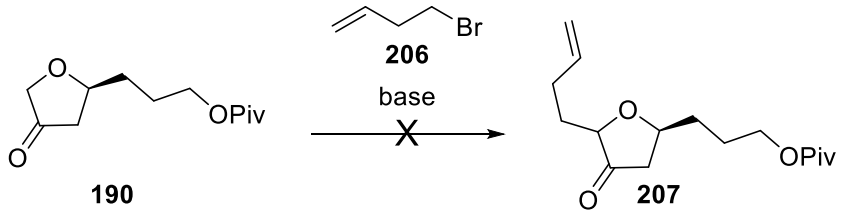

Scheme 2.29. Alkylation of Dihydrofuran-3-one 190 with 4-Bromobut-1-ene 206.

Following conditions used in the few reported alkylations of dihydrofuran-3-ones, treatment of **190** with a strong base such as lithium diisopropylamide (LDA) or lithium *bis*(trimethylsilyl)amide (LiHMDS) followed by addition of the alkyl bromide **206** failed to furnish any desired product **207**. Investigation of solvent, base and reaction temperature failed to improve upon this result and it became clear that we would need a new synthetic strategy to access the ketone **137** (Scheme 2.26). Thus, while a concise and stereoselective synthesis of dihydrofuran-3-one **190** was developed, our failure to alkylate this material precluded access to the targeted 2,5-disubstitutedtetrahydrofuran scaffold **190**. Following this disappointment, the feasibility of each key step was assessed as early as possible using model substrates.

2.2.1.2. Britton group enantioselective synthesis of 2,5-disubstituted-3-hydroxytetrahydrofurans

The Britton group methodology provides a concise and general approach to each configurational isomer of 2,5-disubstituted-3-hydroxytetrahydrofurans.[91] As detailed in Scheme 2.30, this process relies on the diastereoselective aldol reaction of an enolate derived from **208** with an α-chloroaldehyde **209**. The resulting chlorohydrin **210** is then subjected to a *syn*- or an *anti*-reduction depending on which configurational isomer is desired (e.g., **211** and **212**, Scheme 2.30). Direct cyclization, or a two-step chlorine displacement/epoxide opening sequence, can then lead to either one of the 2,5-disubstituted-3-hydroxytetrahydrofuran stereoisomers (e.g., **213**, **214**, **215** and **216**, Scheme 2.30). Consequently, this method could provide a concise and stereoselective approach toward the tetrahydrofuran ring in the C14-C26 fragment **137**.

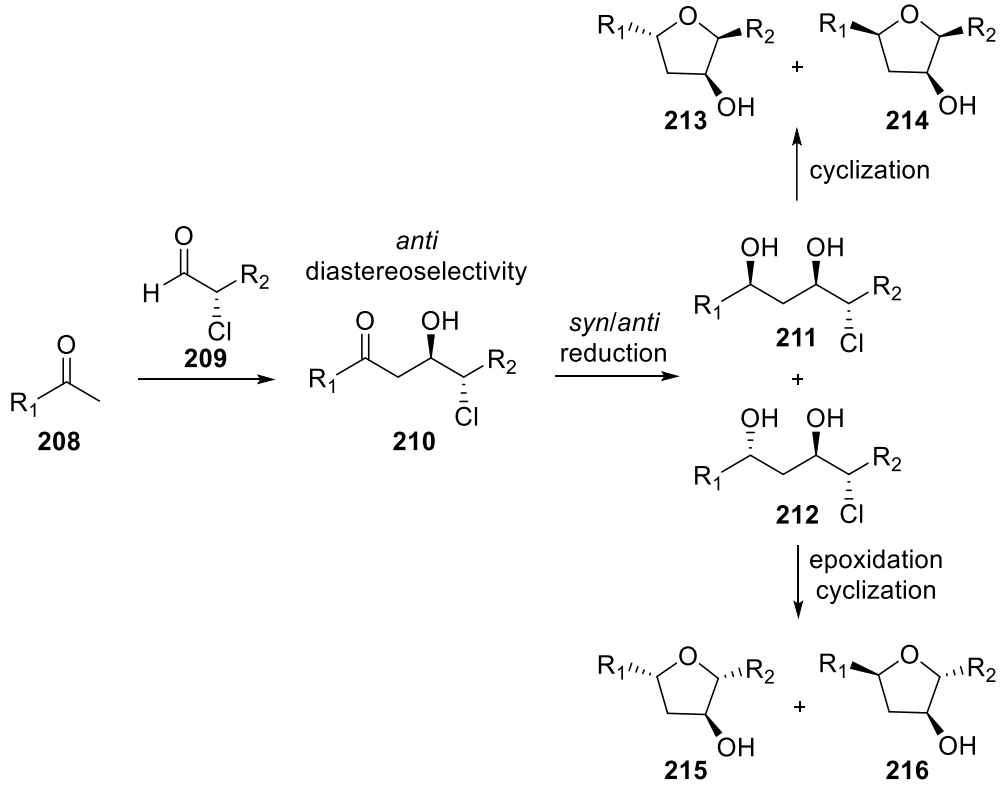

Scheme 2.30. Stereoselective Synthesis of 2,5-Disubstituted-3-hydroxytetrahydrofurans.

As a result, we envisioned that target **189** could be derived from a tetrahydrofuranol precursor such as **217** through straightforward functional group

modifications (Scheme 2.31). Stereoselective reduction of a ketone **218** followed by a 1,5-chlorine displacement could then deliver the tetrahydrofuranol **217**. In turn, reaction of a lithium enolate derived from **219** with aldehyde **220** could achieve the formation of the C18-C19 bond in ketone **218**.

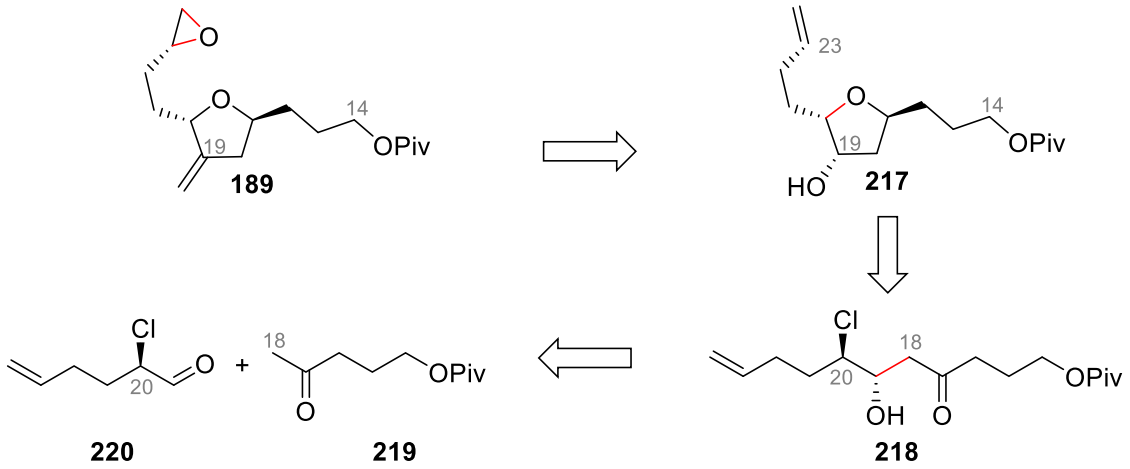

Scheme 2.31. Revised Synthetic Strategy Toward Tetrahydrofuran 189.

The execution of this strategy is shown in Scheme 2.32. PCC oxidation of the commercially available 5-hexen-1-ol **221** and subsequent treatment with *N*-chlorosuccinimide and L-prolinamide afforded the enantioenriched α-chloroaldehyde **220** in moderate yield (Scheme 2.32). It is noteworthy that given the high sensitivity of the planned lithium aldol reaction to impurities (according to our previous experience with lithium aldol reactions),[92] extensive efforts were made to purify aldehyde **220**. Unfortunately, common purification processes such as silica gel chromatography would lead to epimerization of the sensitive α-chloroaldehyde. Ultimately, we found that trituration of the crude reaction product with pentane at -78 °C furnished α-chloroaldehyde **220** (in the pentane) of ~80% purity without epimerization of the α-stereogenic centre (see section 2.2.2.2 for details on e.e. determination of this material). A subsequent lithium aldol reaction of **220** with ketone **219** (synthesized in one step from 5-hydroxy-2-pentanone)[96] provided the desired chlorohydrin **218** in modest yield. Here, the low yield was attributed to the quality of aldehyde used. Eager to assess the synthetic feasibility of the planned strategy, this aldol product was advanced despite the low yield for this key reaction. Thus, 1,3-*syn*-reduction of the hydroxy ketone in **218** using diisobutylaluminum hydride followed by treatment with silver oxide and silver triflate, delivered the

tetrahydrofuranol **217** in 68% overall yield. Thus, the Britton group methodology for the stereoselective synthesis of 2,5-disubstituted-3-hydroxytetrahydrofurans was successfully applied to construct the tetrahydrofuran ring in **217**.

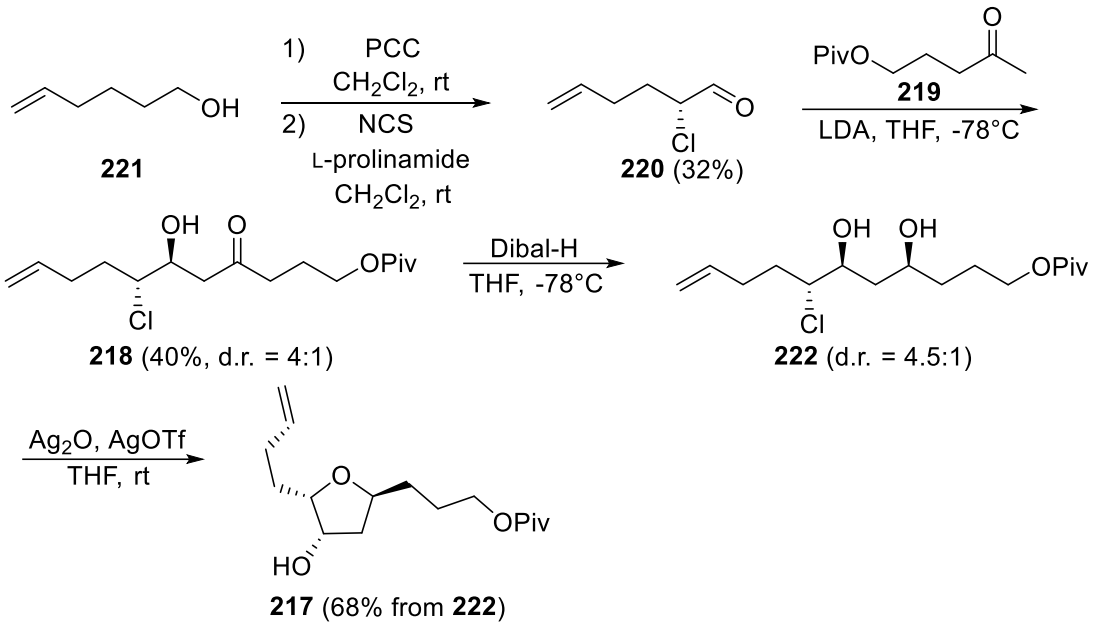

Scheme 2.32. Synthesis of the Tetrahydrofuran Precursor 217.

With intermediate **217** in hand, our next objective was to install the exocyclic alkene on the tetrahydrofuran ring and complete the construction of the C20-C26 side chain (e.g., **189**, Scheme 2.26). Here, transformation of the alkene **217** into the epoxide **189** involved a total of 3 steps. While different orders of execution were investigated, only the sequence shown in Scheme 2.33 selectively provided the epoxide **189**.

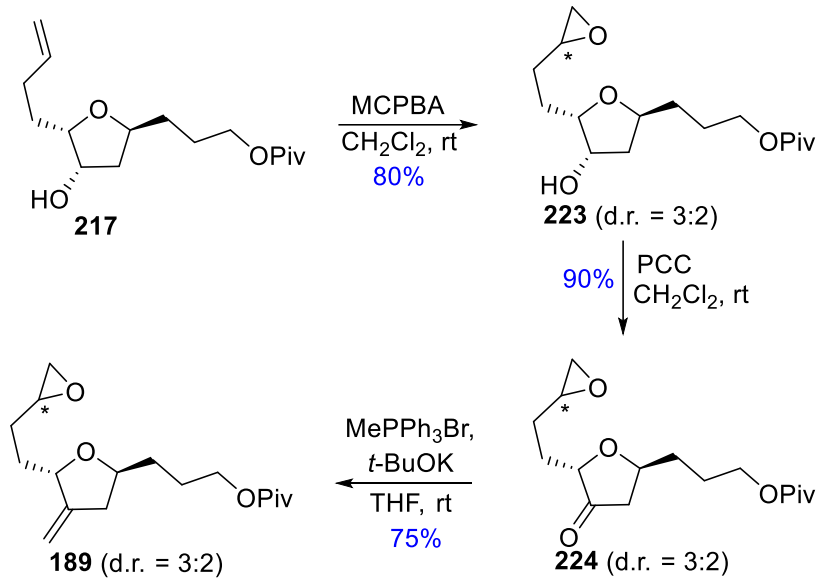

Scheme 2.33. Synthesis of the C14-C19 Building Block 189.
Compounds **223**, **224** and **189** were carried-out as a mixture of diastereoisomers with regard to C* (d.r. = 3:2).

Here, treatment of **217** with MCPBA provided the epoxide **223** as a mixture of diastereoisomers (d.r.= 3:2, Scheme 2.33). Pyridinium chlorochromate oxidation followed by a Wittig olefination then produced the alkene **189** in good yield (90%). It is noteworthy that triethylamine was necessary during the isolation of **189** to minimize its decomposition on silica gel. Moreover, we anticipated that the stereochemical purity of the C23 stereogenic centre in epoxide **189** could later be improved using asymmetric epoxidation methods. Overall, the advanced intermediate **189** was synthesized in a total of 10 steps from commercially available starting materials.

2.2.2. Elaboration of the C20-C26 side chain

2.2.2.1. Nucleophilic ring-opening of a terminal epoxide

With epoxide **189** in hand, the goal then became the installation of the methyl ketone side chain (e.g. **137**, Scheme 2.26). Here, "LG" in **137** could designate an oxygen-containing leaving group such as a tosylate or a mesylate. Thus, the alcohol function resulting from a nucleophilic epoxide-opening could then be further elaborated into a suitable leaving group "LG" to achieve the elaboration of the C14-C26 fragment **137**. Toward this goal, several carbonyl candidates were reacted with a commercially available

model epoxide **225** (1,2-propylene oxide). Importantly, each candidate was carefully chosen such that the product could be further transformed into the desired ketone derivative **137**.

First, we envisioned that a Mukaiyama aldol-like addition could give access to the desired α-methyl-γ-hydroxyketone function.[97] To this end, the silyl ether **227** was synthesized in one step from butane-2-one **226** according to a literature procedure (Scheme 2.39).[98] Unfortunately, subsequent treatment of **227** with titanium chloride failed to give any desired alcohol **228**.

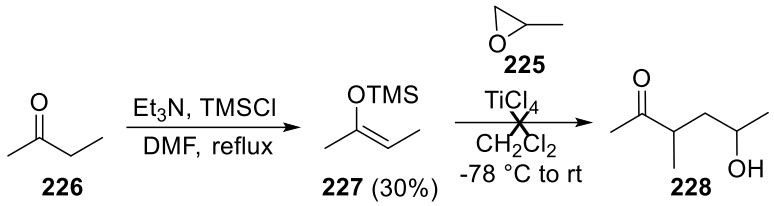

Scheme 2.34. Trimethylsilyl Enol Ether 227 as a Potential Nucleophile for the Epoxide-opening Reaction.

Subsequently, the enolate derived from the Weinreb amide **230** (Scheme 2.40) was investigated. As shown in Scheme 2.35, organic acid anhydride **229** was successfully transformed into the amide **230** using *N*,O-dimethylhydroxylamine and triethylamine. Unfortunately, treatment of **230** with a strong base such as lithium diisopropylamide or lithium bis(trimethylsilyl)amide and subsequent reaction with propylene oxide **225** failed to provide any of desired product **231**. Moreover, modifying the enolate counter anion to potassium or sodium had no effect on this outcome. Notably, a control reaction with 1-bromopropane confirmed the formation of the desired enolate and, thus, we hypothesized that the lack of reactivity of the epoxide was the main challenge.

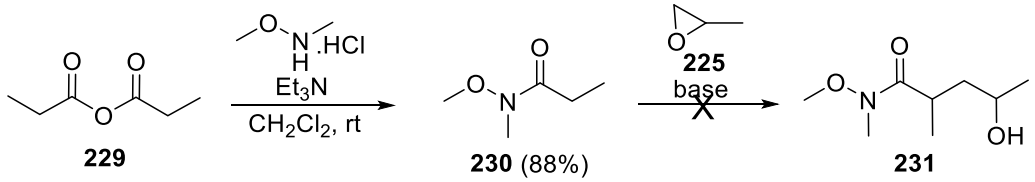

Scheme 2.35. *N*-Methoxy-*N*-methylpropionamide 230 as a Potential Nucleophile for the Epoxide-opening Reaction.

Interestingly, a few examples of nucleophilic epoxide-opening have been reported using enolates derived from β-ketoesters.[99] As shown in Scheme 2.36, a 2- or 3-step sequence could transform ketoesters such as **232** and **233** into the desired hydroxyketone **228**.

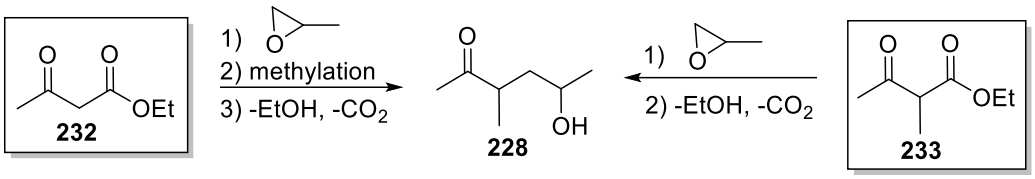

Scheme 2.36. Strategy to Obtain a Methyl Ketone from a Keto-ester.

Encouraged by these reports, various reaction conditions were investigated for the oxirane-opening of **225** using ketoesters **232** and **233**. Unfortunately, most conditions failed to provide any desired product. In fact, only upon treatment with highly concentrated aqueous sodium hydroxide ([5M]), was a small amount of product formed (<5%). Use of water as a solvent resulted in the competitive addition of water to the epoxide. Similar results were observed if methanol or ethanol was employed, and no product was formed in aprotic solvents. Alternatively, reaction of ketoester **232** with potassium *tert*-butoxide and propylene oxide in refluxing *tert*-butanol, provided significant amounts of product. An investigation of co-solvents (acetonitrile, toluene, tetrahydrofuran) indicated that a 1:4 mixture of toluene and *tert*-butanol was optimal. Additionally, the direct addition of methyl iodide to the reaction mixture provided the desired methylated product. The outcomes of this investigation are summarized in Scheme 2.37.

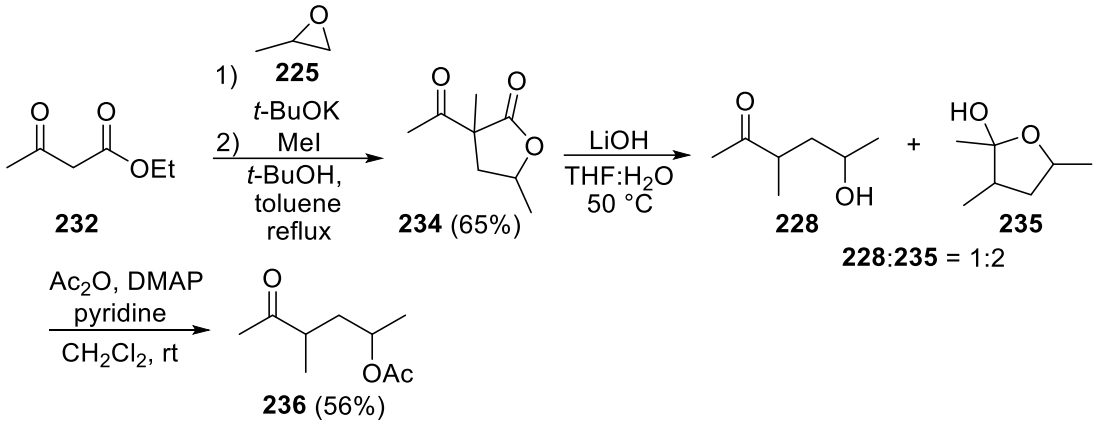

Scheme 2.37. Synthetic Sequence to Transform an Epoxide into a 2-Methyl-4-hydroxyketone.

Here, treatment of ethyl 3-oxobutanoate **232** with potassium *tert*-butoxide and successive addition of propylene oxide **225** and methyl iodide, provided the lactone **234** in 65% yield (Scheme 2.37). Decarboxylation of the resulting keto-ester **234** proceeded smoothly using lithium hydroxide in a mixture of tetrahydrofuran and water at 50 °C. However, the product from this reaction existed as an equilibrating mixture of hydroxyketone **228** and hemiacetal **235** (Scheme 2.37). To avoid the challenge of purification, direct acetate-protection provided the desired methyl ketone **236** in 56% yield from **234**.

Having established a viable route to the desired α-methyl-γ-hydroxy ketone function, this process was applied to the synthesis of the key precursor **238** (Scheme 2.38). To our delight, treatment of ethyl 3-oxobutanoate **232** with potassium *tert*-butoxide followed by the successive addition of epoxide **189** and methyl iodide, provided the corresponding lactone **237** in 60% yield. Pleasingly, despite the relatively harsh reaction conditions (reflux, strong base, high concentration), no other functional group was affected. Subsequently, decarboxylation in basic medium gave the desired product as a mixture of ketone **238** and hemiketal **239** (Scheme 2.38). A subsequent protection provided the *tert*-butyldimethylsilyl ether as a mixture of inseparable protected ketone **240** and protected hemiketal **241**. While overall this sequence still had deficiencies, it provided our first access to the C14-C26 fragment of eribulin. Eager to investigate the key Corey-Chaykovski coupling, the 6-membered ring sulfonium salt **151** was treated with sodium bis(trimethylsilyl)amide and subsequently the mixture of ketone **240** and acetal **241** was

added. Gratifyingly, we observed formation of the desired epoxide **242** (as determined by ^{1}H NMR spectroscopy and mass spectrometric analysis of the crude mixture).

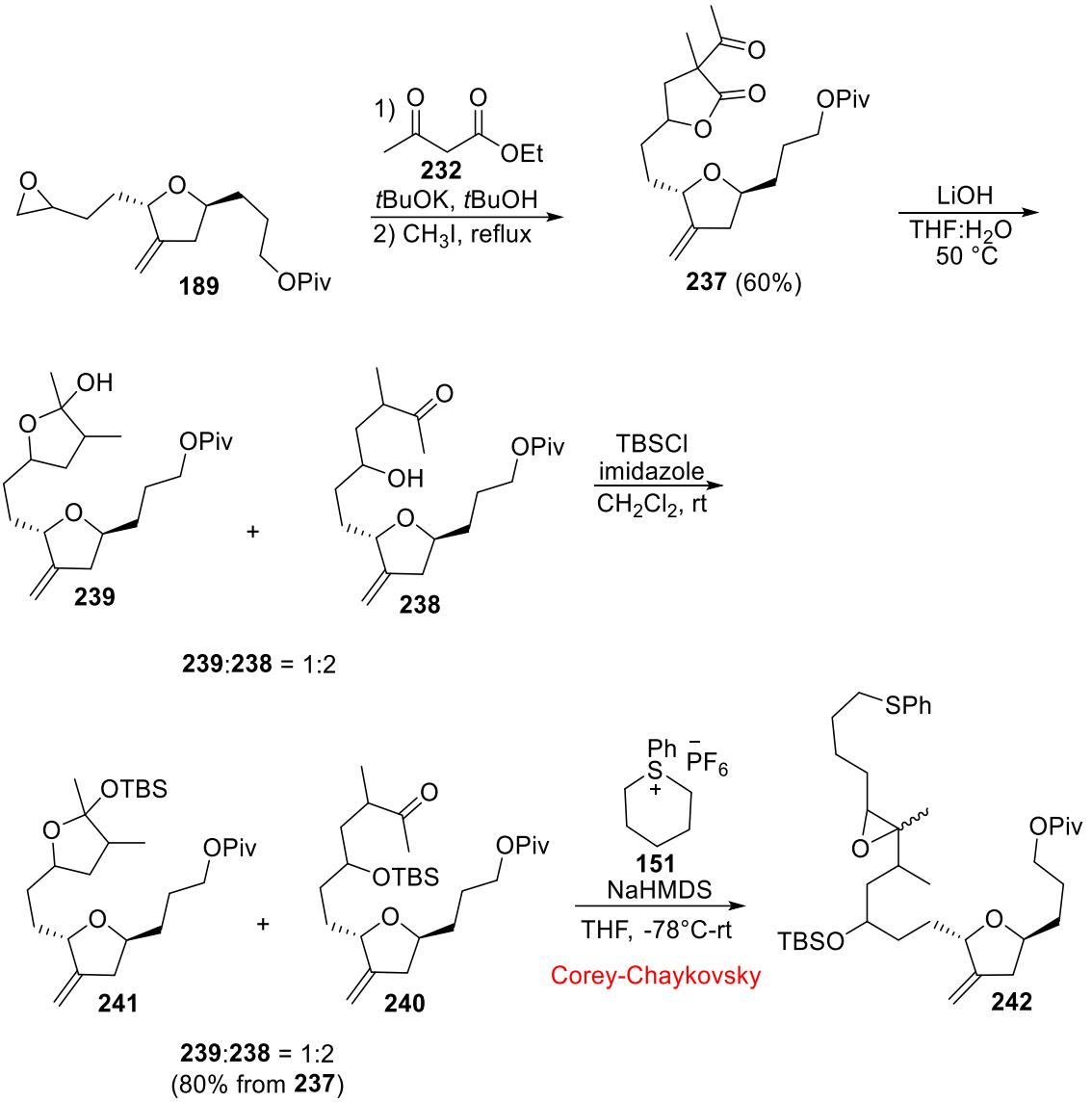

Scheme 2.38. Synthesis of Ketone 240* and Subsequent Exploration of the Corey-Chaykovsky Reaction.

* As a mixture of 4 diastereoisomers.

To summarize, this work demonstrated that the desired α-methyl-γ-hydroxy ketone side chain could be constructed via a short sequence of steps and also that the Corey-Chaykovsky reaction could be used to effect formation of the key C26-C27 bond in the Eisai intermediate **76**. Despite these successes, the challenges faced in selectively

producing the ketone **238** rather than hemiketal **239** represented a significant barrier to advancing material. Further, numerous procedures (solvents, bases, protecting groups) were investigated to effect selective protection of the alcohol function in ketone **238** over the hemiacetal function but all failed to provide a workable solution to this problem. Combined with the lack of stereoselectivity of this sequence, we elected to restrategize in hopes of identifying a more effective and selective process for the construction of the side chain.

2.2.2.2. Horner-Wadsworth-Emmons reaction with an optically pure α-chloroaldehyde

Previously, an oxygen-containing leaving group at C23 was explored for the establishment of the C14-C26 fragment of eribulin. This functionality ultimately led to the production of a mixture of an equilibrating hydroxy ketone and hemiacetal, which complicated the application of this chemistry in an eribulin synthesis. To remedy this problem, we elected to replace the oxygen functionality with a chlorine atom (e.g., ketone **243a**, Scheme 2.39). Moreover, we also found that following olefination at C-19, the alkenyl tetrahydrofurans tended to decompose during silica gel chromatographic purification. As a result, we elected to protect the C19 alcohol as a TBS ether during the following investigation.

As depicted in Scheme 2.39, disconnection of the indicated bond in the *syn*-chloromethyl ketone **243a** provides the aldehyde **244** as a potential precursor. In the synthetic direction, α-chlorination of **244**, and a following a Horner-Wadsworth-Emmons reaction-reduction sequence, could complete the assembly of **243a**. Importantly, the envisioned α-chlorination reaction could in one step, set the stereochemistry at C23 (eribulin numbering), and install a leaving group for a future cyclization. In turn, the aldehyde **244** could be quickly elaborated from the previously synthesized tetrahydrofuranol intermediate **217**.

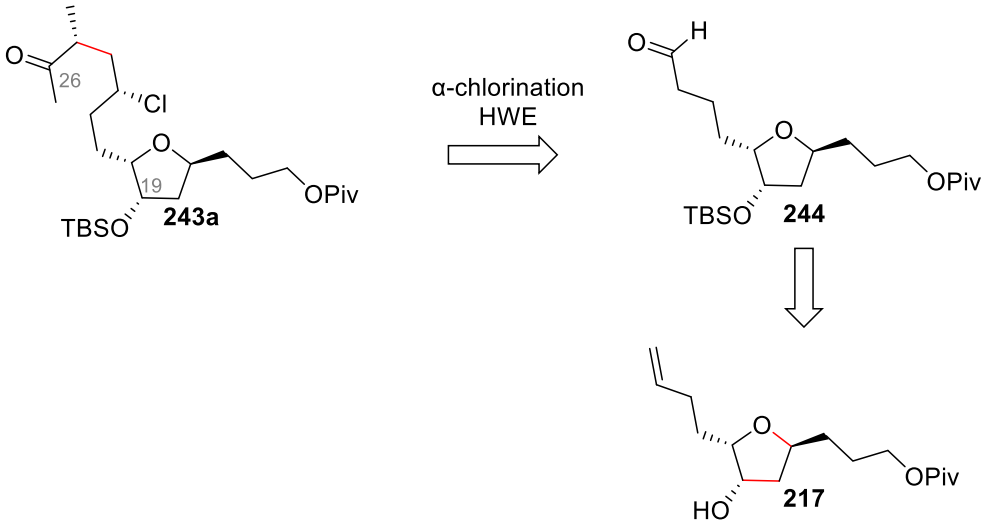

Scheme 2.39. New Retrosynthetic Strategy to Access Terminal Ketone 243a.

Following this strategy, the hydroxy tetrahydrofuran **217** was synthesized in 5 steps from 5-hexen-1-ol following the process shown in scheme 2.32. Subsequent treatment with *tert*-butyldimethylsilyl chloride followed by a Brown hydroboration[100] provided the alcohol **245** in good yield (Scheme 2.40). Pyridinium chlorochromate oxidation of **245** and subsequent treatment with *N*-chlorosuccinimide and L-prolinamide, delivered the α-chloroaldehyde **246** as a mixture of diastereoisomers (d.r. = 2:1). The latter material was then coupled to phosphonate **247** (previously synthesized from 3-iodobutan-2-one in one step) through a barium hydroxide promoted Horner-Wadsworth-Emmons reaction.[101] To our delight, this method, which has been used for coupling of β-ketophosphonates with base-sensitive aldehydes, furnished the desired α,β-unsaturated ketone **248** in good yield.

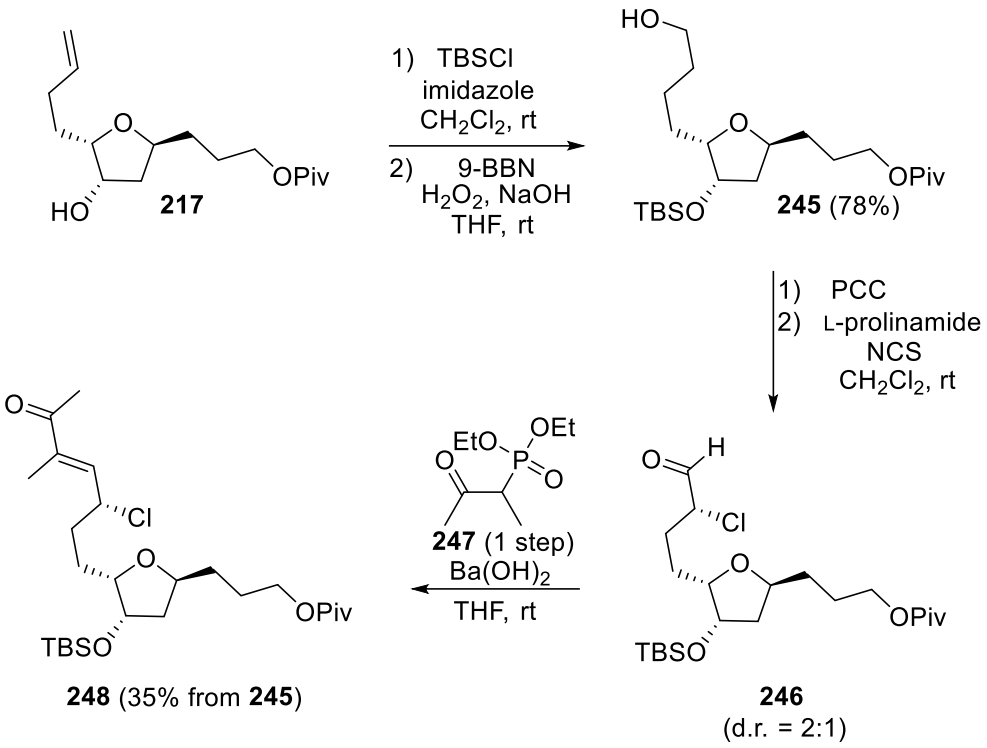

Scheme 2.40. Synthesis of Enone 248 from Hydroxytetrahydrofuran 217.

The following step toward the C14-C26 building block **243a** then involved reduction of the double bond in **248**. Here, we hoped that the stereochemistry at the chloromethine centre would impart diastereoselectivity on the reduction process.

2.2.2.3. Reduction of the α,β-conjugated ketone

While numerous methods exist to reduce α,β-conjugated ketones, hydrogenation is the most common and widely used.[102] Therefore, our first attempts to reduce enone **248**, involved investigations of conventional hydrogenation reactions. As shown in Scheme 2.41, enone **248** was first treated with palladium on carbon (Pd/C) and hydrogen in ethyl acetate. Surprisingly, the major product formed during this reaction was the dechlorinated ketone **249** (**249**:**243** = 2:1, Scheme 2.41). While unexpected, the reduction of allylic chlorides has been reported by others.[103,104] Given the importance of the chlorine atom in the planned construction of the tetrahydropyran ring this moment marked the beginning of a long and exhaustive investigation to find reaction conditions that would selectively reduce the double bound in **248** and minimize the loss of the chlorine atom.

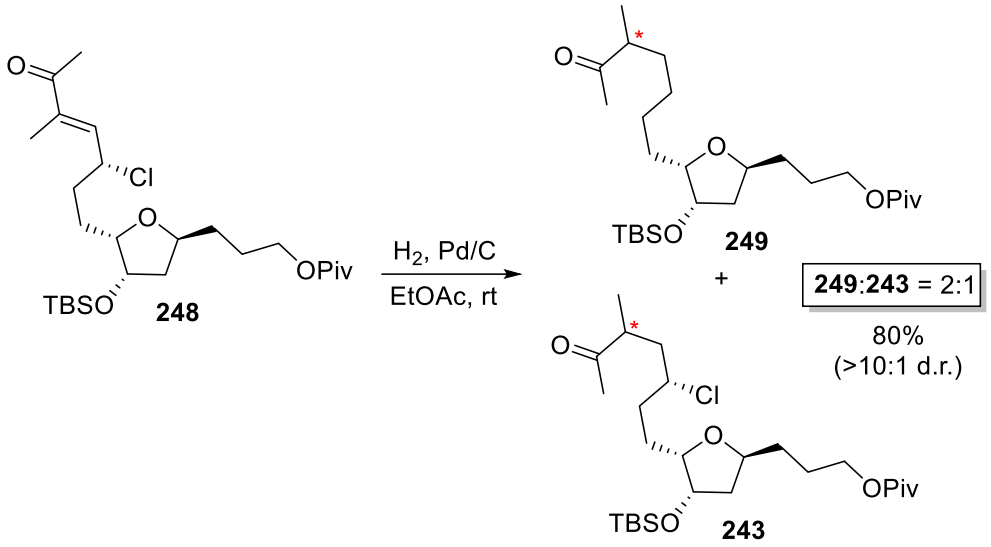

Scheme 2.41. Hydrogenation of Enone 248 Using Pd/C in Ethyl Acetate.

To spare material, most of the following screening of reaction conditions (>70 reaction conditions) was performed on the closely related γ-chloro-α,β-unsaturated carbonyl **253**, synthesized in 4 steps from 1,3-propanediol **250** (Scheme 2.42).

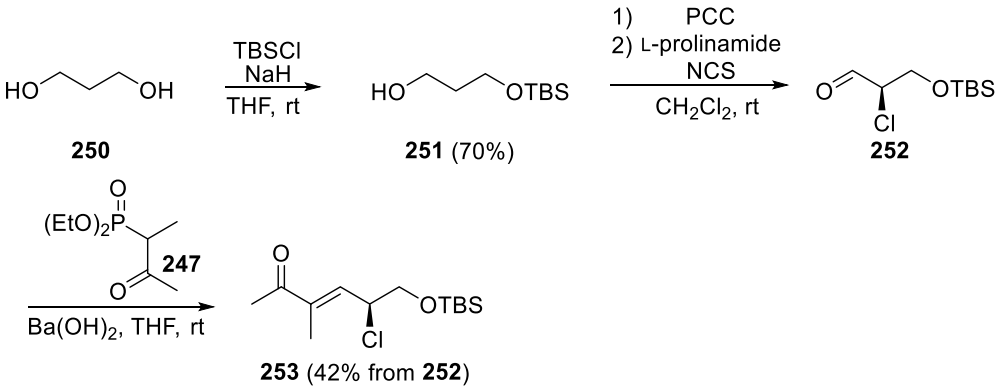

Scheme 2.42. Synthesis of Model Enone 253.

Here, treatment of 1,3-propanediol **250** with sodium hydride and *tert*-butyldimethylsilyl chloride furnished the mono-protected alcohol **251** in good yield. PCC oxidation of **251** followed by α-chlorination with *N*-chlorosuccinimide and L-prolinamide provided the enantioenriched α-chloroaldehyde **252**. A barium promoted Horner-

Wadsworth-Emmons reaction of aldehyde **252** with phosphonate **247** then completed the 4-step synthesis of the model substrate **253**.

Table 2.2. Key Hydrogenation Conditions Investigated on Enones 253 and 248.

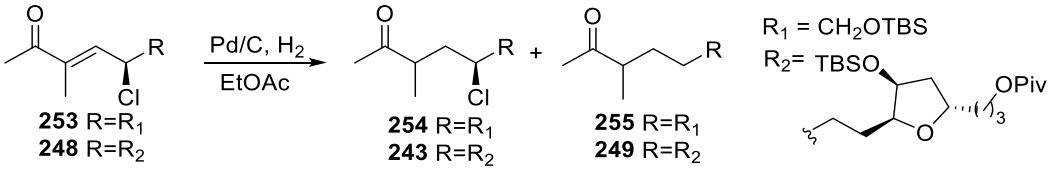

253 R=R_1
248 R=R_2

254 R=R_1
243 R=R_2

255 R=R_1
249 R=R_2

entry	substrate	solvent	catalyst	temp (°C)	ratio of products*	yield
1	**253**	EtOAc	Pd/C	20	**254**:**255** = 2:1	62%
2	**253**	*i*PrOAc	Pd/C	20	**254**:**255** = 4:1	77%
3	**248**	EtOAc	Pd/C	20	**243**:**249** = 1:2	30%
4	**248**	*i*PrOAc	Pd/C	20	**243**:**249** = 1:4	N.D.
5	**253**	EtOAc	Rh/Al_2O_3	20	**254**:**255** = 3:1	25%
6	**253**	EtOAc	Pd/C	0	**254**:**255** = 3:1	72%
7	**248**	EtOAc	Pd/C	0	**243**:**249** = 1:2	N.D.

*From analysis of ^{1}H NMR spectra recorded on crude reaction mixtures. N.D. = not determined.

With the model substrate **253** in hand, we initiated our investigation by studying the solvent effect on the reactivity of the palladium-catalyzed hydrogenation (entries 1 and 2, Table 2.2). Encouragingly, it was discovered that the ratio of saturated chloroketone **254** and the dechlorinated material **255** could be improved from 2:1 in ethyl acetate to 4:1 in isopropyl acetate (entry 1 and 2). Unfortunately, this trend was inverted when the more elaborate chloroenone **248** was subjected to the same reaction conditions (**243**:**249** = 1:2 in EtOAc and **243**:**249** = 1:4 in *i*PrOAc, entries 3 and 4). We next examined a series of metal catalysts from which, some are known to be more efficient for the hydrogenation of substrate containing activated halogens.[105] Unfortunately, among the various metal catalysts investigated, only Rh/Al_2O_3 greatly improved the ratio of desired chloroketone **254** to undesired ketone **255** (entry 5). However, the extended reaction time required to reach complete conversion (3 days) resulted in a low yield of the products. Following several failed attempts to improve upon this result we elected to investigate other reaction conditions. Here, the effect of temperature on the hydrogenation of enone **253** was studied. To our delight, Pd/C catalyzed hydrogenation of **253** at 0 °C improved the yield of desired ketone **254** from 62% to 72% (entries 1 and 5). Excited by these results, hydrogenation of the more elaborate chloroenone **248** was also performed at a lower temperature. Unfortunately, hydrogenation of **248** at 0 °C resulted in a similar ratio of

products as seen before (entries 2 and 7). Other temperatures investigated did not improve upon this result.

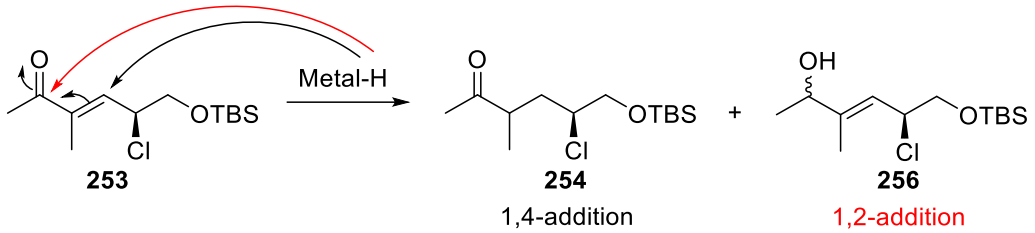

Scheme 2.43. 1,2- and 1,4-Reductions upon Treatment with a Metal Hydride Reducing Agent.

Based on the repeated failure to generate the desired chloroketone **254** as a major product we elected to move away from hydrogenation procedures and explore a series of hydride transfer reactions. It is noteworthy that in the case of α,β-unsaturated ketones, addition of hydride can occur at the carbonyl (e.g. **256**, Scheme 2.43) or on the olefin function (e.g. **254**, Scheme 2.43). Here, it was critical to identify conditions that both favour 1,4-addition and do not reduce the sensitive C-Cl bond. Results of this work are summarized in Table 2.3.

Table 2.3. Reduction Using a Metal Reducing Agent in Combination with Another Metal.

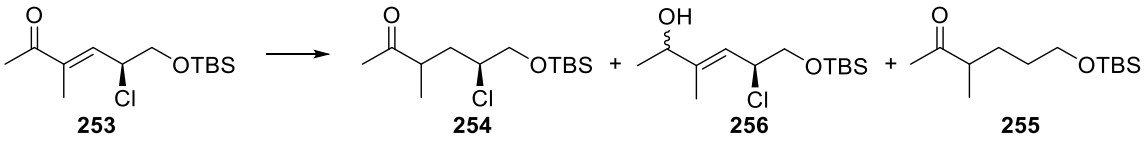

entry	reagents	temp (°C)	solvent	conv.*	ratio of products*
1	Red-Al, CuBr	-78 to 25	THF	0%	N.D.
2	Dibal-H, $Co(acac)_2$	25	THF	0%	N.D.
3	$NaBH_4$, $NiCl_2$	25	THF:MeOH	100%	**254**:**256**:**255** = 0:0:1
4	Stryker's reagent	25	toluene	0%	N.D.

*From analysis of ^1H NMR spectra recorded on crude reaction mixtures. N.D. = not determined.

For example, the combination of Red-Al and copper bromide (entry 1), or *bis*(1,3-diketonato)cobalt(II) complex and diisobutylaluminum hydride (entry 2), both reported to reduce the olefin function in enones,[106] [107] failed to provide any saturated product **254**. Interestingly, the addition of nickel chloride to sodium borohydride has also been shown to induce selectivity in olefin reduction in many α,β-unsaturated carbonyl compounds.[108]

Here, reaction of **253** with this hydride complex successfully promoted the desired 1,4-addition event. Unfortunately, the chloromethine function in **253** was also reduced in the process (entry 3, Table 2.3). Investigation of other combinations of reducing agents and metal catalysts did not improve upon this result. We next explored use of Stryker's reagent, a triphenylphosphine-ligated copper hydride reducing agent well-known for exclusively reducing olefins in α,β-unsaturated carbonyls systems.[109] Unfortunately, no product was formed after two days at room temperature despite using freshly prepared Stryker reagent under careful inert atmosphere (entry 4).[110] Here, we hypothesized that the high steric hindrance of the α,β-unsaturated system was responsible for the lack of reactivity toward the enone **253**.

Interestingly, a more reactive Stryker's reagent that is capable of reducing a broad scope of α,β-unsaturated carbonyls has been described by the Lipshutz group.[111] Here, replacement of the triphenylphosphine ligands in the Stryker reagent by 1,2-bis(diphenylphosphino)benzene (BDP), a readily available achiral bidentate ligand, resulted in a more reactive 16-electron copper hydride complex. Most notably, direct comparison of the Stryker's reagent and the (BDP)CuH complex for the reduction of isophorone revealed a striking difference in reactivity. While 7% of conversion was observed with the Stryker's reagent in 24 hours, the reaction was complete in 5 hours with (BDP)CuH. Based on these insights, we attempted to prepare a solution of (BDP)CuH according to the reported procedure.[111] Unfortunately, the solution failed to turn yellow, the color characteristic of the copper complex. To address this issue, catalytic amounts of BDP were added to a freshly prepared solution of Stryker's reagent.[110] Here, we anticipated that upon ligand exchange the desired (BDP)CuH complex would be formed. To our delight, the solution quickly changed from red to yellow. As a result, different solutions of (BDP)CuH complex were then prepared by addition of varying amounts of BDP to freshly prepared Stryker's reagent and subsequently reacted with the model substrate **253**. The results of this study are summarized in Table 2.4.

Table 2.4. Summary of the (BDP)CuH Reductions of Enones 253 and 248.

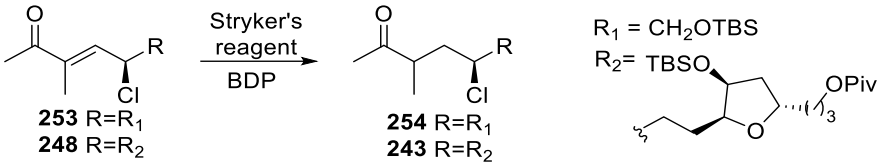

entry	substrate	BDP (equiv.)	time (h)	temp. (°C)	solvent	conv.*	yield
1	**253**	0.3	48	25	toluene	0%	0%
2	**253**	0.3	48	25	THF	0%	0%
3	**253**	0.3	3	60	toluene	50%	45%
4	**253**	0.6	3	60	toluene	55%	52%
5	**253**	1	3	60	toluene	55%	52%
6	**248**	0.6	3	60	toluene	20%	15%

*From analysis of ^{1}H NMR spectra recorded on crude reaction mixtures.

Here, we first investigated the addition of 0.3 equivalent of the BDP ligand to a freshly prepared solution of Stryker's reagent in toluene. Unfortunately, only unreacted starting material was recovered after two days at room temperature (entry 1). Switching the solvent to tetrahydrofuran, a suitable solvent for Stryker's reductions,[112] did not change this result (entry 2). The effect of temperature was then studied and to our delight, 50% of enone **253** were cleanly converted to the corresponding saturated product **254** at 60 °C (entry 3). Importantly, no dehalogenation was detected and thus, further optimization was investigated. For example, longer reaction times and the addition of *tert*-butanol (used as an additive to enhance the reactivity of the (BDP)CuH complex)[111] failed to improve the conversion. Alternatively, doubling the equivalents of BDP slightly increased the conversion and the saturated product **254** was formed in 52% yield (entry 4). However, the yield was not further improved using one equivalent of BDP ligand (entry 5). Based on these insights, the more elaborated chloroenone **248** was subjected to the optimized reaction conditions. Unfortunately, treatment of **248** with a solution of (BDP)CuH at 60 °C only provided small amounts of the corresponding saturated product **243** (entry 6). After many unsuccessful attempts to improve this outcome, we elected to abandon this method of reduction.

We next examined less common enone reduction protocols. Here, different combinations of metal catalysts (the Wilkinson's catalyst, $PdCl_2$, Zn) and hydride sources (organosilanes, ammonium formate and ammonium chloride) were investigated at various temperatures (>15 reaction conditions) but, unfortunately, all resulted in the formation of the undesired saturated ketone **255** as the major product. A microbial reduction described

to stereoselectively reduce the double bond of α,β-unsaturated ketones[113] was also investigated but, disappointedly, treatment of model enone **253** with baker yeast in water only provided a mixture of different reduced products.

At this point, we elected to explore a slightly modified synthetic approach. To avoid the challenges associated with reduction of the activated chloromethine, we anticipated that coupling of sulfonium salt **136** with enone **248** would provide an epoxide **258** that could then be further elaborated into the saturated product **257** through reduction of the double bond (Scheme 2.44). Importantly, the chlorine atom in **258** is not adjacent to an enone function and as a result we hypothesized that it would be less susceptible to reduction.

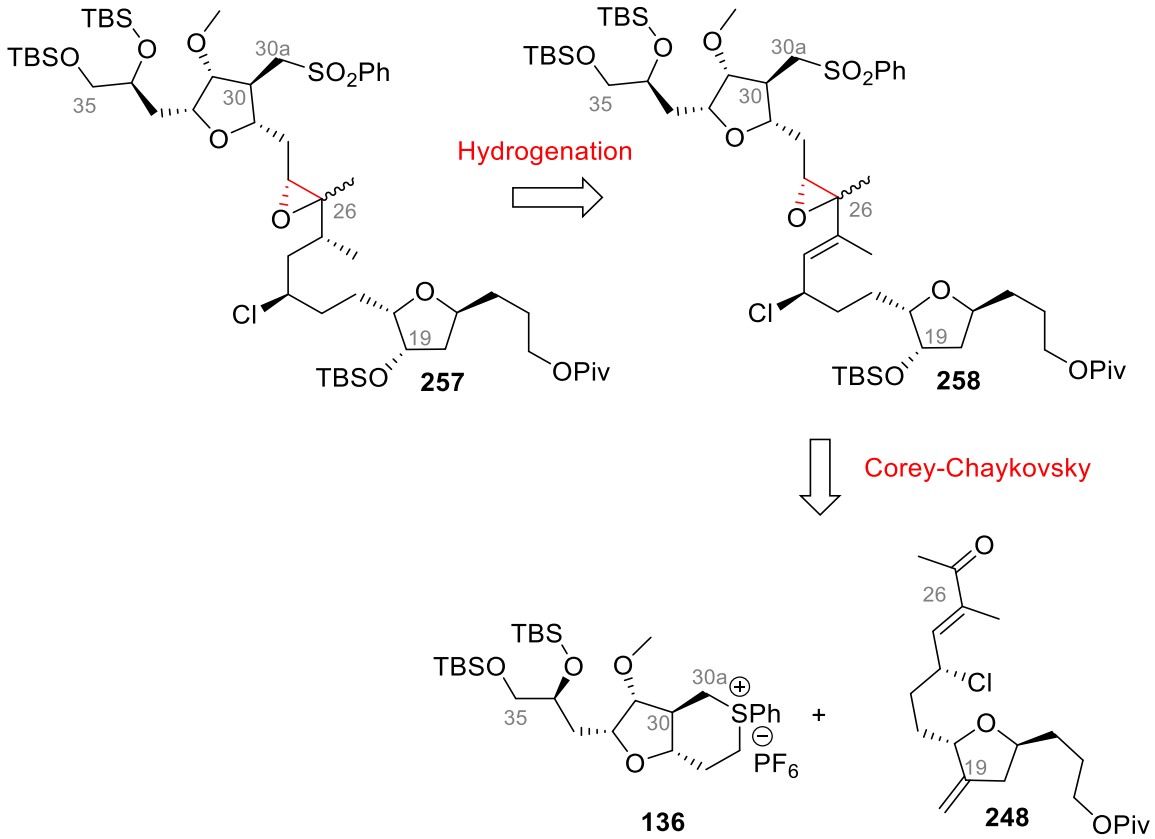

Scheme 2.44. Alternative Retrosynthesis of Epoxide 257.

Although there are examples of Corey-Chaykovsky reactions involving α,β-conjugated carbonyls, the addition of the sulfonium ylide preferentially occurs in 1,4-fashion and thus, this process has become a method for cyclopropane formation.[114]

Fortunately in our case, deprotonation of sulfonium salt **136** with lithium bis(trimethylsilyl)amide followed by addition of the enone **248**, resulted in exclusive formation of the epoxide product. Subsequent oxidation of the thioether function furnished the sulfone **258** in good yield (Scheme 2.45). Unfortunately, re-examining the most productive hydrogenation conditions identified in our earlier studies exclusively reduced the chloromethine function. Following this disappointment, we explored replacement of the chlorine atom by an alcohol function that could be subsequently elaborated into a leaving group to avoid difficulties encountered with the allylic chloride. To our delight, treatment of sulfone **259** with silver tetrafluoroborate in water successfully converted **259** into the corresponding allylic alcohol **260** (Scheme 2.45). However, subjecting **260** to various high-pressure hydrogenations failed to effect olefin reduction.

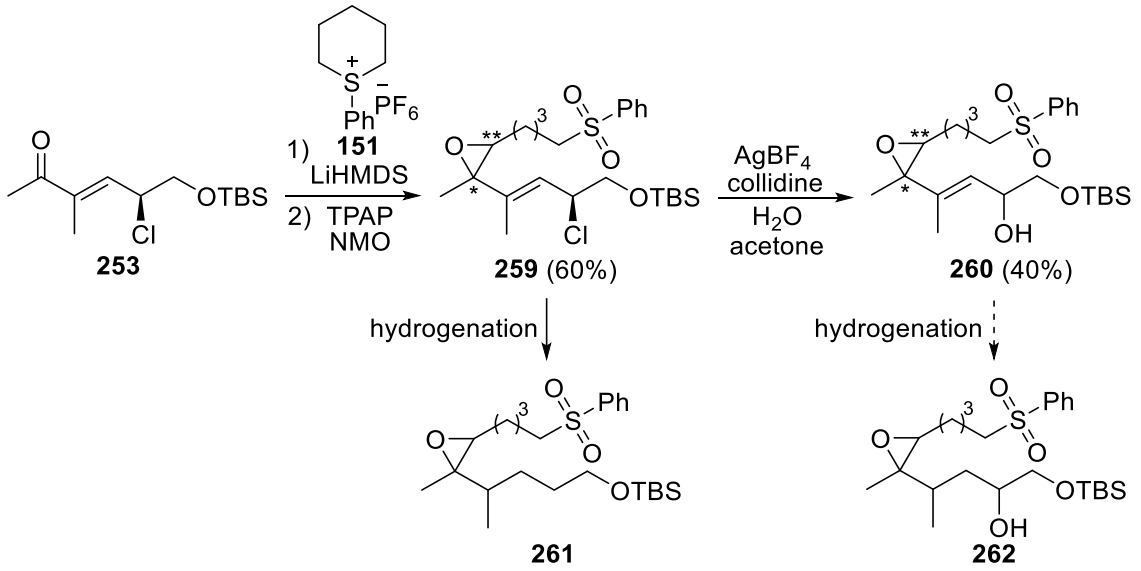

Scheme 2.45. Synthetic Studies Toward the Elaboration of Epoxide 257.
Compounds **259** and **260** were carried out as mixture of diastereoisomers with regard to C* and C**. Formation of these products was confirmed by ^{1}H NMR spectroscopy and mass spectrometric analysis.

Following this investigation, we returned to the reduction of enone **253** and examined a silicon hydride manganese-catalyzed reduction developed in the Magnus group. This reduction has been shown to regioselectively reduce the olefin function in various α,β-unsaturated ketones. [115] Towards this goal, chloroenone **253** was treated with a solution of phenyl silane and $Mn(dpm)_3$ in a mixture of isopropanol and dichloromethane (Scheme 2.46). To our delight, 50% of the desired saturated product **254** was formed

albeit as a mixture with the oxidized product **263** (as determined by ^{1}H NMR and mass spectroscopy).

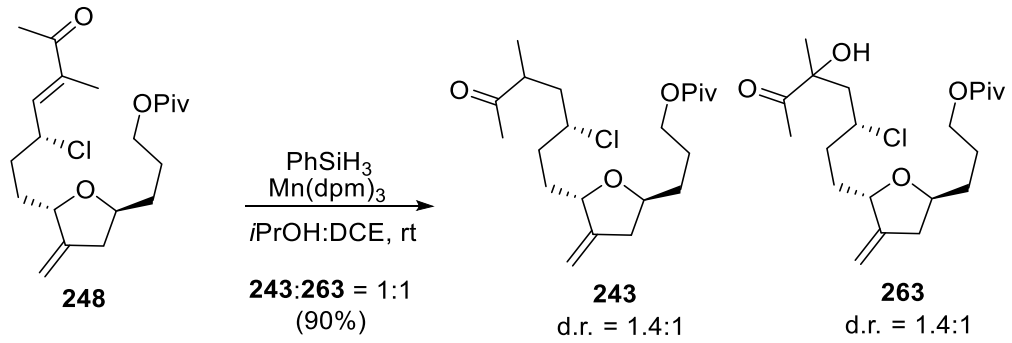

Scheme 2.46. Reduction of Enone 248 Using Mn(Dpm)3 and Phenylsilane.

While we were surprised by the formation of the alpha-hydroxy ketone **263**, the combination of $Mn(dpm)_3$ and phenylsilane has primarily been used for the α-hydroxylation of conjugated carbonyls when the reaction is carried out in the presence of oxygen. This work builds on Mukaiyama's seminal work on cobalt-catalyzed alkene hydrations, also known as the Mukaiyama hydration.[116,117] As a result, we hypothesized that the use of non-deoxygenated solvents was responsible for the formation of the alcohol side-product **263** and thus, the solvents used in the reduction, isopropanol and dichloroethane, were then deoxygenated using freeze-pump-thaw degassing techniques. To our delight, repetition of the reaction using the deoxygenated solvents furnished the desired ketone **243** in 80% yield (Scheme 2.47).

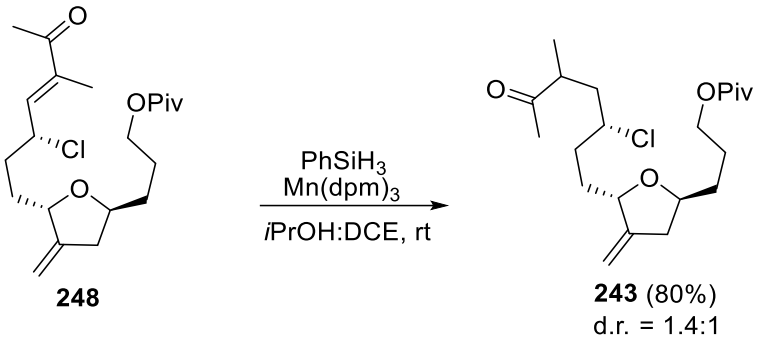

Scheme 2.47. Manganese Reduction of Enone 248 Using Deoxygenated Solvents.

Thus, after months of intense research, conditions capable of reducing the olefin function in **248** and not removing the essential chlorine atom, were finally discovered. Unfortunately, the stereoselectivity of the reaction was low and an almost equivalent mixture of diastereoisomers was produced (d.r. = 1.4:1). To assign the stereochemistry of each diastereoisomer, the model substrate **253** was treated with hydrogen and palladium on carbon to provide a mixture of ketone **254** (d.r. = 12:1, Scheme 2.48) and dechlorinated product **255** (not depicted). Deprotection of the alcohol function in ketone **254** using hydrogen fluoride in pyridine then resulted in the formation of alcohol **264** and tetrahydropyran **265**.

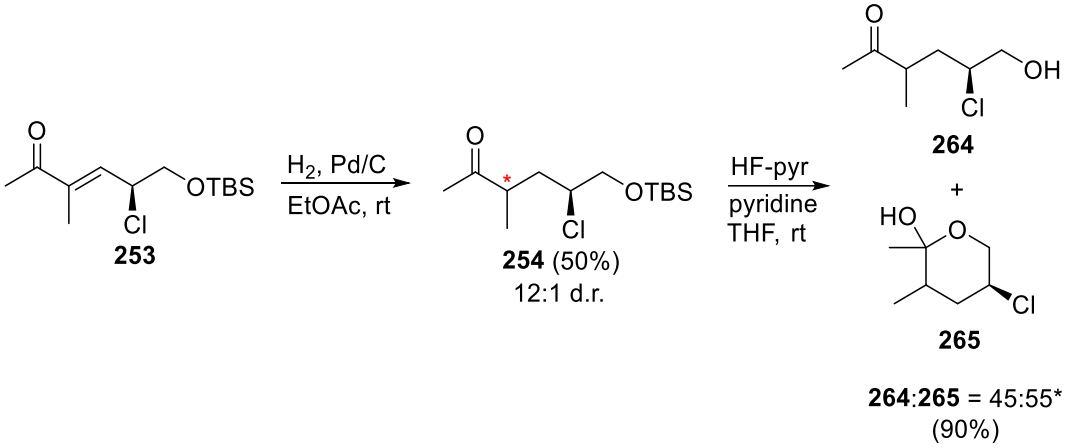

Scheme 2.48. Synthesis of Tetrahydropyran 265.
*As determined by ^{1}H NMR spectroscopic analysis of the mixture.

^{1}H NMR analysis of the cyclized product **265** revealed that the methyl and the chlorine substituents were *syn* to one another (Figure 2.2). As depicted in Figure 2.2 the relative stereochemistry was assigned based on observed coupling constants. Specifically, the resonance in the ^{1}H NMR spectrum that was assigned to H4 appeared as a doublet of doublet of doublets with nearly equivalent 12 Hz coupling constants (an apparent quartet). In the chair conformations depicted for the *syn*- and *anti*- products **265a** and **265b** (Figure 2.2), Hs (see **265a**, Figure 2.2) would have two large diaxial coupling constants (10-12 Hz) and one large geminal coupling constant whereas Ha (see **265b**, Figure 2.2) would have a large geminal coupling constant and two smaller axial-equatorial and equatorial-equatorial coupling constants (~4 Hz).[118] Therefore, the relative stereochemistry for the product of enone reduction was assigned as the *syn*-product **265a**.

Following comparison of the resonances observed in the ^{1}H NMR spectrum of **254** with those of the eribulin fragment **243**, it was clear that the manganese-catalyzed reduction provided the desired *syn*-diastereoisomer **243a** in a slight majority (d.r. =1.4:1, Scheme 2.47).

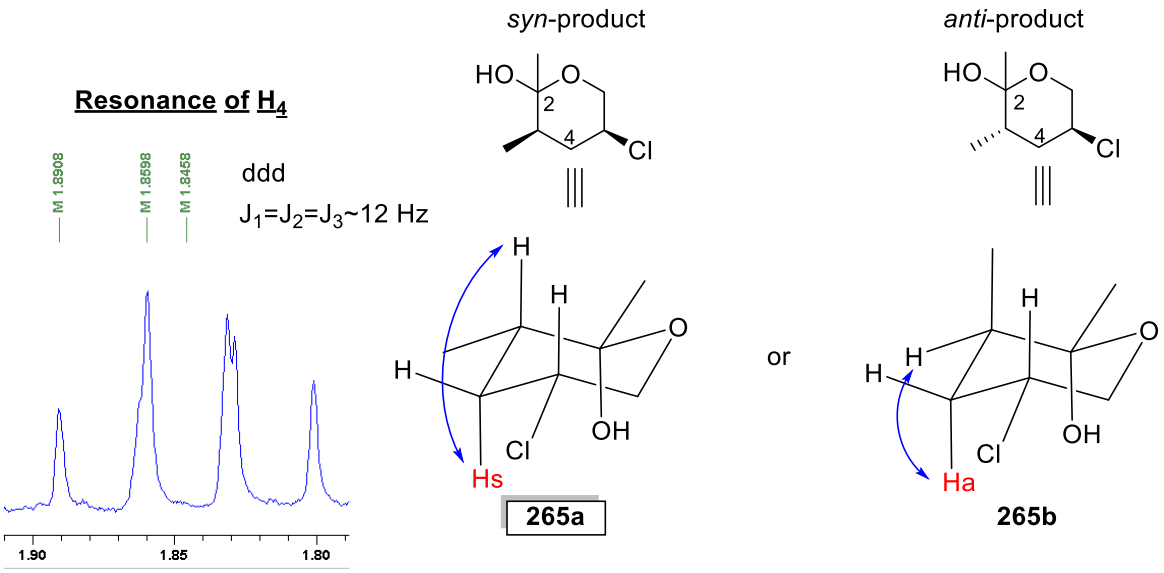

Figure 2.2. Comparison of the ^{1}H NMR coupling constants in the potential *syn*- and *anti*-products 265a and 265b.

2.2.3. Synthetic optimization of the C14-C26 fragment of eribulin

2.2.3.1. Enantiopurity of the C25 stereogenic centre

With a method in hand to produce the desired saturated ketone **243a** we next looked to improve the diastereoselectivity of the reduction. Here, enone **248** was subjected to various combinations of organosilanes ($PhSiH_3$, Ph_2SiH_2, $PhMeSiH_2$, Et_2SiH_2 and TMDS), solvents (*i*PrOH, DCE and DCM) and catalysts ($Mn(dpm)_3$, $Co(dpm)_2$, $Mn(acac)_3$ and $Co(acac)_3$) but, unfortunately, none improved the initial ratio of diastereoisomers in favor of the desired *syn*-chloromethyl ketone **243a**.

Table 2.5. Investigation of Epimerization Reaction Conditions.

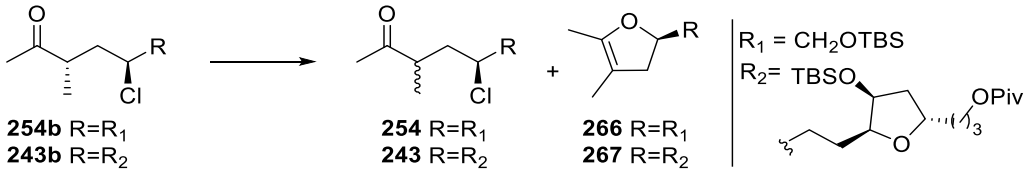

entry	substrate	reagents	temp.(°C)	conv.*	solvent	ratio*	d.r.*
1	R_1	*t*BuOK	35	100%	*t*BuOH	**254**:**266** = 0:1	N.D.
2	R_1	Et_3N	60	0%	DMF	N.D.	1:0
3	R_1	Et_3N	120	100%	DMF	N.D.	N.D.
4	R_1	Et_3N, TMSCl	25	0%	CH_2Cl_2	N.D.	1:0
5	R_1	Et_3N, TMSCl	120	100%	DMF	N.D.	N.D.
6	R_1	DBU	25	0%	CH_2Cl_2	N.D.	1:0
7	R_1	DBU	25	0%	THF	N.D.	1:0
8	R_1	DBU	25	100%	CH_3CN	**254**:**266** = 1:0	1:1
9	R_1	DBU	25	100%	DMSO	**254**:**266** = 1:0	1:1
10	R_2	DBU	25	100%	CH_3CN	**243**:**267** = 4:1	1:1
11	R_2	DBU	4	100%	CH_3CN	**243**:**267** = 1:0	1:1

*From analysis of ^{1}H NMR spectra recorded on crude reaction mixtures. N.D. = not determined.

As we had been unable to improve the diastereoselectivity of the reduction, we next turned to the epimerization of the α-methyl stereogenic centre as a means to recycle the undesired *anti*-diastereoisomer **243b** (Table 2.5). To this end, the model ketone **254b** was first treated with potassium *tert*-butoxide (entry 1), which promoted formation of the cyclized product **266** (as determined by ^{1}H NMR spectroscopy and mass spectrometric analysis) through an intramolecular chlorine displacement involving the intermediate enolate. Triethylamine was then tested in dimethylformamide and again no reaction was observed at room temperature (entries 2) and elevating the reaction temperature eventually led to decomposition (entry 3). The addition of trimethylsilyl chloride to a solution of *anti*-chloromethyl ketone **254b** and triethylamine also failed to produce the corresponding trimethylsilyl enol ether intermediate (entries 4 and 5). 1,8-diazabicyclo[5.4.0]undec-7-ene (DBU) was then explored and while no reaction was observed with DBU in dichloromethane (entry 6), examination of this reaction in a small collection of solvents (entries 7-9) highlighted that in polar solvents such as acetonitrile and DMSO a mixture of both diastereoisomers was produced (d.r. = 1:1, entries 8 and 9). Based on these results, the more elaborate methylketone **243b** was treated with a solution of DBU in acetonitrile. Here, a mixture of diastereoisomers was produced (d.r. = 1:1, entry 10) along with small amounts of the undesired cyclized product **267**. Gratifyingly, when

the reaction was performed at a lower temperature (4 °C), formation of the side-product **267** was avoided (entry 11).

As a result, manganese-catalyzed reduction of the α,β-unsaturated ketone **248**, and recycling of the undesired *anti*-diastereoisomer **243b** upon treatment with DBU (two iterations), produced the desired *syn*-chloromethyl ketone **243a** in 65% overall yield (Scheme 2.49).

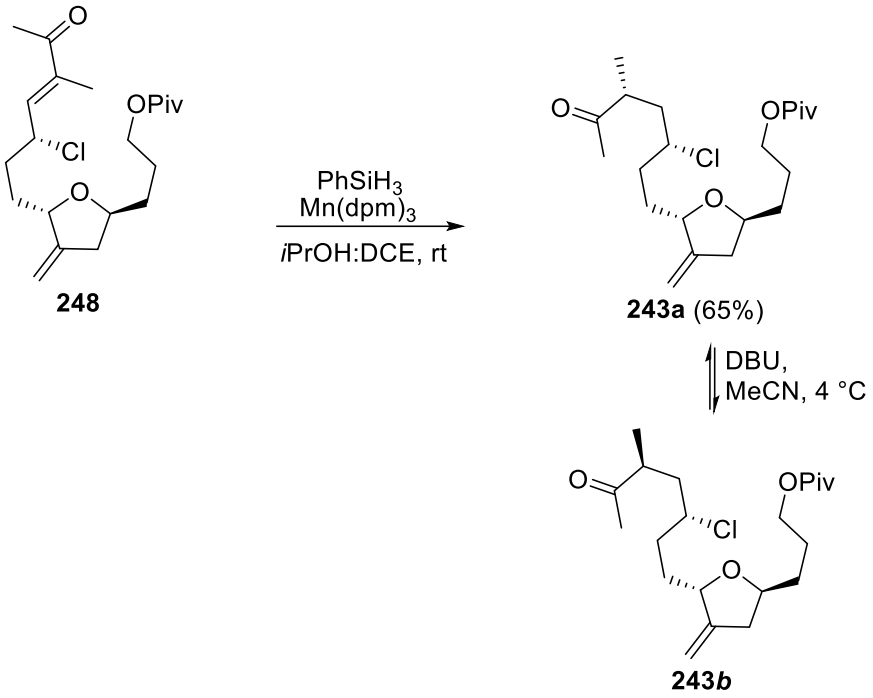

Scheme 2.49. Reduction of Enone 248 to the *Syn*-chloromethyl Ketone 243a.

It is noteworthy that the initial reaction conditions investigated to reduce the olefin function in **248** (H_2, Pd/C in EtOAc) only provided small amounts of the desired saturated product **243a** (~ 30%) and thus, the optimization of this key step has led to a greatly improved process.

2.2.3.2. Enantiopurity of the C20 stereogenic centre

The synthetic strategy to access the C14-C26 fragment **243a** relies on several diastereoselective reactions but is also highly dependent on two enantioselective α-chlorination reactions. It was therefore crucial that each α-chloroaldehyde was formed in high enantiopurity. With a process in hand to produce the methyl ketone required for the

Corey-chaykovsky reaction, it now became critical to carefully evaluate the enantiomeric purity of key intermediates in this sequence.

To this end, the α-chloroaldehyde **220** produced using Jørgensen prolinamide α-chlorination was reduced with sodium borohydride (Scheme 2.50). Following esterification using (*R*)-MTPA furnished the corresponding Mosher[119] ester derivative **269** (d.r. = 4:1, as determined by analysis of the ^{18}F NMR spectrum).

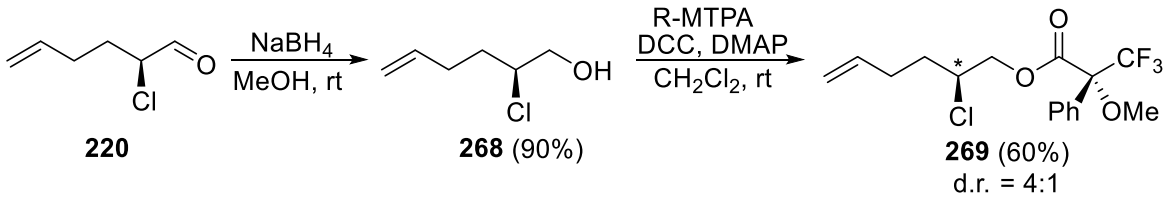

Scheme 2.50. Synthesis of the Mosher Ester Derivative 269.

As a result, the enantiomeric excess of aldehyde **220** was only 56% – a very low e.e. compared to what we would expect using the Jørgensen α-chlorination protocol. To improve upon this result, an alternative route to the α-chloroaldehyde **220** was explored that involves an unpublished route currently under development by colleagues in the Britton group (Allan Brooke, Matthew Sutherland and Marjan Mohammed). This strategy relies on a tandem α-chlorination-aldol reaction also developed in the Britton group (Scheme 2.51).[120]

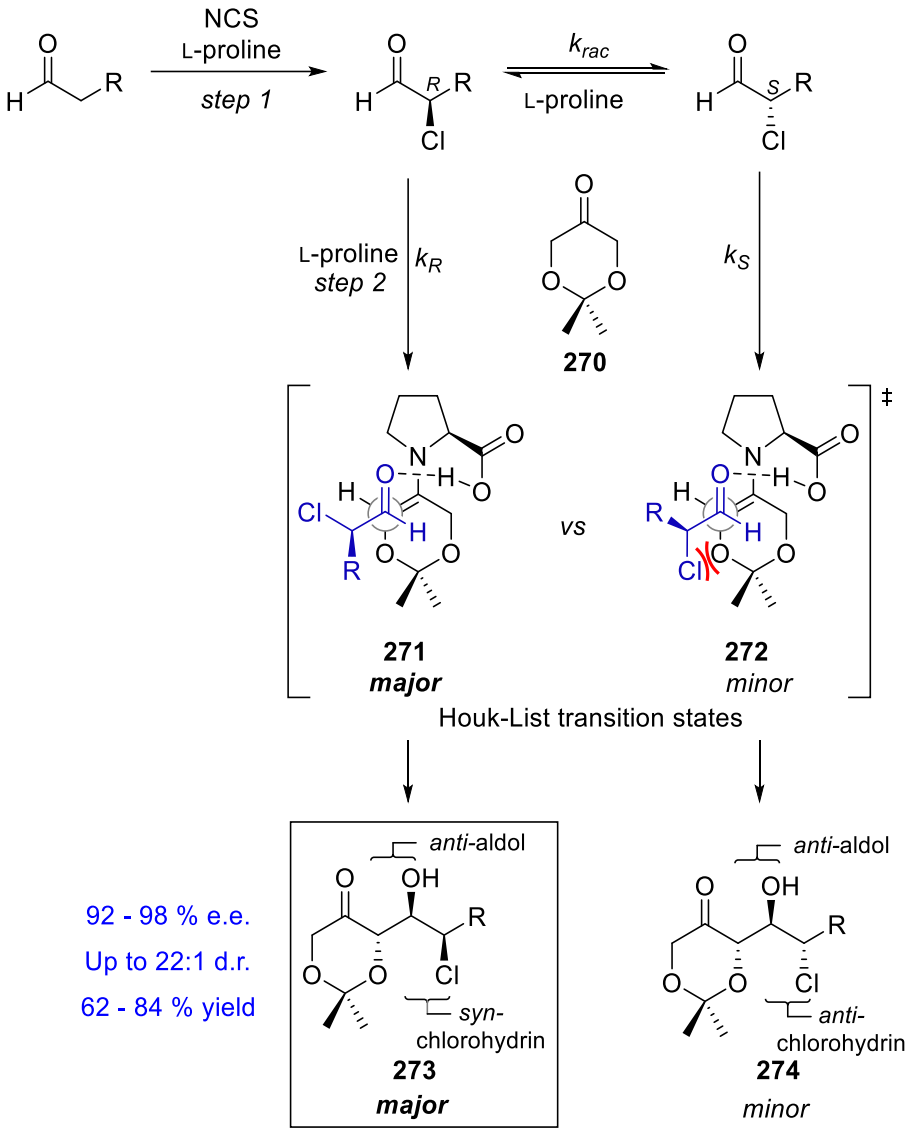

Scheme 2.51. The Dynamic Kinetic Resolution Driving the Britton Group Tandem α-Chlorination-aldol Reaction.

The reaction can be split into three steps: a proline catalyzed α-chlorination resulting in a near racemic mixture of α-chloroaldehydes, condensation of the proline onto the ketone **270**, and subsequent nucleophilic attack of the resulting enamine on the α-chloroaldehyde (Scheme 2.51). Importantly, the second step of the process effects a dynamic kinetic resolution (DKR) controlled by the difference in energy between the two Houk-List transition states (**271** and **272**, Scheme 2.51). It was proposed that electrostatic repulsion between the α-chlorine atom and the endocyclic oxygen of the dioxanone (see)(in **272** of Scheme 2.51) in **272** was responsible for the selectivity of this process.[120,121]

Consequently, the *anti*-aldol *syn*-chlorohydrin **273** obtained via **271** is preferentially formed over the *anti*-aldol *anti*-chlorohydrin **274** (i.e. $k_R > k_S$). Racemization of both α-chloroaldehydes by proline (i.e. $k_{rac} >> k_S, k_R$) is then responsible for the dynamic nature of this process. Typically, the enantiomeric excess of the resulting chlorohydrin is extremely high (92-98%).

While somewhat counterintuitive, colleagues in the Britton lab have developed a process to convert chlorohydrins **274** into α-chloroaldehydes **278** (Scheme 2.52). Here, it was found that treatment of **274** with a solution of hydrochloric acid in methanol gave triol **277**, which was then reacted with sodium periodate to provide the corresponding aldehyde **278** (Scheme 2.52). Most notably, the α-chloroaldehydes **279** and **280** were produced in reasonable yields and high enantiopurity using this process (92% e.e. and 97% e.e. respectively, Scheme 2.52).

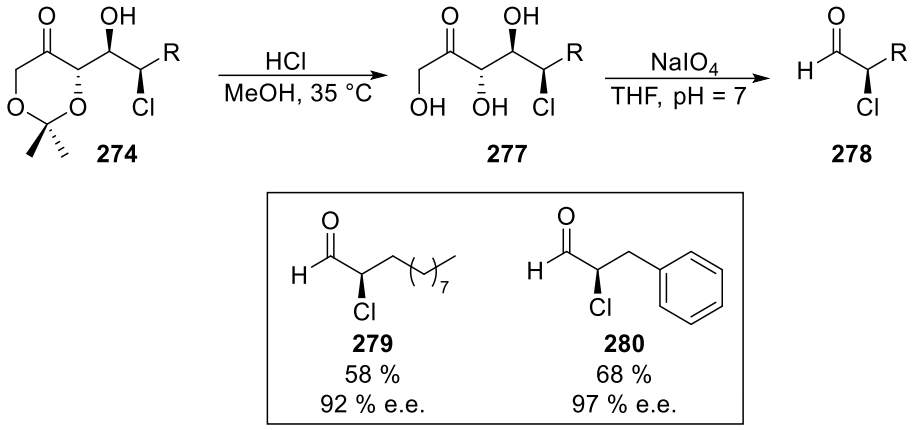

Scheme 2.52. Synthetic Sequence to Access Enantiopure α-Chloroaldehydes.
Work performed by Marjan Mohammed.

Based on these new insights, hexenal **221** was subjected to the above process. Here, the tandem α-chlorination-aldol reaction furnished the *anti*-aldol-*syn*-chlorohydrin **281** in 60% yield (Scheme 2.53). Subsequent acetonide cleavage with a solution of hydrochloric acid in methanol provided the desired triol intermediate **282** in good yield. Unfortunately, treatment with sodium periodate resulted in a mixture of α-chloroaldehyde **220** and hydrate **283**. Upon repetition of this reaction, it appeared that the formation of the hydrate side-product **283** was highly dependent on the acidity of the reaction mixture. For example, more hydrate **283** was formed when sodium bicarbonate was added. Instead,

acidic treatment after completion of the reaction provided only the desired α-chloroaldehyde **220**. Nevertheless, in the case of α-chloroaldehydes acidification increases the risk of epimerization. Moreover, as no such side-product was formed during the preparation of any other α-chloroaldehydes via this process (Scheme 2.52), the formation of the hydrate **283** is likely substrate-dependent and thus, this process was not investigated further.

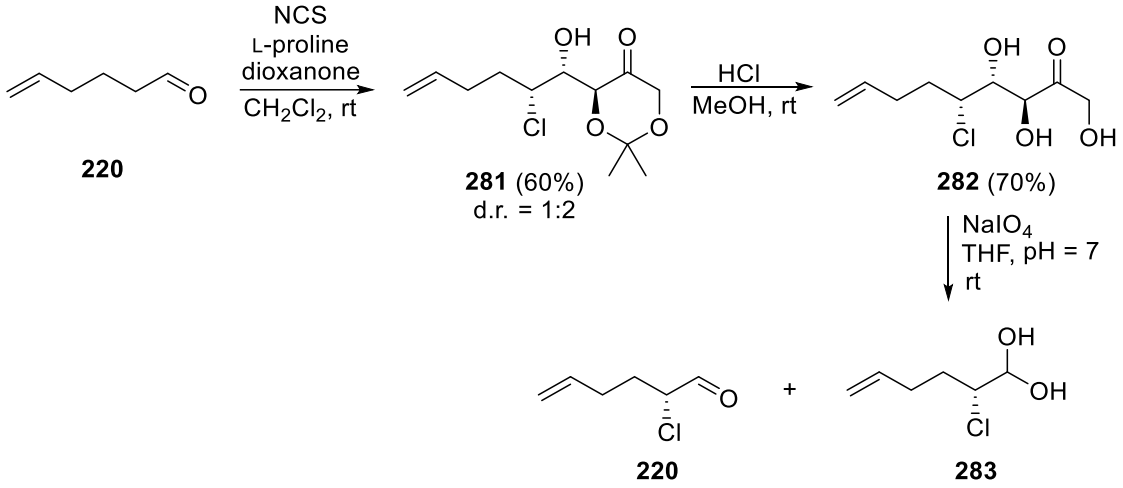

Scheme 2.53. Tandem α-Chlorination-aldol Reaction of Hexanal.

Anecdotally, it has been observed that aldehydes with a terminal alkene function tend to behave poorly (low e.e., low yield) in α-chlorination reactions. Based on our own challenges with 5-hexenal **221**, we elected to explore the α-chlorination of 6-hydroxyhexanal derivatives. With this process in mind, several protected derivatives of 6-hydroxyhexanal were prepared and the yield and enantioselectivity of the α-chlorination were evaluated. As depicted in Scheme 2.54, treatment of 1,6-hexanediol **284** with benzylbromide and sodium hydride furnished the desired mono-protected alcohol **285** in 70% yield. Subsequent pyridinium chlorochromate oxidation and α-chlorination using L-prolinamide and *N*-chlorosuccinimide afforded the corresponding α-chloroaldehyde **287**. Sodium borohydride reduction of aldehyde **287** and subsequent chiral HPLC revealed a 50% e.e.. Moreover, following screen of α-chlorination conditions (catalyst's loading, concentration and temperature) did not improve upon this result.

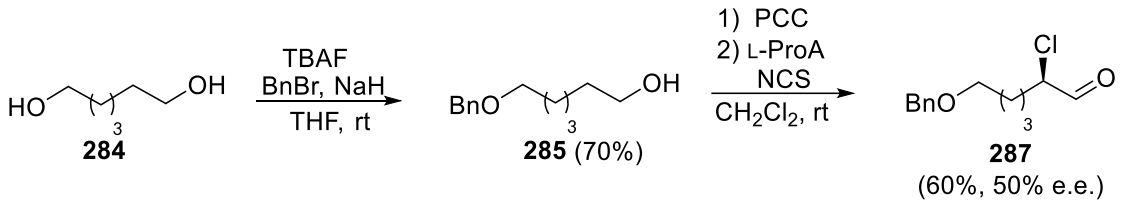

Scheme 2.54. Synthesis of Benzyl Protected α-Chloroaldehyde 287.

As an alternative strategy, the benzyl-protected aldehyde **288** was subjected to the α-chlorination-aldol-cleavage sequence (Scheme 2.55).

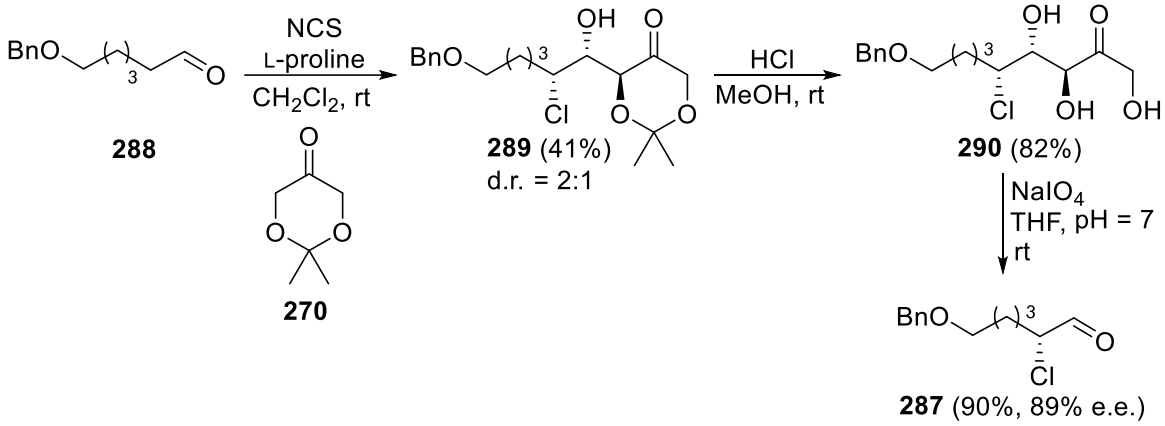

Scheme 2.55. Transformation of Aldehyde 288 into α-Chloroaldehyde 287.

Here, reaction of aldehyde **288** with L-proline and dioxanone **270** furnished the desired *anti*-aldol *syn*-chlorohydrin **289** in 41% yield (Scheme 2.55). Subsequent cleavage of the acetonide and the diol functions provided the α-chloroaldehyde **287** in 74% yield from the aldol adduct **289**. Chiral HPLC of the reduced α-chloroaldehyde (CHIRALCEL-AD column; flow rate 0.5 mL/min; eluent: hexanes-EtOAc 90:10; detection at 215 nm; retention time = 11.7 min and 13.5 min) indicated an enantiomeric excess of 89%. Despite this significant improvement, the low yield of the tandem α-chlorination/aldol reaction effected the overall yield of the sequence and thus, this method was not pursued further.

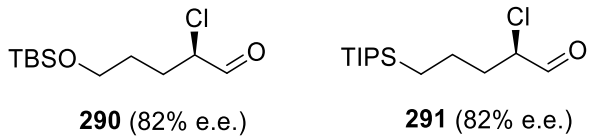

290 (82% e.e.) **291** (82% e.e.)

Figure 2.3. Structure of α-chloroaldehydes 190 and 191.

At this point, we chose to investigate the effect of protecting group and evaluated the TBS-protected α-chloroaldehyde **290** and the TIPS-protected α-chloroaldehyde **291** (Figure 2.3), both synthesized using a protection-oxidation-α-chlorination sequence as exemplified with compound **287** (Scheme 2.54). Determination of the enantiomeric excess using the Mosher ester method revealed an 82% e.e. for both aldehydes **290** and **291**. Here, despite the improved enantioselectivity of the α-chlorination, the TBS-protected α-chloroaldehyde **290** was found to be unstable and thus, only the TIPS-protected α-chloroaldehyde **291** was selected as a potential precursor of the C14-C26 fragment of eribulin. After examination of a small collection of purification methods (chromatography columns using various stationary phases and synthesis of a transient bisulfite salt intermediate), it was found that purification of aldehyde **291** using a C2-modified silica gel[122] chromatography column provided a clean α-chloroaldehyde **291** (>95% purity on ^{1}H NMR) without epimerization of the α-stereogenic centre (as determined by the Mosher ester method).

Before returning to the synthesis of Eisai intermediate **76**, we also explored the production of α-chloroaldehyde **294** (Scheme 2.56), which has one additional carbon and could serve as a late-stage aldehyde precursor through oxidative cleavage of a terminal alkene function. Following a reported procedure,[123] the commercially available epoxide **292** was converted to heptenal **293** and subsequently subjected to Jørgensen's α-chlorination procedure. Unfortunately, this reaction produced only small amount of the desired α-chloroaldehyde **294** and thus, an alternative α-chlorination method was investigated. Notably, **293** was subjected to Christmann's α-chlorination protocol that combines the MacMillan imidazolidinone *ent*-**169** with NCS.[90] To assess this process, the organocatalyst *ent*-**169** was synthesized in 4 steps from D-alanine methyl ester hydrochloride following procedures adapted from the literature (See Scheme 3.13, section 3.2.3 for more details).[124] Unlike Jørgensen's procedure, α-chlorination of heptenal **293** using Christmann's reaction conditions uniquely produced the corresponding α-

chloroaldehyde **294** (Scheme 2.56). Importantly, simple extraction of the reaction mixture with pentane afforded a very clean product (>95% purity) that could directly be used in the next step without further purification. Moreover, further transformation into the para nitrobenzoate ester **295** and subsequent chiral HPLC revealed an excellent enantiomeric purity (95% e.e., Scheme 2.56). Given the better overall purity profile of aldehyde **294** compared to the two other candidates **220** (Scheme 2.50) and **291** (Figure 2.3), it was selected for further investigations.

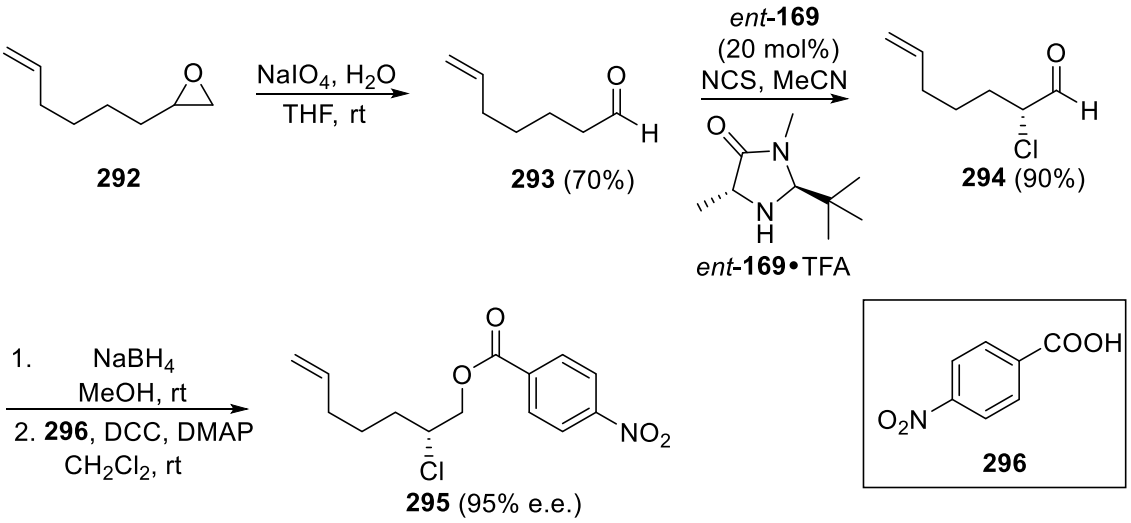

Scheme 2.56. Synthesis of α-Chloroaldehyde 294 from 1,2-Epoxy-7-octene 292.

2.2.3.3. Optimized synthesis of the C14-C26 fragment of eribulin

As depicted in Scheme 2.57, lithium aldol reaction of the α-chloroaldehyde **294**, previously synthesized from the corresponding aldehyde using Christmann modification of the MacMillan α-chlorination, with the enolate derived from **219** delivered the β-hydroxy ketochlorohydrin **297** in 65% yield (d.r. = 1:4). It is noteworthy that efforts directed towards the production of a clean α-chloroaldehyde (**e.g.**, pentane extraction) greatly improved the yield of the aldol reaction (40% previously, Scheme 2.32). Subsequent *syn*-reduction of the 1,3-hydroxyketone moiety in **297** followed by a silver-promoted cyclization, delivered the tetrahydrofuranol **298** in 60% overall yield. Oxidative cleavage of the terminal alkene in **298** using osmium tetroxide and sodium periodate provided a mixture of aldehyde **299** and acetal **300** (as determined by analysis of the crude ^{1}H NMR spectra). While the subsequent L-prolinamide α-chlorination also delivered a similar mixture of acetal and

aldehyde, HWE reaction provided the α,β-unsaturated carbonyl **301** in excellent yield from **298**. DMP oxidation of the alcohol function in **301** and subsequent manganese-catalyzed silicon hydride reduction, then delivered a mixture of diastereoisomers with regards to the C25 stereogenic centre (**302a** and **302b**, d.r. = 1.5:1, Scheme 2.57). The undesired *anti*-chloromethyl ketone **302b** was then treated with a cold solution of DBU in acetonitrile. Unfortunately, under these conditions the stereogenic centre adjacent to the C19 ketone was also epimerized.

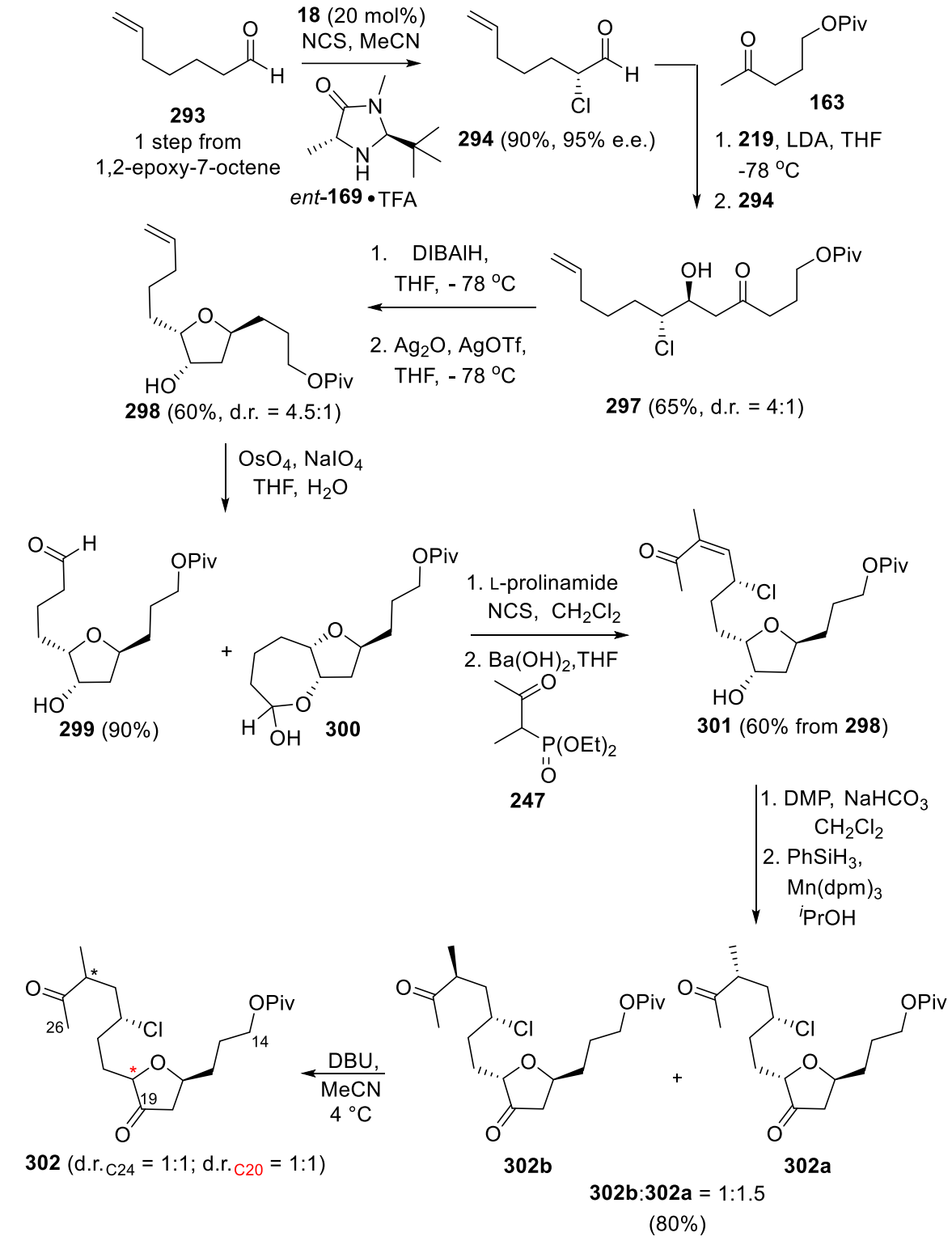

Scheme 2.57. Synthesis of the Advance Intermediate 302.

To avoid this undesired event, investigations directed towards installing the olefin function on the tetrahydrofuran ring before submitting the undesired configurational isomer to the recycling process were initiated. Here, we faced the clear challenge of regioselectively olefinate the C19 ketone over the C26 ketone. Our investigation of this reaction is summarized in Table 2.6.

Table 2.6. Selective Olefination of the C19-Carbonyl in ketone 302a.

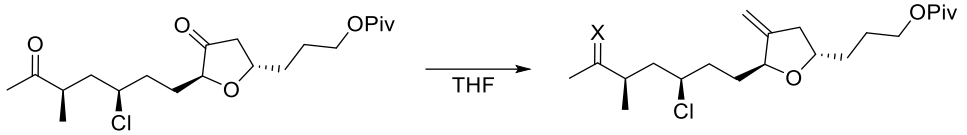

302a

303 (X = O)
304 (X = CH_2)

entry	reagents (equiv.)	temp. (°C)	time (h)	conv.*	303:304*
1	*t*BuOK (3), CH_3PPh_3Br (3)	25	5	100%	0:1
2	*t*BuOK (3), CH_3PPh_3Br (3)	25	2	48%	1:2
3	*t*BuOK (3), CH_3PPh_3Br (3)	0	5	38%	1:2
4	*t*BuOK (2), CH_3PPh_3Br (1),	25	5	0%	N.D.
5	*t*BuOK (1), CH_3PPh_3Br (1)	25	5	0%	N.D.

*From analysis of ^{1}H NMR spectra recorded on crude reaction mixtures. N.D. = not determined.

First, **302a** was submitted to Wittig reaction conditions that have been used for the olefination of closely related tetrahydrofuran substrates.[125] Unfortunately, only the *bis*-olefinated product **304** was formed using these conditions (entry 1). Reducing the reaction time to 2 hours provided small amounts of the desired product **303** but in a mixture with the diene **304** and unreacted starting material **302a** (entry 2). At 0 °C, a similar mixture was produced (entry 3). Moreover, if only one equivalent of phosphonium was used, the reaction did not proceed (entries 4 and 5). Alternative bases such as *n*-Butyllithium and sodium hydride were then investigated but did not provide better results. Moreover, the other olefination reactions tested, such as the Peterson olefination,[126] did not provide better selectivity and thus, we elected to return to the previously prepared TBS-protected derivative **243a** (Scheme 2.49).

Thus, tetrahydrofuranol **298** (synthesized in 4 steps from heptenal **293**, Scheme 2.57) was silylated using TBSOTf in dichloromethane (Scheme 2.58). The following oxidative cleavage delivered the desired aldehyde **244** in excellent yield. Subsequently, the material was subjected to Jørgensen's organocatalytic α-chlorination reaction. Disappointingly, although some of the desired α-chlorinated product **246** was formed, the

diastereoselectivity of the reaction was low (d.r. = 2:1). To our delight, when using the Christmann reaction conditions, the stereoselectivity of the reaction was greatly improved (d.r. = 7:1). Moreover, direct extraction of the reaction mixture with pentane provided a clean α-chloroaldehyde **246** (>95% purity) that was directly used in the next HWE reaction without further purification. Here, the α,β-unsaturated carbonyl **248** was formed in 60% yield from **244**. The subsequent manganese-catalyzed, silicon hydride reduction then produced a mixture of diastereoisomers (**243a**:**243b** = 1.5:1). The undesired configurational isomer **243b** was then treated with DBU in MeCN to provide a clean mixture of **243a** and **243b**. Another iteration of this process delivered the C14-C26 fragment **243a** in 60% yield from **248**.

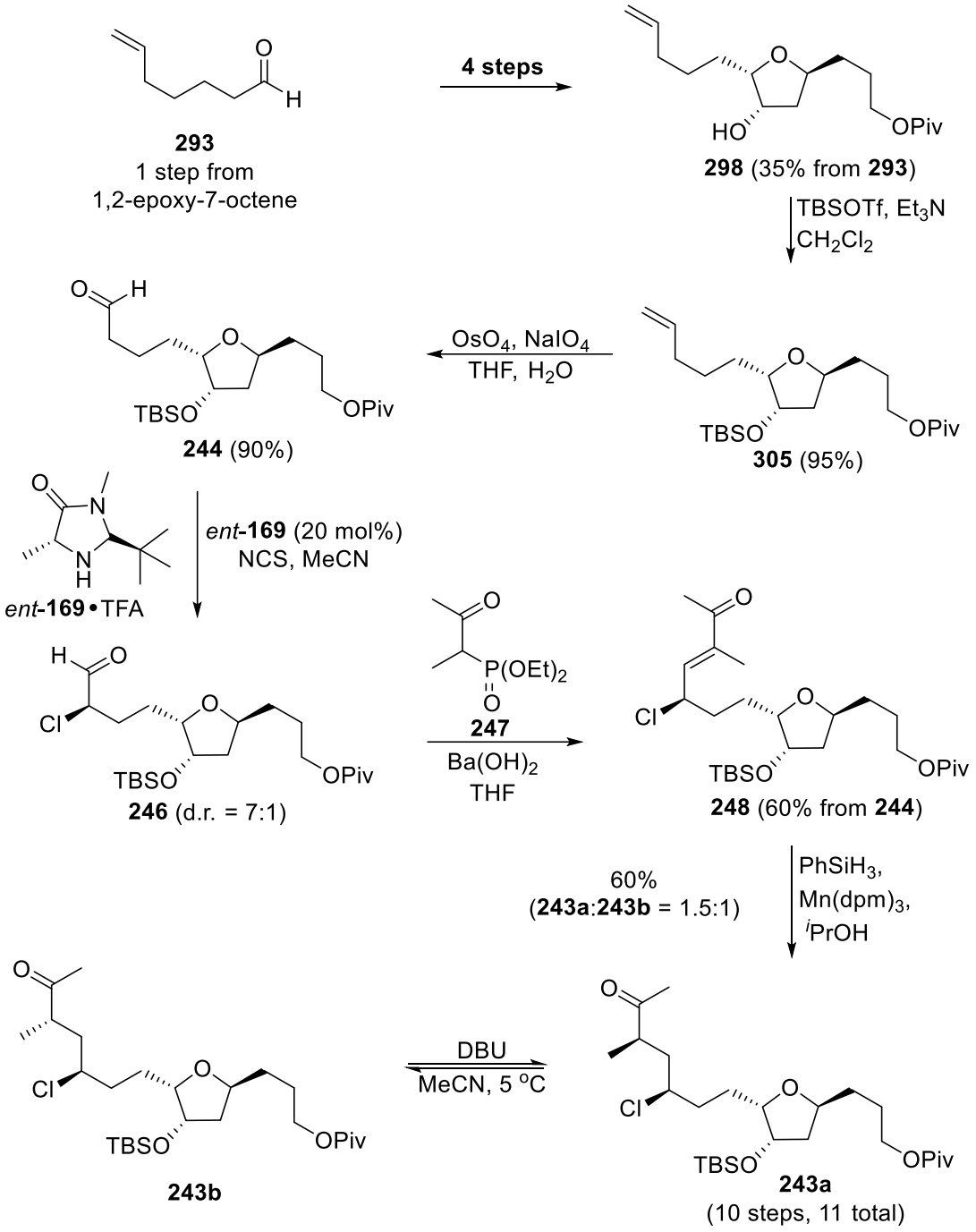

Scheme 2.58. Optimized Synthesis of the C14-C26 Fragment of Eribulin 243a.

To summarize, despite many challenges and difficulties encountered during the construction of the C14-C26 fragment of eribulin, the different synthetic strategies investigated and abandoned, a short and stereoselective synthesis of the advance intermediate **243a** was developed. Overall, this key precursor was synthesized in 10 steps

(longest linear sequence) from cheap, commercially available starting materials and 11% overall yield.

2.3. Synthesis of the C27-C35 fragment of eribulin

As described earlier in this chapter, our synthetic approach toward the Eisai C14-C35 fragment of eribulin is based on a late-stage Corey-Chaykovsky reaction between a sulfonium salt **136** and a ketone **137** (Scheme 2.13). In this chapter, we will summarize the challenges encountered during the elaboration of the C27-C35 building block **136**. Importantly, this work was initiated by Dr. Huimin Zhai and brought to completion by Dimitri Panagopoulos with later assistance from Dr. Guillermo Caballero.

2.3.1. Retrosynthetic analysis

As depicted in Scheme 2.59, the bicyclic derivative **306** was proposed as a potential precursor of the sulfonium salt **136**. Here, arylation of the thioether function in **306**, and a few straightforward functional group modifications that include the inversion of the C31 asymmetric centre, would complete the assembly of **136**. In turn, this material can be easily traced back to the *syn*-chlorohydrin **307** through a reduction-cyclization sequence. Finally, disconnection of the indicated bond in **307** provides ketone **308** and aldehyde **309** as potential precursors. In the synthetic direction, a tandem α-chlorination-aldol reaction (Scheme 2.51) between **308** and **309** could achieve the formation of the C30-C31 bond.

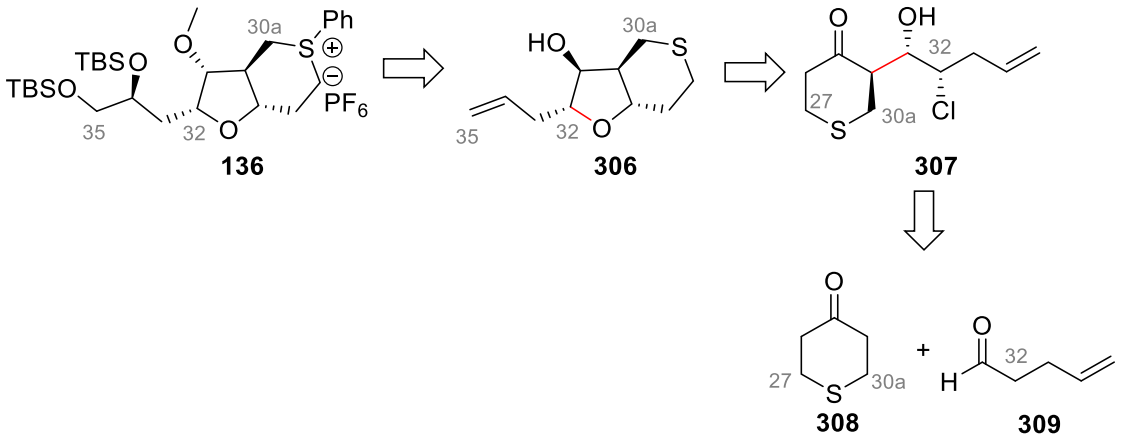

Scheme 2.59. Retrosynthesis of Sulfonium salt 137.

2.3.2. Synthesis

Huimin Zhai initiated this project in 2016 and focused on assessing the synthetic feasibility of the proposed strategy. As depicted in Scheme 2.60, treatment of pentenal **309** with *N*-chlorosuccinimide and D-proline followed by addition tetrahydrothiopyranone **308**, furnished the desired *anti*-aldol *syn*-chlorohydrin **307** albeit in low yield (40%, d.r. = 4:1). Subsequent diisobutylaluminum hydride reduction provided the corresponding *syn*-diol **310** in quantitative yield (d.r. = 4:1). The latter material **310** was then heated at 120 °C in methanol to provide the cyclized product **306**. Methylation of the alcohol function in **306** proceeded smoothly using dimethyl sulfate and sodium hydride. Finally, treatment of the resulting product **311** with diphenyliodonium hexafluorophosphate and catalytic amount of copper benzoate achieved the synthesis of the sulfonium salt **312**. Here, although the C31- stereogenic centre was incorrectly configured, the synthetic feasibility of each key step was validated.

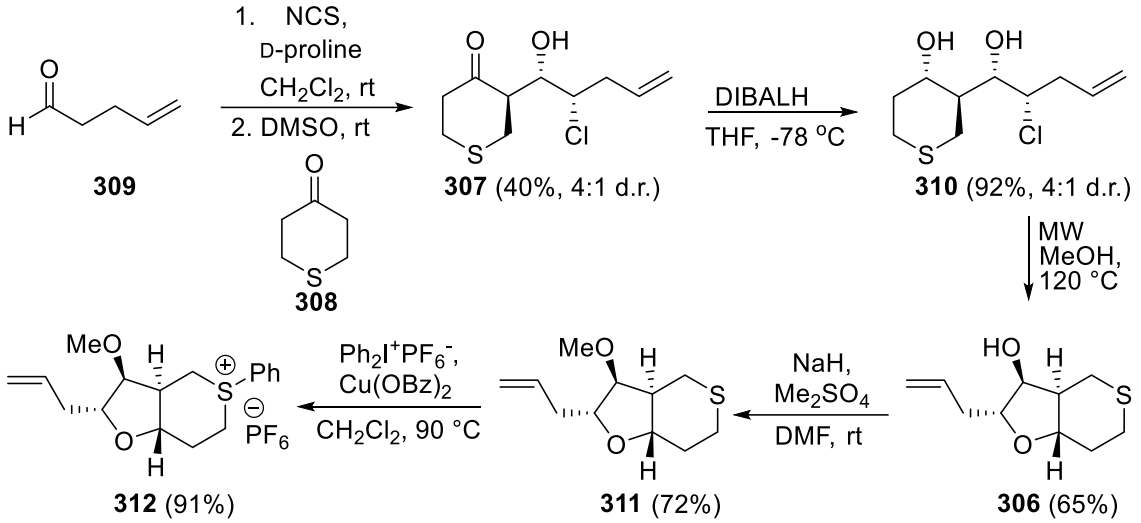

Scheme 2.60. Synthesis of Sulfonium salt 312.
Synthesis performed by Dr. Huimin Zhai.

Following this work, Dimitri Panagopoulos aimed to confirm the relative configuration of the different stereogenic centres established during the sequence. Based on the route shown in Scheme 2.60, the alcohol *ent*-**306** was synthesized in three steps from pentenal **309** (Scheme 2.61). It is noteworthy that L-proline was used in the optimization of the tandem α-chlorination-DKR-aldol reaction instead of D-proline owing to

cost. Esterification of *ent*-**306** using *para*-nitrobenzoyl chloride and triethylamine, and subsequent recrystallization, furnished the ester **313** as a white solid. X-Ray crystallographic analysis of ester **313** (Scheme 2.71) confirmed the originally proposed stereochemistry and thus, a Mitsonobu reaction was necessary to access the correctly configured isomer at C31.

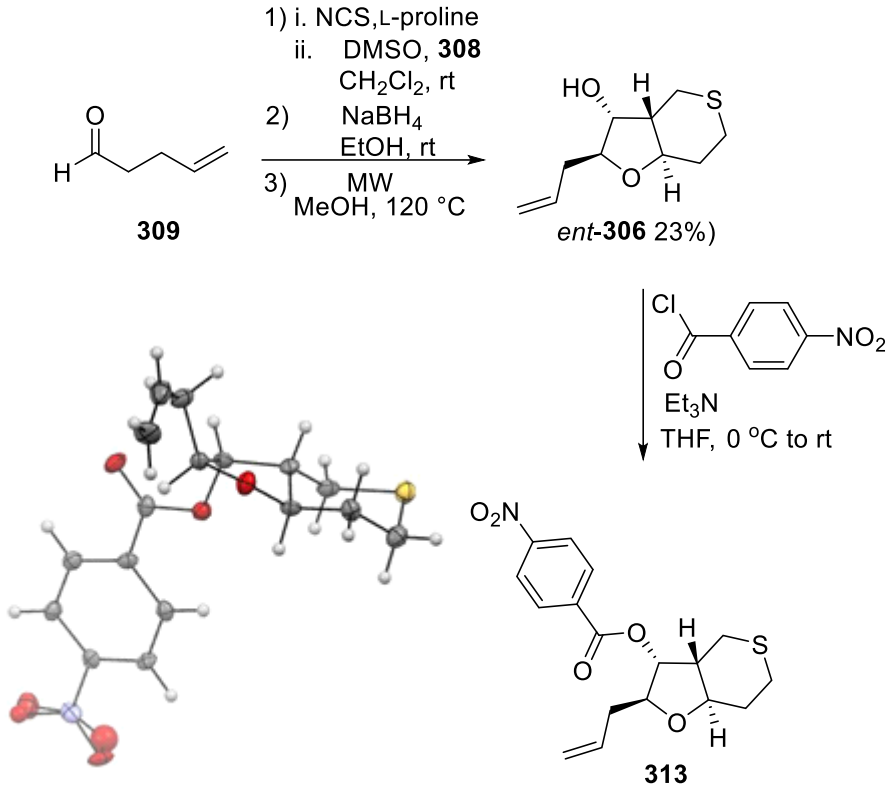

Scheme 2.61. Synthesis of *para*-Nitrobenzene Derivative 313.
Synthesis performed by Dimitri Panagopoulos

Toward this goal, the alcohol *ent*-**306** was treated with *p*-nitrobenzoic acid and DIAD (Scheme 2.62). Subsequent hydrolysis of the resulting ester provided the correctly configured alcohol **314** in 75 % yield. The latter material was then smoothly methylated using the previously established reaction conditions (e.g., **315**, Scheme 2.62). In the subsequent arylation reaction, heating at 120 °C in dichloroethane resulted in improved yields. Thus, the sulfonium salt **316** was formed in 60% yield from the corresponding thioether **315** using the optimized conditions. Overall, a 7-step stereoselective sequence was developed to access the advanced intermediate **316**. The next objective was then to

install the TBS-protected diol moiety on the tetrahydrofuran sidechain (see **137**, Scheme 2.13).

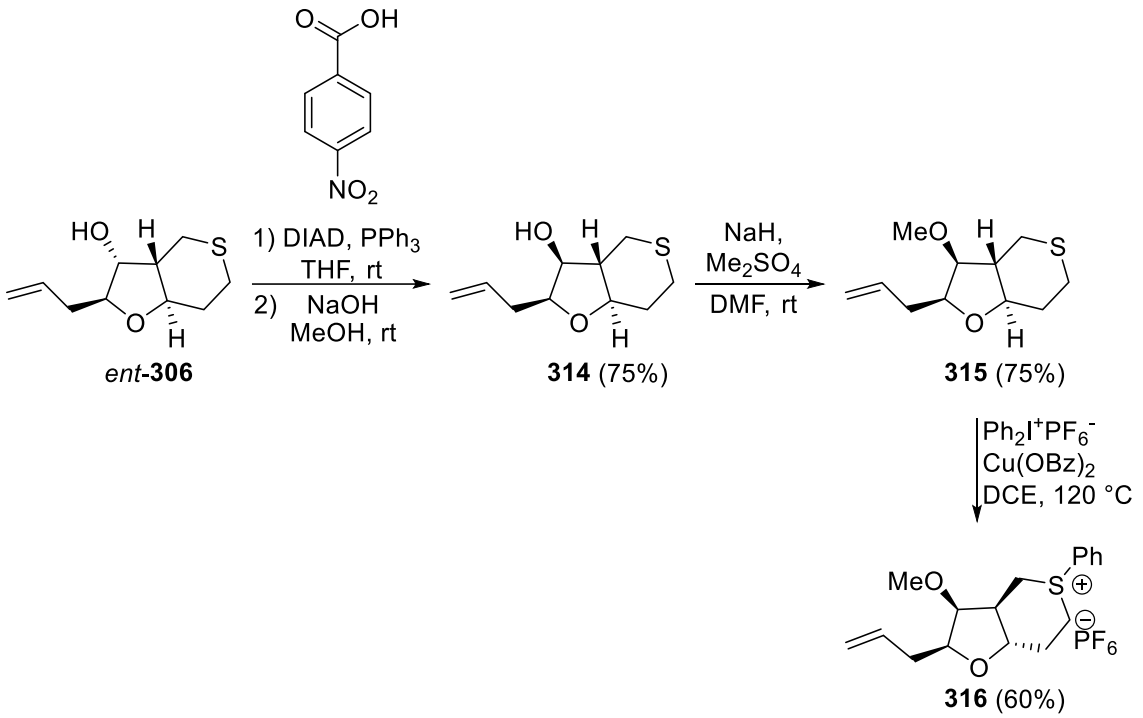

Scheme 2.62. Optimized Synthesis of Sulfonium Salt 316.
Synthesis performed by Dimitri Panagopoulos

In this regard, the Upjohn dihydroxylation[127] conditions were first investigated (Scheme 2.63). These include the use of catalytic amounts of osmium tetroxide along with stoichiometric *N*-methyl morpholine-*N*-Oxide (NMO). Mass and NMR analyses of the reaction mixture revealed that the dihydroxylated compound **317** was formed quantitatively. However, despite concerted efforts, the diol sulfonium salt **317** could not be isolated. Therefore, *tert*-butyldimethylsilyl chloride and imidazole were then directly added to the reaction mixture (Scheme 2.63). Unfortunately, only traces of product *ent*-**137** were detected in the crude mixture (as determined by ^{1}H NMR spectroscopy). Alternatively, the diol moiety was protected with an acetonide upon addition of 2,2-dimethoxypropane and pyridinium *p*-toluenesulfonate (PPTS). Here, up to 50% yield (over two steps) of the product **318** were produced through repetition of this process gave inconsistent results. Moreover, subsequent efforts to install the diol function before arylation of the thioether also failed to provide a workable solution. Combined with the lack of stereoselectivity in

the Upjohn dihydroxylation (d.r. = 1.3:1, Scheme 2.63), it was decided to install the protected diol moiety earlier in the sequence.

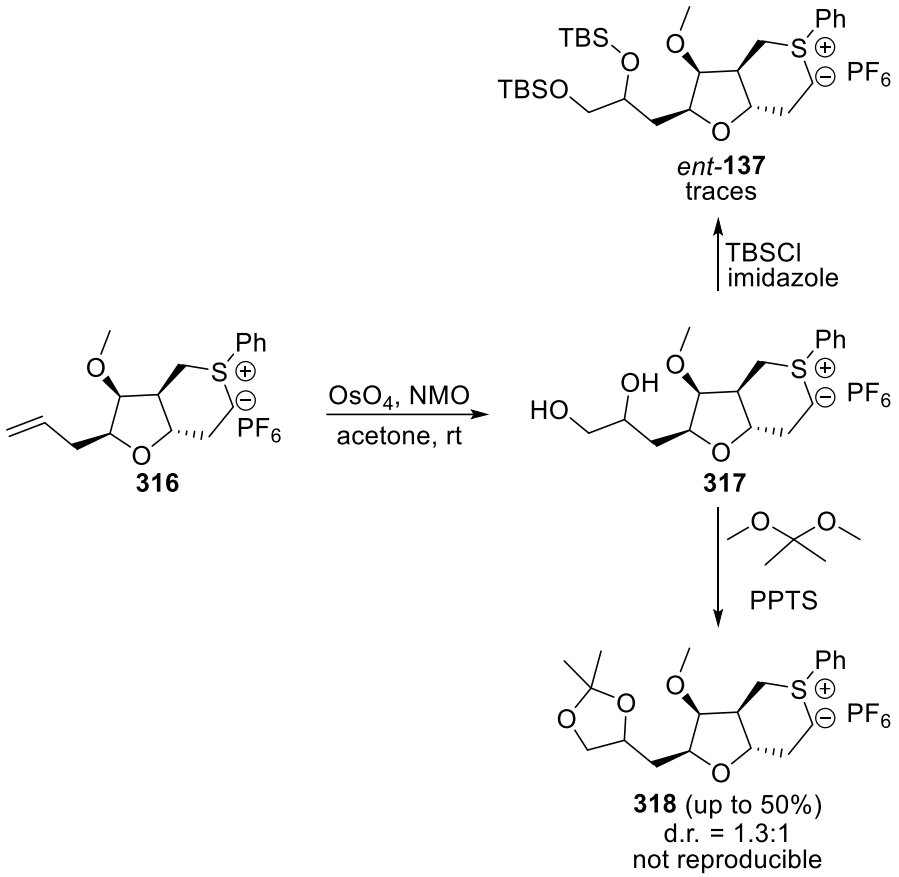

Scheme 2.63. Dihydroxylation Attempts on Alkene 316.
Synthesis performed by Dimitri Panagopoulos.

2.3.3. Revised synthesis

Given the difficulties encountered with a late-stage installation of the diol moiety in the C27-C35 fragment, we elected the known acetonide protected aldehyde **323**[128–130] to produce the sulfonium target **329** (Scheme 2.64). Thus, treatment of L-glutamic acid **319** with sodium nitrite and hydrochloric acid provided the lactone **320** in 65% yield. Subsequent reduction of the carboxylic acid function in **320** furnished the corresponding alcohol **321** quantitatively. Nucleophilic opening of lactone **321** and acetonide protection of the resulting diol were successfully conducted in a one-pot reaction using 2,2-dimethoxypropane (**e.g.**, **321** and **322**, Scheme 2.64). Subsequent diisobutylaluminum

hydride reduction of ester **322** provided the corresponding aldehyde **323** in excellent yield. The latter material was then submitted to a tandem α-chlorination-DKR-aldol with tetrahydrothiopyranone **308**. While the yield was rather low (33%), the desired *syn*-chlorohydrin **324** was formed in good diastereoselectivity. Subsequent reduction with sodium triacetoxyborohydride provided the *syn*-diol **325** (d.r. = 4:1). Based on recent work in the Kishi group, treatment of chlorohydrin **325** with strontium carbonate in refluxing *tert*-butanol delivered the cyclized product **326** in 52% from **324**. We were pleased to find an alternative to the previous microwaved-induced cyclization which limited the scale of the reaction and often leads to removal of acid-sensitive acetonide protecting groups. Inversion of the C31-stereogenic centre was successfully conducted using the previously developed Mitsunobu-hydrolysis reaction conditions. The correctly configured alcohol **327** was then formed in 58% yield from **326**. Subsequent methylation with dimethyl sulfate provided the advance intermediate **328** in excellent yield (89%). Finally, arylation of the sulfide moiety in **328**, using the previous diphenyliodonium reaction conditions, delivered the corresponding sulfonium salt in 74% yield. Thus, the stereoselective synthesis of the C27-C35 building block **329** was achieved in 11 steps and 4% yield from the commercially available L-glutamic acid (**319**).

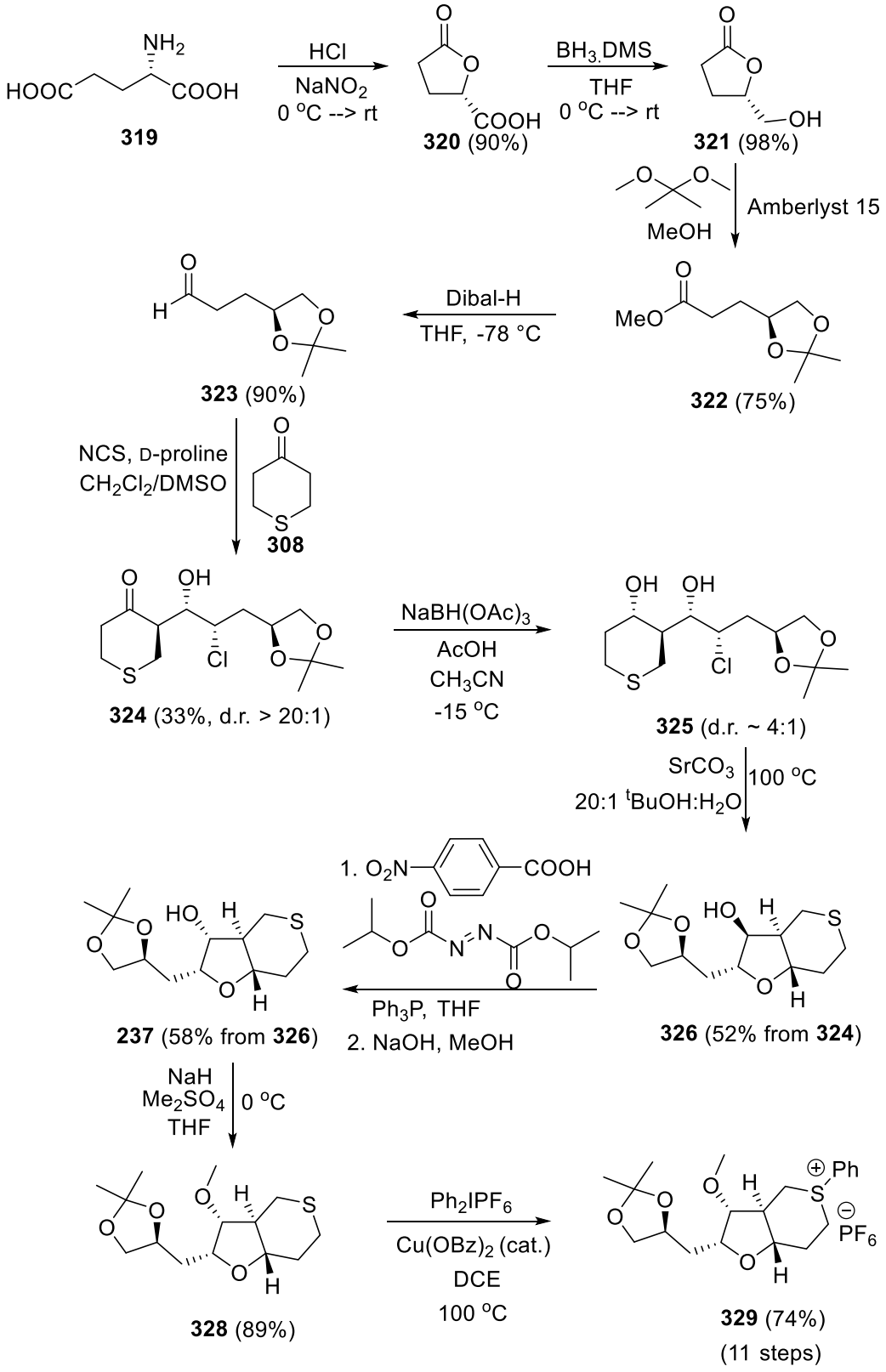

Scheme 2.64. Synthesis of the C27-C35 Building Block 329.
Synthesis and full characterization performed by Dimitri Panagopoulos.

2.4. Synthesis of Eisai key intermediate

As described in the previous sections, our retrosynthetic strategy is based on a late-stage Corey-Chaykovsky reaction (Scheme 2.13). In this section, the development of this key coupling, and the following epoxide-isomerization and cyclization reactions, will be described.

2.4.1. The Corey-Chaykovsky reaction

2.4.1.1. Proof of concept

Having established a short and stereoselective synthesis of the C14-C26 and C27-C35 building blocks, we then explored the key coupling reaction. As described in the introduction (section 2.1.4.3), the Corey-Chaykovsky reaction involves the addition of a sulfur ylide to a ketone to produce an epoxide. Only a few examples of cyclic sulfur ylides are described in the literature, but we were particularly interested in testing reaction conditions developed in the Yamamoto group, who studied the reaction of 5- and 6-membered ring sulfonium ylides with various aldehydes and ketones.[79]

To assess the feasibility of this coupling, preliminary studies with tetrahydrothiopyran and simple terminal ketones were conducted. These reactions provided the corresponding epoxides in good yields and established the effectiveness of this process. Thereafter, reaction of sulfonium salt **316**, which is almost identical to the ultimate C27-C35 building block **329** (Scheme 2.64), with the α-methyl ketone **255** was investigated (Scheme 2.65). Notably, the ketone **255** incorporates a methyl in α-position and a TBS-protected alcohol and thus, we expected that its reactivity with **316** would provide valuable insight into the planned Corey-Chaykovsky reaction.

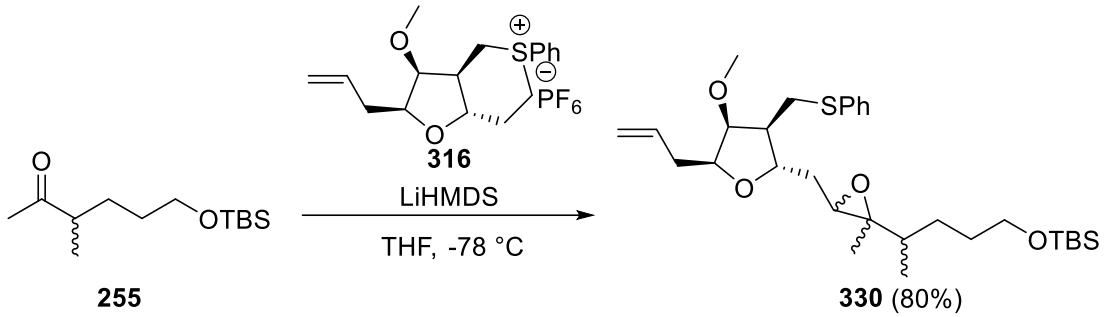

Scheme 2.65. Corey-Chaykovsky Reaction of Ketone 255 and Sulfonium Salt 316.
Formation of epoxide 330 (diastereoisomeric mixture) was confirmed by ^{1}H NMR spectroscopy and mass spectrometric analysis.

We were glad to see that deprotonation of sulfonium salt **330** with sodium *bis*(trimethylsilyl)amide and subsequent nucleophilic attack on ketone **255** provided 60% of the desired epoxide **330** albeit as a mixture of product and unreacted starting material **255**. After investigation of a small collection of bases (LDA, *t*-BuOK, NaH and LiHMDS) at various temperatures (-78 °C to 25 °C), the yield of the Corey-Chaykovsky reaction between ketone **255** and sulfonium salt **316** was increased to 80% (Scheme 2.65). This last set of conditions, LiHMDS at -78 °C, was retained for future Corey-Chaykovsky reactions.

2.4.1.2. Stereoselectivity

As depicted in Scheme 2.66, two new stereogenic centres are established during the Corey-Chaykovsky reaction (see *, **, Scheme 2.66). while the stereoselectivity at C26 (**) would be destroyed in the subsequent transformation, the stereoselectivity at C27 (*) was crucial to the synthesis of Eisai fragment **76**. The absolute configurations of the C23, C25 and C27 stereogenic centres in Eisai intermediate **76** are *S*, *R* and *R*, respectively. Thus, if the epoxide resulting from the Corey-Chaykovsky reaction possessed the wrong stereochemistry at C27 (**e.g.**, **332**, Scheme 2.66), the absolute configuration of this stereogenic centre would need to be inverted during the transformation of **332** into the tetrahydropyran **76** and thus, additional steps would be required.

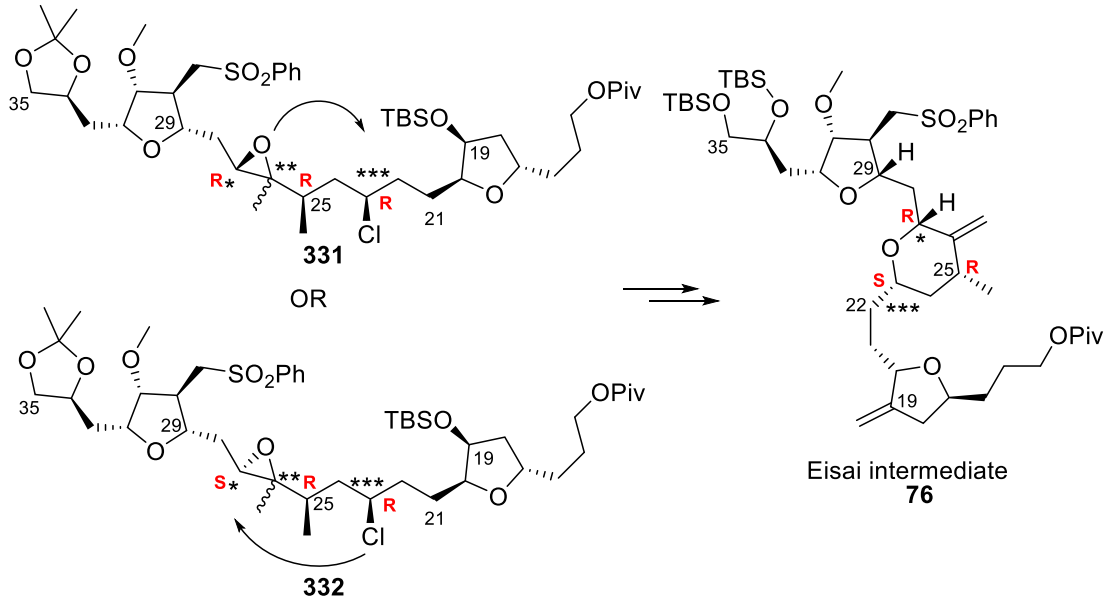

Scheme 2.66. Stereoselectivity of the Corey-Chaykovsky Reaction – a Determinant Factor for the Subsequent Cyclization.

To assess the facial selectivity of the sulfonium salt **329** (Scheme 2.64), a Corey-Chaykovsky reaction between sulfonium salt *ent*-**316** (synthesized in 8 steps using the sequence shown in Scheme 2.60 and Scheme 2.62) and cyclohexanone was performed (Scheme 2.67). Cyclohexanone **333** was chosen as a model ketone as the resulting product contains only one stereogenic centre and would thus minimize complications in determining the stereochemical outcome.

As shown in Scheme 2.67, reaction of sulfonium salt *ent*-**316** with cyclohexanone **333** and subsequent oxidation using TPAP and NMO, furnished epoxide **334** in good yield. To our delight, treatment of this product **334** with aluminum isopropoxide in refluxing tetrahydrofuran provided 40% of the desired allylic alcohol **335**. To determine the absolute configuration at the alcohol stereogenic centre (see * in Scheme 2.67), the alcohol **335** was then transformed into the *(R)*- and the *(S)*-Mosher esters **336** and **337**.

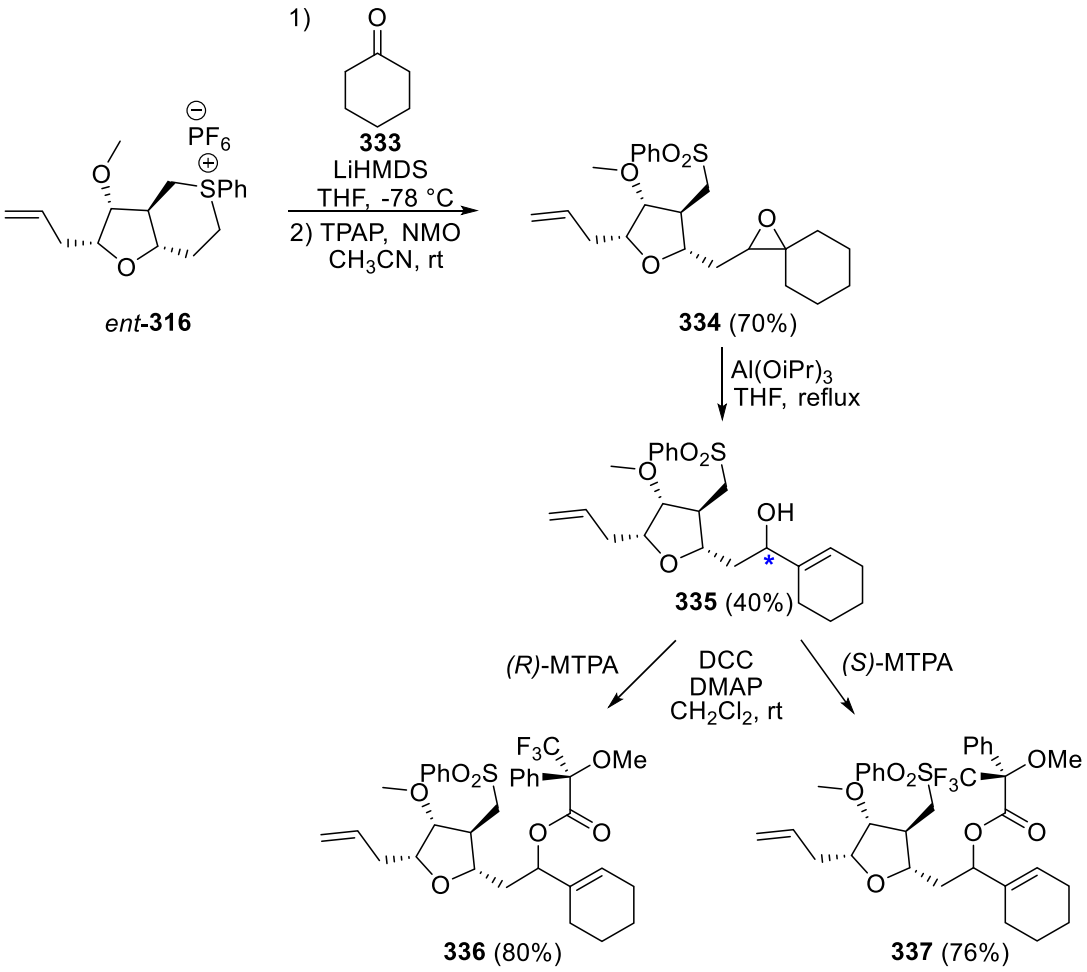

Scheme 2.67. Synthesis of the *(R)*-Mosher Ester 336 and the *(S)*-Mosher Ester 337.

To determine the absolute configuration of C*, chemical shifts of the neighboring protons in the (*S)*-Mosher ester derivative **337** were subtracted from the ones in the (*R*)-Mosher ester **336** (Figure 2.4). Here, the sign of the chemical shift difference on each side of C* indicated that this stereogenic centre is (*R*)-configured.[119] Based on these results, we predicted that the reaction between sulfonium salt **329** (Scheme 2.64) and the C14-C26-ketone **243a** (Scheme 2.58) will favour the formation of epoxide **331** (Scheme 2.66).

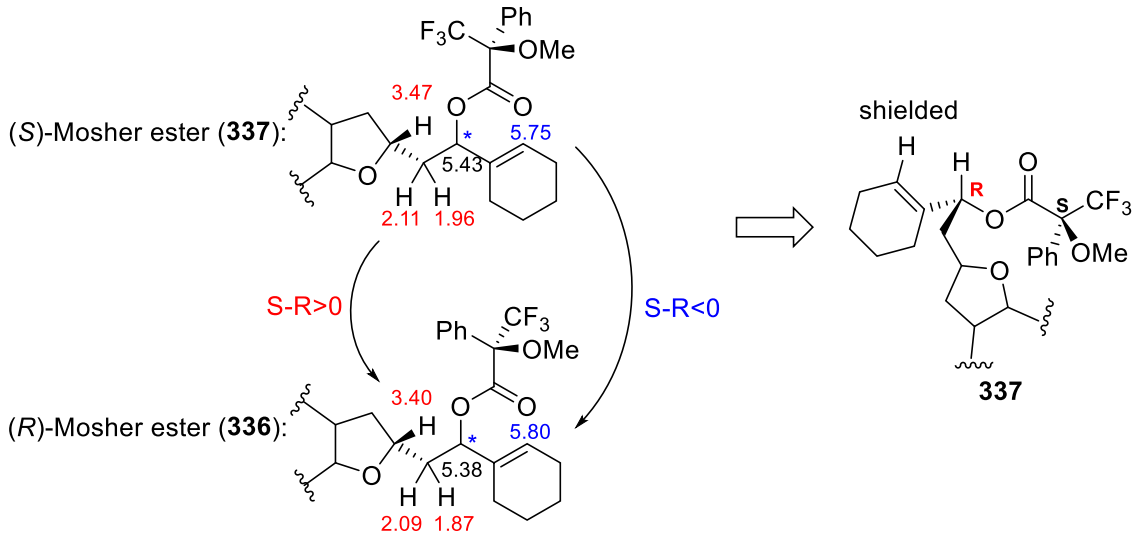

Figure 2.4. **^{1}H NMR comparison of the (*R*)- and (*S*)-Mosher ester derivatives 336 and 337.**

2.4.2. Epoxide isomerization and cyclization

Having found suitable reaction conditions for the Corey-Chaykovsky coupling and determined the stereoselectivity of the reaction, we needed to explore the subsequent transformation. As depicted in Scheme 2.68, reaction of the 6-membered ring sulfonium salt **151** with ketone **338** furnished the epoxide **339** in moderate yield. Subsequent treatment with the *i*-Pr_2NMgBr Hauser base[131] in tetrahydrofuran for three days regioselectively produced the desired allylic alcohol **340**. Unfortunately, this result was not reproducible and as a consequence, we initiated an evaluation of reaction conditions that have been reported to isomerize epoxides into allylic alcohols (Table 2.7).

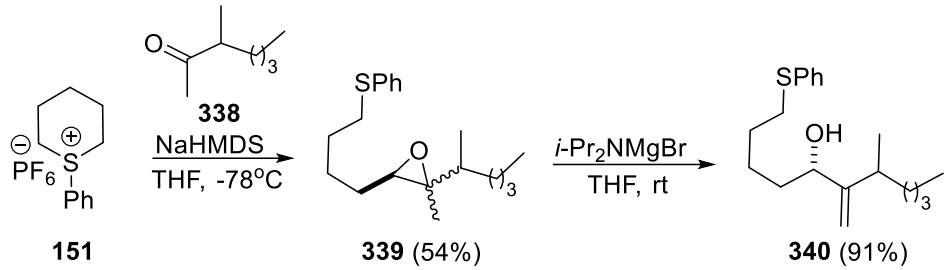

Scheme 2.68. Preliminary Studies on the Isomerization of Epoxide 339.
Synthesis performed by Dr. Huimin Zhai.

Surprisingly, treatment of the more elaborate epoxide **330** with the Hauser base did not provide any alcohol **341** even at temperatures as high as 40 °C (entry 1). Diethylaluminum 2,2,6,6-tetramethylpiperidine (Et_2AlTMP), a combined Lewis acid-base reagent known to isomerize epoxides,[132] was then tested. Encouragingly, 15% of epoxide **330** was converted to the desired allylic alcohol **341** (entry 2). Aluminum isopropoxide, which had been used successfully for the isomerization of epoxide **354** (Scheme 2.67), failed to provide any alcohol **341** (entry 3). Disappointedly, the other Lewis acids investigated did not improve upon this result (entries 4 and 5). Moreover, the TBS-protecting group was removed when **330** was treated with diethylaluminum chloride (entry 6).

Table 2.7. Reaction Conditions Investigated for the Isomerization of epoxide 330.

330 **341**

entry	reagents	solvent	temp. (°C)	conv.*	330:341*
1	iPr_2NMgBr	THF	25 to 40	35%	1:0
2	Et_2AlTMP	toluene	0 to 25	15%	6:1
3	$Al(OiPr)_3$	benzene	110	0%	1:0
4	$Ti(OiPr)_4$	toluene	80	0%	1:0
5	$Ti(OiPr)_4$	toluene	110	0%	1:0
6	Et_2AlCl	CH_2Cl_2	0	100%	0:0

*From analysis of ^1H NMR spectra recorded on crude reaction mixtures. Formation of product **341** (diastereoisomeric mixture) was confirmed by ^1H NMR spectroscopy and spectrometric analysis.

Considering that the epoxide **330** (Table 2.7) is the product of a 12-step sequence of reactions, we elected to examine the effect of a small collection of bases for the isomerization of the more easily accessible γ-chloroepoxide **344** (diastereoisomeric mixture), which was synthesized in 5 steps from hexanal **342** (Scheme 2.69). The results of this study are summarized in Table 2.8.

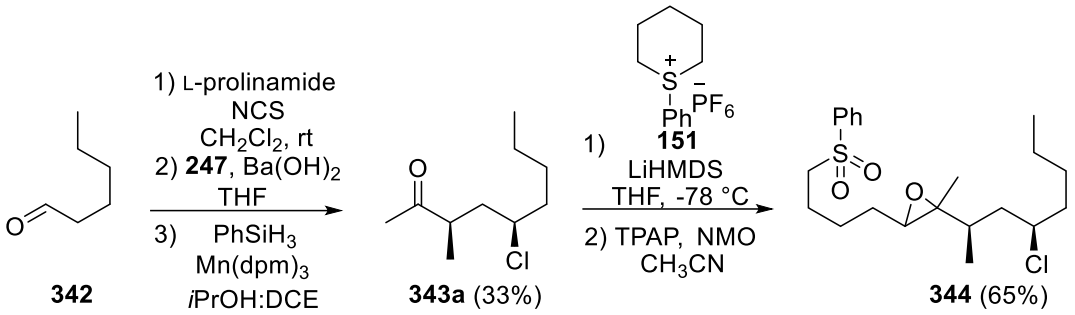

Scheme 2.69. Synthesis of Epoxide 344.
Formation of product 344 (diastereoisomeric mixture) was confirmed by ^{1}H NMR spectroscopy and mass spectrometric analysis.

Encouragingly, treatment of epoxide **344** with Et_2AlTMP furnished 10% of the desired allylic alcohol **345** (entry 1). Unfortunately, longer reaction times and higher temperatures did not improve conversion (entries 2 and 3). Subsequently, a small collection of Hauser bases was investigated. Unfortunately, as exemplified with *i*Pr_2NMgBr (entry 4), no reaction was observed at room temperature and increasing the temperature to 40 °C only resulted in the formation of the alkene side-product **346** (as determined by ^{1}H NMR spectroscopy and mass spectrometric analysis of the crude mixture).

Table 2.8. Base-promoted Isomerization of Epoxide 344.

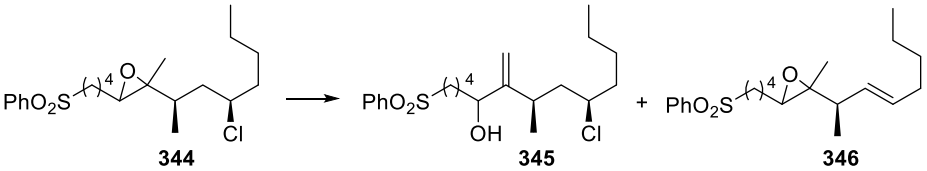

entry	base	solvent	time (h)	temp. (°C)	conv.*	280:281*
1	Et_2AlTMP	toluene	12	25	10%	1:0
2	Et_2AlTMP	toluene	72	25	10%	1:0
3	Et_2AlTMP	toluene	12	40	10%	1:0
4	*i*Pr_2NMgBr	THF	12	25 to 40	50%	0:1

*From analysis of ^{1}H NMR spectra recorded on crude reaction mixtures

As depicted in Scheme 2.70, from this disappointment, we envisioned that an appealing alternative process would involve a combination of silver oxide and silver triflate that may in one step isomerize the epoxide **344** and promote a cyclization event. Based on this hypothesis, epoxide **344** was treated with a silver (I) salt and silver oxide under a variety of conditions (Table 2.9).

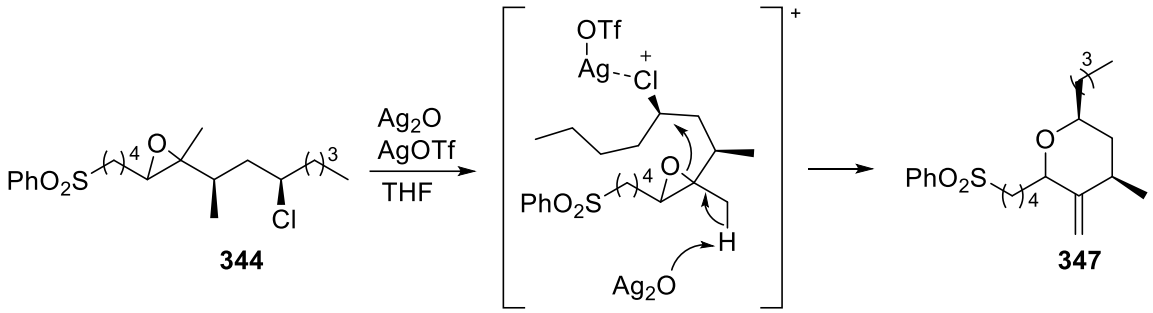

Scheme 2.70. Proposed Mechanism for a Tandem Isomerization-cyclization Reaction.

We were glad to see that the silver reaction conditions used for the cyclization of 1,4-chlorohydrins,[91] that is, sonication with silver triflate and silver oxide for an hour and subsequent stirring overnight, provided 10% of the desired allylic alcohol **345** (entry 1). Efforts to improve upon this result only led to a slightly increased conversion into the alcohol **345** (entry 2) and unfortunately, no cyclized product **347** was formed alongside. Excitingly, when epoxide **344** was solely treated with silver triflate, 30% of the desired allylic alcohol **345** was produced along with 70% of a side-product, which ^{1}H NMR spectroscopy and mass spectrometric analysis matched with a diastereoisomeric mixture of ketone **348** (Table 2.9). Building on this last result, a new screen of silver Lewis acids without silver oxide was performed on the more accessible epoxide **349** (synthesized in 5 steps from hexanal). Here, we found that the allylic alcohol **350** was produced in a 1 to 2 mixture with the ketone side-product **351** when epoxide **349** was treated with silver hexafluoroantimonate (entry 4). After screening of various solvents and temperatures, we then discovered that polar protic solvents such as *i*PrOH and *t*BuOH favoured the formation of the desired allylic alcohol **350** (entries 5 and 6). Excited by these results, isomerization of the chloro-containing derivative **344** was also performed in *t*BuOH at 60 °C, but unfortunately, the reaction did not improve the previous ratio of **345** and **348** (**345**:**348** = 3:7, entry 7).

Table 2.9. Summary of the Lewis Acid-promoted Isomerization.

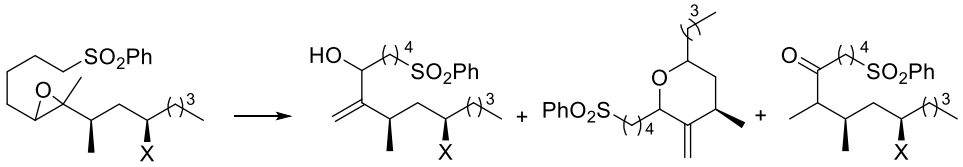

349 (X=H)
344 (X=Cl)

350 (X=H)
345 (X=Cl)

347

351 (X=H)
348 (X=Cl)

entry	subt.	reagents	solvent	temp. (°C)	conv.	ratio of products8
1	**344**	Ag_2O, AgOTf	THF	25 to 45 (sonicator) then 25	10%	**345**:**347**:**348** = 1:0:0
2	**344**	Ag_2O, AgOTf	THF	25 to 45 (sonicator) then 45	25%	**345**:**347**:**348** = 1:0:0
3	**344**	AgOTf	THF	25	100%	**345**:**348** = 3:7
4	**349**	$AgSbF_6$	THF	25	100%	**350**:**351** = 1:2
5	**349**	$AgSbF_6$	*i*PrOH	60	100%	**350**:**351** = 1:1
6	**349**	$AgSbF_6$	*t*BuOH	60	100%	**350**:**351** = 2:1
7	**344**	$AgSbF_6$	*t*BuOH	60	100%	**345**:**348** = 3:7

*From analysis of ^{1}H NMR spectra recorded on crude reaction mixtures

We next examined the so-called “Nugent reagent” (Cp_2TiCl), a single-electron-transfer complex capable of generating a radical from an epoxide.[133,134] Cp_2TiCl can be easily produced upon treatment of commercially available Cp_2TiCl_2 with reductants such as manganese or zinc. Mechanistically, reaction of an epoxide **352** with the Nugent reagent provides the more stable β-titanoxyl radical **353** (Scheme 2.71). Upon addition of another equivalent of Cp_2TiCl, the radical **353** can either undergo a disproportionation process to give the allylic alcohol **355** (Scheme 2.71, **path 1**) or generate an organometallic alkyl-Ti(IV) complex **356** which after β-elimination is transformed into the deoxygenated product **357** (Scheme 2.71, **path 2**). Importantly, which path the radical **353** is subjected to has been found to be substrate-dependent.[135] As a result, a trisubstituted or sterically hindered radical intermediate will most likely not be trapped by a second bulky Cp_2TiCl radical, but instead, it will be converted to the corresponding allylic alcohol through a disproportionation process.

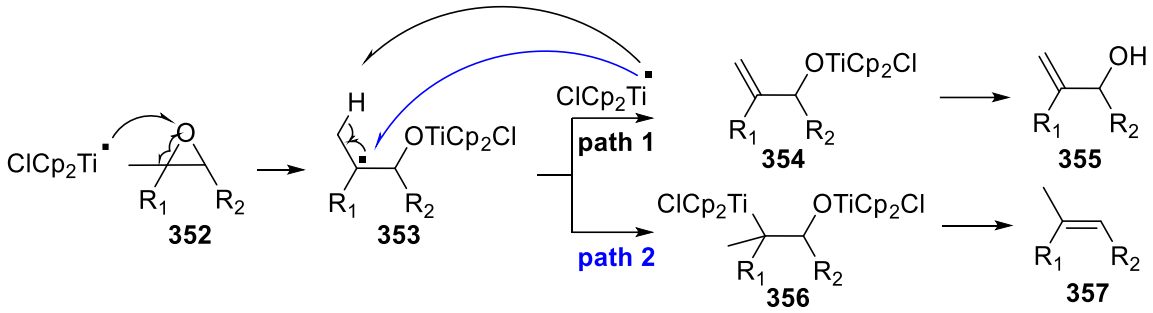

Scheme 2.71. Mechanistic Hypotheses of the Cp_2TiCl-promoted Epoxide-opening

Given the trisubstituted nature of the epoxide in **344**, we anticipated that its reaction with the Nugent reagent would provide the desired allylic alcohol **345** and not the deoxygenated product. Based on these new insights, **344** was subjected to stoichiometric amounts of Cp_2TiCl (Table 2.10).

Table 2.10. Isomerization of Epoxide 344 with Cp_2TiCl_2.

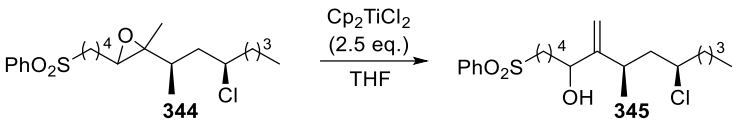

entry	Mn (equiv.)	temp. (°C)	conv.*	yield
1	8	25	10%	N.D.
2	8	45	0%	N.D.
3	24	25	100%	88%

*From analysis of ^1H NMR spectra recorded on crude reaction mixtures. N.D. = not determined.

Encouragingly, addition of epoxide **344** to a solution of Cp_2TiCl, previously formed by reaction of Cp_2TiCl_2 with manganese powder, provided 10% of the desired alcohol **345** along with unreacted starting material **344** (Entry 1). The reaction was then performed at 45 °C (Entry 2), but unfortunately, no product was formed under these conditions. To our delight, when more equivalents of the manganese powder were used, the epoxide **344** was fully converted into the allylic alcohol **345** (Entry 3). Having found suitable reaction conditions for the isomerization of epoxide **344**, we next examined the subsequent cyclization reaction. Here, the alcohol derivative **345** was submitted to the few Williamson ether cyclizations investigated during the development of eribulin.[42] The results of this study are summarized in Table 2.11.

Table 2.11. Cyclization of Alcohol 345.

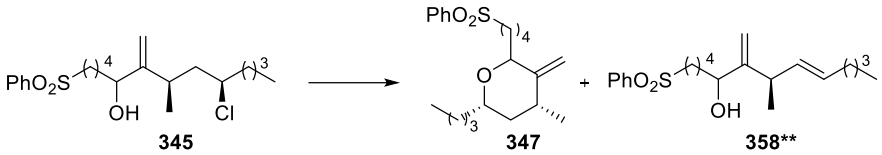

entry	reagents	solvent	temp.	conv.*	347:358*
1	*t*BuOK	THF	- 20	0%	N.D.
2	LiHMDS,	THF	- 30	0%	N.D.
3	*t*BuOK,	THF	25	56%	0:1
4	LiHMDS	THF	25	56%	0:1
5	$AgBF_4$, DTBMP	*t*BuOAc	25	100%	1:0

*From analysis of ^{1}H NMR spectra recorded on crude reaction mixtures. **Formation of product **358** (diastereoisomeric mixture) was confirmed by ^{1}H NMR spectroscopy and mass spectrometric analysis. N.D. = not determined.

Unfortunately, both lithium *bis*(trimethylsilyl)amide and potassium *tert*-butoxide failed to promote the desired cyclization (entries 1 and 2). Moreover, at room temperature, the reaction mixture only resulted in the formation of the alkene side-product **358** (entries 3 and 4). We next examined an acid-promoted cyclization and were particularly interested in the silver tetrafluoroborate reaction conditions used by Kishi for the cyclization of a closely related 1,5-chlorohydrin.[70] To our delight, when the alcohol **345** was treated with silver tetrafluoroborate and DTPMB, the corresponding tetrahydropyran **347** was formed quantitatively (entry 5).

2.4.3. Revised synthesis

As previously noted (section 2.1.3, Scheme 2.10), Kishi's silver-promoted cyclization reaction to form the pyran ring in eribulin involves a double inversion of the chloromethine stereogenic centre and thus, cyclization of the alcohol, derived from epoxide **331** (Scheme 2.66), would not deliver the desired configurational isomer under these reaction conditions. Thus, having established reaction conditions for all of the key steps in the process, we now needed to prepare the methyl ketone **295** with the opposite configuration at the chloromethine stereogenic centre. Based on the extensive studies detailed above, we did not anticipate that this stereochemical change would present difficulties.

As depicted in Scheme 2.72, the aldehyde **244**, which was synthesized in 6 steps from heptenal **293** (Schemes 2.57 and 2.58), was subjected to Christmann's α-chlorination procedure using the imidazolidinone **169** (previously synthesized in 4 steps from L-alanine

methyl ester hydrochloride using procedures adapted from the literature).[124] Here, the corresponding α-chloroaldehyde **359** was produced in excellent diastereoselectivity (d.r. = 10:1, Scheme 2.73). The subsequent HWE reaction with phosphonate **247** provided the α,β-unsaturated carbonyl **360** in 60% yield from **244**. The latter material was then subjected to a manganese-catalyzed silicon hydride reduction to produce a mixture of diastereoisomers **361a** and **361b** (**361a**:**361b** = 1.5:1). The undesired configurational isomer **361a** was subsequently treated with DBU in acetonitrile to furnish a new mixture of diastereoisomers **361a** and **361b** (**361a**:**361b** = 1:1). After chromatography separation, the *syn*-isomer **361a** was subjected to a new recycling event to produce additional amounts of the desired ketone **361b**. Overall, the saturated ketone **361b** was produced in 60% yield from enone **360** (Scheme 2.73). Thus, the route developed to access the epimeric ketone **243a** (Scheme 2.58) was easily adapted to the synthesis of the configurational isomer **361b**. This result shows how robust and versatile our synthetic approach is. In fact, given the full stereocontrol over the 5 stereogenic centres in **361b**, we could in theory access each configurational isomer of **361b** with only slight alterations of the synthetic sequence.

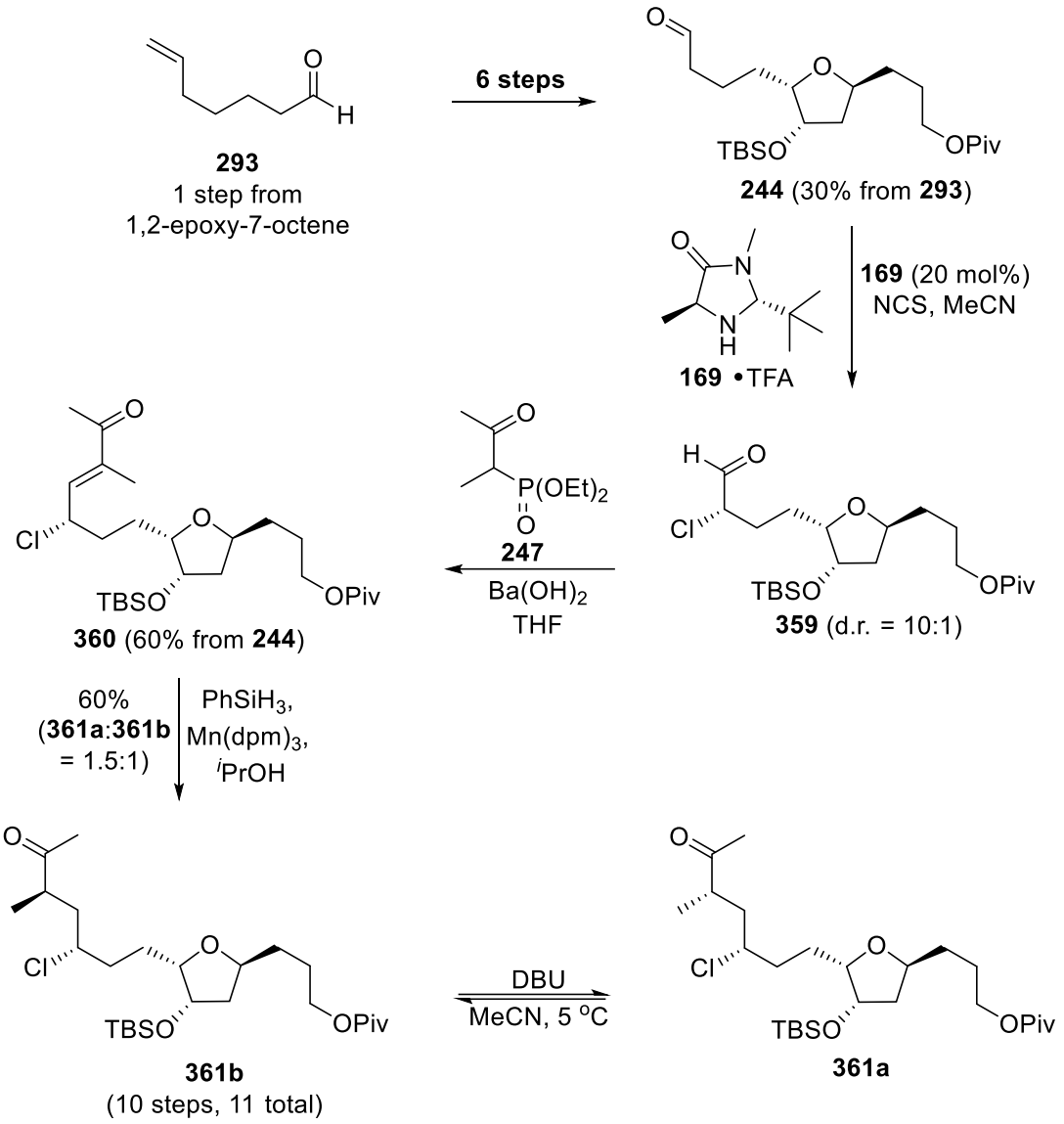

Scheme 2.72. Synthesis of the C14-C26 Building Block 361b.

With the two key fragments **329** and **361b** in hand, we next examined the following steps of the envisioned synthesis (Table 2.12). Here, reaction of the sulfonium salt **329** with LiHMDS and subsequent addition of the ketone **361b** provided a mixture of the desired epoxide **362** along with unreacted ketone **361b** (entry 1). Disappointedly, more equivalents of sulfonium salt **329**, or raising the temperature, failed to improve conversion (entries 2 and 3). However, when more LiHMDS was used, the ketone **361b** was fully consumed to produce the desired epoxide **362** (entry 4). Subsequently, oxidation of the thioether function in **362** was studied. While the desired sulfone **363** was formed using a

TPAP-NMO oxidation, the crude reaction mixture was contaminated with sulfoxide intermediate **364** (entries 5). Alternatively, when compound **362** was treated with MCPBA, oxidation of the thioether function was successful but the acetonide protecting group was also lost in the process (entry 6). We hypothesized that traces of water in combination with the acidic reagent (MCPBA) and side-product (benzoic acid) were responsible for this result. When sodium bicarbonate was added to the MCPBA oxidation, the crude reaction mixture contained several additional products including ones lacking the Piv- or TBS-protecting group (entry 7). Fortunately, when the addition of MCPBA and subsequent treatment with aqueous sodium bicarbonate were performed at -78 °C, the acetonide was not removed and the desired sulfone **363** was formed quantitatively (entry 10).

Table 2.12. Corey-Chaykovsky Reaction and Oxidation.

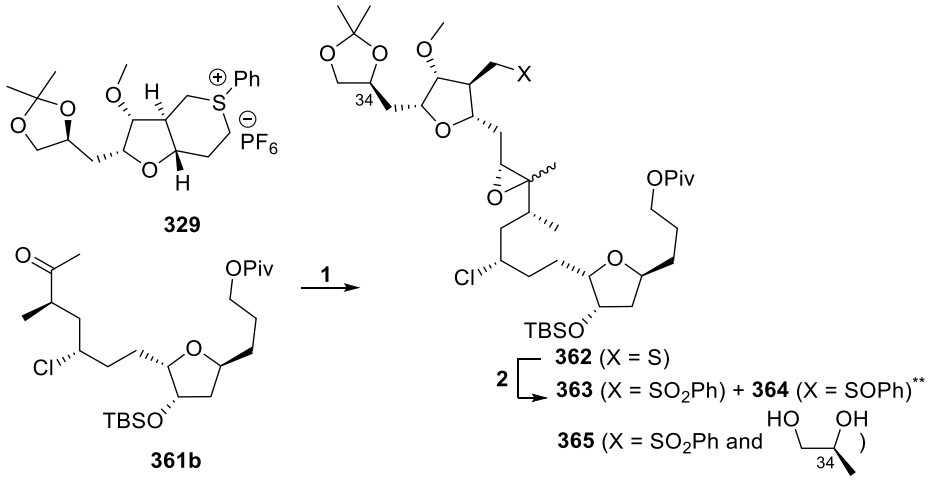

entry	step	reagents (equiv.)	time (h)	solvent	temp. (°C)	conv.[1]	products (yield[1])
1	**1**	**329** (1), LiHMDS (1.5)	5	THF	-78	80%	**362** (80%)
2	**1**	**329** (1.3), LiHMDS (1.5)	5	THF	-78	80%	**362** (80%)
3	**1**	**329** (1), LiHMDS (1.5)	5	THF	-78 then 25	80%	**362** (80%)
4	**2**	**329** (1), LiHMDS (2.8)	5	THF	-78 then 25	100%	**362** (100%)
5	**2**	TPAP (0.4), NMO (3)	12	CH_3CN	25	100%	**363** (56%); **364** (44%)
6	**2**	MCPBA (3)***	1	CH_2Cl_2	25	100%	**365** (100%)
7	**2**	MCPBA (3), $NaHCO_3$ (3)	1	CH_2Cl_2	25	100%	N.D.
8	**2**	MCPBA[2] (3)	1	CH_2Cl_2	25	100%	**363** (100%)

* As determined by ^1H NMR of the crude mixture. ** Formation of **364** was confirmed by 1H NMR spectroscopy and mass spectrometric analysis. ***Reagent added and quenched at -78 °C. N.D. = not determined.

As summarized in Scheme 2.73, the sulfone intermediate **363** was produced in 75% yield using the optimized Corey-Chaykovsky-oxidation sequence. Subsequently, we were happy to see that treatment of **363** with Cp_2TiCl_2 and manganese promoted the desired isomerization and thus, the epoxide **363** was smoothly converted to the corresponding allylic alcohol **366** (69% yield). The latter material was then subjected to Kishi's silver-promoted cyclization conditions. To our delight, the desired tetrahydropyran **367** was formed in excellent yield and thus, the reaction conditions developed on model substrates were successfully adapted to the two subunits **329** and **361b**.

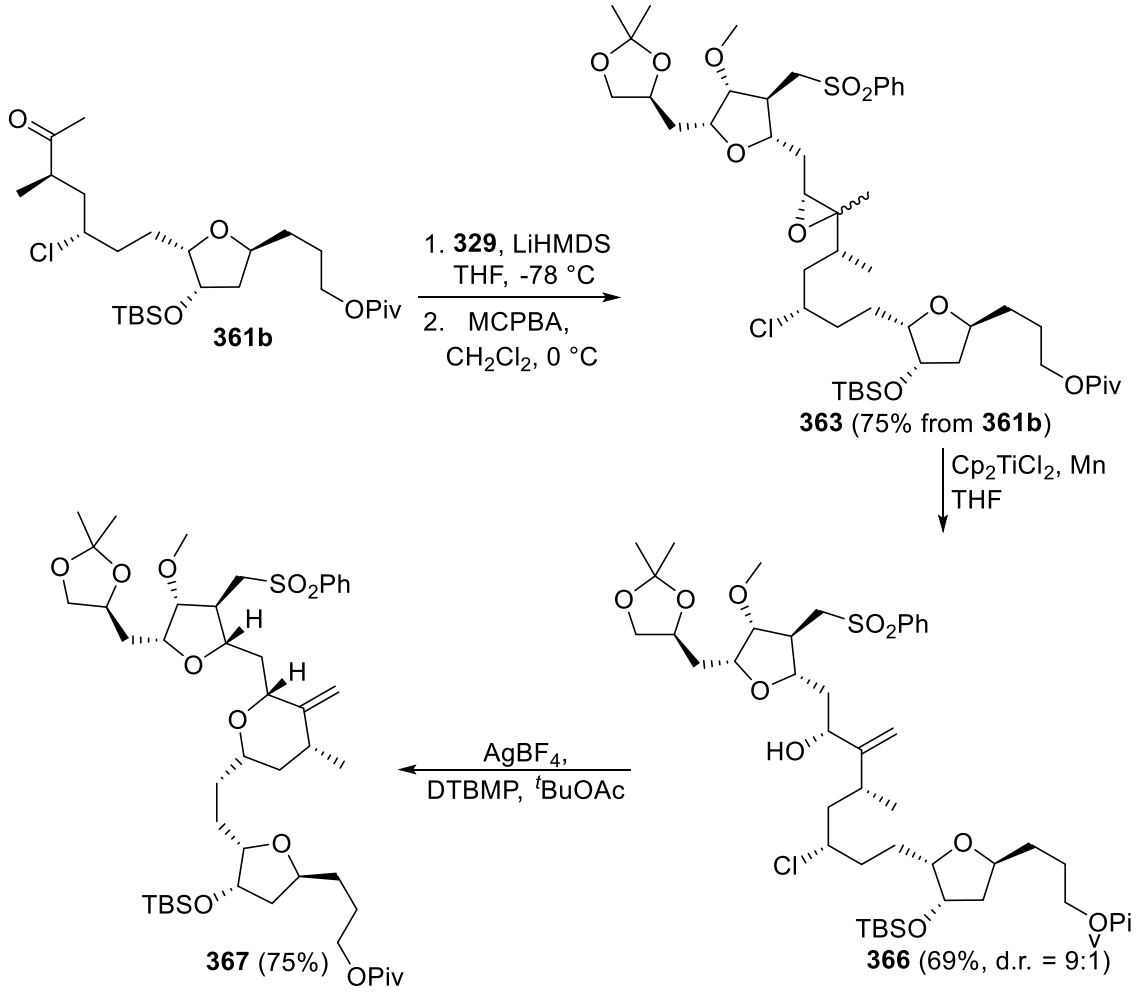

Scheme 2.73. Synthesis of Tetrahydropyran 367.

As depicted in Scheme 2.74, the advanced intermediate **367** was then treated with HF-pyridine in a solution of pyridine and tetrahydrofuran. A Dess-Martin oxidation then provided the ketone **368** in 70% yield from **367**. Thereafter, Wittig olefination of **368** with

potassium *tert*-butoxide and methyltriphenylphosphonium bromide achieved the 24-step synthesis of “Kishi intermediate” **120**.[70] Here, for the first time in the synthetic studies toward Eisai intermediate **76**, we were able to compare the experimental data with reported data and confirm that each stereogenic centre in **76** was properly established throughout the synthesis. Fortunately, the ^{1}H and ^{13}C NMR signals perfectly matched those reported by Kishi (see Table 2.13, section 2.6) and therefore, we were confident that the stereoselectivity of the entire sequence was as planned. To complete the synthesis of Eisai C14-C35 fragment of eribulin, intermediate **120** was then treated with a one molar solution of hydrochloride acid. Subsequent TBS-protection of the resulting diol provided Eisai building block **76** in 69% yield from **120**. Once again, the data of the intermediate produced fully matched that reported (see Table 2.14, section 2.6).[136]

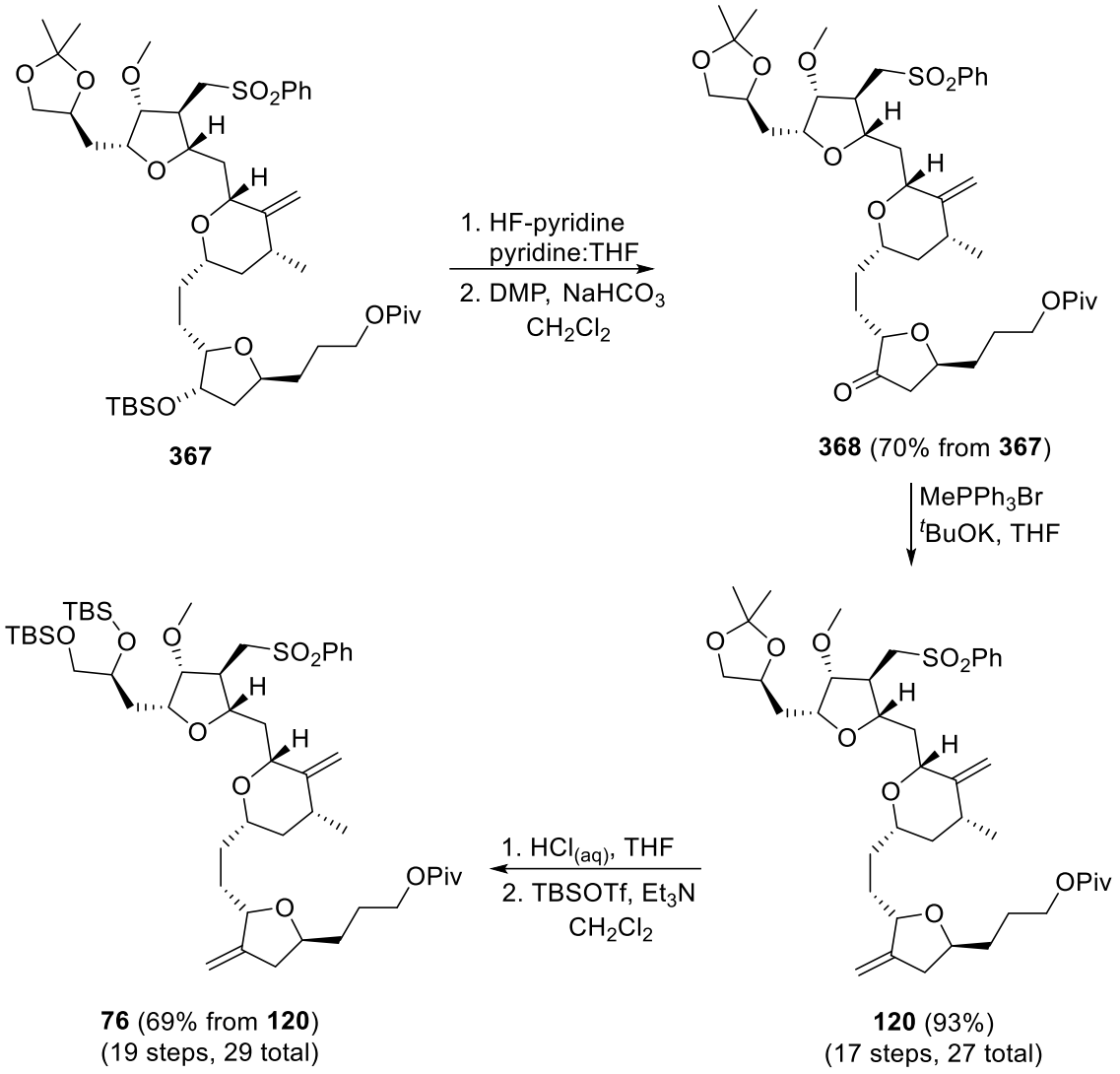

367

368 (70% from **367**)

76 (69% from **120**)
(19 steps, 29 total)

120 (93%)
(17 steps, 27 total)

Scheme 2.74. Syntheses of the Key C14-C35 Fragments of Eribulin 120 and 76.

To summarize, the synthesis of Eisai key intermediate **76** was completed in a total of 29 steps and thus, this route represents more than a 30% reduction in total number of steps compared to the process-scale of this fragment.[66] As a result, despite the sequence was performed at a milligram-scale and therefore, cannot be directly compared to Eisai's process, we are confident that it could dramatically reduce the costs associated with the production of eribulin.

2.5. Conclusion

In conclusion, we have developed a concise, stereoselective synthesis of Eisai C14-C35 fragment of the anticancer drug eribulin. Notably, our unprecedented synthetic approach relies on a doubly diastereoselective Corey-Chaykovsky reaction. In this process, the two building blocks **329** and **361b** are linked-together and the absolute configuration of the central C27 stereogenic centre is properly set. During the synthetic studies toward Eisai intermediate, the key Corey-Chaykovsky reaction smoothly produced the desired epoxide **362**. However, construction of the C14-C26 subunit proved much more challenging. Here, as Nicolaou exquisitely disclosed in his personal account on total synthesis endeavours: “often a “road map” that turns into an adventure, if not an odyssey, as the voyage begins and ends”.[14] Nevertheless, out of resourcefulness and stamina we tackled the numerous difficulties and completed a formal synthesis of eribulin. Importantly, in addition to drastically reducing the total number of steps compared to the other existing sequences,[66] this new approach secures all of the 10 asymmetric centres in **76** without the need of chiral separations or auxiliaries – a clear advantage over the industrial process.

2.6. Experimental

General considerations

All reactions were carried out with commercial solvents and reagents that were used as received. Flash chromatography was carried out with Geduran® Si60 silica gel (Merck). Concentration and removal of trace solvents was done via a Büchi rotary evaporator using dry ice/acetone condenser, and vacuum applied from an aspirator or Büchi V-500 pump. All reagents and starting materials were purchased from Sigma Aldrich, Alfa Aesar, TCI America, and/or Strem, and were used without further purification. All solvents were purchased from Sigma Aldrich, EMD, Anachemia, Caledon, Fisher, or ACP and used without further purification unless otherwise specified.

Nuclear magnetic resonance (NMR) spectra were recorded using chloroform-d ($CDCl_3$) or acetonitrile-d_3 (CD_3CN). Signal positions (δ) are given in parts per million from tetramethylsilane (δ 0) and were measured relative to the signal of the solvent (^{1}H NMR: $CDCl_3$: δ 7.26, CD_3CN: δ 1.96; ^{13}C NMR: $CDCl_3$: δ 77.16, CD_3CN: δ 118.26). Coupling

constants (*J* values) are given in Hertz (Hz) and are reported to the nearest 0.1 Hz. $_1$H NMR spectral data are tabulated in the order: multiplicity (s, singlet; d, doublet; t, triplet; q, quartet; quint, quintet; m, multiplet), coupling constants, number of protons. NMR spectra were recorded on a Bruker Avance 600 equipped with a QNP or TCI cryoprobe (600 MHz), Bruker 500 (500 MHz), or Bruker 400 (400 MHz). Diastereoisomeric ratios (d.r.) are based on analysis of crude ^{1}H-NMR. High performance liquid chromatography (HPLC) analysis was performed on an Agilent 1100 HPLC, equipped with a variable wavelength UV-Vis detector. High-resolution mass spectra were performed on an Agilent 6210 TOF LC/MS, Bruker MaXis Impact TOF LC/MS, or Bruker micrOTOF-II LC mass spectrometer. Infrared (IR) spectra were recorded neat on a Perkin Elmer Spectrum Two FTIR spectrometer. Only selected, characteristic absorption data are provided for each compound. Optical rotation was measured on a Perkin-Elmer Polarimeter 341 at 589 nm.

Synthesis of 4-oxopentyl pivalate 219

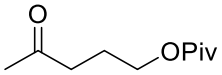

5-hydroxy-2-pentanone (3.42 g, 33 mmol) and DMAP (82 mg, 0.7 mmol) were dissolved in dry CH_2Cl_2 (63 mL) and pyridine (21 mL). The solution was cooled to 0 °C and then PivCl (5.36 mL, 44 mmol) was slowly added. The reaction mixture was then allowed to warm to room temperature over 16 h. The entire reaction mixture was then transferred to a separatory funnel and was washed three times with 1M HCl. The aqueous layers were extracted once with CH_2Cl_2 and the combined organic layers were washed with H_2O and brine, dried over $MgSO_4$, filtered, and concentrated under reduced pressure to afford 6.09 g of a clear liquid. Purification by flash chromatography (silica gel, hexanes-EtOAc 9:1 to 8:2) afforded ketone **219** as a clear liquid (4.22 g, 68%). **^{1}H NMR** (400 MHz, $CDCl_3$) δ 4.05 (t, *J* = 6.4 Hz, 2 H), 2.51 (t, *J* = 7.2 Hz, 2 H), 2.15 (s, 3 H), 1.92 (quint, *J* = 6.7 Hz, 2 H), 1.19 (s, 9 H); **^{13}C NMR** (125 MHz, $CDCl_3$) δ 207.8, 178.6, 63.6, 40.0, 38.9, 30.1, 27.3, 23.0. The data of ketone **219** matched that reported in the literature.[96]

Synthesis of alcohol 251

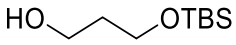

To a cold (0 °C), stirred solution of 1,3-propanediol **250** (1.0 g, 13.1 mmol) in THF (26 mL), was added sodium hydride (60% in mineral oil,769 mg, 17.0 mmol). After 30 minutes at room temperature, TBSCl (2.0 g, 13.1 mmol) was added at 0 °C and the resulting mixture was stirred for 5 hours. The reaction was then quenched with water and the mixture was extracted with Et_2O. The combined organic layers were washed with water and brine, dried over $MgSO_4$, and concentrated to give a crude oil. Purification of the crude product by flash chromatography (silica gel, hexanes-EtOAc 9:1) afforded compound **251** (1.7 g, 70%) as a colorless oil. **^{1}H NMR** (400 MHz, $CDCl_3$): δ 3.84 (t, *J* = 5.6 Hz, 2H), 3.80 (t, *J* = 5.6 Hz, 2H), 2.31 (br s, 1H), 1.78 (quint, *J* = 5.6 Hz, 2H), 0.90 (s, 9H), 0.08 (s, 6H); **^{13}C NMR** (125 MHz, $CDCl_3$) δ 63.1, 62.6, 34.4, 26.0, 18.3, 5.4. The data of ketone **251** matched that reported in the literature.[137]

Synthesis of aldehyde 251b

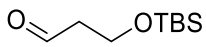

To a cold (0 °C), stirred solution of **251** (300 mg, 1.57 mmol) in CH_2Cl_2 (6.3 mL), were added PCC (441 mg, 2.04 mmol) and molecular sieves 3Å (441 mg). The mixture was stirred at room temperature for 2 hours, diluted with diethyl ether (6 mL), and filtered through a plug of silica gel with CH_2Cl_2. Purification of the crude product by flash chromatography (silica gel, hexanes-EtOAc 9:1) afforded compound **251b** (236 mg, 80%) as a colorless oil. **^{1}H NMR** (400 MHz, $CDCl_3$): δ = 9.80 (t, *J* = 2.1 Hz, 1H), 3.98 (t, *J* = 6.0 Hz, 2H), 2.59 (dt, *J* = 2.1, 6.0 Hz, 2H), 0.88 (s, 9H), 0.06 (s, 6H); **^{13}C NMR** (125 MHz, $CDCl_3$) δ 202.18, 57.55, 46.72, 25.96, 18.37, -5.29. The data of ketone **251b** matched that reported in the literature.[138]

Synthesis of enone 253

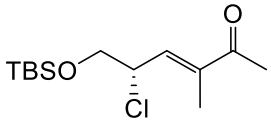

To a cold (0 °C), stirred solution of aldehyde **251b** (110 mg, 0.58 mmol) in CH_2Cl_2 (1.1 mL), was added L-prolinamide (13 mg, 0.11 mmol) and *N*-chlorosuccinimide (78 mg, 0.58 mmol). The ice bath was removed after 30 minutes allowing the solution to slowly warm to room temperature. The reaction mixture was stirred until complete consumption of starting material as determined by ^{1}H NMR spectroscopy. After this time, NH_4Cl (1 mL) and diethyl ether (2 mL) were added, and the layers were separated. Then, the aqueous

layer was extracted with diethyl ether (2 x 2 mL) and the combined organic phases were dried (Na_2SO_4), filtered, and concentrated to provide a crude mixture. The mixture was then diluted with pentane (1 mL), filtered, and concentrated to provide a crude α-chloroaldehyde **252** (92 mg, 80% purity) as a colorless oil. A mixture of ketophosphonate **247** (73 mg, 0.33 mmol, freshly prepared according to the literature) and $Ba(OH)_2.8H_2O$ (84 mg, 0.26 mmol) in THF (0.8 mL) was stirred at room temperature for 30 minutes. A solution of crude α-chloroaldehyde **252** (0.33 mmol) in THF (0.8 mL) was then added and the resulting mixture was stirred for 12 hours. After this time, the reaction mixture was diluted in CH_2Cl_2 (1 mL), washed with $NaHCO_3$ (1 mL) and brine (3 mL), dried with $MgSO_4$, and concentrated to provide a crude yellow oil. Purification of the crude product by flash chromatography (silica gel, hexanes-EtOAc 98:2) afforded compound **253** (48 mg, 52% yield from **251b**) as a colorless oil. **$[\alpha]^{20}_D$** -27.7 (*c* 2.6, $CHCl_3$); **^{1}H NMR** (400 MHz, $CDCl_3$) δ 6.52 (dq, *J* = 9.7, 1.4 Hz, 1H), 4.72 (ddd, *J* = 9.7, 6.8, 5.5 Hz, 1H), 3.91 (dd, *J* = 10.5, 5.5 Hz, 1H), 3.79 (dd, *J* = 10.5, 6.8 Hz, 1H), 2.34 (s, 3H), 1.87 (d, *J* = 1.4 Hz, 3H), 0.89 (s, 11H), 0.08 (d, *J* = 1.4 Hz, 6H); **^{13}C NMR** (101 MHz, $CDCl_3$) δ 199.44, 140.19, 138.38, 66.98, 56.60, 29.85, 25.96, 25.88, 25.76, 18.40, 11.79, -5.18, -5.21. **IR** (cast film, $CHCl_3$) *v* 2949.24, 2923.25, 1677.70, 1262.16, 1153.83; **HRMS (ESI-TOF)** *m/z*: $[M + NH_4]^+$ Calcd for $C_{13}H_{29}ClNO_2Si$ 294.1656; Found 294.1660.

Synthesis of ketone 254

A solution of α,β-conjugated ketone **253** (54 mg, 0.195 mmol) in EtOAc (1.95 mL) was treated with 10% Pd/C (12 mg). The reaction mixture was stirred under a H_2 atmosphere at room temperature for 1 h. The catalyst was removed by filtration over celite (EtOAc) and the filtrate was concentrated *in vacuo* to provide a crude yellow oil as a mixture of products (**255**:**254** = 2:1). Purification by flash chromatography (silica gel, 9:1 hexanes:Et_2O) afforded the desired ketone **254** (27 mg, 50% yield).

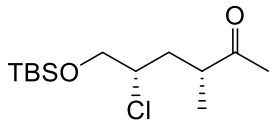

Data for major product **254**: **$[\alpha]^{20}_D$** +5.6 (*c* 0.5, $CHCl_3$); **^{1}H NMR** (400 MHz, $CDCl_3$): δ 3.89-3.81 (m, 1 H), 3.76 (dd, J = 5.21, 10.67 Hz, 1 H), 3.68 (dd, J = 6.00, 10.67 Hz, 1 H), 2.98-2.92 (m, 1 H), 2.27 (ddd, J = 3.08, 9.94, 14.25 Hz, 1 H), 2.19 (s, 3H), 1.54 (ddd, J = 3.70, 10.59, 14.25 Hz, 1 H), 1.16 (d, J = 7.20 Hz, 3 H), 0.90 (s, 9 H), 0.07 (s, 6 H); **^{13}C NMR**

(101 MHz, $CDCl_3$) δ 212.07, 67.74, 61.36, 43.84, 37.36, 29.06, 25.96, 18.46, 17.89, -5.18, -5.24; **IR** (cast film, $CHCl_3$) *v* 2956.24, 2932.08, 2854.77, 1709.53, 1458.26; **HRMS (ESI-TOF)** *m/z*: $[M + NH_4]^+$ Calcd for $C_{13}H_{31}ClNO_2Si$ 296.1813; Found 296.1808.

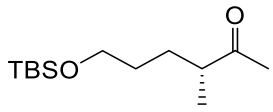

Data for minor side-product **255**: **$[\alpha]^{20}_D$** +1.2 (*c* 0.5, $CHCl_3$); **^{1}H NMR** (400 MHz, $CDCl_3$) δ 3.60 (t, *J* = 6.1 Hz, 2H), 2.52 (h, *J* = 6.8 Hz, 1H), 2.13 (s, 3H), 1.77 – 1.63 (m, 1H), 1.58 – 1.34 (m, 3H), 1.09 (d, *J* = 6.9 Hz, 3H), 0.89 (s, 10H), 0.04 (s, 6H); **^{13}C NMR** (101 MHz, $CDCl_3$) δ 212.80, 63.04, 47.07, 30.51, 29.85, 29.30, 28.03, 26.09, 18.47, 16.30, -5.17; **IR** (cast film, $CHCl_3$) *v* 2926.37, 2855.92, 1708.48, 1255.55, 1094.50; **HRMS (ESI-TOF)** *m/z*: $[M + NH_4]^+$ Calcd for $C_{13}H_{32}NO_2Si$ 262.2202; Found 262.2201.

Synthesis of epoxide 334

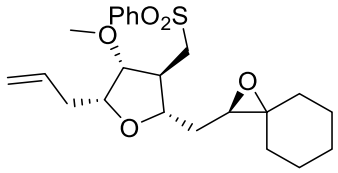

To a cold (-78 °C) solution of sulfonium salt *ent*-**316** (82 mg, 0.19 mmol) in dry THF (1.5 mL) was added LiHMDS (1 M in hexanes, 0.53 mL, 0.53 mmol). The resulting solution was stirred at -78 °C for 1 hour. Cyclohexanone **333** (20 mg, 0.20 mmol) was then slowly added. Stirring was continued for an additional hour at -78 °C and then 15 hours at room temperature. After this time, an aqueous solution of NH_4Cl (1 mL) was added, the mixture was diluted with CH_2Cl_2 (1 mL) and the phases were separated. The aqueous phase was extracted with CH_2Cl_2 (1 ml x 3), and the combined organic phases were washed with water (1 mL) and brine (1 mL), dried ($MgSO_4$) and concentrated to provide a crude yellow solid. The crude product was then dilute in CH_2Cl_2 (1.9 mL) and MCPBA was added (129 mg, 0.57 mmol). After 1 hour, the mixture was quenched with $NaHCO_3$ (2 mL) and the layers were separated. The aqueous phase was extracted with CH_2Cl_2 (2 x 2 mL). The combined organic phases were washed with brine (1 mL), dried (Na_2SO_4), filtered, and concentrated to provide a crude oil. Purification of the crude product by flash chromatography (silica gel, hexanes-EtOAc 3:1) provided sulfone **334** (56 mg, 70%) as a clear oil. **$[\alpha]^{20}_D$** -32.7 (*c* 1.9, $CHCl_3$); **^{1}H NMR** (601 MHz, $CDCl_3$) δ 7.93 (dd, *J* = 8.4, 1.3 Hz, 2H), 7.70 – 7.64 (m, 1H), 7.58 (t, *J* = 7.8 Hz, 2H), 5.81 (ddt, *J* = 17.2, 10.1, 7.0 Hz,

1H), 5.13 (dq, *J* = 17.2, 1.7 Hz, 1H), 5.09 – 5.03 (m, 1H), 3.81 (dd, *J* = 3.6, 1.3 Hz, 1H), 3.71 (s, 1H), 3.39 (s, 3H), 3.14 (t, *J* = 6.9 Hz, 2H), 2.68 (d, *J* = 6.4 Hz, 1H), 2.66 – 2.61 (m, 1H), 2.46 (td, *J* = 6.9, 1.4 Hz, 2H), 1.89 (td, *J* = 6.3, 2.7 Hz, 2H), 1.72 – 1.61 (m, 2H), 1.57 – 1.42 (m, 8H); **^{13}C NMR** (151 MHz, $CDCl_3$) δ 139.53, 134.78, 134.10, 129.60, 128.07, 117.27, 85.92, 81.68, 81.28, 62.66, 60.84, 58.19, 57.64, 43.41, 35.59, 33.41, 33.25, 29.47, 25.78, 24.96, 24.85; **IR** (cast film, $CHCl_3$) *v* 2976.70, 2929.73, 2855.92, 2369.43, 1446.78; **HRMS** (ESI-TOF) *m/z*: $[M + NH_4]^+$ Calcd for $C_{23}H_{36}NO_5S$ 438.2314; Found 438.2310.

Synthesis of alcohol 335

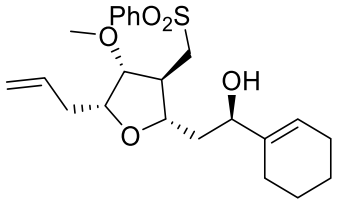

To a solution of epoxide **334** (56 mg, 0.13 mmol) in toluene (1.0 mL) was added Al(O*i*Pr$_4$) (30 mg, 0.14 mmol). The resulting mixture was refluxed for 15 hours. After this time, the mixture was allowed to cool down to rt, filtered through a plug of silica gel (EtOAc), and concentrated to provide a crude oil. Purification of the crude product by flash chromatography (silica gel, hexanes-EtOAc 3:1) provided alcohol **335** (56 mg, 40%) as a clear oil. **$[\alpha]^{20}_D$** -32.9 (*c* 1.9, $CHCl_3$); **^{1}H NMR** (601 MHz, $CDCl_3$) δ 7.93 (br d, *J* = 8.1 Hz, 2H), 7.68 (br t, *J* = 7.4, 1H), 7.59 (br t, *J* = 7.8 Hz, 2H), 5.79 (ddt, *J* = 17.2, 10.2, 7.1 Hz, 1H), 5.64 (br s, 1H), 5.12 (dq, *J* = 17.2, 1.7 Hz, 1H), 5.06 (br d, *J* = 10.3 Hz, 1H), 4.02 (br d, *J* = 9.4 Hz, 1H), 3.78 – 3.71 (m, 3H), 3.39 (s, 3H), 3.12 (d, *J* = 7.0 Hz, 2H), 2.98 (br s, 1H), 2.57 (br q, *J* = 6.2 Hz, 1H), 2.45 (br t, *J* = 6.2 Hz, 2H), 2.07 – 1.98 (m, 3H), 1.90 – 1.83 (m, 2H), 1.78 (dt, *J* = 14.2, 3.6 Hz, 1H), 1.67 – 1.48 (m, 4H); **^{13}C NMR** (151 MHz, $CDCl_3$) 139.60, 139.42, 134.53, 134.17, 129.64, 128.04, 122.68, 117.46, 85.71, 83.58, 81.51, 75.45, 58.26, 57.74, 44.59, 40.67, 33.40, 25.02, 24.09, 22.75, 22.72; **IR** (cast film, $CHCl_3$) *v* 3507.11, 2927.25, 2859.60, 2366.71, 1303.62; **HRMS (ESI-TOF)** *m/z*: $[M + NH_4]^+$ Calcd for $C_{23}H_{36}NO_5S$ 438.2314; Found 438.2312.

Synthesis of (*R*)-Mosher ester derivative 336

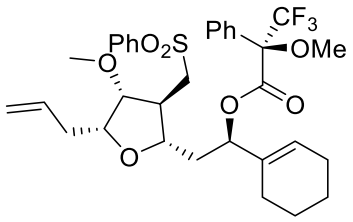

To a solution of alcohol **335** (10 mg, 0.02 mmol) and (*R*)-Mosher acid (10 mg, 0.04 mmol) in CH_2Cl_2 (0.2 mL) were successively added DCC (8 mg, 0.04 mmol) and DMAP (5 mg, 0.04 mmol). The resulting mixture was stirred at rt for 5 hours. After this time, the mixture was filtered and concentrated to provide a crude oil. Purification of the crude product by flash chromatography (silica gel, hexanes-EtOAc 25:3) provided sulfone **336** (10 mg, 80%) as a clear oil. **$[\alpha]^{20}_D$** +4.2 (*c* 0.9, $CHCl_3$); **^{1}H NMR** (600 MHz, $CDCl_3$) δ 8.00 – 7.94 (m, 2H), 7.69 (t, *J* = 7.5 Hz, 1H), 7.61 (t, *J* = 7.7 Hz, 2H), 7.45 (d, *J* = 7.7 Hz, 2H), 7.36 (dt, *J* = 14.4, 6.9 Hz, 3H), 5.84 – 5.74 (m, 2H), 5.38 (t, *J* = 7.2 Hz, 1H), 5.12 (dd, *J* = 17.2, 2.1 Hz, 1H), 5.08 – 5.03 (m, 1H), 3.80 (d, *J* = 3.5 Hz, 1H), 3.67 (td, *J* = 7.0, 3.4 Hz, 1H), 3.48 (s, 3H), 3.39 (s, 3H), 3.06 – 2.99 (m, 2H), 2.46 (ddt, *J* = 41.1, 12.6, 5.7 Hz, 3H), 2.14 – 2.01 (m, 3H), 1.89 (dt, *J* = 34.4, 6.3 Hz, 3H), 1.72 – 1.59 (m, 3H), 1.49 (h, *J* = 4.6, 3.4 Hz, 2H); **^{13}C NMR** (151 MHz, $CDCl_3$) δ 165.95, 139.46, 134.69, 134.17, 132.45, 129.67, 129.65, 129.12, 128.49, 128.14, 127.60, 117.32, 85.58, 81.24, 80.37, 78.92, 58.02, 57.72, 55.42, 43.99, 38.36, 33.38, 29.84, 25.15, 23.39, 22.45, 22.30; **IR** (cast film, $CHCl_3$) *v* 2927.25, 2869.26, 2337.72, 1743.36, 1148.99; **HRMS (ESI-TOF)** *m/z*: $[M + NH_4]^+$ Calcd for $C_{33}H_{43}F_3NO_7S$ 654.2712; Found 654.2708.

Synthesis of (*S*)-Mosherester derivative 337

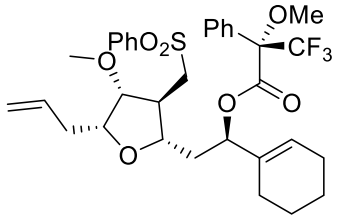

To a solution of alcohol **335** (10 mg, 0.02 mmol) and (*S*)-Mosher acid (10 mg, 0.04 mmol) in CH_2Cl_2 (0.2 mL) were successively added DCC (8 mg, 0.04 mmol) and DMAP (5 mg, 0.04 mmol). The resulting mixture was stirred at rt for 5 hours. After this time, the mixture was filtered and concentrated to provide a crude oil. Purification of the crude product by flash chromatography (silica gel, hexanes-EtOAc 25:3) provided sulfone **337** (9 mg, 76%) as a clear oil. **$[\alpha]^{20}_D$** -41.2 (*c* 0.4, $CHCl_3$); **^{1}H NMR** (600 MHz, $CDCl_3$) δ 7.94

(dt, *J* = 7.1, 1.3 Hz, 2H), 7.72 – 7.66 (m, 1H), 7.60 (t, *J* = 7.8 Hz, 2H), 7.49 – 7.44 (m, 2H), 7.42 – 7.33 (m, 3H), 5.84 – 5.74 (m, 2H), 5.41 (t, *J* = 7.2 Hz, 1H), 5.13 (dq, *J* = 17.2, 1.6 Hz, 1H), 5.06 (ddt, *J* = 10.1, 2.2, 1.1 Hz, 1H), 3.79 (dd, *J* = 3.6, 1.2 Hz, 1H), 3.69 (td, *J* = 7.0, 3.6 Hz, 1H), 3.53 (s, 3H), 3.47 (dt, *J* = 8.0, 5.1 Hz, 1H), 3.39 (s, 3H), 3.09 – 2.99 (m, 2H), 2.52 (dt, *J* = 9.5, 5.4 Hz, 1H), 2.44 (tt, *J* = 7.1, 1.3 Hz, 2H), 2.11 (dt, *J* = 13.7, 7.6 Hz, 1H), 2.04 – 1.93 (m, 3H), 1.82 (d, *J* = 17.1 Hz, 1H), 1.66 (d, *J* = 17.6 Hz, 1H), 1.60 – 1.53 (m, 2H), 1.50 – 1.34 (m, 2H); **^{13}C NMR** (151 MHz, $CDCl_3$) δ 165.61, 139.37, 134.55, 134.05, 133.83, 132.27, 129.53, 129.50, 128.81, 128.31, 127.97, 127.35, 117.23, 85.57, 81.25, 80.48, 78.99, 57.98, 57.60, 55.61, 44.02, 43.93, 38.24, 33.24, 29.73, 25.01, 22.94, 22.23, 22.15; **IR** (cast film, $CHCl_3$) *v* 2932.0, 2872.32, 1743.36, 1699.87, 1163.49; **HRMS (ESI-TOF)** *m/z*: $[M + NH_4]^+$ Calcd for $C_{33}H_{43}F_3NO_7S$ 654.2712; Found 654.2713.

Synthesis of ketone 343a

To a cold (0 °C), stirred solution of aldehyde **342** (200 mg, 2.0 mmol) in CH_2Cl_2 (4.0 mL), was added L-prolinamide (46 mg, 0.40 mmol) and *N*-chlorosuccinimide (267 mg, 2.0 mmol). The ice bath was removed after 30 minutes allowing the solution to slowly warm to room temperature. The reaction mixture was stirred until complete consumption of starting material as determined by ^{1}H NMR spectroscopy. After this time, NH_4Cl (3 mL) and diethyl ether (4 mL) were added, and the layers were separated. Then, the aqueous layer was extracted with diethyl ether (2 x 2 mL) and the combined organic phases were dried (Na_2SO_4), filtered, and concentrated to provide a crude mixture. The mixture was then diluted with pentane (1 mL), filtered, and concentrated to provide a crude α-chloroaldehyde as a colourless oil. After that, a mixture of ketophosphonate **247** (416 mg, 2.0 mmol, freshly prepared according to the literature) and $Ba(OH)_2.8H_2O$ (505 mg, 1.6 mmol) in THF (4 mL) was stirred at room temperature for 30 minutes. A solution of crude α-chloroaldehyde in THF (4 mL) was then added and the resulting mixture was stirred for 12 hours. After this time, the reaction mixture was diluted in CH_2Cl_2 (4 mL), washed with $NaHCO_3$ (4 mL) and brine (4 mL), dried with $MgSO_4$, and concentrated to provide a crude yellow oil. After a quick plug (silica gel, hexanes-EtOAc 1:1), the resulting product was diluted in deoxygenated *i*PrOH (8 mL) under an inert atmosphere. $Mn(dpm)_3$ (242 mg, 0.40 mmol) and phenylsilane (0.29 mL, 2.4 mmol) were then quickly added and the resulting mixture was stirred for 3 hours. After this time, the reaction mixture was filtered through a pad of silica gel and concentrated to provide a crude yellow oil as a mixture of

products (**343a**:**343b** = 1.5:1). Purification by flash chromatography (silica gel, 9:1 hexanes:Et_2O) afforded the desired ketone **343a** (114 mg, 30% yield) as a clear oil.

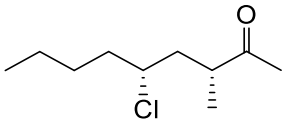

Data for **343a**: $[\alpha]^{20}_D$ +1.7 (*c* 0.7, $CHCl_3$); **^{1}H NMR** (400 MHz, $CDCl_3$) δ 3.85 – 3.80 (m, 1H), 3.05 – 2.97 (m, 1H), 2.20 (s, 3H), 2.18 – 2.12 (m, 1H), 1.76 – 1.63 (m, 2H), 1.56 – 1.45 (m, 2H), 1.41 – 1.19 (m, 3H), 1.14 (d, *J* = 7.4 Hz, 3H), 0.90 (t, *J* = 7.6 Hz, 3H); **^{13}C NMR** (101 MHz, $CDCl_3$) δ 212.29, 62.61, 43.95, 41.34, 38.92, 29.34, 28.52, 22.24, 17.84, 13.99; **IR** (cast film, $CHCl_3$) *v* 2953.22, 2923.05, 2852.56, 1701.77, 1460.21; **HRMS (ESI-TOF)** *m/z*: $[M + NH_4]^+$ Calcd for $C_{10}H_{23}ClNO$ 208.1468; Found 208.1467.

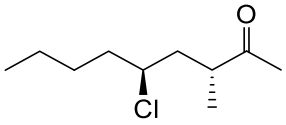

Data for **343b**: **$[\alpha]^{20}_D$** -16.4 (*c* 1.4, $CHCl_3$); **^{1}H NMR** (400 MHz, $CDCl_3$) δ 3.94 – 3.88 (m, 1H), 2.90 – 2.82 (m, 1H), 2.19 (s, 3H), 2.05 (ddd, *J* = 18.9, 8.8, 4.4 Hz, 1H), 1.72 (q, *J* = 7.2 Hz, 2H), 1.65 (ddd, *J* = 12.4, 9.1, 2.9 Hz, 1H), 1.54 – 1.46 (m, 1H), 1.42 – 1.20 (m, 3H), 1.10 (d, *J* = 7.1 Hz, 3H), 0.90 (t, *J* = 7.4 Hz, 3H); **^{13}C NMR** (101 MHz, $CDCl_3$) δ 211.82, 61.69, 44.30, 40.48, 38.78, 29.72, 28.64, 22.24, 15.32, 13.98; **IR** (cast film, $CHCl_3$) *v* 2956.57, 2926.37, 2859.27, 1708.48, 1456.85; **HRMS (ESI-TOF)** *m/z*: $[M + NH_4]^+$ Calcd for $C_{10}H_{23}ClNO$ 208.1468; Found 208.1470.

Synthesis of (*R*)-2-chlorohept-6-enal 294

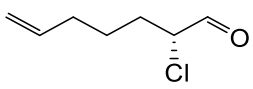

To a cold (0 °C), stirred solution of heptenal **293** (4.43 g, 39.56 mmol, freshly prepared from 1,2-epoxy-7-octene) in CH_3CN (79 mL), was added the MacMillan catalyst *ent*-**169** (2.25 g, 7.91 mmol, freshly prepared according to the litterature[124]) and *N*-chlorosuccinimide (5.28 g, 39.56 mmol). The ice bath was removed after 30 minutes allowing the solution to slowly warm to room temperature. The reaction mixture was stirred until complete consumption of starting material as determined by ^{1}H NMR spectroscopy.

After this time, NH_4Cl (30 mL) and diethyl ether (70 mL) were added and the layers were separated. Then, the aqueous layer was extracted with diethyl ether (2 x 30 mL) and the combined organic phases were dried (Na_2SO_4), filtered, and concentrated to provide a crude mixture. The mixture was then diluted with pentane (5 mL), filtered, and concentrated to provide a crude α-chloroaldehyde **293** (5.80.g, 94% purity, 95% e.e.) as a colourless oil. **^{1}H NMR** (400 MHz, $CDCl_3$) δ 9.48 (t, *J* = 2.4 Hz, 1H), 5.77 (ddt, *J* = 17.1, 10.2, 6.7 Hz, 1H), 5.06 – 4.97 (m, 2H), 4.16 (ddd, *J* = 8.3, 5.4, 2.3 Hz, 1H), 2.10 (br q, *J* = 7.2 Hz, 2H), 2.05 – 1.95 (m, 1H), 1.87 – 1.77 (m, 1H), 1.70 – 1.49 (m, 2H), 1.33 – 1.20 (m, 1H).

Synthesis of ester 295

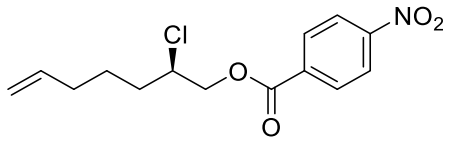

ee determination of aldehyde **294**: Crude aldehyde **294** (49 mg, 0.2 mmol) was dissolved in CH_3OH (1 mL) and $NaBH_4$ (23 mg, 0.6 mmol) was added. After stirring for 1 hour at room temperature, NH_4Cl (1 mL) was added and the aqueous layer was extracted with ethyl acetate (3 × 1 mL). The combined organic phases were washed with brine (1 mL), dried (Na_2SO_4), filtered, and concentrated. The resulting mixture was then dissolved in CH_2Cl_2 (0.8 mL) and para-nitrobenzoic acid (33.4 mg, 0.2 mmol), DCC (41.2 mg, 0.2 mmol) and DMAP (24.4 mg, 0.2 mmol) were successively added. After 2 hours at room temperature, the reaction mixture was filtered and concentrated to provide a crude oil. Purification of the crude product by flash chromatography (silica gel, hexanes-EtOAc 95:5) furnished ester **295** (44 mg, 75%). Chiral separation of using Amylose (50 × 4.6 mm, IPA:hexanes 1:99, 0.250 mL/min) revealed an 95% enantiomeric excess (t_{R1} = 15.4 min, t_{R2} = 16.9 min). **^{1}H NMR** (400 MHz, $CDCl_3$) δ 8.31 (br d, *J* = 8.9 Hz, 2H), 8.23 (br d, *J* = 8.9 Hz, 2H), 5.80 (ddt, *J* = 16.9, 10.2, 6.6 Hz, 1H), 5.04 (dq, *J* = 17.4, 1.9 Hz, 1H), 4.99 (br d, *J* = 10.2, 1H), 4.55 (dd, *J* = 11.8, 4.8 Hz, 2H), 4.48 (dd, *J* = 11.8, 6.9 Hz, 1H), 2.18 – 2.06 (m, 2H), 1.94 – 1.68 (m, 3H), 1.64 – 1.56 (m, 1H).

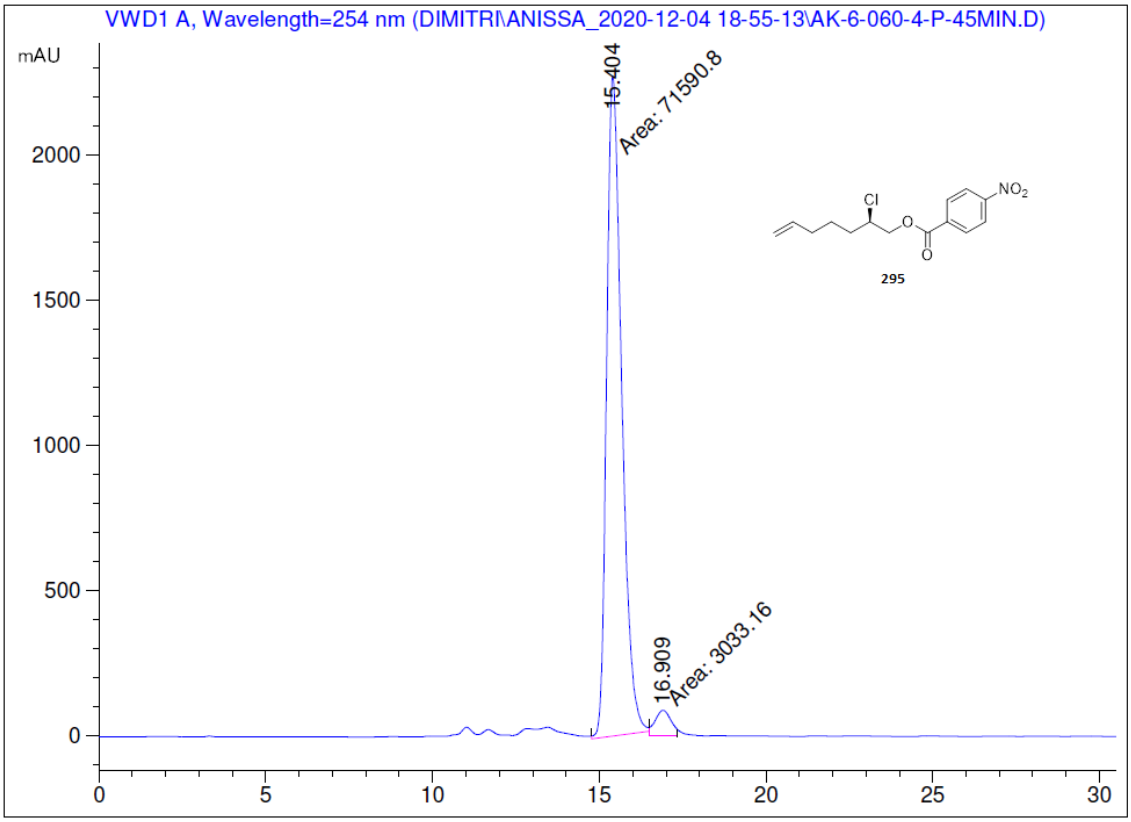

Synthesis of ketochlorohydrin 297

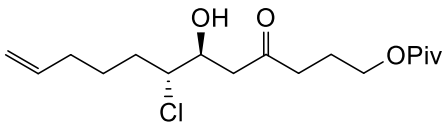

To a cold (–78 °C) solution of diisopropylamine (2.16 mL, 15.4 mmol) in THF (91 mL) was added *n*-butyllithium dropwise (2 M soln. in hexane, 7.42 mL, 14.8 mmol). The resulting solution was stirred at –78 °C for 30 minutes. After this time, ketone **219** (2.62 g, 14.1 mmol) in THF (2 mL) was added in one portion. The reaction mixture was stirred for 30 minutes. A solution of **297** (2.09 g, 13.4 mmol) in THF (10 mL) was then added dropwise over 10 minutes at –78 °C and the resulting mixture was stirred for an additional 75 minutes. Saturated aqueous NH_4Cl (50 ml) was then added, the mixture was diluted with EtOAc (50 ml) and the phases were separated. The aqueous phase was extracted with EtOAc (3 × 50 ml) and the combined organic phases were washed with brine (50 mL), dried (Na_2SO_4), filtered, and concentrated to provide a crude oil which showed a 4:1 diastereoisomeric ratio as determined by ^1H NMR. Purification of the crude product by flash chromatography (silica gel, hexanes-acetone 9:1) provided the title compound **297**

as a colourless oil (2.89 g, 65%). **[α]$^{20}_{D}$** -5.0 (*c* 1.0, $CHCl_3$); **^{1}H NMR** (400 MHz, $CDCl_3$) δ 5.79 (ddt, *J* = 16.9, 10.2, 6.6 Hz, 1H), 5.06 – 4.95 (m, 2H), 4.15 – 4.09 (m, 1H), 4.07 (t, *J* = 6.4 Hz, 2H), 3.91 (ddd, *J* = 9.3, 6.1, 3.1 Hz, 1H), 3.21 (d, *J* = 5.2 Hz, 1H), 2.82 (dd, *J* = 17.4, 3.5 Hz, 1H), 2.76 (dd, *J* = 17.5, 8.0 Hz, 1H), 2.56 (t, *J* = 7.2 Hz, 2H), 2.17 – 2.01 (m, 2H), 1.98 – 1.86 (m, 3H), 1.78 – 1.44 (m, 3H), 1.19 (s, 9H); **^{13}C NMR** (101 MHz, $CDCl_3$) δ 210.31, 178.65, 138.24, 115.21, 71.09, 65.93, 63.39, 45.31, 40.11, 38.91, 33.34, 33.23, 27.34, 25.64, 22.72; **IR** (cast film, $CHCl_3$) *v* 3476.61, 2963.28, 1718.55, 1282.39, 1158.25; **HRMS (ESI-TOF)** *m/z*: $[M + NH_4]^+$ Calcd for $C_{17}H_{29}ClNO_4$ 450.2098; Found 450.2079.

Synthesis of *syn*-diol 297b

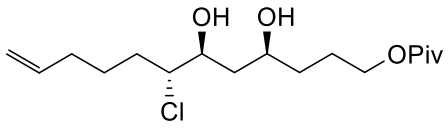

To a cold (–78 °C) solution of ketone **297** (3.37 g, 10.14 mmol) in THF (149 mL) was added diisobutylaluminum hydride (1.00 M solution in THF, 20.3 mL, 20.3 mmol) and the reaction mixture was stirred for 3.5 hours at the same temperature. After this time, an aqueous solution of HCl (1.0 M, 100 mL) was added, the mixture was diluted with ether (100 mL) and the phases were separated. The aqueous phase was extracted with ether (2 × 75 mL), and the combined organic phases were washed with water (100 mL) and brine (100 mL), dried (Na_2SO_4), filtered, and concentrated to provide a crude oil. Purification of the crude product by flash chromatography (silica gel, hexanes-EtOAc 8:1) afforded 1,3-diol **297b** (2.72 g, 80%) as a colorless oil. **[α]$^{20}_{D}$** +11.3 (*c* 0.83, $CHCl_3$); **^{1}H NMR** (400 MHz, $CDCl_3$) δ 5.80 (ddt, *J* = 16.9, 10.2, 6.7 Hz, 1H), 5.06 – 5.00 (m, 1H), 4.98 (ddt, *J* = 10.1, 2.1, 1.2 Hz, 1H), 4.09 (t, *J* = 6.5 Hz, 2H), 3.97 (d, *J* = 10.4 Hz, 0H), 3.94 – 3.87 (m, 2H), 3.27 (s, 1H), 2.99 (s, 1H), 2.16 – 2.04 (m, 2H), 1.88 – 1.46 (m, 10H), 1.20 (s, 9H); **^{13}C NMR** (101 MHz, $CDCl_3$) δ 178.79, 138.22, 115.23, 75.87, 72.10, 67.79, 64.31, 38.88, 38.82, 34.44, 33.21, 32.28, 27.32, 25.89, 24.73; **IR** (cast film, $CHCl_3$) *v* 3410.47, 2956.24, 2874.09, 1724.03, 1284.30; **HRMS (ESI-TOF)** *m/z*: $[M + H]^+$ Calcd for $C_{17}H_{32}ClO_4$ 335.1989; Found 335.1980.

Synthesis of tetrahydrofuran 298

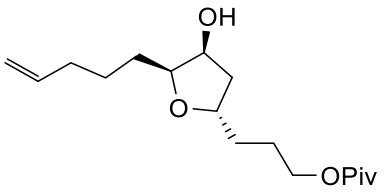

To a cold (0 °C), stirred solution of 1,3-diol **297b** (2.71 g, 8.11 mmol) in THF (16 mL) was added AgOTf (1.88 g, 8.11 mmol) and Ag_2O (2.08 g, 8.11 mmol) and the reaction mixture was sonicated at rt for 1 h. The reaction mixture was then stirred for another 15 hours. The resulting suspension was then filtered through Celite and washed with Et_2O and concentrated to provide a crude oil. The crude oil was dissolved in Et_2O (30 mL) and washed with saturated aq $NaHCO_3$ (15 mL) and the layers were separated. The aqueous layer was extracted with Et_2O (2 × 30 mL), and the combined organic layers were dried (Na_2SO_4), filtered, and concentrated to provide a crude oil. Purification of the crude product by flash chromatography (silica gel, hexanes-acetone 9:1) afforded the desired alcohol **298** (1.94 g, 82%) as a colorless oil. **$[\alpha]^{20}_D$** +2.07 (*c* 0.82, $CHCl_3$); **^{1}H NMR** (400 MHz, $CDCl_3$) δ 5.81 (ddt, *J* = 16.9, 10.2, 6.7 Hz, 1H), 5.01 (ddt, *J* = 17.1, 2.0, 1.6 Hz, 1H), 4.95 (ddt, *J* = 10.2, 2.2, 1.2 Hz, 1H), 4.26 – 4.16 (m, 2H), 4.08 (t, *J* = 6.1 Hz, 2H), 3.77 (ddd, *J* = 7.3, 6.2, 2.9 Hz, 1H), 2.15 – 2.06 (m, 3H), 1.82 – 1.41 (m, 9H), 1.19 (s, 9H); **^{13}C NMR** (101 MHz, $CDCl_3$) δ 178.71, 138.71, 114.87, 81.84, 76.55, 73.48, 64.38, 41.92, 38.89, 33.99, 32.77, 28.65, 27.36, 25.80, 25.62; **IR** (cast film, $CHCl_3$) *v* 3449.13, 2917.58, 2223.22, 1728.86, 1279.46; **HRMS (ESI-TOF)** *m/z*: $[M + NH_4]^+$ Calcd for $C_{17}H_{34}NO_4$ 316.2488; Found 316.2485.

Synthesis of TBS-protected tetrahydrofuran 305

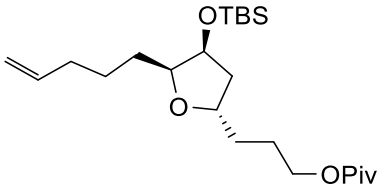

To a cold (0 °C) solution of alcohol **298** (1.93 g, 6.49 mmol) and Et_3N (2.17 mL, 15.6 mmol) in CH_2Cl_2 (32.5 mL) was added TBSOTf (1.79 mL, 7.79 mmol) and the reaction mixture was stirred for 1 hour. After this time, water (15 mL) was added and the phases were separated. The aqueous phase was extracted with CH_2Cl_2 (2 × 25 mL), and the combined organic phases were washed with water (10 mL) and brine (10 mL), dried (Na_2SO_4),

filtered, and concentrated to provide a crude oil. Purification of the crude product by flash chromatography (silica gel, hexanes-EtOAc 97:3) afforded compound **305** (2.41, 90%) as a colorless oil. **$[\alpha]^{20}_D$** +13.7 (*c* 1.1, $CHCl_3$); **^{1}H NMR** (400 MHz, $CDCl_3$) δ 5.81 (ddt, *J* = 17.0, 10.2, 6.7 Hz, 1H), 4.99 (ddt, *J* = 17.1, 2.2, 1.5 Hz, 1H), 4.93 (ddt, *J* = 10.2, 2.2, 1.2 Hz, 1H), 4.22 (td, *J* = 3.8, 3.3, 1.4 Hz, 1H), 4.21 – 4.13 (m, 1H), 4.07 (t, *J* = 6.1 Hz, 2H), 3.78 (ddd, *J* = 7.1, 5.9, 3.3 Hz, 1H), 2.12 – 2.05 (m, 2H), 1.95 (ddd, *J* = 12.8, 5.8, 1.4 Hz, 1H), 1.82 – 1.33 (m, 9H), 1.19 (s, 9H), 0.89 (s, 9H), 0.07 (s, 3H), 0.05 (s, 3H); **^{13}C NMR** (101 MHz, $CDCl_3$) δ 178.73, 138.97, 114.57, 82.76, 76.67, 73.67, 64.57, 42.31, 38.89, 34.20, 32.75, 29.33, 27.37, 25.93, 25.89, 25.63, 18.22, -4.31, -4.88; **IR** (cast film, $CHCl_3$) *v* 2956.24, 2927.25, 2854.77, 1724.03, 1153.83; **HRMS (ESI-TOF)** *m/z*: $[M + NH_4]^+$ Calcd for $C_{23}H_{48}NO_4Si$ 430.3353; Found 430.3353.

Synthesis of α,β-conjugated ketone 360

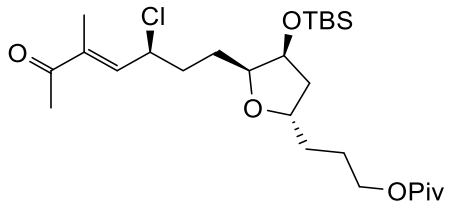

To a solution of alkene **305** (2.11 g, 5.12 mmol) in a 1:1 mixture of THF:H_2O (50.2 mL) was added OsO_4 (5% in H_2O, 0.54 mL, cat) and the reaction mixture was stirred for 10 min. After this time, $NaIO_4$ (2.74 g, 12.8 mmol) was added and the resulting mixture was stirred for another 4 hours. The reaction was then quenched with $NaHCO_3$:$Na_2S_2O_3$ (1:1, 30 mL) and EtOAc (50 mL) was added. The layers were separated, and the aqueous phase was extracted with EtOAc (2 × 50 mL). The combined organic phases were washed with water (50 mL) and brine (50 mL), dried (Na_2SO_4), filtered, and concentrated. The resulting oil was filtered through a plug of silica (hexanes-ethylacetate 4:1) and directly used in the next step without further purification. Subsequently, the crude aldehyde **244** (1.91 g, 4.60 mmol) was diluted in CH_3CN (9.2 mL) and cooled to (0 °C). The MacMillan catalyst **169**.TFA (262 mg, 0.92 mmol, freshly prepared according to the litterature[1]) and *N*-chlorosuccinimide (615 mg, 4.60 mmol) were then added. The ice bath was removed after 30 minutes allowing the solution to slowly warm to room temperature. The reaction mixture was stirred until complete consumption of starting material as determined by ^{1}H NMR spectroscopy. After this time, NH_4Cl (10 mL) and diethyl ether (10 mL) were added and the layers were separated. Then, the aqueous layer was extracted with diethyl ether

(2 x 10 mL) and the combined organic phases were dried (Na_2SO_4), filtered, and concentrated to provide a crude mixture. The mixture was diluted with pentane (2 mL), filtered and concentrated to provide a crude α-chloroaldehyde **359** as a colourless oil. After that, a mixture of ketophosphonate **247** (959 mg, 4.60 mmol) and $Ba(OH)_2.8H_2O$ (1.16 g, 3.68 mmol) in THF (6.8 mL) was stirred at room temperature for 30 minutes. A solution of crude α-chloroaldehyde **359** in THF (6.8 mL) was then added and the resulting mixture was stirred for 24 hours. After this time, the reaction mixture was diluted in CH_2Cl_2 (15 mL), washed with $NaHCO_3$ (15 mL) and brine (15 mL), dried with $MgSO_4$, and concentrated to provide a crude yellow oil. Purification of the crude product by flash chromatography (silica gel, hexanes-EtOAc 95:5) afforded compound **360** (1.39 g, 54% yield from **305**) as a colorless oil. **$[\alpha]^{20}_D$** +13.7 (*c* 1.1, $CHCl_3$); **^{1}H NMR** (400 MHz, $CDCl_3$) δ 6.51 (dq, *J* = 9.9, 1.5 Hz, 1H), 4.80 (dt, *J* = 9.8, 6.9 Hz, 1H), 4.25 – 4.22 (m, 1H), 4.19 – 4.11 (m, 1H), 4.07 (td, *J* = 6.4, 1.1 Hz, 2H), 3.83 (ddd, *J* = 8.3, 4.7, 3.5 Hz, 1H), 2.33 (s, 3H), 2.12 – 2.04 (m, 1H), 1.98 – 1.85 (m, 2H), 1.83 (d, *J* = 1.4 Hz, 3H), 1.82 – 1.45 (m, 7H), 1.19 (s, 9H), 0.88 (s, 9H), 0.07 (s, 3H), 0.05 (s, 3H); **^{13}C NMR** (101 MHz, $CDCl_3$) δ 199.57, 178.70, 140.87, 138.14, 81.79, 76.91, 73.91, 64.46, 57.39, 42.21, 38.90, 35.37, 32.65, 27.37, 26.70, 25.89, 25.76, 25.61, 18.21, 11.55, -4.34, -4.86; **IR** (cast film, $CHCl_3$) *v* 2956.24, 2347.38, 1724.03, 1675.70, 1153.83; **HRMS (ESI-TOF)** *m/z*: $[M + NH_4]^+$ Calcd for $C_{26}H_{51}ClNO_5Si$ 520.3225; Found 520.3221.

Synthesis of ketone 361b

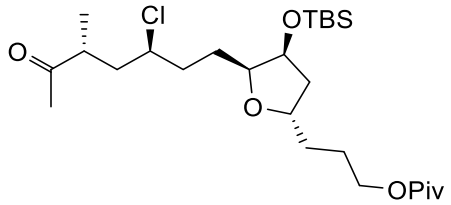

Phenylsilane (0.55 mL, 4.46 mmol) was added to a strictly deoxygenated solution of enone **360** (1.87 g, 3.72 mmol) and $Mn(dpm)_3$ (450 mg, 0.74 mmol) in isopropyl alcohol (12.4 mL). After completion of the reaction (TLC monitoring), the reaction mixture was filtered through a pad of silica gel and concentrated to provide a crude yellow oil (dr = 1.5:1). Purification by flash chromatography (silica gel, hexanes-ethylacetate 95:5) afforded a mixture of compounds **361a** + **361b** (1.31 g) and clean **361b** (540 mg) as clear oils. Subsequently, to a cold (0 °C) solution of mixed fraction **361a** + **361b** (1.31 g, 2.57 mmol) in acetonitrile (26 mL), was added DBU (0.78 mL, 5.14 mmol) and the resulting mixture

was stirred at 4 °C for 48 hours. After this time, water (10 mL) and EtOAc (10 mL) were added and the layers were separated. The aqueous phase was extracted with EtOAc (2 × 25 mL). The combined organic phases were washed with water (10 mL) and brine (10 mL), dried (Na_2SO_4), filtered, and concentrated to provide a crude oil. Purification of the crude product by flash chromatography (silica gel, hexanes-EtOAc 95:5) afforded 869 mg of **361a** + **361b** and 250 mg of **361b**. The above procedure was repeated with 869 mg of **361a** + **361b** to furnish another 340 mg of **361b**. The different fractions of **361b** were combined to provide the desired ketone **361b** (1.13 g, 60%) as a colorless oil. **$[\alpha]^{20}_D$** +6.82 (*c* 1.7, $CHCl_3$); **^{1}H NMR** (400 MHz, $CDCl_3$) δ 4.25 – 4.21 (m, 1H), 4.16 (dt, *J* = 9.1, 5.9 Hz, 1H), 4.11 – 4.02 (m, 2H), 3.97 (ddt, *J* = 11.2, 8.0, 3.9 Hz, 1H), 3.80 (tq, *J* = 9.0, 4.9 Hz, 1H), 2.91 – 2.80 (m, 1H), 2.18 (s, 3H), 2.07 (ddd, *J* = 14.8, 10.6, 4.5 Hz, 1H), 1.95 (ddd, *J* = 12.8, 5.8, 1.5 Hz, 1H), 1.89 – 1.45 (m, 10H), 1.19 (s, 9H), 1.10 (d, *J* = 7.0 Hz, 3H), 0.89 (d, *J* = 0.9 Hz, 9H), 0.07 (d, *J* = 1.1 Hz, 3H), 0.06 (s, 3H); **^{13}C NMR** (101 MHz, $CDCl_3$) δ 211.70, 178.71, 81.74, 76.77, 73.81, 64.50, 61.54, 44.46, 42.20, 40.73, 38.88, 35.75, 32.64, 28.40, 27.36, 26.74, 25.91, 25.59, 18.22, 15.46, -4.34, -4.84; **IR** (cast film, $CHCl_3$) *v* 2951.41, 2864.43, 1724.03, 1158.66; 839.73. **HRMS (ESI-TOF)** *m/z*: $[M + NH_4]^+$ Calcd for $C_{26}H_{53}ClNO_5Si$ 522.3382; Found 522.3391.

Synthesis of carboxylic acid 320

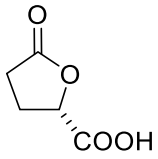

To a solution of L-glutamic acid **319** (15.06 g, 102 mmol) in H_2O (48 mL) and concentrated HCl (22 mL) at 0 ºC was added over 30min a solution of $NaNO_2$ (10.59 g, 154 mmol) in H_2O (48 mL). The slightly yellow mixture was then allowed to warm to room temperature overnight. The solvent was then removed under reduced pressure and the residue was diluted with EtOAc (~80 mL). It was then filtered to remove the white solids. The filtrate was dried over $MgSO_4$, filtered and concentrated under reduced pressure to afford a thick yellow oil, which solidified on standing. The crude product **320** was used in the next step without purification (12.76 g, 95% purity, 90% crude yield). **^{1}H NMR** (400 MHz, $CDCl_3$) δ 11.09 (br s, 1H), 5.32 – 4.59 (m, 1H), 2.81 – 2.51 (m, 3H), 2.48 – 2.35 (m, 1H); **^{13}C NMR** (101 MHz, $CDCl_3$) δ 176.40, 174.75, 75.41, 26.86, 25.91. Synthesis of the title compound was performed by Dimitri Panagopoulos.

Synthesis of alcohol 321

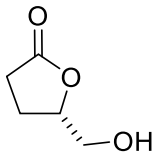

To a solution of carboxylic acid **320** (1.44 g, 11 mmol) in THF (74 mL) at 0 ºC was added BH_3.DMS (1.2 mL, 13 mmol) over 10min. After 1h at 0 ºC, the solution was allowed to warm to rt over 4h. The reaction mixture was then opened to the atmosphere and the reaction was carefully quenched with the slow addition of MeOH (2.2 mL). The solvents were then removed under reduced pressure and the residue was dried under a stream of air overnight to afford the title compound as a slightly yellow oil (1.29 g, 97% purity, 98% crude yield). The crude product **321** was used in the next step without purification. **^{1}H NMR** (400 MHz, $CDCl_3$) δ 4.70 – 4.58 (m, 1H), 3.91 (dd, *J* = 12.5, 2.9 Hz, 1H), 3.66 (dd, *J* = 12.5, 4.7 Hz, 1H), 2.78 – 2.50 (m, 2H), 2.45 (br s, 1H), 2.34 – 2.22 (m, 1H), 2.21 – 2.08 (m, 1H). Synthesis of the title compound was performed by Dimitri Panagopoulos.

Synthesis of ester 322

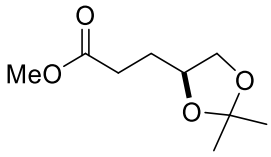

To a solution of **321** (13.87 g, 119 mmol) in MeOH (40 mL) at rt was added 2,2-dimethoxypropane (161 mL, 1.31 mol). Then, Amberlyst 15 (2.5 g) was added as well and the mixture was stirred at rt overnight. The reaction mixture was then quenched with the addition of saturated $NaHCO_3$ (~30 mL) and further diluted with H_2O (30 mL). The aqueous was then extracted with EtOAc (3 x 40 mL) and the combined organic layers were washed with saturated $NaHCO_3$ (40 mL) and brine (40 mL), dried over $MgSO_4$, filtered and concentrated under reduced pressure to afford 17.33 g of an orange oil. Purification of the crude material by flash chromatography (silica gel, hexanes-EtOAc 7:3 to 1:1) afforded the title compound as a yellow oil (13.88 g, 62%). **^{1}H NMR** (400 MHz, $CDCl_3$) δ 4.16 – 4.08 (m, 1H), 4.04 (dd, *J* = 7.9, 6.1 Hz, 1H), 3.67 (s, 3H), 3.54 (dd, *J* = 7.9, 6.7 Hz, 1H), 2.54 – 2.32 (m, 2H), 1.95 – 1.79 (m, 2H), 1.39 (s, 3H), 1.33 (s, 3H); **^{13}C NMR** (101 MHz, $CDCl_3$) δ 173.77, 109.17, 75.07, 69.21, 51.78, 30.34, 28.96, 27.04, 25.74. Synthesis of the title compound was performed by Dimitri Panagopoulos.

Synthesis of aldehyde 324

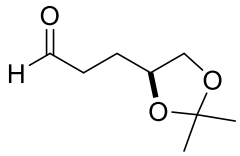

To a solution of **322** (13.88 g, 74 mmol) in dry CH_2Cl_2 (147 mL) at -78 ºC was added DIBAL-H 1M solution in Hexanes (77 mL, 77 mmol) dropwise over 25min. After stirring for 15min, the reaction was quenched with the addition of MeOH (60 mL). The mixture was then stirred at -78 ºC for another 20min and then it was allowed to warm to 0 ºC over 1h. Following that, it was allowed to warm to rt over 1h. Upon reaching rt, the reaction mixture was diluted with Et_2O (~100 mL) and saturated Rochelle's salt solution (~150 mL). The biphasic mixture was then stirred vigorously overnight at rt for the layers to separate. The layers were then separated and the aqueous was further extracted with EtOAc (3 x 150 mL). The combined organic layers were then dried over $MgSO_4$, filtered and concentrated under reduced pressure to afford the title compound as a yellow oil (11.47 g, 92% purity, 90% crude yield). This material was used immediately for the next step without purification. **^{1}H NMR** (400 MHz, $CDCl_3$) δ 9.80 (s, 1H), 4.18 – 4.08 (m, 1H), 4.09 – 4.01 (m, 1H), 3.59 – 3.51 (m, 1H), 2.66 – 2.50 (m, 2H), 1.99 – 1.88 (m, 1H), 1.88 – 1.77 (m, 1H), 1.40 (s, 3H), 1.33 (s, 3H). Synthesis of the title compound was performed by Dimitri Panagopoulos.

Synthesis of chlorohydrin 324

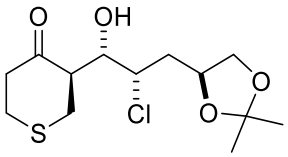

To a slurry of NCS (3.19 g, 24 mmol) and D-proline (3.22 g, 29 mmol) in CH_2Cl_2 (70 mL) at 0 ºC was added a solution of **323** (3.78 g, 24 mmol) in CH_2Cl_2 (10 mL). After 1h 10min, tetrahydriothiopyran-4-one **308** (8.33 g, 72 mmol) was added, followed by DMSO (16 mL). The reaction mixture was then allowed to warm to rt over 4 days. It was then quenched with the addition of brine (100 mL) and the layers were separated. The aqueous was extracted with CH_2Cl_2 (3 x 80 mL) and the combined organic layers were washed with brine (150 mL), dried over $MgSO_4$, filtered and concentrated under reduced pressure to afford 13.18 g of a brown solid. Purification of the crude material by flash

chromatography (silica gel, hexanes-EtOAc 4:1 to 3:2) afforded the title compound as a slightly yellow, semi-crystalline solid (2.40 g, 33%). **^{1}H NMR** (500 MHz, $CDCl_3$) δ 4.47 – 4.31 (m, 1H), 4.24 (dt, *J* = 10.7, 2.4 Hz, 1H), 4.12 (td, *J* = 7.2, 6.1, 3.7 Hz, 2H), 3.59 (dd, *J* = 8.1, 6.6 Hz, 1H), 3.19 (d, *J* = 4.6 Hz, 1H), 3.14 (ddd, *J* = 9.6, 8.4, 4.8 Hz, 1H), 3.07 – 3.02 (m, 1H), 3.02 – 2.94 (m, 2H), 2.86 – 2.68 (m, 3H), 2.24 (ddd, *J* = 14.7, 10.7, 2.7 Hz, 1H), 1.90 (ddd, *J* = 14.7, 9.7, 2.8 Hz, 1H), 1.40 (s, 3H), 1.36 (s, 3H); **^{13}C NMR** (126 MHz, $CDCl_3$) δ 211.54, 109.38, 73.18, 72.92, 69.41, 60.52, 56.56, 44.58, 39.99, 31.89, 30.77, 27.27, 25.77. Synthesis of the title compound was performed by Dimitri Panagopoulos.

Synthesis of diol 325

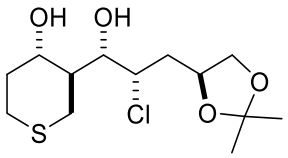

To a solution of **324** (3.12 g, 10 mmol) in MeCN (101 mL) at -15 ºC was added glacial acetic acid (5.78 mL, 101 mmol). Then, $NaBH(OAc)_3$ (10 g, 47 mmol) was also added and the resulting slurry was stirred at -15 ºC overnight. After 16h, the reaction mixture was warmed to 0 ºC and quenched with saturated Rochelle's salt solution (~100 mL). The mixture was further diluted with EtOAc (~100 mL) and stirred vigorously for 1h. The layers were then separated and the aqueous was extracted with EtOAc (2 x 100 mL). The combined organic layers were then washed with brine (200 mL), dried over $MgSO_4$, filtered and concentrated under reduced pressure to afford a yellow oil, which was an inseparable mixture of diastereoisomers (3.65 g, 100%, d.r. ~ 4:1). This material was advanced to the next step without further purification. **^{1}H NMR** (400 MHz, $CDCl_3$) δ 4.46 – 4.25 (m, 2H), 4.26 – 4.18 (m, 0.5H), 4.18 – 4.07 (m, 2H), 4.01 – 3.94 (m, 0.5H), 3.87 – 3.67 (m, 1H), 3.66 – 3.51 (m, 1H), 3.03 – 2.92 (m, 1H), 2.81 – 2.58 (m, 2H), 2.46 – 2.32 (m, 1H), 2.31 – 2.12 (m, 2H), 1.98 – 1.73 (m, 2H), 1.41 (s, 3H), 1.36 (s, 3H). Synthesis of the title compound was performed by Dimitri Panagopoulos.

Synthesis of cyclic alcohol 326

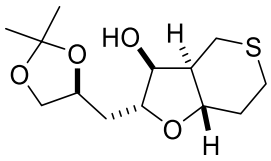

To a solution of **324** (1.64 g, 5.3 mmol) in ^{t}BuOH (168 mL) and H_2O (8.5 mL) was added $SrCO_3$ (38.9 g, 264 mmol). The resulting white slurry was then stirred at 100 ºC for 25h. It was then allowed to cool to rt and was diluted with EtOAc (~100 mL). The slurry was then filtered through a plug of silica and the filtrate was concentrated under reduced pressure to afford 1.56 g of a brown oil. Purification of the crude material by flash chromatography (silica gel, hexanes-EtOAc 1:1 to 3:7) afforded the title compound as a yellow oil (753 mg, 52% over two steps). **^{1}H NMR** (400 MHz, $CDCl_3$) δ 4.20 – 4.13 (m, 1H), 4.09 (dt, *J* = 8.1, 5.4 Hz, 1H), 3.80 (td, *J* = 6.3, 1.6 Hz, 1H), 3.61 (dd, *J* = 8.1, 7.4 Hz, 1H), 3.41 (td, *J* = 11.0, 3.7 Hz, 1H), 2.87 (t, *J* = 12.3 Hz, 1H), 2.78 – 2.59 (m, 3H), 2.47 (dt, *J* = 12.2, 3.4 Hz, 1H), 1.99 – 1.89 (m, 1H), 1.86 – 1.58 (m, 4H), 1.41 (s, 3H), 1.35 (s, 3H); **^{13}C NMR** (101 MHz, $CDCl_3$) δ 109.02, 83.97, 79.35, 77.03, 72.92, 69.44, 49.59, 37.33, 33.97, 27.53, 27.48, 27.08, 25.84. Synthesis of the title compound was performed by Dimitri Panagopoulos.

Synthesis of alcohol 327

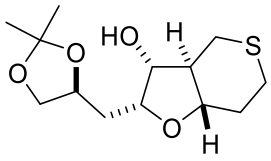

To a solution of **326** (1.12 g, 4 mmol) in THF (27 mL) were added p-nitrobenzoic acid (1.02 g, 6 mmol) and Ph_3P (1.61 g, 6 mmol). The yellow solution was cooled to 0 ºC and then DIAD (1.2 mL, 6 mmol) was added dropwise. After stirring at 0 ºC for 1h, the reaction mixture was allowed to warm to rt over 3h. The solvent was then removed under reduced pressure and the thick yellow residue was redissolved in MeOH (58 mL). Then, freshly ground NaOH (490 mg, 12 mmol) was added and the reaction mixture was stirred at rt for 1h. It was then quenched by the addition of H_2O (~40 mL). The mixture was further diluted with brine (~20 mL) and extracted with EtOAc (3 x 40 mL). The combined organic layers were washed with saturated NH_4Cl (40 mL) and brine (40 mL), dried over $MgSO_4$, filtered and concentrated under reduced pressure to afford 4.44 g of a thick yellow oil. This material was dissolved in a minimum amount of CH_2Cl_2 and then diluted with Et_2O, then placed in the freezer overnight. The following day the mixture was filtered, the white solid was discarded and the filtrate was concentrated under reduced pressure to afford 2.2 g of a yellow oil. Purification of this material by flash chromatography (silica gel, hexanes-EtOAc 1:1 to 1:4) afforded the title compound as a low melting white solid (653 mg, 58%

over two steps). **^{1}H NMR** (400 MHz, $CDCl_3$) δ 4.49 – 4.33 (m, 1H), 4.12 (ddd, *J* = 10.5, 8.0, 5.9 Hz, 2H), 4.00 (q, *J* = 8.4 Hz, 1H), 3.81 – 3.68 (m, 1H), 3.63 (t, *J* = 8.0 Hz, 1H), 3.12 – 2.88 (m, 2H), 2.81 – 2.66 (m, 2H), 2.60 (dd, *J* = 12.9, 11.5 Hz, 1H), 2.38 (dq, *J* = 12.1, 3.3 Hz, 1H), 2.10 (ddd, *J* = 15.1, 7.2, 2.8 Hz, 1H), 1.93 – 1.64 (m, 3H), 1.45 (s, 3H), 1.39 (s, 3H). Synthesis of the title compound was performed by Dimitri Panagopoulos.

Synthesis of methyl ether 328

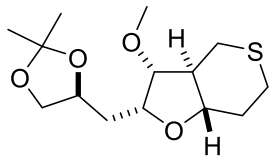

To a slurry of 60% NaH (206 mg, 124 mg active reagent, 5.2 mmol) in THF (5 mL) at 0 ºC was added dropwise a solution of **327** (354 mg, 1.3 mmol) in THF (4 mL). Then, Me_2SO_4 (140 µL, 1,5 mmol) was added as well and then the reaction mixture was stirred at 0 ºC for 2h. It was then quenched (while still at 0 ºC) with H_2O (10 mL) and the aqueous was extracted with Et_2O (3 x 10 mL). The combined organic layers were washed with H_2O (10 mL) and brine (10 mL), dried over $MgSO_4$, filtered and evaporated to afford 471 mg of a white solid. Purification of the crude material by flash chromatography (silica gel, hexanes-EtOAc 3:2) afforded the title compound as a white solid (330 mg, 89%). **^{1}H NMR** (400 MHz, $CDCl_3$) δ 4.37 – 4.23 (m, 1H), 4.08 (dd, *J* = 8.0, 5.9 Hz, 1H), 4.00 – 3.91 (m, 1H), 3.69 – 3.58 (m, 2H), 3.39 (s, 3H), 3.04 – 2.87 (m, 2H), 2.77 – 2.62 (m, 3H), 2.37 (dq, *J* = 12.2, 3.3 Hz, 1H), 1.99 – 1.80 (m, 2H), 1.73 (qd, *J* = 11.5, 4.9 Hz, 1H), 1.41 (s, 3H), 1.36 (s, 3H). Synthesis of the title compound was performed by Dimitri Panagopoulos.

Synthesis of sulfonium salt 329

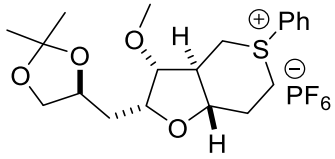

A sealed tube was charged with $Cu(OBz)_2$ (13 mg, 0.04 mmol) and **328** (485 mg, 1.7 mmol) in $ClCH_2CH_2Cl$ (11 mL). Then, Ph_2IPF_6 (721 mg, 1.7 mmol) was added as well, the tube was sealed and the reaction mixture was stirred at 100 ºC for 3.5h. The mixture was then allowed to cool to rt and it was loaded directly onto a chromatography column. Purification by flash chromatography (silica gel, hexanes-EtOAc 1:1 to acetone:CH_2Cl_2

1:1) afforded the title compound, contaminated with ~2% Ph_2IPF_6, as a white foam (638 mg, 74%). **^{1}H NMR** (400 MHz, $CDCl_3$) δ 8.03 (d, *J* = 7.6 Hz, 2H), 7.81 (t, *J* = 7.5 Hz, 1H), 7.73 (t, *J* = 7.7 Hz, 2H), 4.28 (td, *J* = 12.5, 5.8 Hz, 2H), 4.22 – 4.13 (m, 1H), 4.13 – 4.04 (m, 2H), 4.00 – 3.80 (m, 3H), 3.75 – 3.67 (m, 1H), 3.67 – 3.54 (m, 1H), 3.39 (s, 3H), 2.81 – 2.70 (m, 1H), 2.14 – 1.91 (m, 2H), 1.86 – 1.74 (m, 1H), 1.43 (s, 3H), 1.36 (s, 3H). Synthesis of the title compound was performed by Dimitri Panagopoulos.

Synthesis of sulfone 363

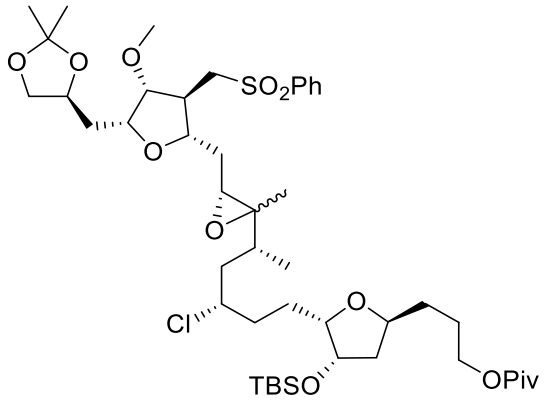

To a cold (-78 °C) solution of sulfonium salt **329** (103 mg, 0.20 mmol) in dry THF (1.5 mL) was added LiHMDS (1 M in hexanes, 0.56 mL, 0.56 mmol). The resulting solution was stirred at -78 °C for 1 hour. Ketone **361b** (110 mg, 0.20 mmol), diluted in a minimum amount of THF (0.3 mL), was then slowly added. Stirring was continued for an additional hour at -78 °C and then 15 hours at room temperature. After this time, an aqueous solution of NH_4Cl (1 mL) was added, the mixture was diluted with CH_2Cl_2 (1 mL) and the phases were separated. The aqueous phase was extracted with CH_2Cl_2 (1 ml x 3), and the combined organic phases were washed with water (1 mL) and brine (1 mL), dried ($MgSO_4$) and concentrated to provide a crude yellow solid **362**. The crude product **362** was then dilute in CH_2Cl_2 (2 mL) and cooled to -78 °C. MCPBA was added (150 mg, 0.60 mmol) and the resulting mixture was allowed to warm up to ambient temperature for 1 hour. After this time, the mixture was cooled to -78 °C and quenched with $NaHCO_3$ (2 mL). After slowly warming up to room temperature, the layers were separated, and the aqueous phase was extracted with CH_2Cl_2 (2 x 2 mL). The combined organic phases were washed with brine (1 mL), dried (Na_2SO_4), filtered, and concentrated to provide a crude oil. Purification of the crude product by flash chromatography (silica gel, hexanes-EtOAc 3:1) provided sulfone **363** (135 mg, 75%) as a clear oil. **$[\alpha]^{20}_D$** -12.1 (*c* 0.33, $CHCl_3$); **^{1}H NMR**

(400 MHz, $CDCl_3$) δ 7.97 – 7.91 (m, 2H), 7.71 – 7.64 (m, 1H), 7.63 – 7.56 (m, 2H), 4.25 (t, *J* = 3.2 Hz, 1H), 4.16 (p, *J* = 6.1 Hz, 2H), 4.10 – 3.96 (m, 3H), 3.86 – 3.79 (m, 2H), 3.67 (q, *J* = 5.8 Hz, 1H), 3.62 (t, *J* = 7.5 Hz, 1H), 3.42 – 3.39 (m, 1H), 3.40 (s, 3H), 3.20 – 3.11 (m, 2H), 2.67 – 2.60 (m, 1H), 2.03 – 1.60 (m, 15H), 1.57 (s, 3H), 1.55 – 1.45 (m, 2H), 1.40 (s, 3H), 1.35 (s, 3H), 1.19 (s, 9H), 0.90 (s, 9H), 0.08 (s, 3H), 0.07 (s, 3H); **^{13}C NMR** (151 MHz, $CDCl_3$) δ 178.76, 139.39, 134.19, 134.03, 129.70, 129.64, 129.53, 129.48, 128.12, 128.10, 109.03, 86.05, 81.97, 81.73, 78.59, 76.79, 73.74, 73.47, 69.52, 64.52, 63.54, 61.47, 59.82, 58.11, 57.39, 43.31, 42.19, 40.91, 38.87, 35.76, 33.66, 32.67, 32.44, 29.85, 27.36, 27.09, 26.69, 25.92, 25.91, 25.57, 18.23, 15.47, 12.87, -4.31, -4.82; **IR** (cast film, $CHCl_3$) *v* 2956.57, 1725.26, 1151.54; 1081.08, 829.45; **HRMS (ESI-TOF)** *m/z*: $[M + NH_4]^+$ Calcd for $C_{46}H_{81}ClNO_{11}SSi$ 918.4988; Found 918.4997.

Synthesis of alcohol 366

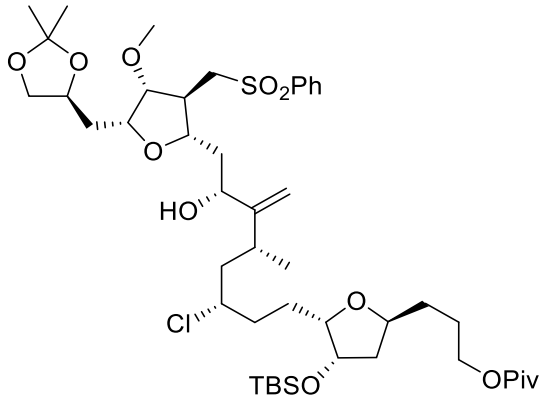

Thoroughly deoxygenated THF (1.5 mL) was added to a mixture of commercial Cp_2TiCl_2 (0.33 mmol) and Mn dust (143 mg, 2.6 mmol) under an Ar atmosphere and the suspension was stirred at room temperature until it turned lime green (after about 15 min). A solution of epoxide **363** (90 mg, 0.1 mmol) in THF (1 mL) was then added and the mixture was stirred for 15 h, after which the reaction was quenched with a saturated solution of NaH_2PO_4 (1 mL). The resulting mixture was filtered through celite and the layers were separated. The organic phase was washed with brine (1 mL), dried (Na_2SO_4), filtered, and concentrated to provide a crude oil. Purification of the crude product by flash chromatography (silica gel, hexanes-EtOAc 7:3) provided alcohol **366** (54 mg, 60%) as a clear oil. **$[\alpha]^{20}_D$** -12.1 (*c* 0.66, $CHCl_3$); **^{1}H NMR** (400 MHz, $CDCl_3$) δ 7.97 – 7.90 (m, 2H), 7.73 – 7.65 (m, 1H), 7.63 – 7.57 (m, 2H), 5.15 (s, 1H), 4.87 (s, 1H), 4.27 – 4.21 (m, 1H), 4.20 – 4.10 (m, 3H), 4.05 (ddt, *J* = 8.5, 4.3, 2.3 Hz, 3H), 3.97 (td, *J* = 8.5, 7.7, 3.4 Hz, 1H),

3.90 (td, *J* = 6.7, 3.6 Hz, 4H), 3.86 – 3.78 (m, 1H), 3.74 (dt, *J* = 9.0, 4.6 Hz, 1H), 3.59 (dd, *J* = 7.9, 7.1 Hz, 1H), 3.39 (s, 3H), 3.14 (d, *J* = 6.8 Hz, 2H), 2.64 – 2.57 (m, 1H), 2.42 – 2.32 (m, 1H), 2.01 – 1.91 (m, 2H), 1.91 – 1.70 (m, 3H), 1.54 – 1.44 (m, 0H), 1.40 (s, 3H), 1.35 (s, 4H), 1.18 (s, 9H), 1.06 (d, *J* = 6.7 Hz, 2H), 0.89 (s, 9H), 0.07 (s, 3H), 0.06 (s, 2H); **^{13}C NMR** (101 MHz, $CDCl_3$) δ 178.71, 156.75, 139.62, 134.22, 129.68, 128.07, 109.19, 85.77, 83.77, 81.80, 79.33, 77.36, 76.75, 73.78, 73.68, 73.53, 69.56, 64.51, 62.30, 58.21, 57.47, 46.33, 44.33, 42.18, 41.64, 38.88, 36.79, 35.81, 32.77, 32.71, 32.64, 29.83, 29.79, 27.36, 27.07, 27.06, 26.81, 25.95, 25.93, 25.91, 25.85, 25.57, 24.83, 19.36, 18.22, -4.33, -4.78, -4.82; **IR** (cast film, $CHCl_3$) *v* 3486.67, 2959.93, 1725.26, 1151.54, 836.16; **HRMS (ESI-TOF)** *m/z*: $[M + NH_4]^+$ Calcd for $C_{46}H_{81}ClNO_{11}SSi$ 918.4988; Found 918.4980.

Synthesis of tetrahydropyran 367

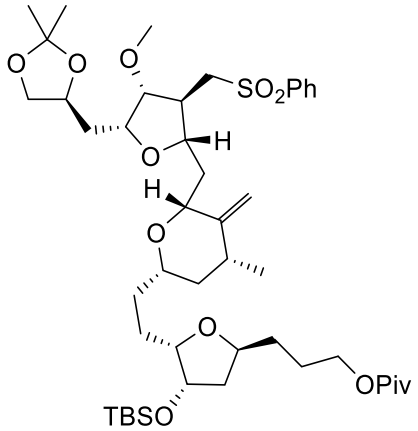

To a solution of alcohol **366** (60 mg, 0.067 mmol) in *t*-BuOAc (5.7 ml) at 0 °C were added 2,6-di-*tert*-butyl-4-methylpyridine (69 mg, 0.33 mmol) and $AgBF_4$ (39 mg, 0.20 mmol). The resulting reaction flask was wrapped with aluminum foil and warmed to rt. After stirring 12 h at rt, the reaction mixture was treated with a NH_4Cl (5 mL). The layers were separated, and the aqueous phase was extracted with EtOAc (2 x 5 mL). The combined organic phases were washed with brine (5 mL), dried (Na_2SO_4), filtered, and concentrated to provide a crude oil. Purification of the crude product by flash chromatography (silica gel, hexanes-EtOAc 5:1) provided tetrahydropyran **367** (43 mg, 75%) as a clear oil. **$[\alpha]^{20}_D$** +4.78 (*c* 0.69, $CHCl_3$); **^{1}H NMR** (400 MHz, $CDCl_3$) δ 7.99 – 7.92 (m, 2H), 7.71 – 7.64 (m, 1H), 7.64 – 7.58 (m, 2H), 4.84 (s, 1H), 4.77 (d, *J* = 1.8 Hz, 1H), 4.23 – 4.10 (m, 3H), 4.09 – 4.00 (m, 3H), 3.89 (d, *J* = 3.2 Hz, 1H), 3.79 – 3.66 (m, 3H), 3.63 (t, *J* = 7.6 Hz, 1H), 3.57 (dd, *J* = 10.1, 3.4 Hz, 1H), 3.44 (s, 3H), 3.40 – 3.33 (m, 1H), 3.18 – 3.03 (m, 2H), 2.57 (dt, *J* = 10.1, 4.5 Hz, 1H), 2.26 – 2.12 (m, 2H), 2.09 – 1.91 (m, 3H), 1.91 – 1.83 (m, 1H), 1.78

– 1.43 (m, 10H), 1.41 (s, 3H), 1.36 (s, 3H), 1.28 – 1.22 (m, 1H), 1.19 (s, 9H), 1.06 (d, *J* = 6.5 Hz, 3H), 0.90 (s, 8H), 0.07 (s, 3H), 0.04 (s, 2H); **^{13}C NMR** (101 MHz, $CDCl_3$) δ 178.70, 150.83, 139.89, 134.01, 129.69, 128.12, 108.96, 104.96, 86.10, 82.69, 81.14, 78.32, 77.35, 76.68, 75.40, 73.58, 73.44, 69.52, 64.51, 58.22, 57.60, 43.36, 42.78, 42.30, 38.89, 37.71, 35.61, 32.67, 32.33, 27.38, 27.12, 25.98, 25.95, 25.71, 25.64, 18.21, 18.10, -4.19, -4.70; **IR** (cast film, $CHCl_3$) *v* 2956.24, 2849.93, 2347.38, 1724.03, 1144.16; **HRMS (ESI-TOF)** *m/z*: $[M + NH_4]^+$ Calcd for $C_{46}H_{80}NO_{11}SSi$ 882.5221; Found 882.5230.

Synthesis of ketone 368

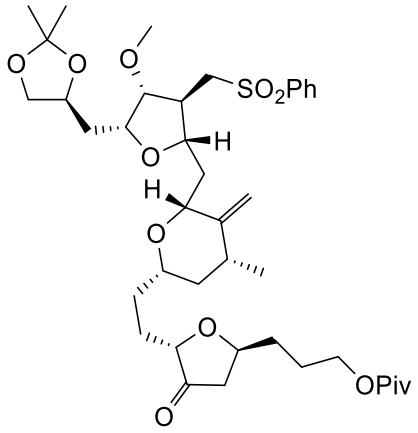

To a cold (0 °C) solution of compound **367** (56 mg, 0.065 mmol) in THF (0.2 mL) and pyridine (0.36 mL) was added HF-pyridine (70% in pyridine, 0.18 mL, 5 mmol). The resulting solution was stirred at room temperature for 15 hours. After this time, an aqueous solution of $NaHCO_3$ (0.5 mL) was added, the mixture was diluted with EtOAc (0.5 mL) and the phases were separated. The aqueous phase was extracted with EtOAc (0.5 ml x 3), and the combined organic phases were washed with water (1 mL) and brine (1 mL), dried ($MgSO_4$) and concentrated to provide a crude yellow oil that was directly used in the next step without further purification. The crude alcohol was diluted in CH_2Cl_2 (0.6 mL) and cooled to 0 °C. $NaHCO_3$ (28 mg, 0.32 mmol) in and DMP (28 mg, 0.071 mmol) were then added and the mixture was stirred at room temperature for 1 hour. After this time, the reaction was quenched with $H_2O/Na_2S_2O_3$(aq)/NaHCO3(aq) = 1/1/1 (1 mL) and the resulting mixture was stirred for another 30 minutes. The mixture was extracted with CH_2Cl_2 (0.5 ml x 3), washed with brine, dried over anhydrous $MgSO_4$, and concentrated to provide a crude oil. Purification by flash chromatography (silica gel, hexanes-EtOAc 5:1) provided ketone **368** (34 mg, 70%) as a clear oil. **$[\alpha]^{20}_D$** -8.23 (*c* 1.2, $CHCl_3$); **^{1}H NMR** (400 MHz, $CDCl_3$) δ 7.98 – 7.93 (m, 2H), 7.71 – 7.66 (m, 1H), 7.64 – 7.58 (m, 2H), 4.86

(s, 1H), 4.79 (d, *J* = 1.8 Hz, 1H), 4.32 – 4.22 (m, 1H), 4.16 (h, *J* = 6.1 Hz, 1H), 4.08 (tdd, *J* = 7.9, 5.9, 3.8 Hz, 3H), 3.85 (d, *J* = 3.3 Hz, 1H), 3.76 (ddd, *J* = 15.8, 8.2, 4.4 Hz, 3H), 3.67 – 3.59 (m, 2H), 3.41 (s, 4H), 3.16 (dd, *J* = 14.4, 10.8 Hz, 1H), 3.02 (dd, *J* = 14.4, 2.7 Hz, 1H), 2.61 (ddd, *J* = 10.8, 5.4, 2.7 Hz, 1H), 2.53 (dd, *J* = 18.0, 6.7 Hz, 1H), 2.26 – 2.11 (m, 3H), 2.09 – 1.95 (m, 2H), 1.91 (ddd, *J* = 13.2, 9.4, 3.4 Hz, 1H), 1.83 – 1.44 (m, 10H), 1.41 (s, 3H), 1.36 (s, 3H), 1.20 (s, 9H), 1.07 (d, *J* = 6.4 Hz, 3H); **^{13}C NMR** (101 MHz, $CDCl_3$) δ 216.16, 178.65, 150.62, 140.04, 134.05, 129.67, 128.11, 109.00, 105.18, 86.04, 81.20, 78.72, 78.42, 77.36, 76.32, 75.47, 74.81, 73.58, 69.57, 64.02, 58.29, 57.59, 43.34, 42.80, 42.52, 38.91, 37.65, 35.66, 32.43, 32.15, 31.60, 27.37, 27.12, 26.84, 25.94, 25.08, 18.06; IR (cast film, $CHCl_3$) *v* 2956.24, 2864.43, 1757.85, 1724.03, 1148.93; **HRMS (ESI-TOF)** *m/z*: $[M + NH_4]^+$ Calcd for $C_{40}H_{64}NO_{11}S$ 766.4200; Found 766.4193.

Synthesis of alkene 120

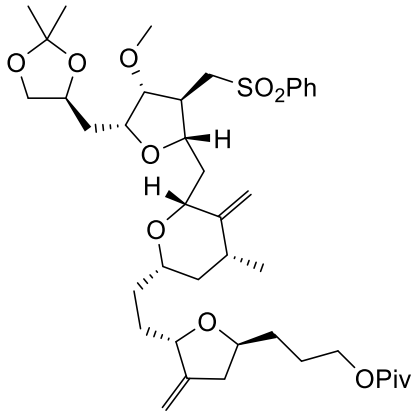

To a suspension of methyltriphenylphosphonium bromide (17 mg, 0.048 mmol) in dry THF (0.3 mL) was added *t*BuOK (48 µL of 1.0 M solution in THF, 0.048 mmol) at 0 °C. After the mixture was stirred for 30 minutes at the same temperature, a solution of ketone **368** (12 mg, 0.016 mmol) in dry THF (0.3 mL) was slowly added. After stirring for an additional 3 hours at room temperature, the resulting mixture was quenched with water (0.5 mL). The mixture was extracted with EtOAc (0.5 mL), washed with brine (0.5 mL), dried over anhydrous $MgSO_4$, and concentrated to provide the crude product as a yellow oil. Purification by flash chromatography (silica gel, hexanes-EtOAc 9:1) afforded the desired alkene **120** (11 mg, 90%). **$[\alpha]^{20}_D$** -7.6 (*c* 0.3, $CHCl_3$); **^{1}H NMR** (500 MHz, $CDCl_3$) δ 8.00 – 7.92 (m, 2H), 7.72 – 7.66 (m, 1H), 7.61 (t, J = 7.7 Hz, 2H), 4.90 (q, J = 2.1 Hz, 1H), 4.85 (s, 1H), 4.78 (d, J = 1.9 Hz, 1H), 4.64 (q, J = 2.2 Hz, 1H), 4.23 (br s, 1H), 4.17 (p, J = 6.2 Hz, 1H), 4.11 – 4.01 (m, 3H), 3.94 (p, J = 6.2 Hz, 1H), 3.91 (d, J = 3.3 Hz, 1H), 3.77 (td, J

= 6.8, 3.2 Hz, 1H), 3.72 (dt, J = 9.8, 5.0 Hz, 1H), 3.65 – 3.57 (m, 2H), 3.44 (s, 3H), 3.41 – 3.33 (m, 1H), 3.12 (dd, J = 14.3, 10.9 Hz, 1H), 3.04 (dd, J = 14.3, 2.7 Hz, 1H), 2.65 – 2.57 (m, 2H), 2.27 – 2.15 (m, 3H), 2.05 – 2.00 (m, 2H), 1.88 (ddd, *J* = 13.2, 9.5, 3.4 Hz, 1H), 1.77 – 1.70 (m, 1H), 1.67 – 1.39 (m, 7H), 1.41 (s, 3H), 1.37 (s, 3H), 1.35 – 1.25 (m, 2H), 1.19 (s, 9H), 1.07 (d, *J* = 6.4 Hz, 3H). **^{13}C NMR** (126 MHz, $CDCl_3$) δ 178.70, 151.38, 150.72, 139.94, 134.12, 129.67, 128.13, 109.02, 105.11, 105.09, 85.84, 81.12, 79.54, 78.42, 77.25, 76.89, 75.43, 73.55, 69.57, 64.37, 58.14, 57.58, 43.28, 42.86, 38.92, 37.64, 35.67, 32.35, 31.89, 31.72, 31.64, 27.36, 27.10, 25.93, 25.43, 18.07. **IR** (cast film, $CHCl_3$) *v* 2956.24, 2932.08, 2864.43, 1757.85, 1724.03; **HRMS (ESI-TOF)** *m/z*: $[M + NH_4]^+$ Calcd for $C_{41}H_{66}NO_{10}S$ 764.4407; Found 766.4411.

Table 2.13. Comparison of experimental and reported[70] data of compound 120.

^{1}H NMR (600 MHz, $CDCl_3$) δ (ppm) experimental	^{1}H NMR (300 MHz, $CDCl_3$) δ (ppm) reported	^{13}C NMR (151 MHz, $CDCl_3$) δ (ppm) experimental	^{13}C NMR (151 MHz, $CDCl_3$) δ (ppm) reported
8.0 – 7.92 (m, 2H)	7.96 (dd, *J* = 7.0, 1.5 Hz, 2H)	178.70	178.60
7.72 – 7.66 (m, 1H)	7.70 (dd, *J* = 8.0, 1.5 Hz, 1H)	151.38	151.26
7.61 (t, *J* = 7.7 Hz, 2H)	7.61 (dd, *J* = 8.0, 7.0 Hz, 2H)	150.72	150.51
4.90 (q, *J* = 2.1 Hz, 1H)	4.90 (d, *J* = 1.5 Hz, 1H),	139.94	139.81
4.85 (s, 1H)	4.85 (s, 1H)	134.12	134.03
4.78 (d, *J* = 1.9 Hz, 1H)	4.78 (s, 1H)	129.67	129.57
4.64 (q, *J* = 2.2 Hz, 1H)	4.64 (q, *J* = 1.5 Hz, 1H)	128.13	128.02
4.23 (br s, 1H)	4.26 – 4.21 (br s, 1H)	105.11	105.01
4.17 (p, *J* = 6.0 Hz, 1H)	4.18 (p, *J* = 6.0 Hz, 1H)	105.09	104.97
4.11 – 4.01 (m, 3H)	4.10 – 4.02 (m, 3H)	85.84	85.72
3.94 (p, *J* = 6.2 Hz, 1H)	3.95 (p, *J* = 6.0 Hz, 1H)	81.12	81.01
3.91 (d, *J* = 3.3 Hz, 1H)	3.91 (d, *J* = 3.0 Hz, 1H)	78.42	78.30
3.77 (td, *J* = 6.8, 3.2 Hz, 1H)	3.77 (dt, *J* = 10.0, 3.0 Hz, 1H)	77.25	77.14
3.72 (dt, *J* = 9.8, 5.0 Hz, 1H)	3.73 (p, *J* = 5.0 Hz, 1H)	76.89	76.78
3.65 - 3.57 (m, 2H)	3.62 (dd, *J* = 15.0, 8.0 Hz, 1H), 3.60 (dd, *J* = 10.0, 2.5 Hz, 1H)	75.43	75.32
3.44 (s, 3H)	3.44 (s, 3H)	73.55	73.44
3.41 - 3.33 (m, 1H)	3.41 - 3.33 (m, 1H)	69.357	69.46
3.12 (dd, J = 14.3, 10.9 Hz, 1H)	3.12 (dd, J = 14.3, 10.9 Hz, 1H)	64.37	64.27
3.04 (dd, J = 14.3, 2.7 Hz, 1H)	3.04 (dd, J = 14.3, 2.7 Hz, 1H)	58.14	58.02
2.65 – 2.57 (m, 2H)	2.64 – 2.58 (m, 2H)	57.58	57.46
2.27 – 2.15 (m, 3H)	2.25 – 2.17 (m, 3H)	43.28	43.16
2.05 – 2.00 (m, 3H)	2.04 – 2.01 (m, 2H)	42.86	42.75
1.88 (ddd, *J* = 13.2, 9.5, 3.4 Hz, 1H)	1.88 (dt, *J* = 12.5, 3.0 Hz, 1H)	38.92	38.81
1.77 – 1.70 (m, 1H)	1.77 – 1.71 (m, 1H)	37.64	37.53
1.67 – 1.39 (m, 7H),	1.66 – 1.40 (m, 7H),	35.67	35.55
1.41 (s, 3H)	1.41 (s, 3H)	32.35	32.24
1.37 (s, 3H)	1.37 (s, 3H)	31.89	31.78
1.35 – 1.25 (m, 2H)	1.35 – 1.25 (m, 2H)	31.71	31.61
1.19 (s, 9H)	1.19 (s, 9H)	31.64	31.54
1.07 (d, *J* = 6.4 Hz, 3H)	1.07 (d, *J* = 6.5 Hz, 3H)	27.36	27.26
		27.10	26.99
		25.93	25.83
		25.43	25.32
		18.07	17.97

Synthesis of alkene 76

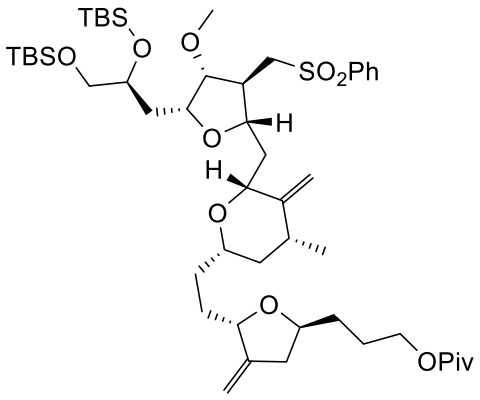

To a cold (0 °C) solution of compound **120** (13 mg, 0.017 mmol) in THF (0.25 mL) was added HCl (1 M in H_2O, 0.25 mL, 0.25 mmol). The resulting solution was stirred at room temperature for 5 hours. After this time, an aqueous solution of $NaHCO_3$ (0.5 mL) was added, the mixture was diluted with EtOAc (0.5 mL) and the phases were separated. The aqueous phase was extracted with EtOAc (0.5 ml x 3), and the combined organic phases were washed with water (1 mL) and brine (1 mL), dried ($MgSO_4$) and concentrated to provide a crude yellow oil that was directly used in the next step without further purification. The crude diol was diluted in CH_2Cl_2 (0.3 mL) and cooled to 0 °C. Et_3N (12 µL, 0.088 mmol) and TBSOTf (19 µL, 0.083 mmol) were then added and the reaction mixture was stirred for 1 hour. After this time, water (0.5 mL) was added and the phases were separated. The aqueous phase was extracted with CH_2Cl_2 (2 × 0.5 mL), and the combined organic phases were dried (Na_2SO_4), filtered, and concentrated to provide a crude oil. Purification of the crude product by flash chromatography (silica gel, hexanes-EtOAc 95:5) afforded compound **76** (11 mg, 69%) as a colorless oil. **^{1}H NMR** (600 MHz, $CDCl_3$) δ 7.98 – 7.91 (m, 2H), 7.73 – 7.65 (m, 1H), 7.64 – 7.57 (m, 2H), 4.90 (q, *J* = 2.2 Hz, 1H), 4.85 (s, 1H), 4.78 (d, *J* = 1.9 Hz, 1H), 4.67 (q, *J* = 2.2 Hz, 1H), 4.25 (s, 1H), 4.06 (td, *J* = 6.3, 2.5 Hz, 2H), 3.96 (p, *J* = 6.4 Hz, 1H), 3.89 – 3.75 (m, 3H), 3.68 (dt, *J* = 9.7, 4.9 Hz, 1H), 3.62 – 3.54 (m, 2H), 3.51 – 3.45 (m, 1H), 3.43 (s, 3H), 3.42 - 3.34 (m, 1H), 3.10 – 2.96 (m, 2H), 2.67 – 2.51 (m, 2H), 2.26 – 2.14 (m, 3H), 2.06 – 1.96 (m, 1H), 1.94 – 1.69 (m, 4H), 1.68 - 1.24 (m, 7H), 1.19 (s, 9H),1.07 (d, *J* = 6.4 Hz, 3H), 1.05 – 0.99 (m, 1H), 0.90 (s, 18H), 0.10 (s, 3H), 0.09 (s, 3H), 0.05 (s, 3H), 0.04 (s, 3H). **^{13}C NMR** (151 MHz, $CDCl_3$) δ 178.73, 151.41, 150.71, 139.87, 134.09, 129.66, 128.12, 105.07, 85.91, 80.85, 79.48, 78.46, 76.9, 75.49, 71.54, 68.00, 64.39, 58.22, 57.71, 43.45, 42.84, 38.92, 37.64, 35.65, 33.25, 31.84,

31.72, 31.59, 29.85, 27.35, 26.15, 26.11, 25.41, 18.09, -3.90, -4.56, -5.17. The data of compound **76** matched that reported in the literature.[136]

1H NMR (600 MHz, CDCl3) of compound 76

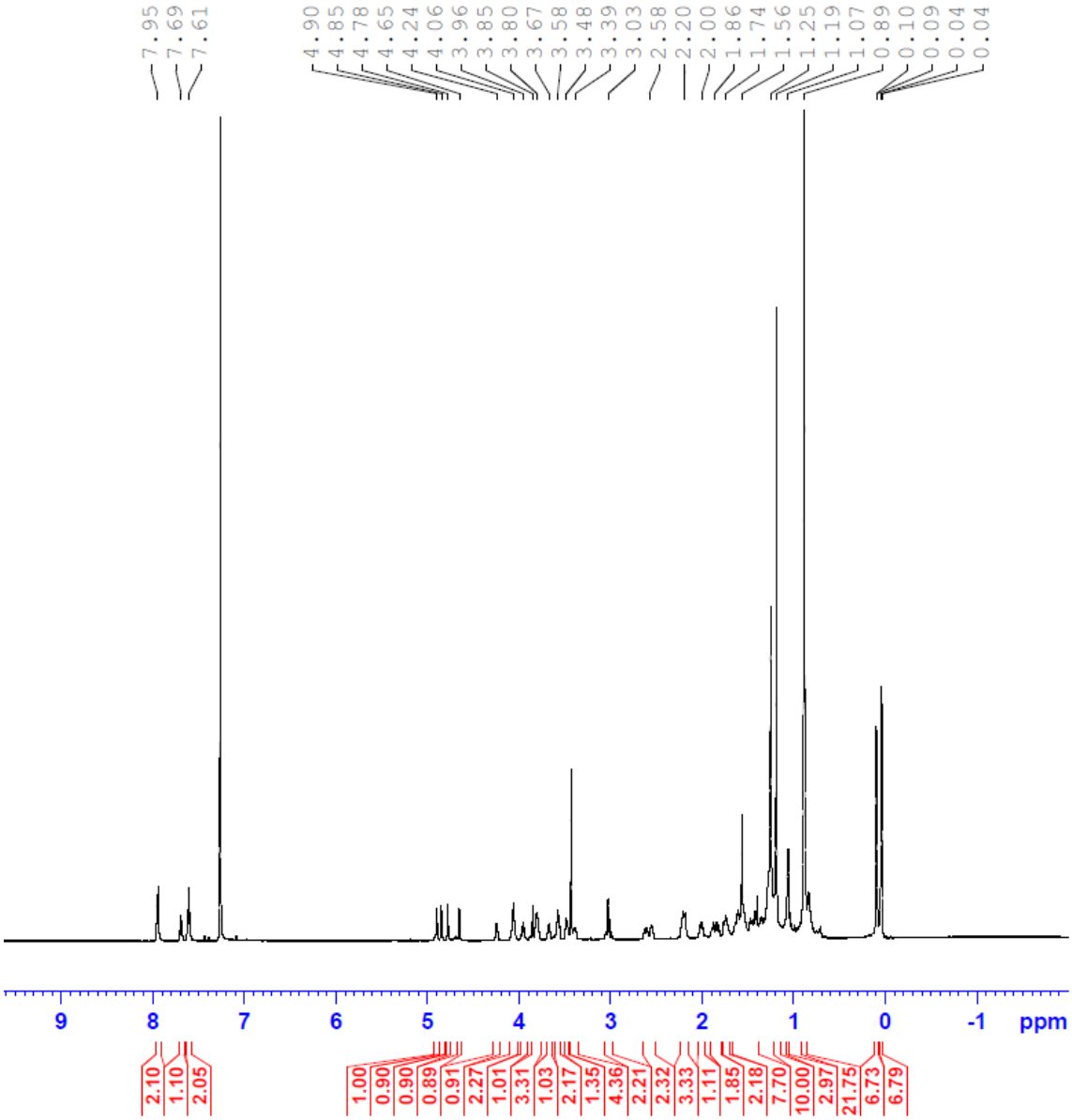

^{13}C NMR (151 MHz, $CDCl_3$) of compound 76

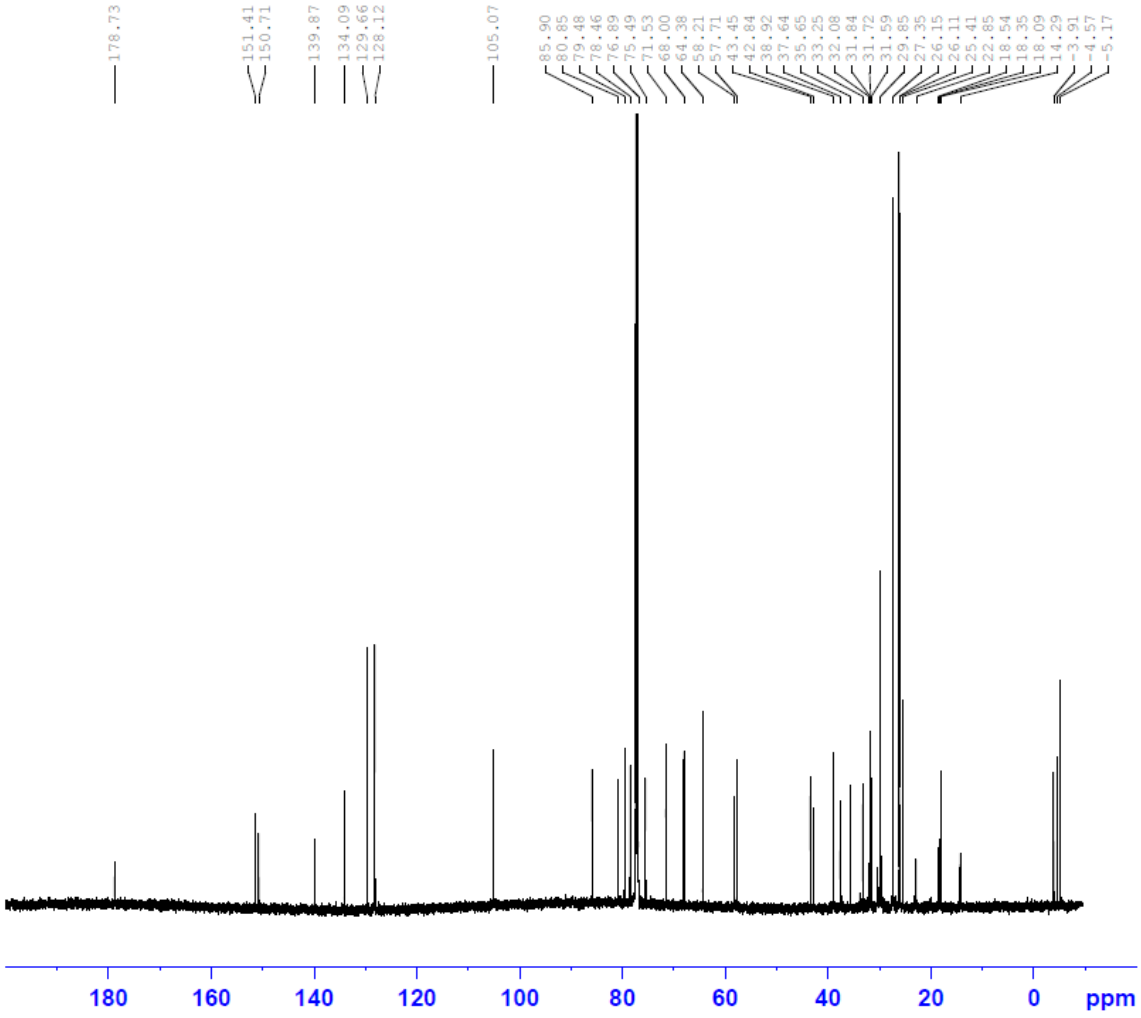

Table 2.14. Comparison of experimental and reported[136] data of compound 76.

^{1}H NMR (600 MHz, $CDCl_3$) δ (ppm) experimental	^{1}H NMR (300 MHz, $CDCl_3$) δ (ppm) reported	^{13}C NMR (151 MHz, $CDCl_3$) δ (ppm) experimental	^{13}C NMR (126 MHz, $CDCl_3$) δ (ppm) reported
7.98 – 7.91 (m, 2H)	7.96 – 7.93 (m, 2H),	178.73	178.5
7.73 – 7.65 (m, 3H)	7.71 – 7.57 (m, 3H)	151.41	151.3
4.90 (q, *J* = 2.2 Hz, 1H)	4.90 (q, *J* = 1.8 Hz, 1H),	150.71	150.6
4.85 (s, 1H)	4.85 (s, 1H)	139.87	139.8
4.78 (d, *J* = 1.9 Hz, 1H)	4.78 (d, *J* = 1.2 Hz, 1H)	134.09	133.9
4.67 (q, *J* = 2.2 Hz, 1H)	4.67 (q, *J* = 1.8 Hz, 1H)	129.66	129.5
4.25 (s, 1H)	4.25 (s, 1H)	128.12	128.0
4.06 (td, *J* = 6.3, 2.5 Hz, 2H)	4.08 – 4.02 (m, 2H)	105.07	104.9
3.96 (p, *J* = 6.4 Hz, 1H)	4.00 – 3.92 (m, 1H)	85.91	85.8
3.89 – 3.75 (m, 3H)	3.85 – 3.76 (m, 3H)	80.85	80.7
3.68 (dt, *J* = 9.7, 4.9 Hz, 1H)	3.71 – 3.64 (m, 1H)	79.48	79.4
3.62 – 3.54 (m, 2H)	3.63 – 3.54 (m, 2H)	78.46	78.3
3.51 – 3.45 (m, 1H)	3.53 – 3.47 (m, 1H)	76.9	
3.43 (s, 3H)	3.44 (s, 3H)	75.49	75.4
3.42 - 3.34 (m, 1H)	3.42 - 3.34 (m, 1H)	71.54	71.4
3.10 – 2.96 (m, 2H)	3.12 – 2.97 (m, 2H)	68.00	67.9
2.67 – 2.51 (m, 2H)	2.63 (br dd, *J* = 5.87, 15.65 Hz, 1H), 2.59 - 2.50 (m, 1H)	64.39	64.2
2.26 – 2.14 (m, 3H)	2.28 – 2.13 (m, 3H)	58.22	58.1
2.06 – 1.96 (m, 1H)	2.12 – 1.95 (m, 1H)	57.71	57.6
1.94 – 1.69 (m, 4H)	1.93 – 1.69 (m, 4H),	43.45	43.4
1.68 - 1.24 (m, 7H)	1.68 - 1.33 (m, 7H)	42.84	42.7
1.19 (s, 9H)	1.20 (s, 9H)	38.92	38.8
1.07 (d, *J* = 6.4 Hz, 3H)	1.08 (d, *J* = 5.9 Hz, 3H)	37.64	37.2
1.05 – 0.99 (m, 1H)	1.06 – 1.00 (m, 1H)	35.65	35.5
0.90 (s, 18H)	0.90 (s, 18H)	33.25	33.2
0.10 (s, 3H), 0.09 (s, 3H)	0.10 (d, *J* = 3.4 Hz, 6H)	31.84	31.7
0.05 (s, 3H), 0.04 (s, 3H)	0.08 – 0.03 (m, 6H)	31.72	31.6
		31.59	31.4
		29.85	29.7
		27.35	27.2
		26.15	26.0
		26.11	26.0
		25.41	25.3
		18.09	17.9, 18.2, 18.4
		-3.90	-4.1
		-4.56	-4.7
		-5.17	-5.3

Chapter 3.

Synthesis of Alphora Fragments of Eribulin

3.1. Introduction

3.1.1. Alphora

Alphora Research Inc. was acquired by Eurofins Scientific (EUFI.PA), a world leader in biopharmaceutical testing, in 2017.[139] The company provides research contracts for the development of active pharmaceutical ingredients (APIs) and drug substances in the pharmaceutical and biotechnology domains. They offer a wide range of services such as the development of technologies and analytical controls to manufacture APIs, the discovery of new solid forms to enhance bioavailability, as well as pre-formulation and formulation studies. Moreover, through the production of highly potent APIs, the company has developed great expertise in large-scale multi-step syntheses. In this regard, Alphora was contracted in 2012 to develop an innovative and economically viable synthetic route to one of the most complex pharmaceutical molecules, eribulin mesylate. In two years, they were able to elaborate an elegant and innovative route to the marketed API. Since then, they have initiated the daunting task of converting an academic, laboratory-scale synthesis into a commercially viable manufacturing process.[140] At the time Alphora became involved in this project, 5 patents related to the drug were active. The first patent expired in June 2019 and the last is set to expire in June 2027, thereby leaving room for the development of a generic version of the drug.

3.1.2. Generic

To cover the high costs (estimated to $2.8 billion in 2020)[141] and risks associated with the development of a new drug, companies routinely file patent applications to protect the structure or the synthetic process of a potential drug candidate. In most countries, once the application is filed, the patent is valid for a duration of 20 years.[142] Given the length of the drug discovery process is about 10 years, the company will be granted another 10 years of exclusivity. After this time, so-called “generic drugs”, which contain the same API but often differ in some characteristics such as the manufacturing process,

formulation, and packaging, will be authorized on the market. Here, the price of the original brand-name product and its generic equivalents drop significantly compared to the original cost. In this regard, Emcure Pharmaceuticals, a global pharmaceutical company from India (a leading country in the world's generic drugs market), has announced in April 2019 the launch of a generic version of Eisai Pharmaceutical's Halaven (eribulin) to treat metastatic breast cancer. The drug will be sold under the tradename of "eribilin" and is expected to be priced 40% lower than Halaven.[143]

3.1.3. Alphora synthesis of eribulin

Also aiming for a generic version of Halaven, researchers at Eurofins-Alphora have spent the last 10 years developing a large-scale synthesis of the anticancer drug eribulin mesylate. While details of this process are not publicly available, we will describe in this section the general synthetic approach toward the macrocyclic ketone that is described in the patent literature.[144]

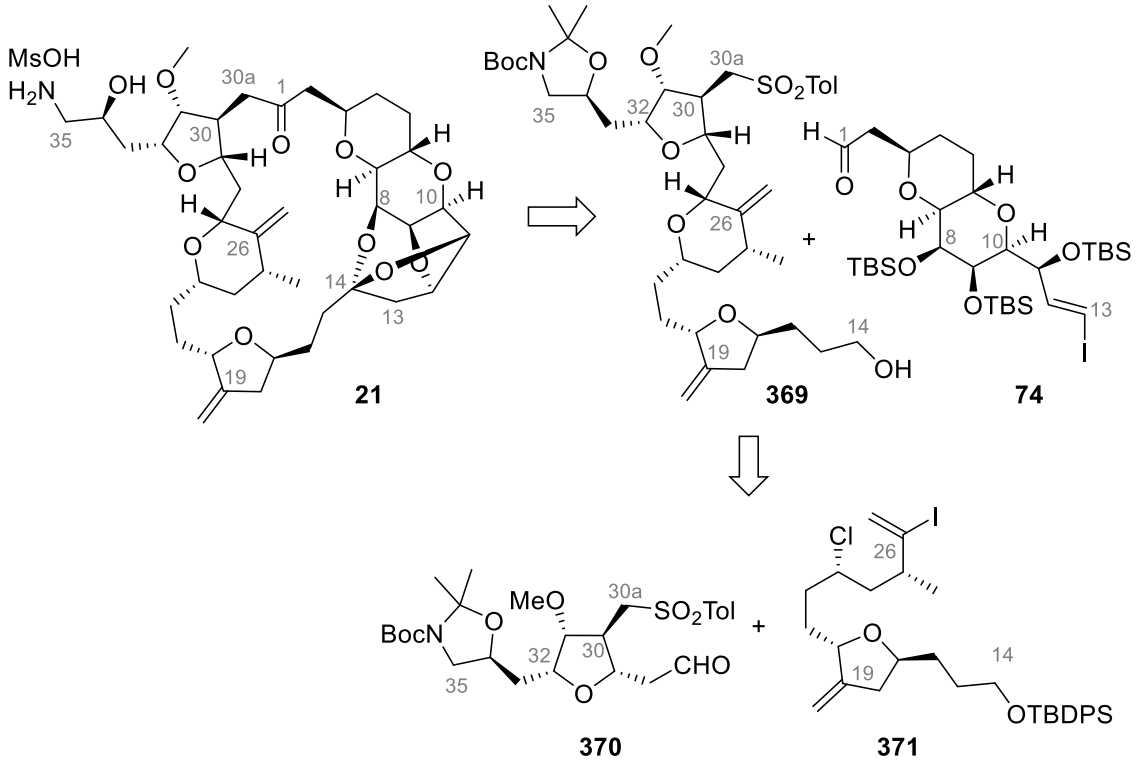

Scheme 3.1. Alphora Retrosynthesis of Eribulin (21).

The route, mainly inspired by recent work of Kishi, Eisai and Alphora, relies on several key Nozaki Hiyama Kishi couplings to link or build fragments of eribulin (Scheme 3.1). A noticeable difference with the previous syntheses of eribulin is the early introduction of the amino alcohol moiety at the C32-side chain (e.g., **369**, Scheme 3.1). In this regard, the synthesis of Alphora C27-C35 fragment of eribulin **370** is shown in Scheme 3.2.[145]

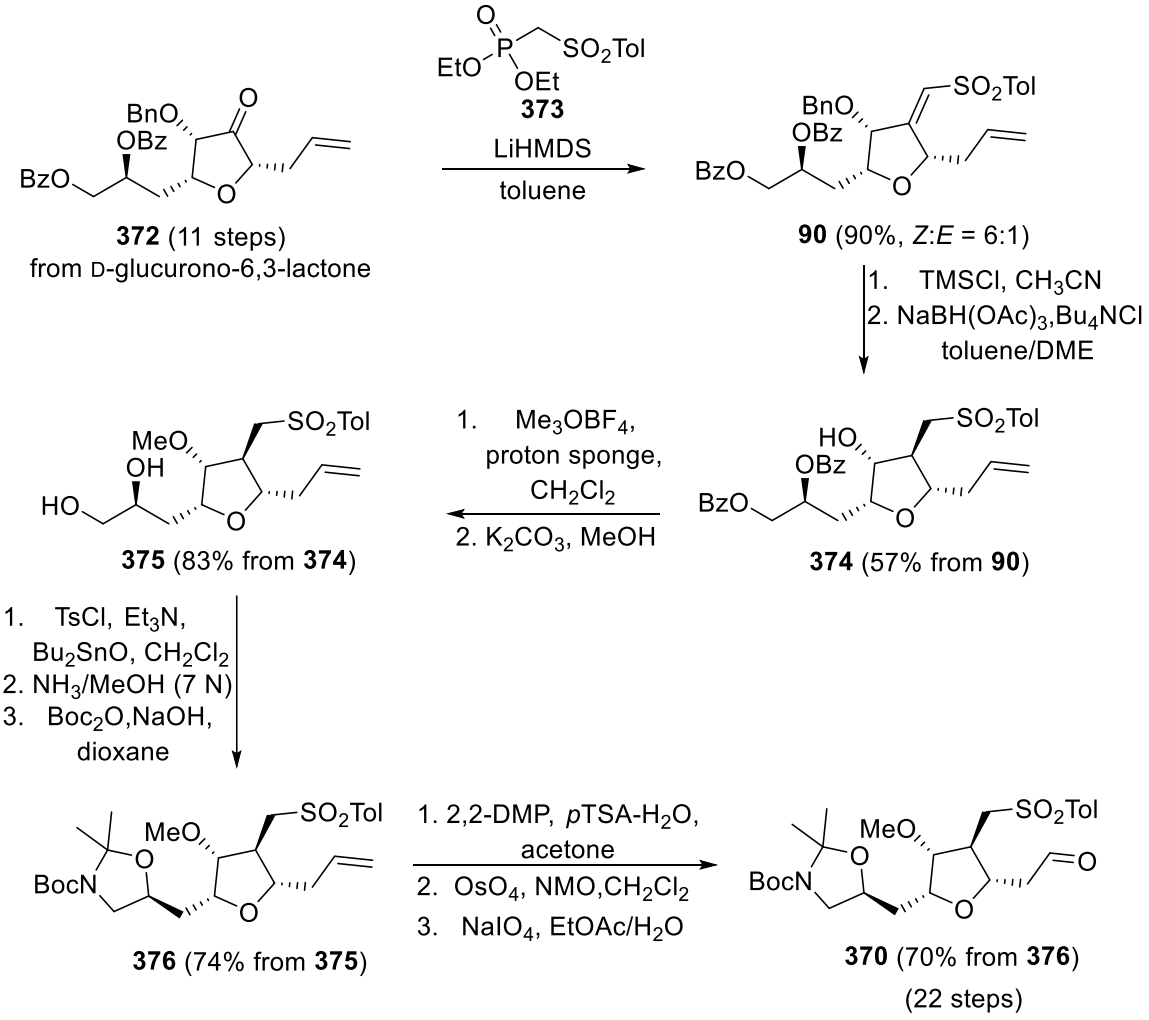

Scheme 3.2. Alphora Synthesis of the C27-C35 Fragment of Eribulin 370.

Starting from the known intermediate **372** (synthesized in 11 steps from D-glucurono-3,6-lactone according to Eisai process-scale synthesis),[146] a subsequent Horner–Wadsworth–Emmons (HWE) reaction provided the unsaturated aryl sulfone **90** as a mixture of *Z:E* geometrical isomers (*Z:E* = 6:1). Benzyl deprotection and following

sodium triacetoxyborohydride reduction, then furnished the sulfone **374** in decent yield (57% from **372**). Subsequent methylation of the secondary alcohol in **374** and removal of the benzoyl protecting groups provided the diol **375** in excellent yield. The latter material **375** was then smoothly converted to the corresponding amino alcohol via successive selective tosylation and nucleophilic substitution with ammonia. Subsequent Boc- and acetonide protection provided the advance intermediate **376** in 80% from **375**. Finally, a 2-step oxidative cleavage of the olefin in **376** completed the assembly of Alphora C27-C35 fragment **370**. Overall, the aldehyde **370** was synthesized in a total of 21 synthetic steps from D-glucurono-3,6-lactone.

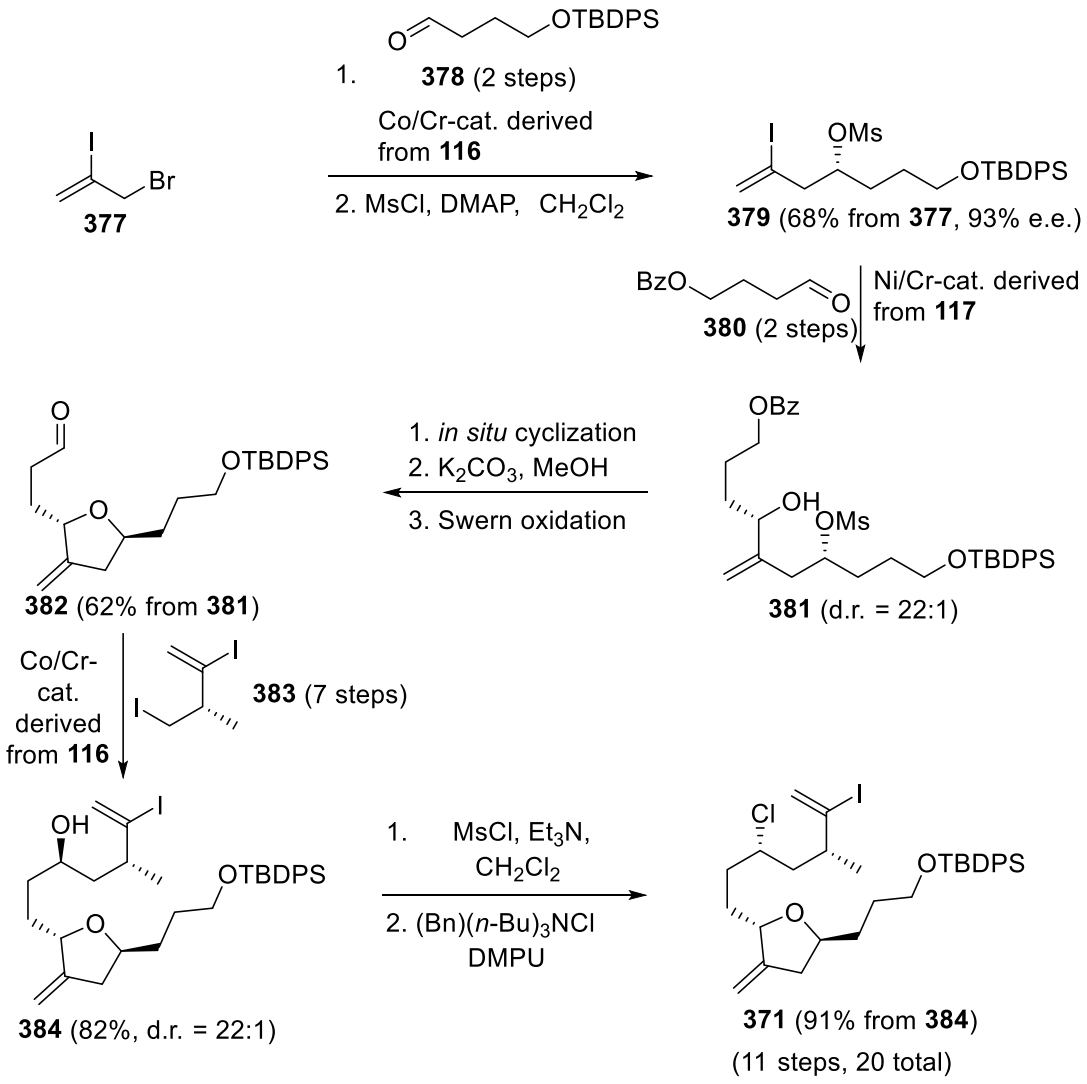

Scheme 3.3. Alphora Synthesis of the C14-C26 Fragment of Eribulin 371.

Alternatively, the route toward the C14-C26 fragment **371** initiates with the stereoselective 2-haloallylation of aldehyde **378** (synthesized in 2 steps from 1,4-

butanediol) using 10 mol% of the Cr complex of (*S*)-catalyst **116** and 0.2 mol% of cobalt phthalocyanine (Scheme 3.3). Mesylation of the resulting alcohol then delivered the vinyl iodide **379** in 68% yield from **378**. Subsequent Ni/Cr-mediated coupling of **379** with aldehyde **380** (synthesized in 2 steps from 1,4-butanediol) furnished **381** in excellent yield (90%) and diastereoselectivity (d.r. = 22:1). Spontaneous cyclization of **381** to the corresponding tetrahydrofuran was followed by removal of the benzoyl protecting group. Swern oxidation of the resulting alcohol provided the aldehyde **382** in 62% yield from **381**. A second Ni/Cr-mediated coupling of aldehyde **382** with the diiodide **383** furnished the vinyl iodide **384** in 82% yield. Subsequent mesylation and nucleophilic substitution of the alcohol in **384**, achieved the synthesis of Alphora C14-C26 fragment of eribulin **371**. Noteworthy, two 7-step synthetic routes of the diiodide coupling partner **383** have been disclosed and thus, it is likely that Alphora synthesis of the diiodide derivative **383** is derived from one of these routes. As a result, while the longest synthetic sequence to Alphora C14-C26 fragment **371** is 11 steps, the overall process involves at least 20 steps.

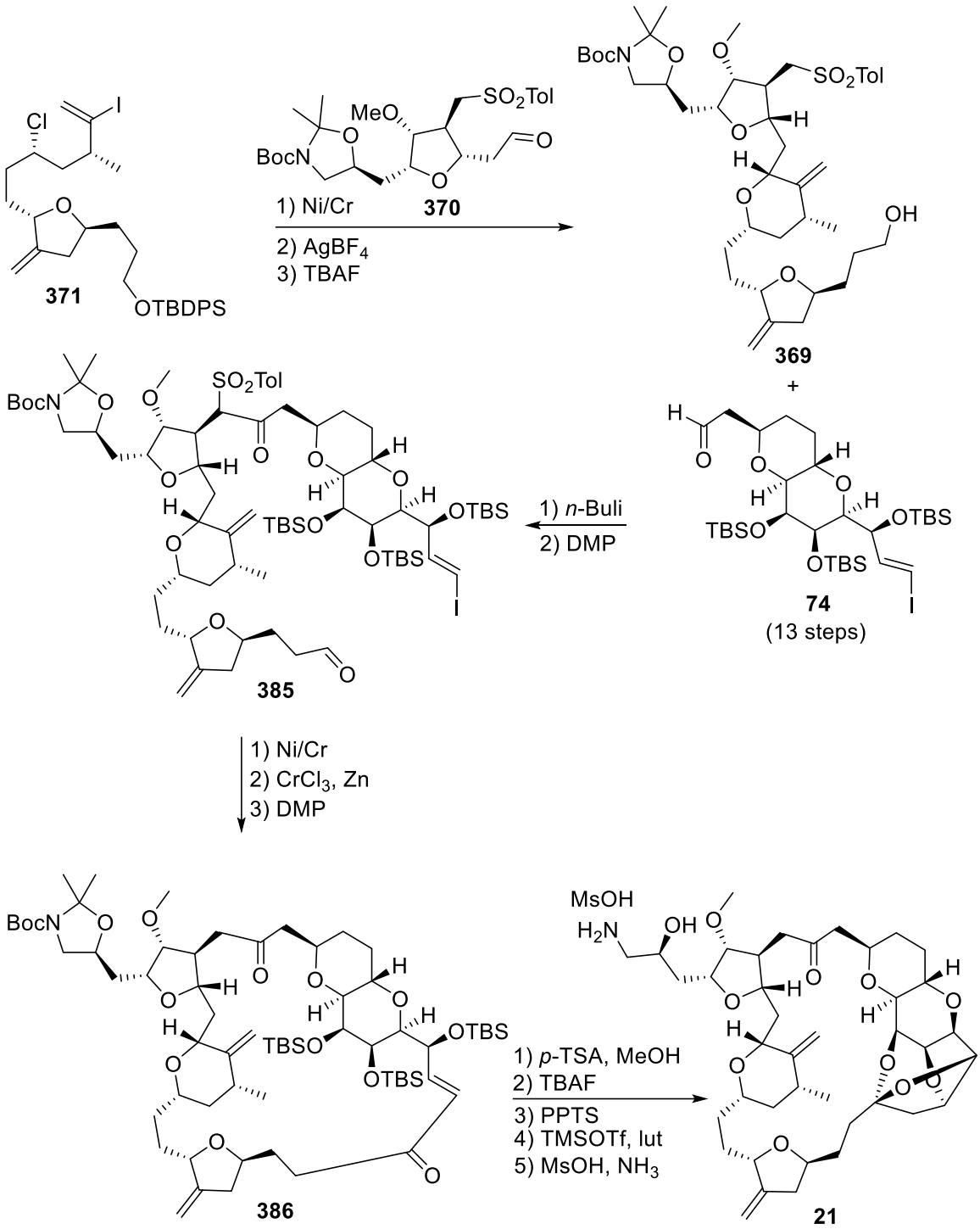

Scheme 3.4. Alphora Synthesis of Eribulin (21).

As depicted in Scheme 3.4, Ni/Cr-mediated coupling of aldehyde **370** with vinyl iodide **371** was followed by a silver-promoted cyclization reaction and subsequent

treatment with TBAF completed the assembly of Alphora C14-C35 fragment of eribulin **369**. Thereafter, coupling of vinyl iodide **369** and aldehyde **74** (synthesized in 13 steps from D-gulonolactone, Scheme 2.6) under basic conditions and following DMP-oxidation provided the aldehyde **385**. Subsequently, an intramolecular Ni/Cr-mediated coupling was followed by a chromium-promoted desulfonylation and another DMP-oxidation, to provide the macrolactone intermediate **386**. Finally, a 5-step sequence that involves the successive deprotections of the amino alcohol moiety and the TBS-protected alcohols, an acid-promoted cyclization and a crystallization, completed Alphora synthesis of eribulin (**21**).

3.2. Development of a concise and scalable synthesis of Alphora C14-C26 fragment of eribulin

3.2.1. Retrosynthesis

About two years after the beginning of the "eribulin project" in the Britton group, we engaged in a collaboration with researchers at Alphora to develop a concise and scalable synthesis of the C14-C23 fragment **382** (Scheme 3.3). Elaboration of a kilogram-scale route derived from this work by researchers at Alphora was then the ultimate goal.

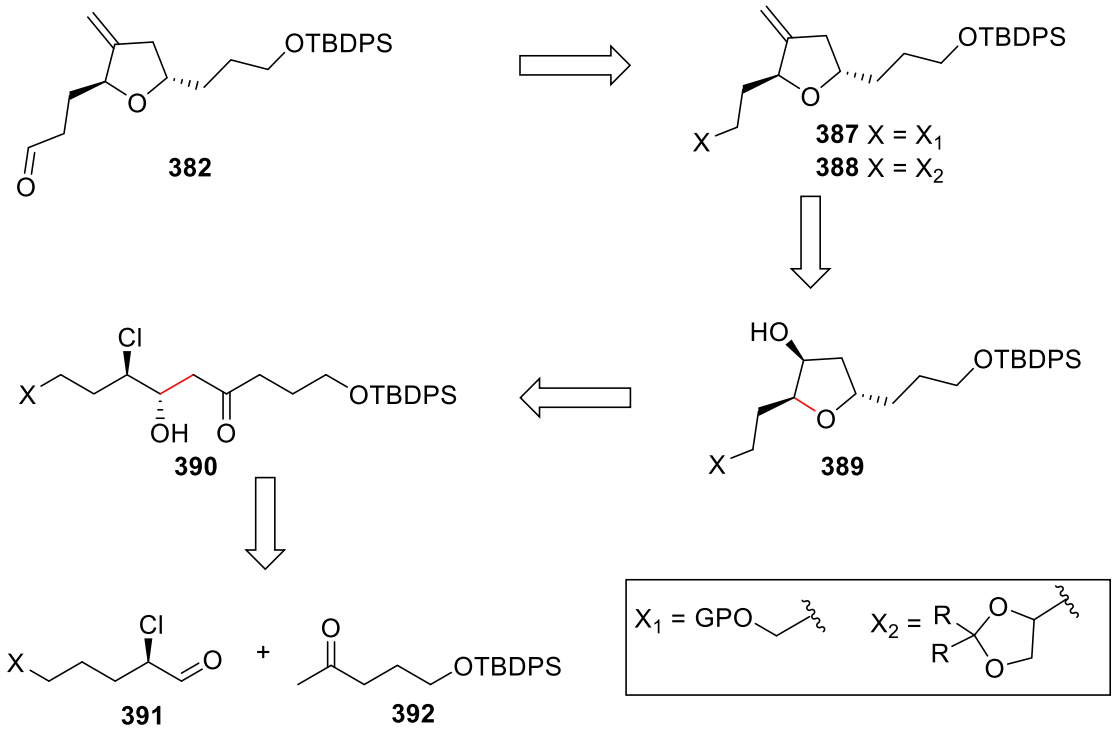

Scheme 3.5. Retrosynthetic Analysis of Alphora Intermediate 382.

As depicted in Scheme 3.5, we anticipated that the aldehyde in **382** could result from the successive deprotection and oxidation of a protected alcohol **387** (X = X_1). Alternatively, deprotection and cleavage of a protected diol **388** (X = X_2) would deliver the key intermediate **382**. In turn, the olefin function in **387** (or **388**) could be easily elaborated from the alcohol **389** using straightforward functional group modifications. Retrosynthetic disconnection of the indicated bond in **389** provides the β-chlorohydrin **390** as a potential precursor. In the synthetic direction, stereoselective reduction of the ketone function in **390** and subsequent cyclization could achieve the formation of the tetrahydrofuran ring in **389**. Finally, disassembly of the 1,3-hydroxyketone in **390** furnishes the aldehyde **391** and the ketone **392** as potential precursors. Synthetically, a stereoselective aldol condensation between an enolate derived from ketone **392** and the aldehyde **391** could complete the desired connection.

3.2.2. Aldehyde candidates

Having in mind an ultimate goal of a kilogram-scale synthesis, we initiated this project by seeking protecting groups that could produce crystalline α-chloroaldehydes. Here, recrystallization of this material could then at once provides a mild means of purification and an opportunity for improving the enantiopurity. Moreover, we envisioned that other solid intermediates could result from these aldehydes throughout the sequence and thus offer more straightforward isolation and purification options.

Toward this goal, a trityl protecting group, an acetonide and a benzylidene acetal were first investigated. Here, protection of 1,6-hexanetriol **393** using 2,2-dimethoxy propane followed by pyridinium chlorochromate oxidation and L-prolinamide α-chlorination, delivered the desired α-chloroaldehyde **395**, but unfortunately, not as a solid (Scheme 3.6).

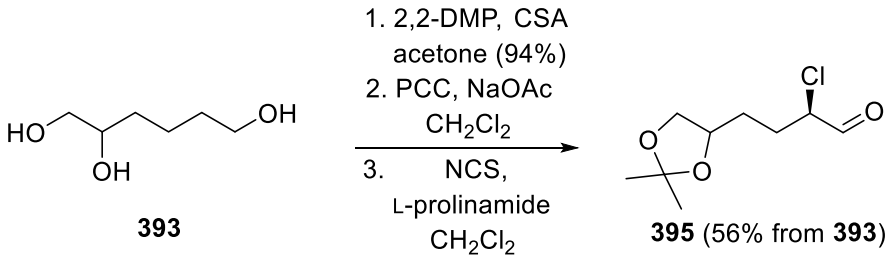

Scheme 3.6. Synthesis of Acetonide Protected Aldehyde 395.
Formation of aldehyde 395 was confirmed by ^{1}H NMR spectroscopic analysis.

The trityl-protected α-chloroaldehyde **396** and the benzylidene-protected diol **398** were then synthesized in a 3-step sequence (Scheme 3.7). Here, treatment of 1,5-hexanediol with tritylchloride, subsequent pyridinium chlorochromate oxidation and α-chlorination, furnished the α-chloroaldehyde **396** in 60% overall yield. Following a similar approach, the α-chloroaldehyde **398** was produced from the commercially available 1,6-hexanetriol **393** (scheme 3.7). Unlike aldehyde **396**, which was an oil, the benzylidene-protected diol **398** appeared as a foamy solid, but unfortunately, attempts to purify this material by recrystallization were unsuccessful.

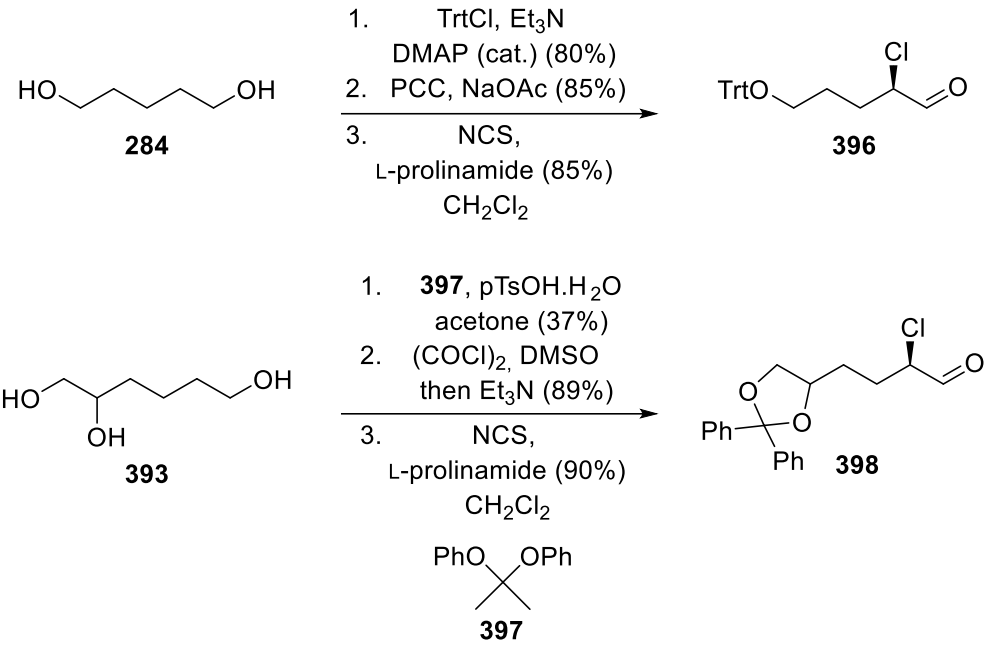

Scheme 3.7. Synthesis of α-Choroaldehydes 396 and 398.
Synthesis performed by Dimitri Panagopoulos.

We next examined the transformation of these aldehydes into solid bisulfite salts. Here, it was anticipated that a simple filtration could provide a clean bisulfite salt intermediate that could then be converted back to the corresponding aldehyde.[147]

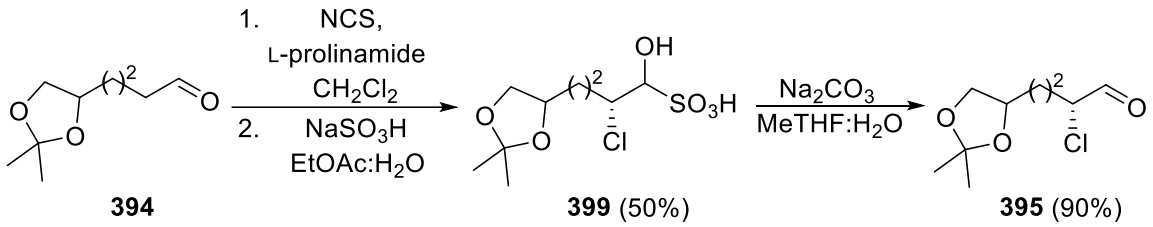

Scheme 3.8. Transient Transformation of Aldehyde 394 into a Bisulfite Salt 399.

Following this strategy, α-chlorination of aldehyde **394** and subsequent treatment with sodium bisulfite in a mixture of ethyl acetate and water, provided the bisulfite salt **399** in 50% yield (Scheme 3.8). To our delight, reaction with aqueous sodium carbonate furnished a clean α-chloroaldehyde **395**. Thereafter, enantiomeric excess of aldehyde **395** was assessed before, and after the bisulfite salt process, by ^{19}F NMR spectroscopic

analysis of the (*R*)-Mosher ester derivative. Here, we discovered that the enantiomeric excess of the α-chloroaldehyde **395** dropped from 60% e.e. (before) to 33% e.e. (after). Following these new insights, a small screen of reaction conditions was performed. Notably, we envisioned that a buffered solution could prevent the undesired epimerization event. Unfortunately, no bisulfite salt was formed when water was switched with buffered solutions (pH = 5; pH = 7 and pH = 9) and no further investigations were conducted. At this point, the enantiomeric excess of aldehydes **396** and **397** were also determined using the Mosher ester method and revealed both compounds had an unsatisfactory 77% and 46% e.e., respectively (Figure 3.1).

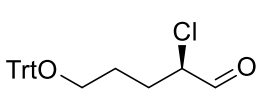

396 (77% e.e., Mosher ester)

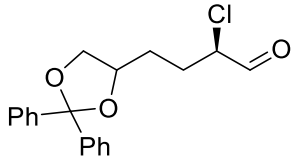

398 (46% e.e., Mosher ester)

Figure 3.1. Enantiomeric Excess of α-Chloroaldehyde 395 and 398.
Work performed by Dimitri Panagopoulos

Finally, a TIPS-protected α-chloroaldehyde **401** was prepared (Scheme 3.9). while we did not anticipate this material to be a solid, improved enantiopurity (82% e.e.) and reactivity of a closely related analogue prepared previously in the Britton group (e.g., aldehyde **291**, Scheme 3.9) inspired us to examine this protecting group. As shown in Scheme 3.9, mono-TIPS protection of pentanediol **284** using sodium hydride and TIPSCl followed by a PCC oxidation and a prolinamide catalyzed α-chlorination, provided the α-chloroaldehyde **401** in 27% overall yield. ^{19}F NMR spectroscopic analysis of the (*R*)-Mosher ester derivative revealed a modest enantiopurity of 70% e.e..

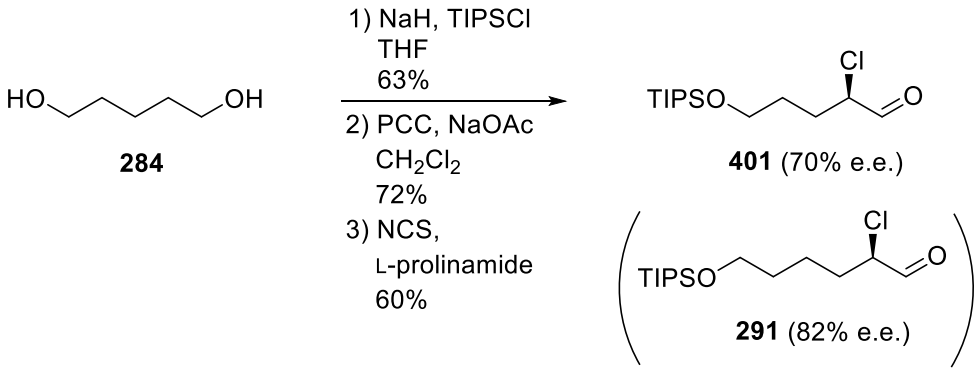

Scheme 3.9. Synthesis of Aldehyde 401 from 1,5-Pentanediol (284).

3.2.3. Synthesis of Alphora C14-C23 fragment

Having synthesized a series of potential aldehyde precursors, the synthetic feasibility of the proposed strategy was then assessed. In this regard, the candidates were subjected to a lithium aldol reaction with an enolate derived from the TBDPS-protected ketone **392** (previously synthesized in one step from 5-hydroxy-2-pentanone).[148] Results of this study are summarized in Table 3.1.

Table 3.1. Lithium Aldol Reaction of α-Chloroaldehydes 395, 396, 398 and 400.

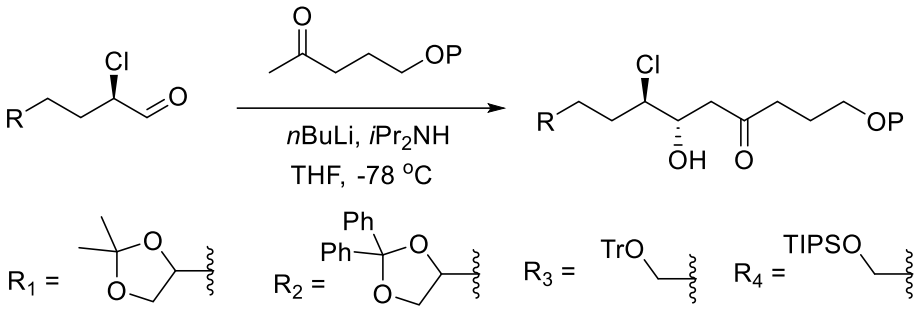

entry	aldehyde	P	base	temp. (°C)	conv.*
1	**395** (R = R_1)	TBDPS	DIPA	-78	0%
2	**396** (R = R_2)	TBDPS	DIPA	-78	0%
3	**398** (R = R_3)	TBDPS	DIPA	-78	0%
4	**401** (R = R_4)	TBDPS	DIPA	-78	0%
5	hexanal (**342**)	TBDPS	LiHMDS	-78	80%
6	**395** (R = R_1)	TBDPS	LiHMDS	-78	5%
7	**395** (R = R_1)	TBDPS	LiHMDS	0	100%
8	**395** (R = R_1)	TBDPS	DIPA	0	100%
9	**395** (R = R_1)	Piv	DIPA	-78	85%
10	**396** (R = R_2)	Piv	DIPA	-78	80%
11	**398** (R = R_3)	Piv	DIPA	-78	75%
12	**401** (R = R_4)	Piv	DIPA	-78	90%

*From analysis of ^{1}H NMR spectra recorded on crude reaction mixtures

As summarized in Table 3.1, the lithium enolate derived from ketone **392** (P = TBDPS) was reacted with aldehydes **395**, **396**, **398**, and **401** at -78 °C, but unfortunately, none of these reactions produced the desired chlorohydrin product (entries 1 to 4). Encouragingly, when ketone **392** was treated with LiHMDS instead of LDA, and subsequently reacted with hexanal **342**, 80% of ketone **392** was converted to the corresponding aldol adduct (entry 5). Unfortunately, when the same reaction conditions were used with aldehyde **395**, only trace amounts of product were formed (entry 6). Moreover, increasing the temperature to 0 °C resulted in decomposition of the ketone **392** (entries 7 and 8). Disappointed by these results, we next examined the Piv-protected ketone **219**. It is noteworthy that this ketone has been successfully coupled with a series of α-chloroaldehydes in the Britton group and thus, we were confident it would deliver the desired chlorohydrins. To our delight, much improved reactivity was observed when ketone **219** was reacted with aldehydes **395**, **396**, **398**, and **401** using the initial reaction conditions (entries 9-12) and thus, it was selected for further investigations.

Regarding the aldehyde coupling partner, given the low enantiopurity of benzylidene protected diol **398** (46% e.e.) and the stability issue associated with trityl protected aldehyde **396**, neither were selected to advance.

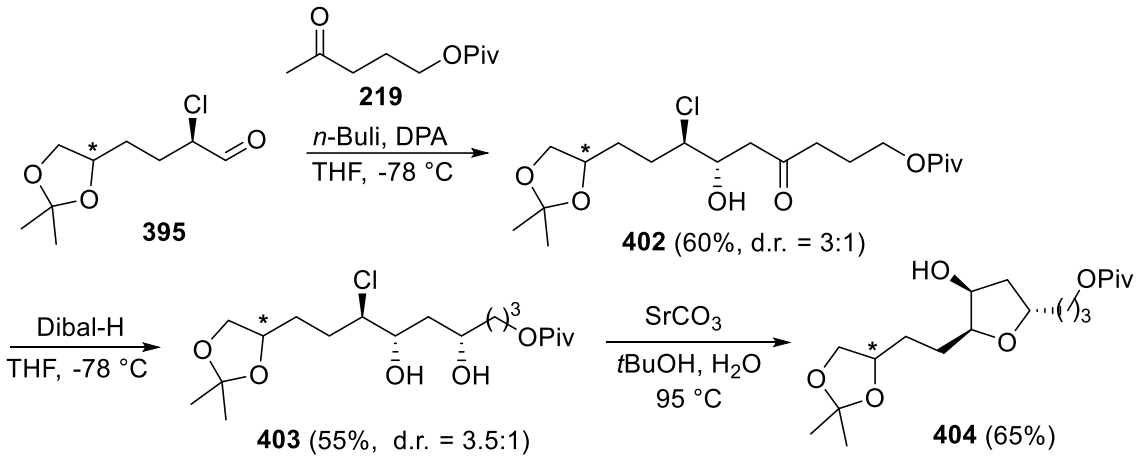

Scheme 3.10. Aldol/Reduction/Cyclization Sequence using Aldehyde 395.
Formation of intermediates 402, 403 and 404 (diastereoisomeric mixture at C*) was confirmed by ^{1}H NMR spectroscopy and mass spectrometric analysis.

As shown in Scheme 3.10, reaction of ketone **219** with α-chloroaldehyde **395** provided the corresponding chlorohydrin **402** in 60% yield (d.r. = 3:1). Subsequent treatment with Dibal-H at -78 °C furnished diol **403** in good yield. Finally, while both the silver-promoted cyclization developed in the Britton group[91] and the strontium carbonate-initiated cyclization recently disclosed by Kishi[149] successfully produced the tetrahydrofuranol **404**, we elected the latter option which was thought less expensive. Here, reaction of diol **403** with strontium carbonate in *tert*-butanol at 95 °C provided the alcohol **404** in 65% yield.

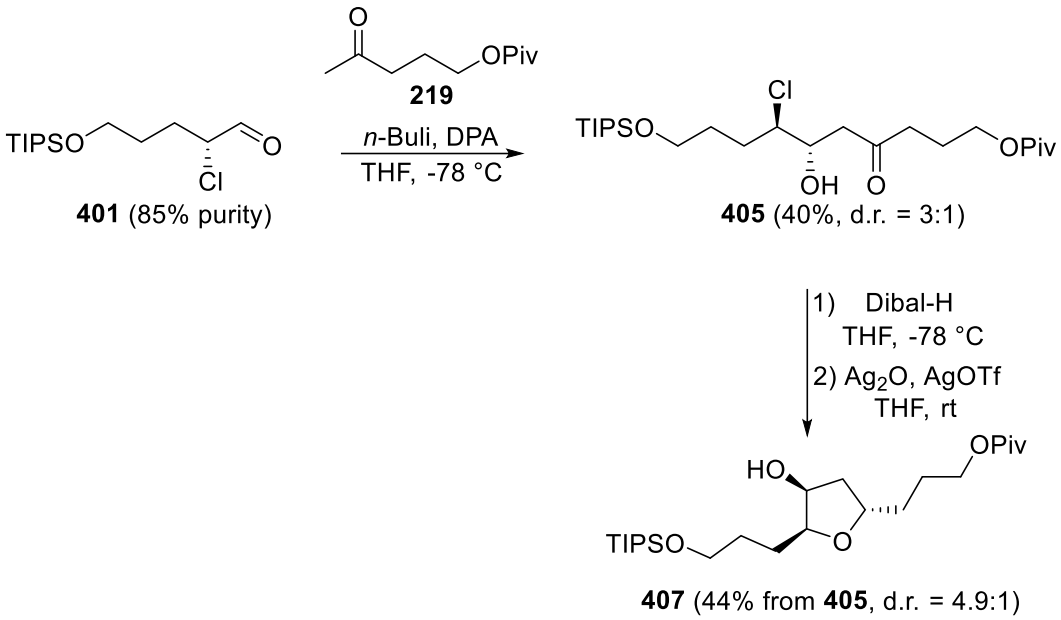

Scheme 3.11. Aldol/Reduction/Cyclization Sequence using Aldehyde 401.

Alternatively, the α-chloroaldehyde **401** was also subjected to the proposed aldol/reduction/cyclization sequence (Scheme 3.11). Here, lithium aldol reaction of aldehyde **401** (~85% purity) with the enolate derived from **219** provided the β-chlorohydrin **405** in 40% yield (Scheme 3.12). Successive diisobutylaluminium hydride reduction and silver oxide-promoted cyclization successfully furnished the tetrahydrofuranol **407** in 44% yield. It is noteworthy that Kishi's strontium carbonate cyclization conditions were also tolerated but showed a reduced reactivity compared to the silver conditions (66% conversion after 24h). As a result of these preliminary studies, it was deemed that both aldehydes **395** and **401** were compatible with the proposed strategy. Subsequently, efforts were made to improve the enantiomeric purity of each aldehyde (60% and 70% e.e., respectively). Here, Christmann's modification of the MacMillan α-chlorination was investigated.[90]

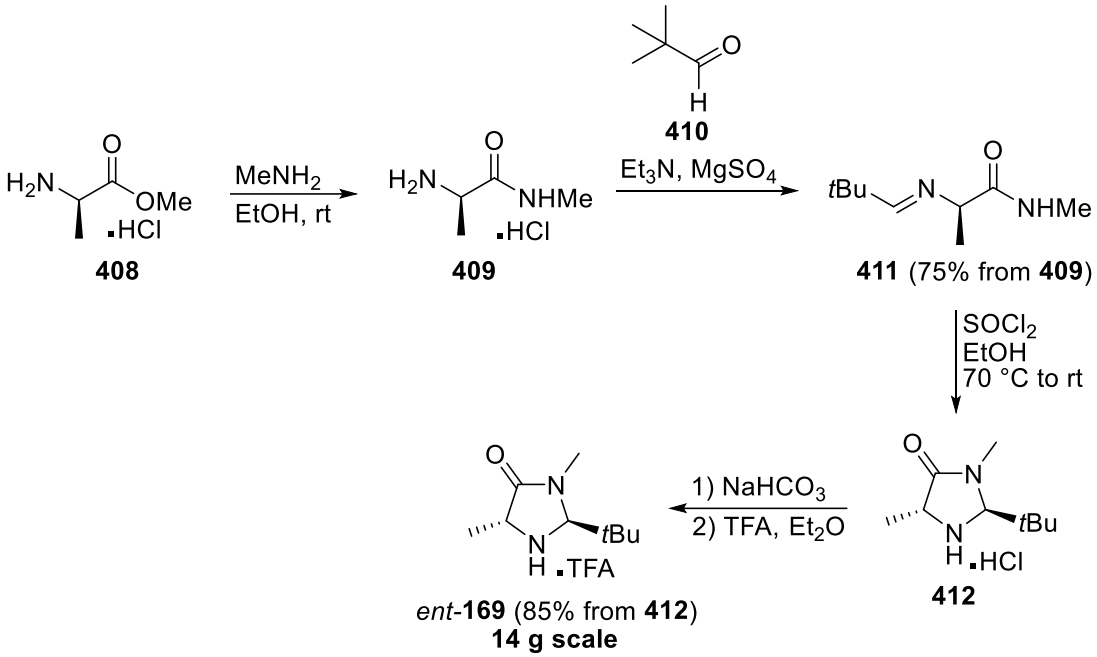

Scheme 3.12. Synthesis of Imidazolidinone *ent*-169.

In this regard, the imidazolidinone *ent*-**169** was synthesized in 4 steps following procedures adapted from the literature (Scheme 3.12).[124] Notably, treatment of D-alanine methyl ester hydrochloride **408** with methylamine and subsequent reaction with pivaldehyde **410**, provided the imine **411** in excellent yield. However, while reported reaction conditions using acetyl chloride to generate hydrogen chloride gave only limited amounts of the desired cyclized product **412**, excellent conversion was observed with thionyl chloride. Finally, sodium bicarbonate wash of the resulting salt followed by treatment with trifluoroacetic acid in diethyl ether, furnished the desired salt *ent*-**169** in 64% overall yield.

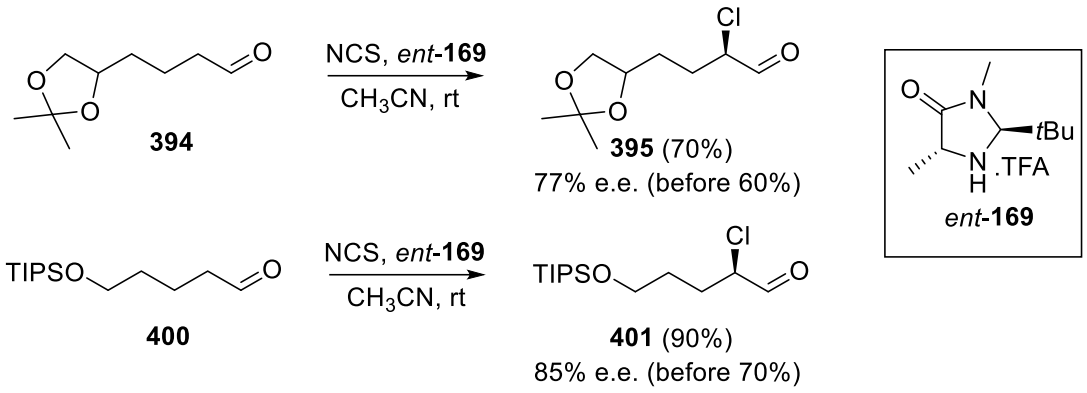

Scheme 3.13. Christmann's Modification of the MacMillan α-Chlorination.
e.e. determined using the Mosher ester method.

As shown in Scheme 3.13, aldehydes **395** and **401** were subjected to Christmann's modification of the MacMillan α-chlorination. Here, the corresponding α-chloroaldehydes **395** and **401** were produced in improved yields and enantioselectivity (77% and 85% e.e., respectively). Moreover, direct extraction of the crude mixture with pentane provided a sufficiently clean aldehyde **401** (purity >95%) to be directly used in the next step without further purification. Given the superior profile of the TIPS-aldehyde **401** (yield and enantiomeric purity), it was selected for further investigations. It is noteworthy that the oily nature of TIPS derivatives precluded any enantiomeric enrichment via recrystallization throughout the sequence. It was expected then that the ultimate Nozaki Hiyama Kishi (NHK) coupling of the aldehyde **401** with Alphora diiodide **383** (e.e. >97%) would upgrade the enantiomeric purity of the material produced (Scheme 3.14).

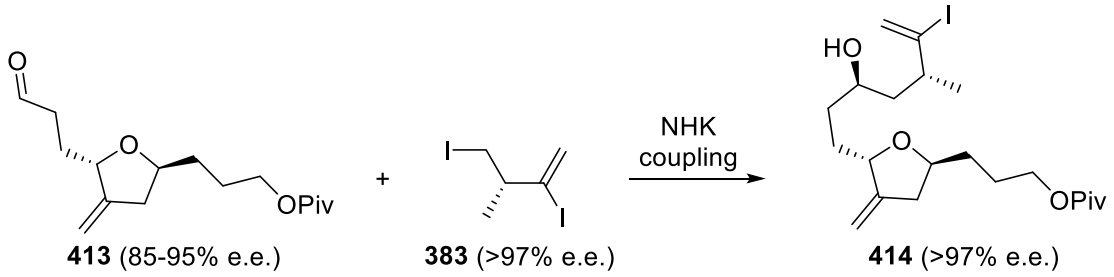

Scheme 3.14. NHK Coupling with Diiodide 383 as a Means of e.e. Upgrade.

Following this strategy, a lithium aldol reaction of ketone **219** with α-chloroaldehyde **401** furnished the corresponding chlorohydrin **405** in 70% yield (d.r. = 3:1,

Scheme 3.15). A subsequent diastereoselective reduction of the ketone function in **405** using Dibal-H resulted in production of the desired 1,3-syn diol **406** in >72% yield (d.r. = 4.9:1). Subsequent cyclization using a combination of Ag_2O and AgOTf gave the 2,5-disubstituted tetrahydrofuranol **407** in 88% yield. Here, several other cyclization conditions were also examined and notably, the thermal $SrCO_3$-promoted cyclization derived from Kishi's protocol[149] provided the desired product **407** in comparable efficiency (86% yield). Swern oxidation[150] of alcohol **407** then furnished the corresponding ketone **414** in 93% yield. Following olefination using methyltriphenylphosphonium bromide and potassium *tert*-butoxide provided the alkene **415** in excellent yield. TIPS deprotection was then achieved using TBAF and treatment of the resulting alcohol **417** with pyridinium chlorochromate furnished the desired aldehyde **413** (83% from **417**). Overall, the Alphora C_{14}-C_{23} fragment of eribulin **413** was produced in 10 steps and 12.6% overall yield.

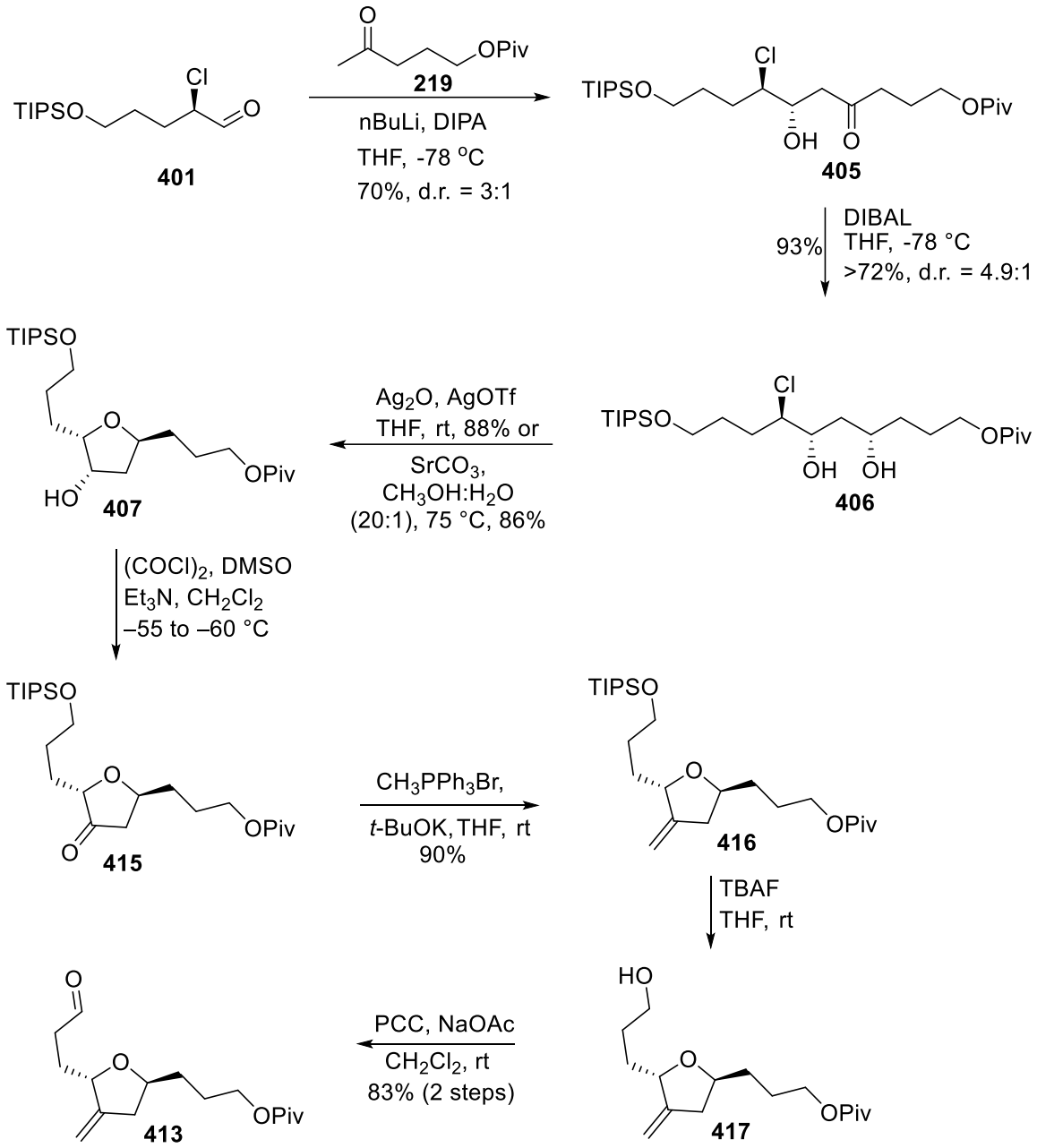

Scheme 3.15. Concise Synthesis of the C_{14}-C_{23} Fragment of Eribulin 413.
In collaboration with Dr V Narasimharao Thota.

Subsequently, the upgrade in enantiopurity of the produced aldehyde **413** was examined. To this end, the aldehyde **413** was reacted with Alphora diiodide **383** through a NHK coupling using Alphora's optimal protocol. Gratifyingly, the resulting alcohol **414** was produced in good diastereoselectivity (d.r. = 8:1, Scheme 3.16). Moreover, while we

were not able to reproduce the reported yields for this air-sensitive glove box reaction, we were pleased to find that the desired product **414** could be isolated from the other configurational isomers and thus, this coupling would generate vinyl iodide **414** in >97 e.e..

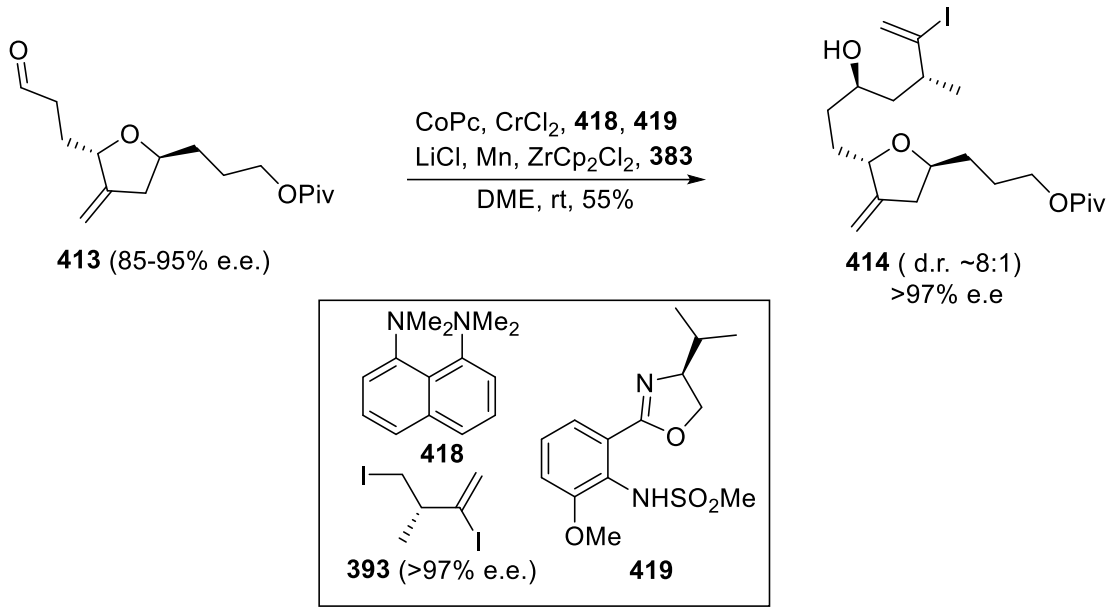

Scheme 3.16. Nozaki-Hiyama-Kishi Reaction of Aldehyde 413 with Diiodide 383.

3.3. New synthetic approach toward Alphora C14-C35 fragment of eribulin

3.3.1. Retrosynthesis

As described in Chapter 2, we had developed a new approach to the Eisai C14-C35 fragment of eribulin **76**. Most notably, this strategy relies on a doubly diastereoselective Corey-Chaykovsky reaction between two subunits **361b** and **329** and allows for a drastic reduction in total number of steps required to produce the key fragment **76**. It is noteworthy that α-chloroaldehyde building blocks proved crucial to the elaboration of concise and stereoselective syntheses of the C14-C26 and C27-C35 fragments **361b** and **329**. Eager to demonstrate the versatility of this new α-chloroaldehyde-based synthetic route to produce eribulin fragments, a synthesis of the C14-C35 fragment of eribulin used in the Alphora process was contemplated. Most notably, researchers at Alphora routinely perform an 11-step sequence to produce eribulin from the C1-C13 and

C14-C35 subunits **74** and **369**. While Alphora C14-C35 fragment **369** is closely related to Eisai intermediate **76**, a few key differences exist (Figure 3.2). Most notably, the C32-C35 side chain in Eisai intermediate **76** incorporates a *bis*-TBS-protected diol, while it is an acetonide-protected amino alcohol in the Alphora route (Figure 3.2). Additionally, a tolyl group is attached to the sulfone in **369** instead of a phenyl group in **76** and the hydroxy at the C14-position is protected with a *tert*-butyldiphenylsilyl group instead of a pivaloyl. These differences, albeit minor, led to slight modifications in the synthetic strategy. Here, while the amino alcohol moiety in **369** could have been elaborated from the acetonide-protected diol intermediate **120** (Scheme 2.74), we aimed for a more convergent, early introduction of this functional group.

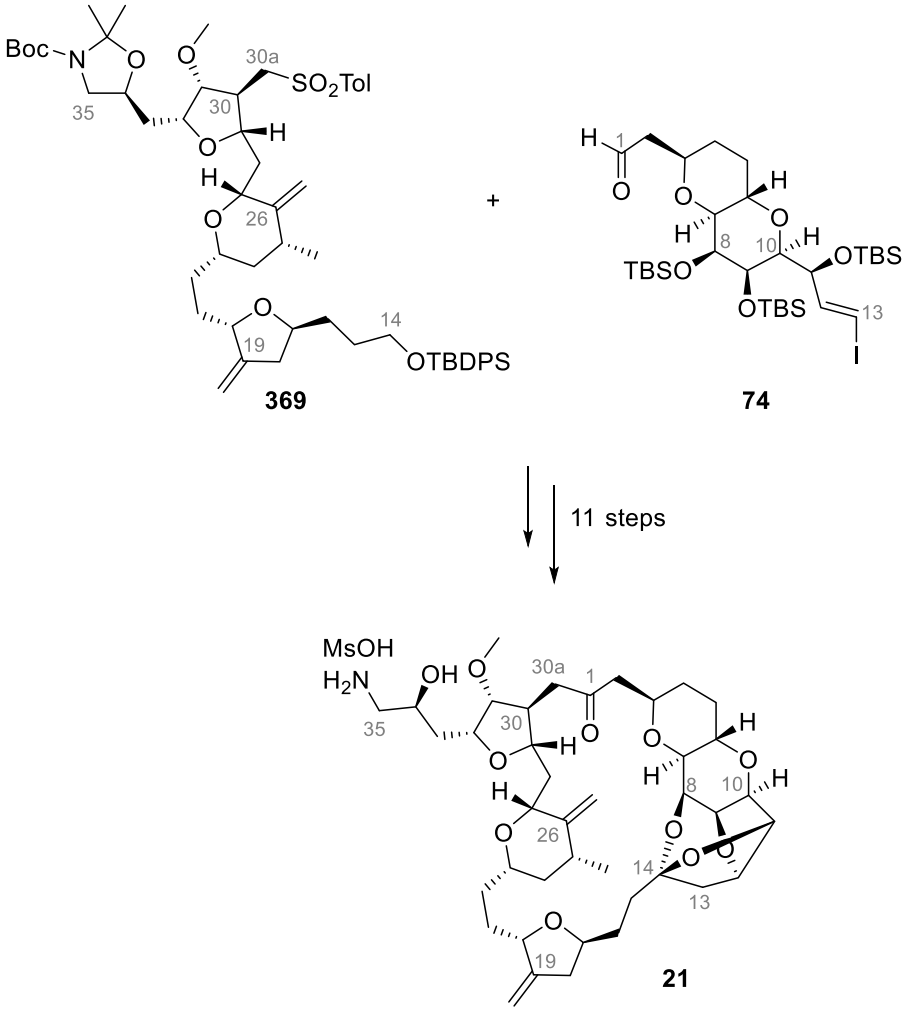

Scheme 3.17. Alphora 11-Step Synthesis of Eribulin (21) from the Subunits 369 and 74.

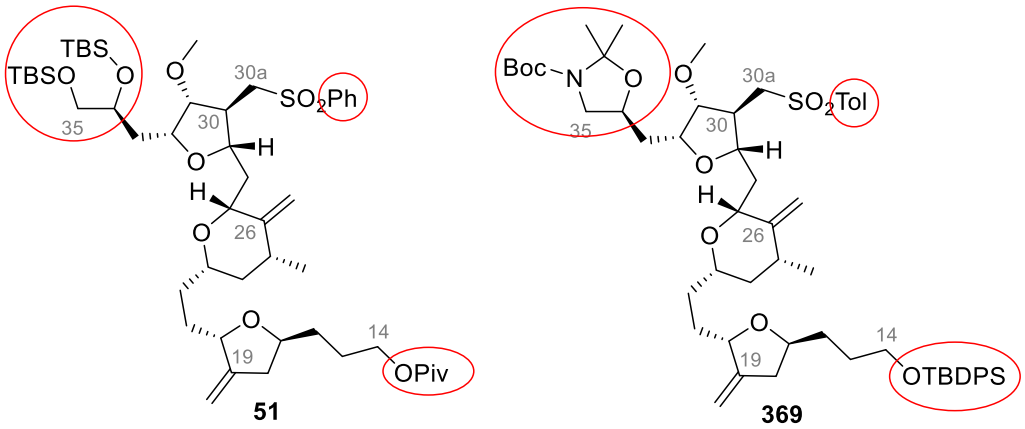

Figure 3.2. Differences Between the C14-C35 Fragments 76 and 369.

As depicted in Scheme 3.18, our previous strategy was adapted to the production of Alphora intermediate **369**. Given the difficulties encountered with a *tert*-butyldiphenylsilyl protecting group at C14 during our earlier collaboration with Alphora (see section 3.2), we aimed for the production of the pivaloyl analogue **420**. Here, retrosynthetic disconnection of the indicated bond in **420** provides the epoxide **421** as potential precursor. In the synthetic direction, isomerization of the epoxide in **421** and a subsequent cyclization upon chlorine displacement could achieve the formation of the tetrahydropyran ring. A few straightforward functional group modifications would then complete the assembly of **420**. In turn, a Corey-Chaykovsky reaction of a sulfonium salt **422** and a ketone **361b** would result in the formation of an epoxide intermediate, which upon oxidation, would be further converted into the precursor **421**. It is noteworthy that a stereoselective synthesis of the C14-C26 fragment **361b** has already been elaborated during the synthetic studies toward Eisai intermediate **76** (Scheme 2.72) and thus, we focused on the synthesis of the new C27-C35 fragment **422**.

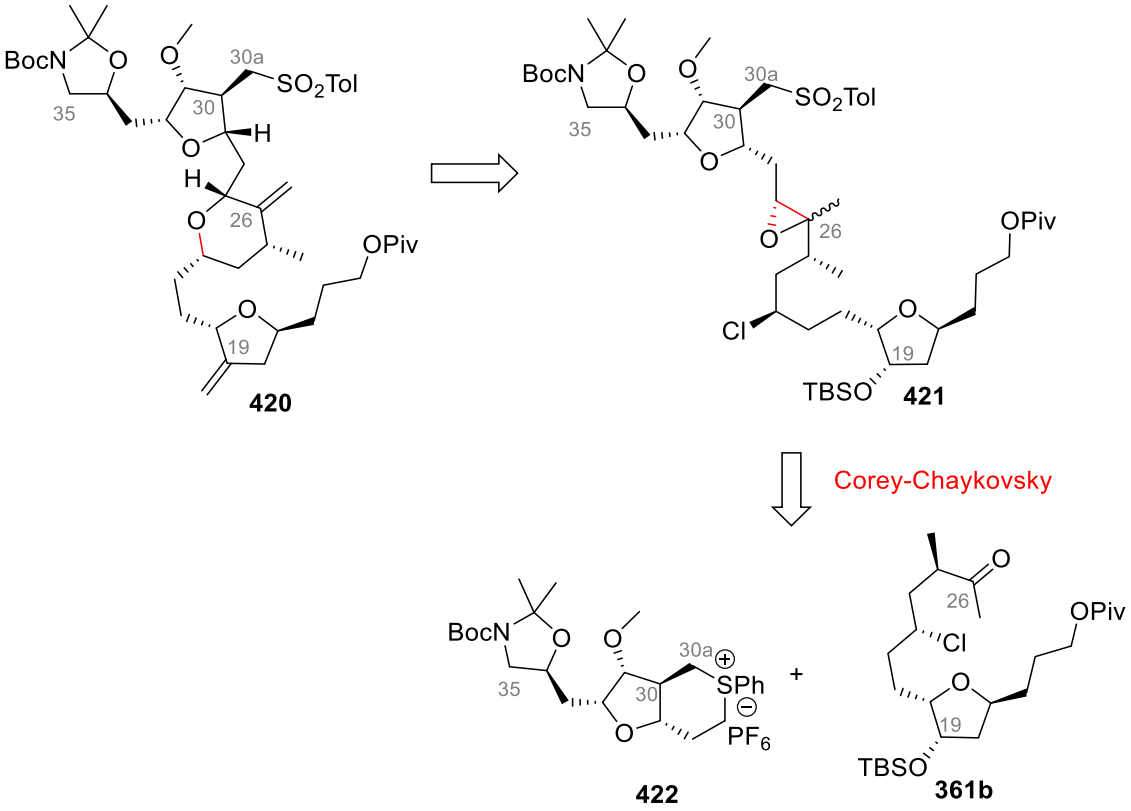

Scheme 3.18. Retrosynthesis of Alphora C14-C35 Fragment 420.

3.3.2. Synthesis of the C27-C35 subunit

Based on the route developed for the Eisai C27-C35 fragment **329**, we elected the aldehyde **423** as a potential precursor of the sulfonium salt **422** (Scheme 3.19). Moreover, we anticipated that the aldehyde **423** could be elaborated from commercially available chiral starting materials such as (*S*)-tetrahydrofurfurylamine **425** or L-glutamic acid **319** in a limited number of steps.[151]

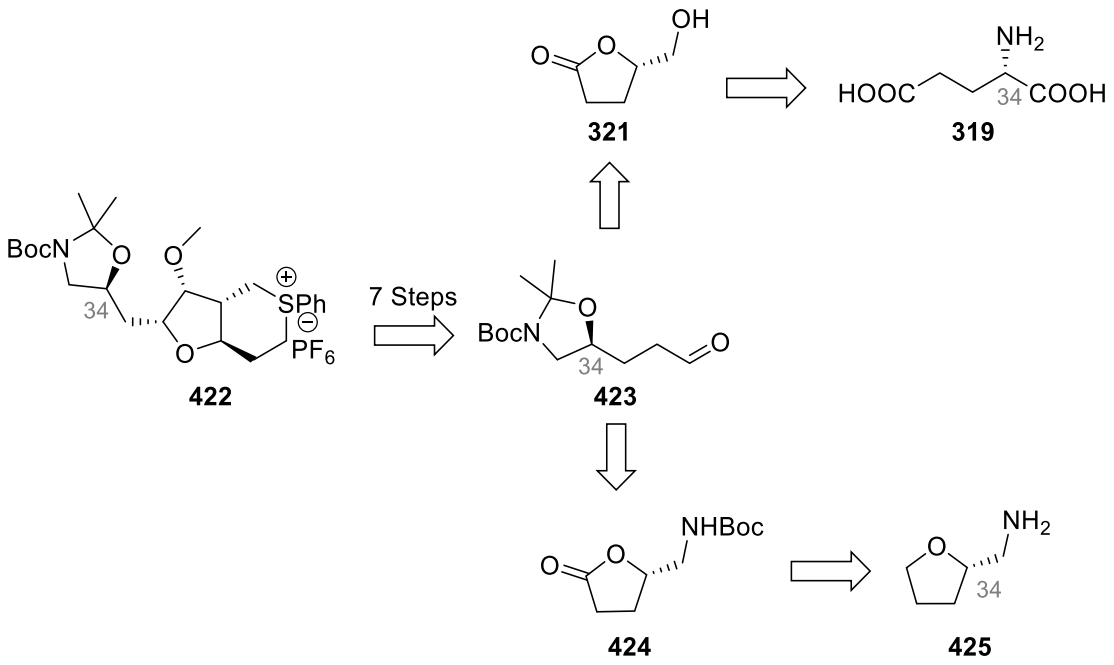

Scheme 3.19. Retrosynthesis of Sulfonium Salt 422.

Following this strategy, several syntheses of the key aldehyde **423** were elaborated. First, a straightforward, but rather lengthy, route was developed from the cheap, commercially available L-glutamic acid **319**.

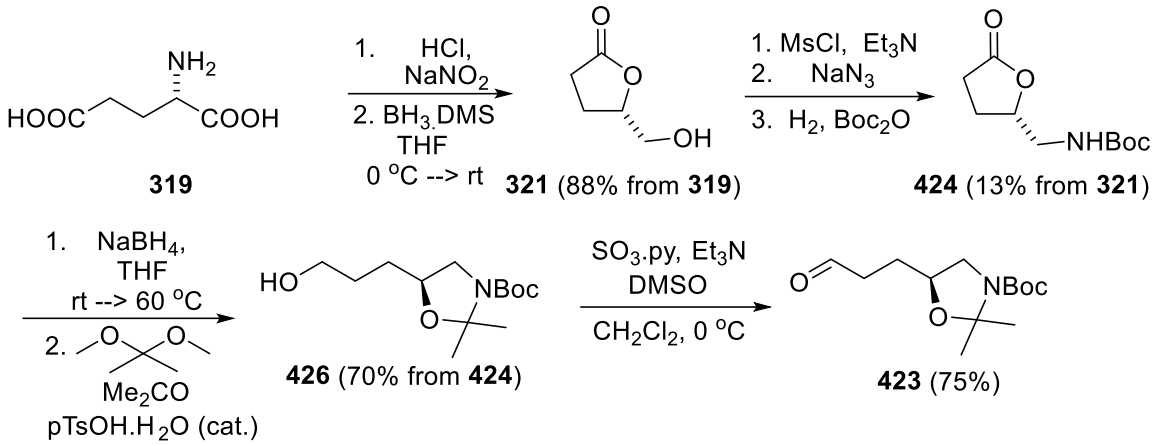

Scheme 3.20. Synthesis of Aldehyde 423 from L-Glutamic acid.
Synthesis performed by Dimitri Panagopoulos.

As shown in Scheme 3.20, L-glutamic acid was converted to the lactone **321** in excellent yield through an acid-promoted cyclization and a subsequent reduction. A 3-step sequence that included mesylation of the alcohol function in **321**, a nucleophilic substitution and a tandem reduction-protection reaction of the resulting azide function, provided the Boc-protected derivative **424** in 13% yield. Sodium borohydride reduction of the lactone **424** and subsequent acetonide protection, furnished the alcohol **426** in 70% overall yield. Finally, a Parikh–Doering oxidation achieved the 8-step sequence to the aldehyde precursor **423**.

Alternatively, a shorter route was developed from the commercially available tetrahydrofurfurylamine **425**. Initially, the optically pure (*S*)-tetrahydrofurfurylamine **425** was used to initiate the synthesis but later, kinetic resolution[152] of the racemate provided large quantities of the desired configurational isomer.

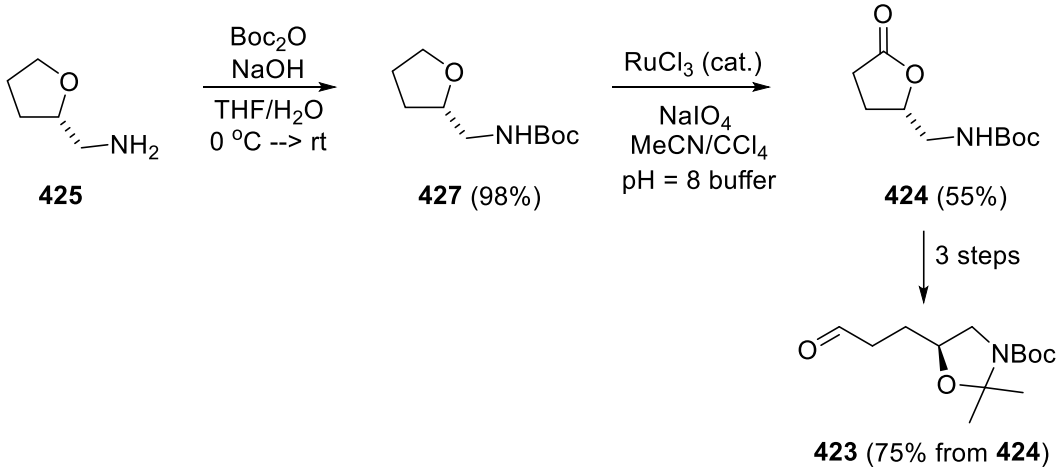

Scheme 3.21. Synthesis of Aldehyde 423 from (*S*)-Tetrahydrofurfurylamine 425.
Synthesis performed by Dimitri Panagopoulos.

As shown in Scheme 3.21, treatment of (*S*)-tetrahydrofurfurylamine **425** with di-tert-butyl decarbonate delivered the Boc-protected derivative **428** in excellent yield. Subsequently, a $RuCl_3$-catalyzed oxidation of the tetrahydrofuran derivative **427** provided the corresponding lactone **424** in 55% yield. The latter material **424** could then be converted to the aldehyde **423** following the synthetic route shown in Scheme 3.20. As a result, the key aldehyde **423** was synthesized in a total of 5 steps from a commercially available starting material.

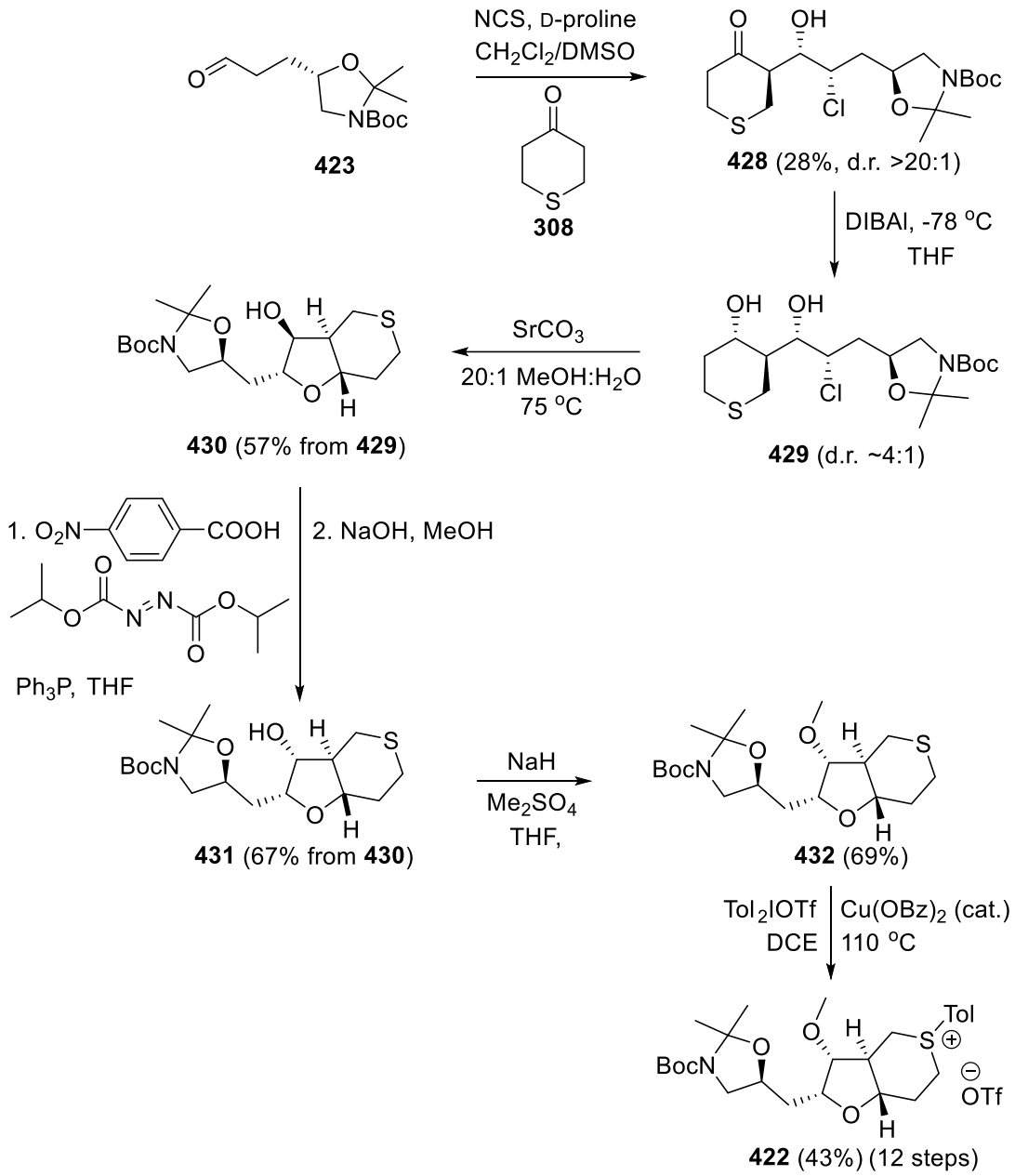

Scheme 3.22. Synthesis of the C27-C35 Building Block 422.
Synthesis performed by Dimitri Panagopoulos.

Subsequently, aldehyde **423** was submitted to a tandem α-chlorination-DKR-aldol reaction with tetrahydrothiopyranone **308** (Scheme 3.22). We were glad to see that the desired chlorohydrin **428** was formed in excellent diastereoselectivity (d.r. >20:1). However, despite extended reaction times (2 to 5 days), unreacted α-chloroaldehyde intermediate was recovered in the crude mixture. Moreover, while the conversion was

increasing up to five days of reaction, the yield of the reaction was decreasing if longer reaction times were used. DIBAL reduction of the β-hydroxy ketone in **428** provided the *syn*-diol intermediate **429** with good selectivity (d.r. = 4:1). Next, treatment with strontium carbonate at 75 °C delivered the cyclized product **430** in 57% yield from the aldol adduct **428**. Subsequently, a Mitsunobu reaction and hydrolysis of the resulting ester furnished the desired configurational isomer **431** in 67% overall yield. The alcohol **431** was then treated with sodium hydride and dimethylsulfate and finally, a copper-catalyzed arylation of the thioether function in **432** achieved the 12-step synthesis of the key C27-C35 building block **422**.

3.3.3. Concise and stereoselective synthesis of Alphora C14-C35 fragment of eribulin

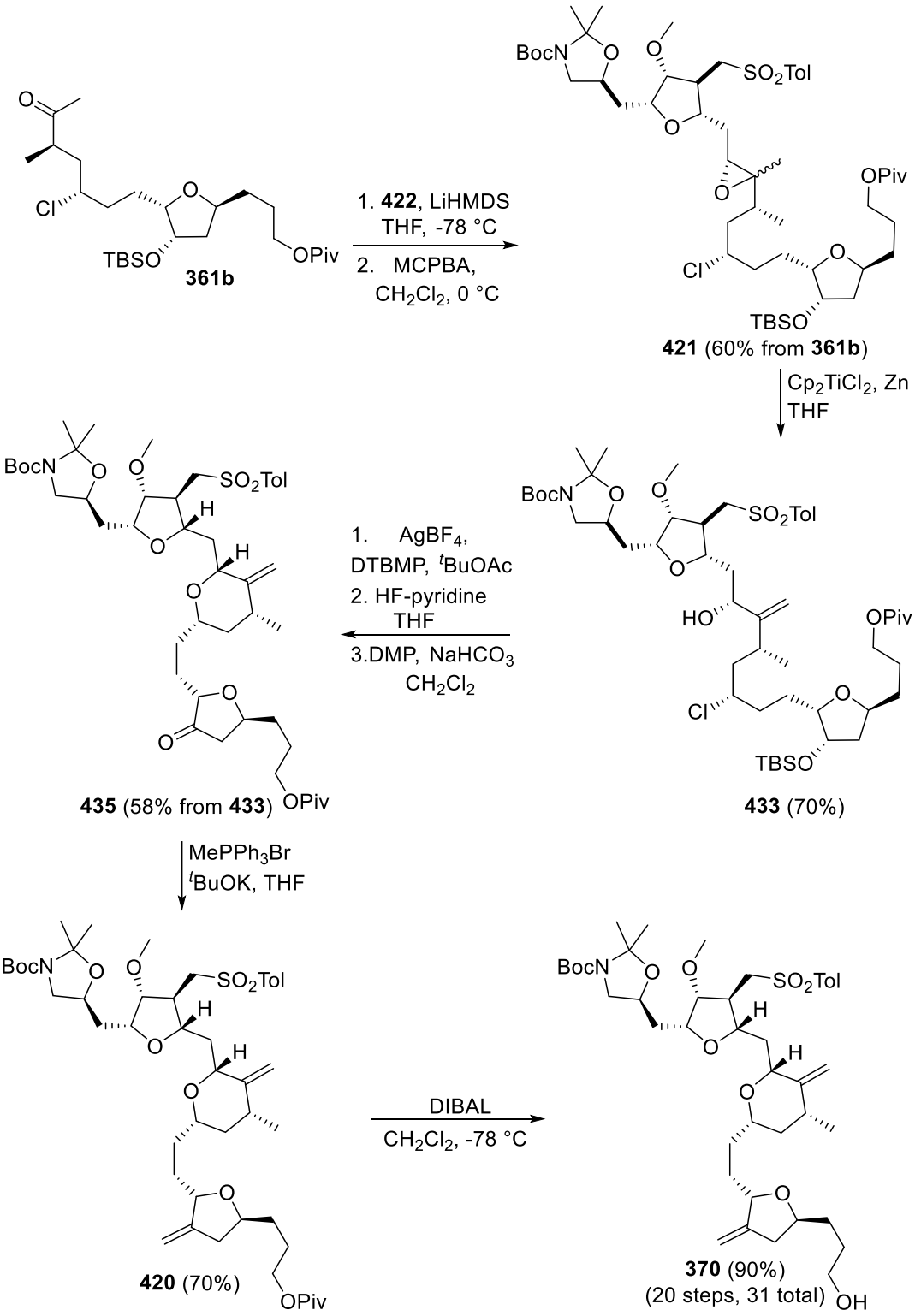

Scheme 3.23. Synthesis of Alphora C14-C35 Fragment of Eribulin 370.

With both fragments **361b** and **422** in hand, we were able to assess the feasibility of using our previously developed 7-step sequence to produce the Alphora C14-C35 fragment. Here, the sulfonium salt **422** was treated with LiHMDS and subsequently reacted with ketone **361b**. Using the optimized reaction conditions, we observed a full consumption of both starting materials **361b** and **422**. Following treatment of the crude product with MCPBA furnished the desired sulfone **421** in 60% yield. Subsequently, the epoxide **421** was submitted to the Cp_2TiCl-reaction conditions used in the synthesis of Eisai intermediate, but surprisingly, the titanocene dichloride reagent failed to turn bright green, a colour characteristic of the Cp_2TiCl complex, when treated with manganese powder. As a result, no desired alcohol **433** was formed when the epoxide was added to this mixture. However, when zinc powder was used instead, the reaction mixture quickly turned from red to green. Therefore, following addition of epoxide **421** resulted in the formation of the corresponding allylic alcohol **433** in good yield (70%). This material was then submitted to the $AgBF_4$-promoted cyclization conditions.[70] To our delight, the alcohol **433** was fully converted to the corresponding tetrahydropyran **434** (not depicted). TBS-deprotection with HF-pyridine followed by oxidation of the resulting alcohol function, then delivered the advance intermediate **435** in 58% yield from **433**. Subsequently, the ylide derived from methyltriphenylphosphonium bromide was reacted with the ketone **435** to provide the alkene **420** in excellent yield. A final treatment with DIBAL-H deprotected the pivalate protected alcohol in **420** and achieved the 31-step synthesis of Alphora C14-C35 fragment of eribulin **370**. As depicted in Figure 3.3, the spectroscopic data of this material and Alphora's were entirely identical and thus, the desired configurational isomer was produced using this sequence.

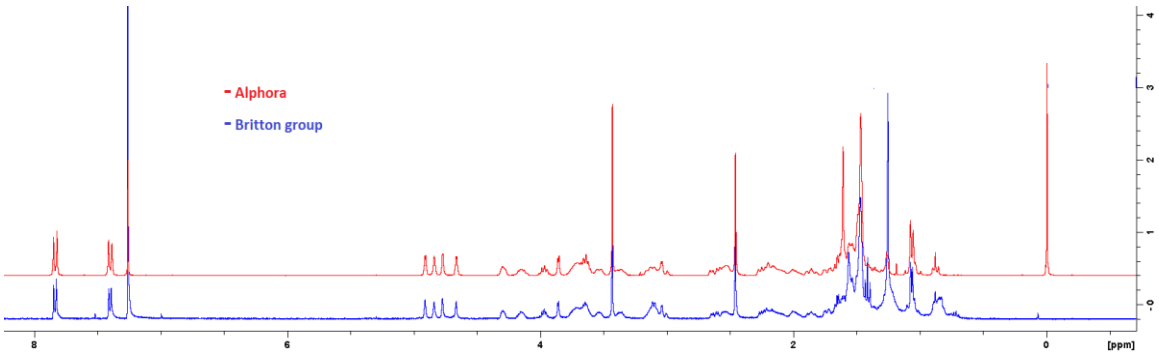

Figure 3.3. Direct comparison of our ^1H NMR spectrum of alcohol 370 and Alphora's.

3.4. Conclusion

In conclusion, the collaboration with Alphora-Eurofins first led to the development of a concise, stereoselective synthesis of the C14-C23 building block **413**. Importantly, while the sequence is not shorter than Alphora initial route, evaluation of the process metrics at an industrial scale revealed a drastic reduction in terms of costs and time. As a result, a kilogram-scale process of this route is under development at Alphora and might eventually serve as a means to produce this key fragment. Moreover, the concomitant development of both Alphora and Eisai fragments has led to valuable discoveries for both projects. Most notably, the synthetic studies toward the C14-C26 building block described in chapter 2 greatly contributed to the rapid construction of Alphora target. Alternatively, the “MacMillan” catalyst investigated during the Alphora project turned out crucial for the completion of the Eisai fragment. Alternatively, the structural differences of the Alphora C14-C35 fragment with Eisai’s, which notably incorporates the western amino alcohol function, drove us to adapt our new synthetic approach toward the synthesis of this fragment. In this regard, a slightly modified C27-C35 subunit **422** was elaborated and coupled with the previously synthesized ketone **361b**. The resulting product was then successfully carried-out toward the previously developed 6-step sequence to provide Alphora C14-C35 fragment in a total of 30 synthetic steps.

3.5. Experimental

General considerations

All reactions were carried out with commercial solvents and reagents that were used as received. Flash chromatography was carried out with Geduran® Si60 silica gel (Merck). Concentration and removal of trace solvents was done via a Büchi rotary evaporator using dry ice/acetone condenser, and vacuum applied from an aspirator or Büchi V-500 pump. All reagents and starting materials were purchased from Sigma Aldrich, Alfa Aesar, TCI America, and/or Strem, and were used without further purification. All solvents were purchased from Sigma Aldrich, EMD, Anachemia, Caledon, Fisher, or ACP and used without further purification, unless otherwise specified.

Nuclear magnetic resonance (NMR) spectra were recorded using chloroform-d ($CDCl_3$) or acetonitrile-d_3 (CD_3CN). Signal positions (δ) are given in parts per million from

tetramethylsilane (δ 0) and were measured relative to the signal of the solvent (^{1}H NMR: $CDCl_3$: δ 7.26, CD_3CN: δ 1.96; ^{13}C NMR: $CDCl_3$: δ 77.16, CD_3CN: δ 118.26). Coupling constants (*J* values) are given in Hertz (Hz) and are reported to the nearest 0.1 Hz. $_1$H NMR spectral data are tabulated in the order: multiplicity (s, singlet; d, doublet; t, triplet; q, quartet; quint, quintet; m, multiplet), coupling constants, number of protons. NMR spectra were recorded on a Bruker Avance 600 equipped with a QNP or TCI cryoprobe (600 MHz), Bruker 500 (500 MHz), or Bruker 400 (400 MHz). Diastereoisomeric ratios (d.r.) are based on analysis of crude ^{1}H-NMR. High performance liquid chromatography (HPLC) analysis was performed on an Agilent 1100 HPLC, equipped with a variable wavelength UV-Vis detector. High-resolution mass spectra were performed on an Agilent 6210 TOF LC/MS, Bruker MaXis Impact TOF LC/MS, or Bruker micrOTOF-II LC mass spectrometer. Infrared (IR) spectra were recorded neat on a Perkin Elmer Spectrum Two FTIR spectrometer. Only selected, characteristic absorption data are provided for each compound. Optical rotation was measured on a Perkin-Elmer Polarimeter 341 at 589 nm.

Synthesis of imidazolidinone *ent*-169

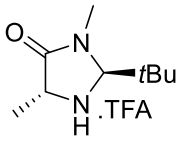

Imine **411** (11.18 g, 65.67 mmol) was synthesized in 2 steps from D-alaninemethyl ester hydrochloride **408** (10.34 g, 74.08 mmol) according to the literature.[124] To a cold solution of ethanol (34 mL) at 0 °C, $SOCl_2$ (2.65 mL, 36.3 mmol) was added dropwise and the resulting mixture was stirred at 0 °C for 15 min. Crude intermediate **412** (11.18 g, 65.67 mmol) was then quickly added at the same temperature and the ice bath was removed. After 10 min, crystallization occurred. The resulting mixture was warmed to 70 ± 2 °C over 30 min and held at this temperature for 20 min. The heating mantle was removed, and the stirred mixture was allowed to cool to 23 °C over 1.5 h and stirring was continued for 2 h at ambient temperature. After this time, the resulting crystals were vacuum filtered, washed with ethanol (2 x 10 mL) and air-dried to afford (2*R*,5*S*)-2-*tert*-butyl-3,5-dimethylimidazolidin-4-one **412** (10.4 g, 50.3 mmol) as white crystalline material. The imidazolidinone **412** was then stirred for 15 min in saturated aq. $NaHCO_3$ (65 mL) and extracted 3 times with dichloromethane (100 mL). The combined organic layers were washed with H_2O and brine, dried over Na_2SO_4, filtered, and concentrated under reduced

pressure to afford 8.84 g of a clear liquid. The latter material was dissolved in diethylether (9.5 mL), and TFA (4.0 mL, 52 mmol) was added at 0 °C. The mixture was then stored in the freezer for 24 h. The resulting mixture was filtered, washed with cold diethyl ether and air-dried to afford 14 g of *ent*-**169** (66 % yield from **412**) as a white solid. **^{1}H NMR** (400 MHz, $CDCl_3$) δ 4.51 (s, 1 H), 4.06 (q, J = 7.1 Hz, 1 H), 3.05 (s, 3 H), 1.50 (d, J = 7.1 Hz, 3 H), 1.13 (s, 9 H). The ^{1}H NMR spectroscopic data of compound *ent*-**169** matched that reported in the literature.[124]

Synthesis of the TIPS-alcohol 400a

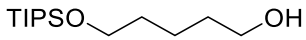

To a suspension of 60% NaH in mineral oil (136 mg, 3.4 mmol) in dry THF (4 mL) at 0 °C was slowly added a solution of 1,5-pentanediol (350 mg, 3.4 mmol) in dry THF (2 mL). After 30 min at that temperature, a solution of TIPSCl (0.72 mL, 3.4 mmol) in dry THF (0.75 mL) was added. The reaction mixture was then stirred for 1 h at 0 °C and then quenched with H_2O. The aqueous layer was removed and extracted three times with Et_2O and the combined organic layers were washed with brine, dried over Na_2SO_4, filtered, and concentrated under reduced pressure to afford 1.23 g of a colourless oil. Purification by flash chromatography (silica gel, hexanes-EtOAc 8:2) afforded the title compound as a colourless oil (552 mg, 63%). **^{1}H NMR** (400 MHz, $CDCl_3$) δ 3.67 (dt, J = 15.3, 6.5 Hz, 4 H), 1.66–1.52 (m, 4 H), 1.49–1.37 (m, 2 H), 1.16–1.01 (m, 21 H). The ^{1}H NMR spectroscopic data of alcohol **400a** matched that reported in the literature.[153]

Synthesis of TIPS-aldehyde 400

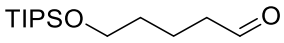

To a suspension of PCC (3.95 g, 18.3 mmol), NaOAc (1 g, 12.2 mmol) and celite (3.95 g, 1 g per 1 g of PCC) in dry CH_2Cl_2 (60 mL) was slowly added a solution of alcohol **336a** (3.18 g, 12.2 mmol) in dry CH_2Cl_2 (10 mL) and the resulting brown slurry was then stirred at room temperature for 2 h. The reaction mixture was then filtered through a Celite pad and the filter pad was further washed with CH_2Cl_2 (~50 mL). Evaporation of solvents afforded 2.98 g of a crude yellow oil. Purification by flash chromatography (silica gel, hexanes-EtOAc 8:2) afforded the title compound as a colourless oil (2.28 g, 72%). **^{1}H NMR** (400 MHz, $CDCl_3$) δ 9.77 (t, J = 1.8 Hz, 1 H), 3.70 (t, J = 6.2 Hz, 2 H), 2.47 (td, J = 7.3, 1.8

Hz, 2 H), 1.79–1.68 (m, 2 H), 1.63–1.52 (m, 2 H), 1.08–1.02 (m, 21 H). The ^{1}H NMR spectroscopic data of aldehyde **400** matched that reported in the literature.[153]

Synthesis of α-chloroaldehyde 401

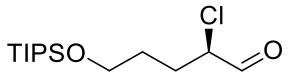

To a cold (0 °C), stirred solution of aldehyde **400** (30 mg, 0.115 mmol) in CH_3CN (0.23 mL), was added the MacMillan catalyst *ent*-**169** (6.6 mg, freshly prepared according to the literature) and *N*-chlorosuccinimide (15.3 mg). The ice bath was removed after 30 minutes allowing the solution to slowly warm to room temperature. The reaction mixture was stirred until complete consumption of starting material as determined by ^{1}H NMR spectroscopy. After this time, the mixture was extracted with pentane and concentrated to provide the title compound as a colourless oil (30.4 mg, 90%). **^{1}H NMR** (400 MHz, $CDCl_3$) δ 9.50 (d, J = 2.3 Hz, 1 H), 4.26 (ddd, *J* = 8.0, 5.4, 2.3 Hz, 1 H), 3.74 (td, *J* = 5.9, 1.4 Hz, 2 H), 2.15 (ddt, *J* = 14.8, 9.4, 5.8 Hz, 1 H), 2.03–1.85 (m, 1 H), 1.80–1.63 (m, 2 H), 1.08–1.02 (m, 21 H).

Synthesis of ester 401b

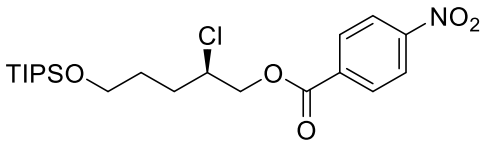

e.e. determination of **401**: Crude aldehyde **401** (58 mg, 0.2 mmol) was dissolved in CH_3OH (1 mL) and $NaBH_4$ (23 mg, 0.6 mmol) was added. After stirring for 1 hour at room temperature, NH_4Cl (1 mL) was added and the aqueous layer was extracted with EtOAc (3 × 1 mL). The combined organic phases were washed with brine (1 mL), dried (Na_2SO_4), filtered, and concentrated. The resulting mixture was then dissolved in CH_2Cl_2 (0.8 mL) and para-nitrobenzoic acid (33.4 mg, 0.2 mmol), DCC (41.2 mg, 0.2 mmol) and DMAP (24.4 mg, 0.2 mmol) were successively added. After 2 hours at room temperature, the reaction mixture was filtered and concentrated to provide a crude oil. Purification of the crude product by flash chromatography (silica gel, hexanes-EtOAc 95:5) furnished **401b** (62 mg, 70%). Chiral separation of ester **401b** using Amylose (50 × 4.6 mm, IPA:hexanes 1:99, 0.250 mL/min) revealed an 85% enantiomeric excess (t_{R1} = 4.63 min, t_{R2} = 5.46 min).

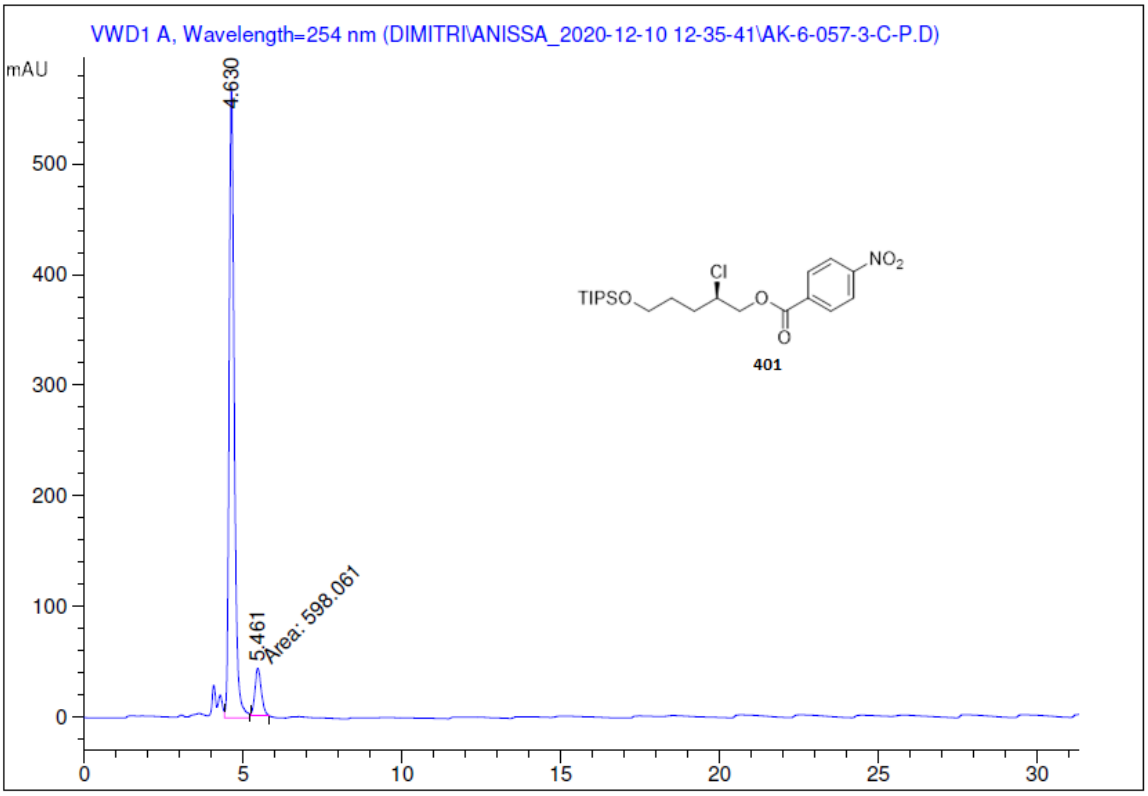

Synthesis of ketochlorohydrin 405

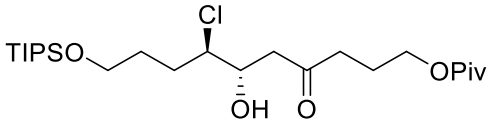

To a cold (–40 °C) solution of diisopropylamine (2.10 mL, 14.9 mmol) in THF (7 mL) was added *n*-butyllithium (2.35 M soln. in hexane, 5.50 mL, 12.9 mmol). The resulting solution was stirred at –40 °C for 40 minutes. After this time, the slightly yellow solution was cooled to –78 °C and ketone **219** (1.86 g, 9.99 mmol) in THF (3 mL) was added in one portion. The reaction mixture was stirred for 35 minutes. A solution of **401** (2.77 g, 9.46 mmol) in THF (6 mL) was then added dropwise over 10 minutes at –78 °C and the resulting mixture was stirred for an additional 75 minutes. Saturated aqueous NH_4Cl (20 ml) was then added, the mixture was diluted with EtOAc (75 ml) and the phases were separated. The aqueous phase was extracted with EtOAc (3 × 50 ml) and the combined organic phases were washed with brine (20 mL), dried (Na_2SO_4), filtered, and concentrated to provide a crude oil which showed a 3:1 diastereoisomeric ratio as determined by ^1H NMR spectroscopy. Purification of the crude product by flash chromatography (silica gel, hexanes-acetone 96:4) removed the unreacted ketone completely to afford the majority of

the major isomer. The obtained remaining mixture was purified by flash chromatography (silica gel, hexanes- EtOAc 9:1) to separate the mixture of diastereoisomers. Three purifications provided ketochlorohydrin **405** (2.4 g, 53%) as a colourless oil. **[α]$^{20}_{D}$** –4.9 (*c* 1.72, $CHCl_3$); **^{1}H NMR** (500 MHz, $CDCl_3$) *δ* 4.19–4.11 (m, 1 H), 4.07 (t, *J* = 6.3 Hz, 2 H), 3.97 (ddd, *J* = 9.5, 6.0, 3.3 Hz, 1 H), 3.78–3.67 (m, 2 H), 3.22 (d, *J* = 5.0 Hz, 1 H), 2.79–2.72 (m, 1 H), 2.56 (t, *J* = 7.3 Hz, 2 H), 2.10–2.00 (m, 1 H), 1.98–1.89 (m, 2 H), 1.84 (dddd, *J* = 13.0, 10.4, 6.4, 4.3 Hz, 1 H), 1.78–1.58 (m, 3 H), 1.19 (s, 9 H), 1.14–1.01 (m, 21 H); **^{13}C NMR** (125 MHz, $CDCl_3$) *δ* 210.1, 178.6, 71.0, 66.1, 63.4, 62.7, 45.3, 40.1, 38.9, 30.4, 29.7, 27.3, 22.7, 18.1, 12.1; **IR** (cast film, $CHCl_3$) *v* 3359, 2862, 1722, 1104, 789 cm^{-1}; **HRMS (ESI-TOF)** *m/z*: $[M + H]^+$ Calcd for $C_{24}H_{48}ClO_5Si$ 479.2954; Found 479.2949.

Synthesis of diol 406

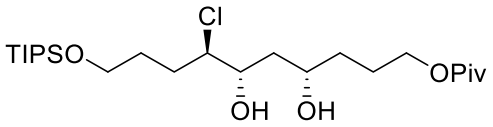

To a cold (–78 °C) solution of ketone **405** (1.22 g, 2.55 mmol) in THF (24 mL) was added diisobutylaluminum hydride (1.00 M solution. in THF, 6.50 mL, 6.50 mmol) and the reaction mixture was stirred for 3.5 hours. After this time, an aqueous solution of HCl (1.0 M, 15 mL) was added, the mixture was diluted with ether (75 mL) and the phases were separated. The aqueous phase was extracted with ether (2 × 50 mL), and the combined organic phases were washed with water (10 mL) and brine (10 mL), dried (Na_2SO_4), filtered, and concentrated to provide a crude oil. Purification of the crude product by flash chromatography (silica gel, hexanes-EtOAc 84:16) afforded 1,3-diol **406** (0.73 g, 60%) as a colorless oil. **[α]$^{20}_{D}$** +4.2 (*c* 1.81, $CHCl_3$); **^{1}H NMR** (500 MHz, $CDCl_3$) *δ* 4.08 (t, *J* = 6.6 Hz, 2 H), 4.02–3.86 (m, 3 H), 3.73 (td, *J* = 5.8, 1.5 Hz, 2 H), 3.49 (br s, 1 H), 3.36 (br s, 1 H), 2.04–1.93 (m, 1 H), 1.90–1.48 (m, 10 H), 1.19 (s, 9 H), 1.14–1.01 (m, 21 H); **^{13}C NMR** (125 MHz, $CDCl_3$) *δ* 178.8, 75.8, 77.0, 67.6, 64.4, 62.8, 38.89, 38.84, 34.4, 29.5, 29.2, 27.3, 24.7, 18.1, 12.1; **IR** (cast film, $CHCl_3$) *v* 3594, 2946, 1729, 1151, 715 cm^{-1}; **HRMS (ESI-TOF)** *m/z*: $[M + H]^+$ Calcd for $C_{24}H_{50}ClO_5Si$ 481.3111; Found 481.3009.

Synthesis of tetrahydrofuran 407

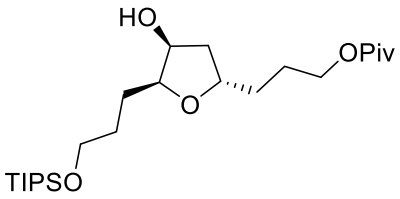

To a cold (0 °C), stirred solution of 1,3-diol **406** (299 mg, 0.621 mmol) in THF (12 mL) was added AgOTf (160 mg, 0.623 mmol) and freshly prepared Ag_2O (145 mg, 0.626 mmol) and the reaction mixture was sonicated at rt for 3 h. The reaction mixture was then stirred for ~36 hours. The resulting suspension was then filtered through Celite and washed with Et_2O and concentrated to provide a crude oil. The crude oil was redissolved in Et_2O (30 mL) and washed with saturated aq $NaHCO_3$ (15 mL) and the layers were separated. The aqueous layer was extracted with Et_2O (2 × 30 mL), and the combined organic layers were dried (Na_2SO_4), filtered, and concentrated to provide a crude oil. Purification of the crude product by flash chromatography (silica gel, hexanes-acetone 9:1) afforded the desired alcohol **407** (565 mg, 73%) as a colorless oil. **$[\alpha]^{20}_D$** +1.4 (*c* 0.86, $CHCl_3$); **^{1}H NMR** (500 MHz, $CDCl_3$) *δ* 4.30–4.25 (m, 1 H), 4.25–4.17 (m, 1 H), 4.10–4.03 (m, 2 H), 3.81 (ddd, *J* = 8.2, 5.9, 2.8 Hz, 1 H), 3.77–3.69 (m, 2 H), 2.31 (d, *J* = 4.4 Hz, 1 H), 2.12 (dd, *J* = 13.3, 6.1 Hz, 1 H), 1.81–1.45 (m, 10 H), 1.18 (s, 9 H), 1.15–1.02 (m, 21 H); **^{13}C NMR** (125 MHz, $CDCl_3$) *δ* 178.7, 82.3, 76.7, 73.3, 64.4, 63.2, 41.5, 38.9, 32.8, 29.2, 25.6, 25.0, 18.1, 12.1; **IR** (cast film, $CHCl_3$) *v* 3450, 2940, 1719, 1702, 1148 cm^{-1}; **HRMS (ESI-TOF)** *m/z*: $[M + H]^+$ Calcd for $C_{24}H_{49}O_5Si$ 445.3344; Found 445.3315.

Synthesis of ketone 415

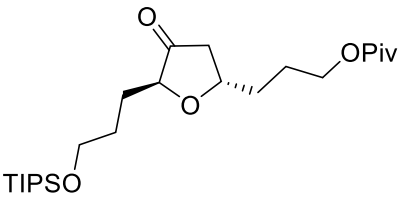

To a solution of oxalyl chloride (170 µL, 1.95 mmol) in CH_2Cl_2 (6 mL) at –60 °C was added DMSO (185 µL, 2.60 mmol) in CH_2Cl_2 (0.5 mL) over 2 minutes. This solution was stirred for 40 minutes at approximately –55 to –60 °C. Alcohol **407** (565 mg, 1.27 mmol) in CH_2Cl_2 (3 mL) was then added dropwise over 5 minutes and the resulting mixture was stirred for an additional 90 minutes. Et_3N (0.7 mL, 5.0 mmol) was then added and the reaction

mixture was stirred for an additional 1 h. Saturated aqueous NH_4Cl (10 mL) was then added, the mixture was diluted with CH_2Cl_2 (30 mL) and the layers were separated. The aqueous layer was extracted with CH_2Cl_2 (3 × 30 ml) and the combined organic layers were washed with brine (15 mL), dried (Na_2SO_4), filtered, and concentrated to provide a crude oil. Purification of the crude product by flash chromatography (silica gel, hexanes-EtOAc 9:1) afforded ketone **415** (526 mg, 93%) as a colorless oil: **$[\alpha]^{20}_D$** –22.5 (*c* 2.88, $CHCl_3$); **^{1}H NMR** (500 MHz, $CDCl_3$) *δ* 4.37–4.28 (m, 1 H), 4.11–4.04 (m, 2 H), 3.93 (dd, *J* = 8.1, 4.4 Hz, 1 H), 3.69 (t, *J* = 5.9 Hz, 2 H), 2.58 (dd, *J* = 18.0, 6.8 Hz, 1 H), 2.20 (ddd, *J* = 18.0, 7.3, 1.0 Hz, 1 H), 1.87–1.56 (m, 8 H), 1.18 (s, 9 H), 1.12–0.98 (m, 21 H); **^{13}C NMR** (125 MHz, $CDCl_3$) *δ* 216.4, 178.6, 79.3, 74.7, 64.0, 63.0, 42.6, 38.9, 32.1, 28.9, 27.3, 27.2, 25.1, 18.1, 12.1; **IR** (cast film, $CHCl_3$) *v* 2943, 1759, 1722, 1145, 876 cm^{-1}; **HRMS (ESI-TOF)** *m/z*: $[M + NH_4]^+$ Calcd for $C_{24}H_{50}NO_5Si$ 460.3453; Found 460.3420.

Synthesis of alkene 416

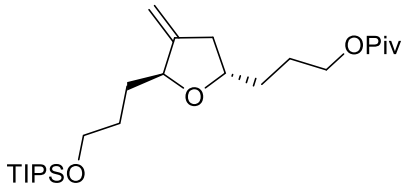

To a suspension of methyltriphenylphosphonium bromide (1.06 g, 2.97 mmol) in dry THF 911 mL) was added *t*BuOK (2.97 mL of 1.0 M solution in THF, 2.97 mmol) at 0 °C. After the mixture was stirred for 30 minutes at the same temperature, a solution of ketone **415** (526 mg, 1.19 mmol) in dry THF (7 mL) was slowly added. After stirring for an additional 3 h at room temperature, the resulting mixture was quenched with water. The mixture was extracted with EtOAc, washed with brine, dried over anhydrous $MgSO_4$, and concentrated to provide the crude product as a yellow oil. Purification by flash chromatography (silica gel, hexanes-EtOAc 19:1) afforded the desired alkene **416** (471 mg, 90%). **$[\alpha]^{20}_D$** –28.0 (*c* 1.50, $CHCl_3$); **^{1}H NMR** (400 MHz, $CDCl_3$) *δ* 4.97 (q, *J* = 2.2 Hz, 1 H), 4.84 (q, *J* = 2.2 Hz, 1 H), 4.39 (br d, *J* = 7.4 Hz, 1 H), 4.07 (td, *J* = 6.4, 3.6 Hz, 2 H), 4.03–3.98 (m, 1 H), 3.71 (t, *J* = 5.4 Hz, 2 H), 2.67 (ddd, *J* = 15.5, 6.5, 1.9 Hz, 1 H), 2.25 (dd, *J* = 15.5, 6.6, 1 H), 1.80–1.44 (m, 8 H), 1.19 (s, 9 H), 1.08–1.02 (m, 21 H); **^{13}C NMR** (126 MHz, CDCl3) *δ* 178.7, 151.8, 104.9, 79.8, 77.4, 76.8, 64.4, 63.4, 39.0, 38.9, 31.8, 31.8, 29.2, 27.4, 25.5, 18.2, 12.2; **IR** (cast film, $CHCl_3$) *v* 2937, 2864, 1724, 1158, 801 cm^{-1}; **HRMS (ESI-TOF)** *m/z*: $[M + H]^+$ Calcd for $C_{24}H_{50}ClO_5Si$ 481.3111; Found 481.3009.

Synthesis of alcohol 417

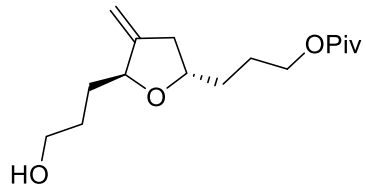

To a stirred solution of alkene **416** (200 mg, 0.42 mmol) in THF (3.2 mL) at 0 °C was added TBAF (1 mL of 1.0 M solution in THF, 1.05 mmol) and the reaction mixture was stirred for 5 hours. After this time, the resulting mixture was concentrated, diluted with EtOAc and filtered through a pad of silica gel to afford a crude product **417** which was used in the next step without further purification. **^{1}H NMR** (400 MHz, $CDCl_3$) *δ* 4.97 (q, *J* = 2.2 Hz, 1 H), 4.84 (q, *J* = 2.2 Hz, 1 H), 4.41 (br d, *J* = 8.7 Hz, 1 H), 4.10–4.02 (m, 3 H), 3.70–3.60 (m, 2 H), 2.72 (ddd, *J* = 15.5, 6.5, 1.9 Hz, 1 H), 2.30 (ddd, *J* = 15.5, 6.6, 0.9 Hz, 1 H), 1.80–1.46 (m, 8 H), 1.18 (s, 9 H).

Synthesis of aldehyde 413

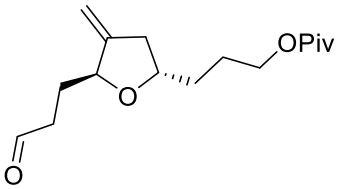

To a cold (0 °C), stirred solution of alcohol **417** (120 mg, 0.42 mmol) were added 3Å molecular sieves (118 mg) in CH_2Cl_2 (1.5 mL), PCC (118.2 mg, 0.55 mmol) and NaOAc (34.6 mg, 0.42 mmol). The mixture was stirred at room temperature for 4 hours, diluted with Et_2O, filtered through a plug of silica gel and concentrated to provide the crude product as a yellow oil. Purification by flash chromatography (silica gel, hexanes-EtOAc 20:1) of the crude product afforded the desired aldehyde **413** (79 mg, 66% over 2 steps). **$[\alpha]^{20}_D$** –35.4 (*c* 1.11, $CHCl_3$); **^{1}H NMR** (500 MHz, $CDCl_3$) *δ* 9.78 (t, *J* = 1.7 Hz, 1 H), 5.02 (q, *J* = 2.2 Hz, 1 H), 4.88 (q, *J* = 2.2 Hz, 1 H), 4.44–4.40 (m, 1 H), 4.06 (td, *J* = 6.4, 3.6 Hz, 2 H), 4.02–3.96 (m, 1 H), 2.67 (ddd, *J* = 15.6, 6.5, 1.9 Hz, 1 H), 2.54 (br q, *J* = 7.1 Hz, 2 H), 2.27 (ddd, *J* = 15.6, 6.8, 0.9 Hz, 1 H), 2.01–1.94 (m, 1 H), 1.87–1.79 (m, 1 H), 1.77–1.43 (m, 4 H), 1.18 (s, 9 H); **^{13}C NMR** (126 MHz, CDCl3) *δ* 202.4, 178.7, 150.8, 105.6, 78.8, 77.4, 77.1, 64.3, 40.1, 39.0, 38.9, 31.7, 27.9, 27.3, 25.4; **IR** (cast film, $CHCl_3$) *v* 2956,

2869, 1729, 1154, 883 cm^{-1}; **HRMS (ESI-TOF)** *m/z*: $[M + NH_4]^+$ Calcd for $C_{16}H_{30}NO_4$ 300.2175; Found 300.2179.

Synthesis of vinyl iodide 414

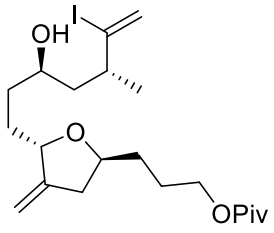

(*S*)-Sulfonamide ligand **419** (29 mg, 0.092 mmol) and CoPc (3.2 mg, 0.0056 mmol) were weighed outside a glove box and put in a flask. In a glove box, proton sponge **418** (19.9 mg, 0.092 mmol), $CrCl_2$ (10.4 mg, 0.092 mmol) and DME (1 mL) were added and the resulting mixture was then stirred at rt for 1 h. To the resulting green solution, LiCl (23.9 mg, 0.092 mmol), Mn powder (31 mg, 0.092 mmol) and $Zr(Cp)_2Cl_2$ (164.8 mg, 0.092 mmol) were successively added. After 15 min at rt, a solution of aldehyde **413** (79.6 mg, 0.28 mmol) and Alphora's diiodide **383** (181.5 mg, 0.092 mmol) in DME (0.2 mL) were added. The reaction mixture was stirred at rt in a glove box for 48 h. The resulting mixture was then poured into a slurry of Florisil in Et_2O. The mixture was stirred vigorously for 0.5 h and then filtered through a short pad of silica gel with MTBE. The filtrate was concentrated under reduced pressure. Flash chromatography (hexanes-acetone 44:1) provided alcohol **414** (46 mg, 20% yield) as a 4:1 mixture of two C23 diastereoisomers in the form of a pale yellow oil. Separation of the two diastereoisomers was achieved with silica gel column chromatography (CH_2Cl_2-EtOAc:hexanes 30:1:20). **$[\alpha]^{20}_D$** –35.4 (*c* 0.99, $CHCl_3$); **^{1}H NMR** (500 MHz, $CDCl_3$) *δ* 6.24 (d, *J* = 1.1 Hz, 1 H), 5.76 (d, *J* = 1.3 Hz, 1 H), 5.00 (d, *J* = 2.2 Hz, 1 H), 4.86 (d, *J* = 2.3 Hz, 1 H), 4.42–4.36 (m, 1 H), 4.12–4.04 (m, 3 H), 3.62–3.53 (m, 1 H), 2.70 (dd, *J* = 15.6, 6.4 Hz, 1 H), 2.45 (d, *J* = 5.1 Hz, 1 H), 2.28 (dd, *J* = 15.9, 6.3 Hz, 1 H), 2.15–2.07 (m, 1 H), 1.79–1.44 (m, 10 H), 1.19 (s, 9 H), 0.99 (d, *J* = 6.6 Hz, 2 H); **^{13}C NMR** (101 MHz, $CDCl_3$) *δ* 178.7, 151.2, 151.1, 125.2, 123.6, 105.4, 79.7, 77.4, 77.1, 68.7, 64.3, 43.7, 42.7, 38.9, 38.9, 34.5, 31.6, 31.2, 27.4, 25.5, 22.6; **IR** (cast film, $CHCl_3$) *v* 3439, 2966, 1724, 1154, 888 cm^{-1}; **HRMS (ESI-TOF)** *m/z*: $[M + H]^+$ Calcd for $C_{21}H_{36}IO_4$ 479.1658; Found 479.1662.

Synthesis of carbamate 427

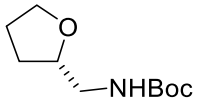

To a solution of (*S*)-tetrahydrofurfurylamine **425** (3 g, 30 mmol) in THF (74 mL), H_2O (74 mL) was added. The biphasic mixture was cooled to 0 ºC and then NaOH (1.78 g, 44 mmol) was added, followed by Boc_2O (8.41 g, 39 mmol). The white slurry was then allowed to warm to rt overnight. After 23h, the reaction mixture was quenched with saturated NH_4Cl solution (~150 mL) and the aqueous layer was extracted with EtOAc (3 x 150 mL). The combined organic layers were washed with brine (250 mL), dried over $MgSO_4$, filtered and concentrated under reduced pressure to afford 7.72 g of a colourless oil. Purification of the crude material by flash chromatography (silica gel, hexanes-EtOAc 1:1) afforded the title compound as a solid (5.85 g, 98%). **^{1}H NMR** (400 MHz, $CDCl_3$) δ 4.86 (br s, 1H), 4.00 – 3.89 (m, 1H), 3.89 – 3.81 (m, 1H), 3.79 – 3.69 (m, 1H), 3.50 – 3.29 (m, 1H), 3.06 (dt, *J* = 13.1, 6.1 Hz, 1H), 2.03 – 1.82 (m, 3H), 1.58 – 1.51 (m, 1H), 1.44 (s, 9H); **^{13}C NMR** (101 MHz, $CDCl_3$) δ 156.28, 79.33, 78.21, 68.21, 44.58, 28.60, 28.55, 26.00. Synthesis of the title compound was performed by Dimitri Panagopoulos.

Synthesis of lactone 424

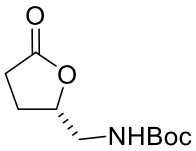

To a solution of carbamate **427** (68 mg, 0.34 mmol) in MeCN (690 µL) and CCl_4 (690 µL), a pH = 8 buffer was added (1.03 mL). To this biphasic mixture, $NaIO_4$ (217 mg, 1 mmol) was added, followed by $RuCl_3.(H_2O)_3$ (2 mg, 0.007 mmol). The resulting brown biphasic mixture was stirred at rt overnight. After 19h the reaction mixture was quenched with saturated $Na_2S_2O_3$ (~1 mL) and then the aqueous was extracted with CH_2Cl_2 (3 x 2 mL). The combined organic layers were then washed with saturated $NaHCO_3$ (2 mL) and brine (2 mL), dried over $MgSO_4$, filtered and concentrated under reduced pressure to afford the title compound as a colourless oil (40 mg, 55%). **^{1}H NMR** (400 MHz, $CDCl_3$) δ 4.88 (br s, 1H), 4.70 – 4.50 (m, 1H), 3.63 – 3.42 (m, 1H), 3.27 (dt, *J* = 14.6, 6.2 Hz, 1H), 2.64 – 2.45 (m, 2H), 2.42 – 2.16 (m, 1H), 2.11 – 1.86 (m, 1H), 1.44 (s, 9H); **^{13}C NMR** (101

MHz, $CDCl_3$) δ 176.83, 156.17, 80.09, 79.78, 44.21, 28.72, 28.46, 24.69. Synthesis of the title compound was performed by Dimitri Panagopoulos.

Synthesis of diol 426

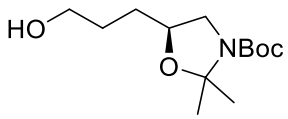

To a solution of lactone **424** (3.49 g, 16 mmol) in THF (162 mL) was added $NaBH_4$ (1.47 g, 39 mmol). The mixture was stirred at rt for 5min and then it was heated to 60 ºC. At that temperature, MeOH (30 mL) was added portionwise over 40min. After the addition was complete, the resulting solution was stirred at 60 ºC for an additional 45min. It was then allowed to cool to rt and then the reaction mixture was quenched with saturated NH_4Cl (100 mL) at 0 ºC. The aqueous was then extracted with EtOAc (3 x 150 mL) and the combined organic layers were washed with brine (200 mL), dried over $MgSO_4$, filtered and concentrated under reduced pressure to afford the product as a solution in EtOAc. Acetone (86 mL), and then 2,2-dimethoxypropane (10.5 mL, 86 mmol) were added, followed by pTsOH.H_2O (82 mg, 0.43 mmol). The reaction mixture was then stirred at rt overnight. After 17h the reaction was quenched with saturated $NaHCO_3$ (100 mL) and was further diluted with saturated LiCl (100 mL). The aqueous was then extracted with EtOAc (3 x 200 mL) and the combined organic layers were washed with saturated LiCl (200 mL), dried over $MgSO_4$, filtered and concentrated under reduced pressure to afford 3.79 g of a pink oil. Purification of the crude material by flash chromatography (silica gel, acetone:hexanes 80:20) afforded alcohol **426** (3.34 g, 70%) as a thick yellow oil. **^{1}H NMR** (400 MHz, $CDCl_3$) δ 4.19 – 3.97 (m, 1H), 3.81 – 3.56 (m, 3H), 3.13 – 2.96 (m, 1H), 1.92 (t, *J* = 5.7 Hz, 1H), 1.80 – 1.61 (m, 4H), 1.53 (m, 15H). Synthesis of the title compound was performed by Dimitri Panagopoulos.

Synthesis of aldehyde 423

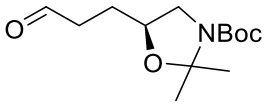

To a solution of alcohol **426** (917 mg, 3.5 mmol) in dry CH_2Cl_2 (18 mL) was added dry Et_3N (1.5 mL, 11 mmol). The solution was cooled to 0 ºC and then a solution of SO_3.py

(1.13 g, 7 mmol) in dry DMSO (9 mL) was added dropwise. After 1h at 0 ºC, the reaction was quenched by the addition of H_2O (20 mL). The layers were separated and the aqueous layer was extracted with CH_2Cl_2 (3 x 15 mL). The combined organic layers were washed with 1M HCl (15 mL), saturated $NaHCO_3$ (15 mL) and brine, dried over $MgSO_4$, filtered and concentrated under reduced pressure to afford 1.36 g of a pink oil. Purification of the crude material by flash chromatography (silica gel, hexanes-EtOAc 3:2) afforded aldehyde **423** (686 mg, 75%) as a slightly yellow oil. **^{1}H NMR** (400 MHz, $CDCl_3$) δ 9.80 (t, *J* = 1.4 Hz, 1H), 4.17 – 3.99 (m, 1H), 3.66 (br d, *J* = 24.4 Hz, 1H), 3.06 (br s, 1H), 2.59 (br s, 2H), 2.03 – 1.93 (m, 1H), 1.92 – 1.78 (m, 1H), 1.69 – 1.35 (m, 15H). Synthesis of the title compound was performed by Dimitri Panagopoulos.

Synthesis of chlorohydrin 428

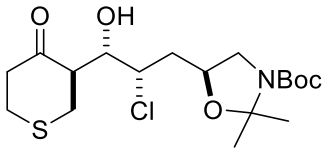

To a suspension of NCS (356 mg, 2.7 mmol) and D-proline (359 mg, 3.2 mmol) in CH_2Cl_2 (3 mL) at 0 ºC was added a solution of aldehyde **423** (686 mg, 2.7 mmol) in CH_2Cl_2 (6 mL). After 1h 10min, tetrahydrothiopyran-4-one **308** (929 mg, 8 mmol) was added, followed by DMSO (1.7 mL). The mixture was then allowed to warm to rt for 3 days. After 70h, the reaction was quenched with brine (15 mL) and the layers were separated. The aqueous was extracted with CH_2Cl_2 (2 x 20 mL) and the combined organic layers were washed with brine (20 mL), dried over $MgSO_4$, filtered and concentrated under reduced pressure to afford 1.74 g of a brown solid. This material was dissolved in a minimum amount of Et_2O and then Hexanes were added. The solution was placed in a freezer for 20min and then it was filtered. The brown solid was discarded and the filtrate was concentrated under reduced pressure to afford 1.35 g of a brown oil. Purification of this material by flash chromatography (silica gel, hexanes-EtOAc 8:2) afforded chlorohydrin **428** (305 mg, 28%) as a yellow oil. **^{1}H NMR** (400 MHz, $CDCl_3$) δ 4.38 – 4.27 (m, 1H), 4.23 (d, *J* = 10.6 Hz, 1H), 3.72 (br d, *J* = 26.5 Hz, 1H), 3.20 (br s, 1H), 3.18 – 3.01 (m, 3H), 2.98 (dd, *J* = 7.9, 5.0 Hz, 2H), 2.85 – 2.66 (m, 3H), 2.32 (t, *J* = 12.9 Hz, 1H), 1.96 – 1.81 (m, 1H), 1.67 – 1.39 (m, 15H). Synthesis of the title compound was performed by Dimitri Panagopoulos.

Synthesis of diol 429

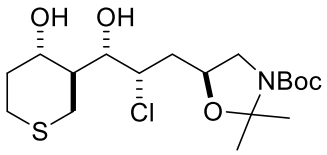

To a solution of **428** (837 mg, 2 mmol) in THF (14 mL) at -78 ºC was added 1M DIBAL in Hexanes (4 mL, 4 mmol) dropwise. After 1h, the reaction mixture was diluted with EtOAc (20 mL) and quenched with saturated Rochelle's salt solution (~30 mL). The biphasic mixture was allowed to warm to rt with vigorous stirring for 45min. The layers were then separated and the aqueous was extracted with EtOAc (2 x 30 mL). The combined organic layers were then washed with brine (30 mL), dried over $MgSO_4$, filtered and concentrated under reduced pressure to afford the diol **429** as a ~4:1 mixture of inseparable diastereoisomers (731 mg, white foam, 87%). This material was used immediately for the next step. **^{1}H NMR** (500 MHz, $CDCl_3$) δ 4.41 – 4.18 (m, 2H), 3.88 – 3.58 (m, 3H), 3.10 (br s, 2H), 2.82 – 2.71 (m, 1H), 2.72 – 2.55 (m, 2H), 2.47 – 2.32 (m, 1H), 2.33 – 2.22 (m, 1H), 2.12 – 2.01 (m, 1H), 2.03 – 1.89 (m, 1H), 1.88 – 1.77 (m, 1H), 1.66 – 1.39 (m, 15H). Synthesis of the title compound was performed by Dimitri Panagopoulos.

Synthesis of cyclized alcohol 430

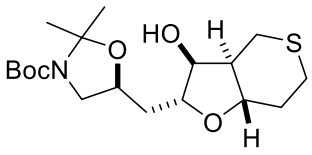

To a solution of the mixture of **429** (731 mg, 1.8 mmol) in MeOH (85 mL), H_2O was added (4 mL). Then, $SrCO_3$ (5.26 g, 36 mmol) was added as well and the resulting white slurry was stirred at 75 ºC overnight. After 12h, the reaction mixture was allowed to cool to rt and then it was filtered through a Celite pad. The filtrate was dried over $MgSO_4$, filtered and concentrated under reduced pressure to afford 1.21 g of a yellow oil. Purification of the crude material by flash chromatography (silica gel, hexanes-EtOAc 3:2) afforded alcohol **430** (379 mg, 57% from **428**) as a white foam. **^{1}H NMR** (400 MHz, $CDCl_3$) δ 4.27 – 4.18 (m, 1H), 4.18 – 4.14 (m, 1H), 3.79 (td, *J* = 6.3, 1.7 Hz, 1H), 3.41 (t, *J* = 10.7 Hz, 1H), 3.13 (br s, 1H), 2.93 – 2.81 (m, 1H), 2.77 – 2.62 (m, 3H), 2.47 (dd, *J* = 12.1, 3.5 Hz, 1H), 2.00

– 1.90 (m, 1H), 1.89 – 1.80 (m, 1H), 1.79 – 1.61 (m, 3H), 1.51 (d, *J* = 33.9 Hz, 15H). Synthesis of the title compound was performed by Dimitri Panagopoulos.

Synthesis of cyclized alcohol 431

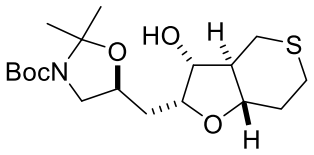

To a solution of Ph_3P (399 mg, 1.5 mmol) in THF (6 mL) at 0 ºC was added DIAD (300 µL, 1.5 mmol). The yellow solution was stirred at 0 ºC for 30 min, by which time it had turned into a white suspension. A solution of alcohol **430** (379 mg, 1 mmol) and p-nitrobenzoic acid (254 mg, 1.5 mmol) in THF (4 mL) was then added dropwise over 5min. The resulting yellow solution was stirred at 0 ºC for 50min, then it was allowed to warm to rt over 2.5h. The solvents were then removed under reduced pressure and the residue was redissolved in MeOH (14.5 mL). Freshly ground NaOH (122 mg, 3 mmol) was then added and the mixture was stirred at rt overnight. After 15h, the reaction was quenched by the addition of saturated NH_4Cl (~20 mL) and the aqueous were then extracted with Et_2O (3 x 30 mL). The combined organic layers were washed with brine (30 mL), dried over $MgSO_4$, filtered and concentrated under reduced pressure to afford 1.25 g of a yellow oil. This material was dissolved in a minimum amount of hot benzene and then cold cyclohexane was added. The solvents were removed under reduced pressure and this process was repeated once more. The residue was suspended in Et_2O, filtered, the white solid was discarded and the filtrate was concentrated under reduced pressure to afford 1.18 g of a yellow oil. Purification of this material by flash chromatography (silica gel, hexanes-EtOAc, 7:3) afforded alcohol **431** (254 mg, 67% from **430**) as a white foam. **^{1}H NMR** (400 MHz, $CDCl_3$) δ 4.46 – 4.35 (m, 1H), 4.22 – 4.06 (m, 2H), 3.71 (br s, 1H), 3.51 (br s, 1H), 3.16 (br s, 1H), 3.10 – 2.89 (m, 2H), 2.78 – 2.67 (m, 2H), 2.65 – 2.54 (m, 1H), 2.46 – 2.32 (m, 1H), 2.19 – 2.07 (m, 1H), 1.93 – 1.76 (m, 2H), 1.74 – 1.64 (m, 1H), 1.63 – 1.40 (m, 15H). Synthesis of the title compound was performed by Dimitri Panagopoulos.

Synthesis of methyl ether 432

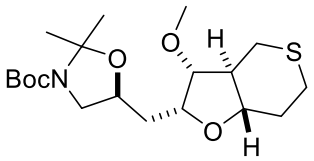

370

To a suspension of 60% NaH (109 mg, 65 mg active reagent, 2.7 mmol) in THF (2.5 mL) at 0 ºC was added a solution of alcohol **431** (254 mg, 0.68 mmol) in THF (2 mL). Then, Me_2SO_4 (71 µL, 0.75 mmol) was added as well and the suspension was allowed to warm to rt overnight. After 22h the reaction was quenched at 0 ºC with H_2O (5 mL) and the aqueous was extracted with Et_2O (3 x 5 mL). The combined organic layers were washed with brine (5 mL), dried over $MgSO_4$, filtered and concentrated under reduced pressure to afford 279 mg of a yellow oil. Purification of the crude material by flash chromatography (silica gel, hexanes-EtOAc 7:3) afforded methyl ether **432** (181 mg, 69%) as a white solid. **^{1}H NMR** (500 MHz, $CDCl_3$) δ 4.31 – 4.19 (m, 1H), 3.93 (br s, 1H), 3.75 (br d, *J* = 39.4 Hz, 1H), 3.64 (br s, 1H), 3.38 (s, 3H), 3.18 – 3.03 (m, 1H), 3.01 – 2.89 (m, 2H), 2.75 – 2.63 (m, 3H), 2.37 (br s, 1H), 1.97 (ddd, *J* = 13.7, 8.5, 5.1 Hz, 1H), 1.91 – 1.67 (m, 3H), 1.51 (d, *J* = 35.8 Hz, 15H). Synthesis of the title compound was performed by Dimitri Panagopoulos.

Synthesis of sulfonium salt 422

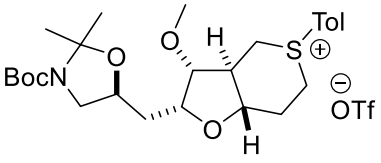

357

A sealed tube was charged with compound **432** (79 mg, 0.20 mmol) in $ClCH_2CH_2Cl$ (1.36 mL), $(Tol)_2IOTf$ (93 mg, 0.20 mmol) and $Cu(OBz)_2$ (1.6 mg, 0.005 mmol). The tube was then sealed and the reaction mixture was stirred at 110 ºC for 30min. It was then allowed to cool to rt and the solvent was removed under reduced pressure. The residue was dissolved in a minimum amount of acetone and then Et_2O was added to afford 154 mg of a green-brown tar. Purification of the crude material by flash chromatography (silica gel, MeOH:CH_2Cl_2 5:95 to 40:60) afforded sulfonium salt **422** (55 mg, 43%) as a brown foam. **^{1}H NMR** (500 MHz, $CDCl_3$) δ 8.0 (d, *J* = 8.4 Hz, 2H), 7.52 (d, *J* = 8.2 Hz, 2H), 4.85 – 4.67

(m, 1H), 4.40 – 4.31 (m, 1H), 4.29 – 4.04 (m, 4H), 3.90 – 3.69 (m, 2H), 3.54 (dd, *J* = 12.1, 3.2 Hz, 1H), 3.38 (s, 3H), 3.24 – 3.01 (m, 1H), 2.76 (d, *J* = 13.9 Hz, 1H), 2.48 (s, 3H), 2.11 – 1.91 (m, 3H), 1.89 – 1.65 (m, 1H), 1.65 – 1.42 (m, 15H). Synthesis of the title compound was performed by Dimitri Panagopoulos.

Synthesis of sulfone 421

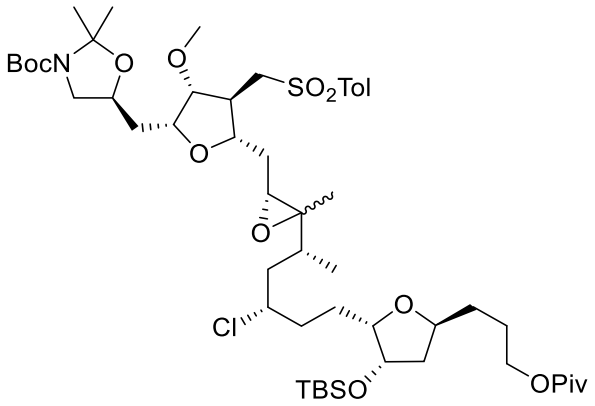

To a cold (-78 °C) solution of sulfonium salt **422** (20 mg, 0.03 mmol) in dry THF (0.3 mL) was added LiHMDS (1 M in hexanes, 64 µL, 0.08 mmol). The resulting solution was stirred at -78 °C for 1 hour. Ketone **361b** (16 mg, 0.03 mmol), diluted in a minimum amount of THF (0.1 mL), was then slowly added. Stirring was continued for an additional hour at -78 °C and then 15 hours at room temperature. After this time, an aqueous solution of NH_4Cl (1 mL) was added, the mixture was diluted with CH_2Cl_2 (1 mL) and the phases were separated. The aqueous phase was extracted with CH_2Cl_2 (1 ml x 3), and the combined organic phases were washed with water (1 mL) and brine (1 mL), dried ($MgSO_4$) and concentrated to provide a crude yellow solid. The crude product was then dilute in CH_2Cl_2 (0.3 mL) and cooled to -78 °C. MCPBA was added (21 mg, 0.09 mmol) and the resulting mixture was allowed to warm up to ambient temperature for 1 hour. After this time, the mixture was cooled to -78 °C and quenched with $NaHCO_3$ (1 mL). After slowly warming up to room temperature, the layers were separated, and the aqueous phase was extracted with CH_2Cl_2 (2 x 1 mL). The combined organic phases were washed with brine (1 mL), dried (Na_2SO_4), filtered, and concentrated to provide a crude oil. Purification of the crude product by flash chromatography (silica gel, hexanes-EtOAc 3:1) provided sulfone **421** (19.5 mg, 60%) as a foamy solid. **$[\alpha]^{20}_D$** + 2.3 (*c* 1.6, $CHCl_3$); **^{1}H NMR** (400 MHz, $CDCl_3$) δ 7.81 (d, *J* = 8.0 Hz, 2H), 7.38 (d, *J* = 8.0 Hz, 2H), 4.24 (br s, 1H), 4.20 – 4.10 (m, 2H), 4.06 (dt, *J* = 6.4, 2.9 Hz, 2H), 4.04 – 3.90 (m, 2H), 3.88 – 3.75 (m, 3H), 3.74 – 3.54 (m, 3H),

3.39 (s, 3H), 3.18 – 3.04 (m, 2H), 2.66 – 2.55(br s, 1H), 2.45 (s, 3H), 2.11 – 1.51 (m, 20H), 1.47 (s, 15H), 1.19 (s, 9H), 1.13 (s, 3H), 0.89 (s, 9H), 0.07 (d, *J* = 1.8 Hz, 6H); **^{13}C NMR** (101 MHz, $CDCl_3$) δ 178.70, 145.22, 136.58, 130.32, 130.27, 130.19, 128.18, 128.13, 86.27, 81.97, 81.73, 78.34, 77.36, 76.75, 73.80, 64.51, 64.48, 63.48, 61.46, 59.78, 58.24, 57.51, 51.02, 43.64, 42.20, 40.98, 38.93, 38.88, 35.80, 33.68, 32.68, 32.13, 32.07, 29.84, 28.62, 27.36, 26.72, 25.93, 25.59, 21.79, 18.23, 15.47, 12.86, -4.33, -4.80; **IR** (cast film, $CHCl_3$) *v* 2953.22, 2926.37, 2855.92, 1725.26, 1701.77; **HRMS (ESI-TOF)** *m/z*: $[M + NH_4]^+$ Calcd for $C_{52}H_{92}ClN_2O_{12}SSi$ 1031.5829; Found 1031.5834.

Synthesis of alcohol 433

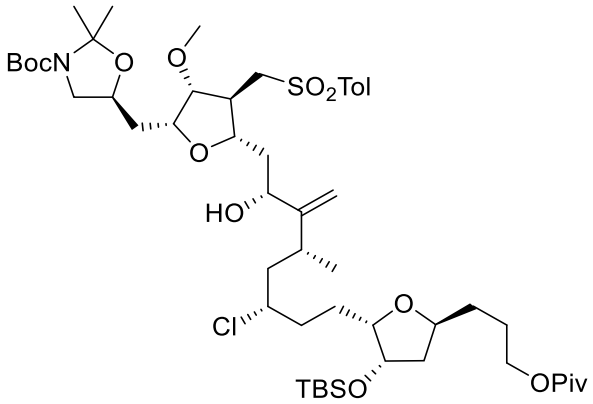

Thoroughly deoxygenated THF (0.4 mL) was added to a mixture of commercial Cp_2TiCl_2 (30 mg, 0.12 mmol) and Zn dust (52 mg, 0.80 mmol) under an Ar atmosphere and the suspension was stirred at room temperature until it turned lime green (after about 5 min). A solution of epoxide **421** (41 mg, 0.04 mmol) in THF (0.4 mL) was then added and the mixture was stirred for 2 h, after which the reaction was quenched with a saturated solution of NaH_2PO_4 (1 mL). The resulting mixture was filtered through celite, and the layers were separated. The organic phase was washed with brine (1 mL), dried (Na_2SO_4), filtered, and concentrated to provide a crude oil. Purification of the crude product by flash chromatography (silica gel, hexanes-EtOAc 3:1) provided the alcohol **433** (29 mg, 70%) as a foamy solid. **$[\alpha]^{20}_D$** -3.3 (*c* 0.7, $CHCl_3$); **^{1}H NMR** (500 MHz, $CDCl_3$) δ 7.84 – 7.77 (m, 2H), 7.38 (d, *J* = 7.9 Hz, 2H), 5.15 (s, 1H), 4.87 (s, 1H), 4.27 – 4.21 (m, 1H), 4.20 – 4.08 (m, 3H), 4.06 (td, *J* = 6.4, 2.3 Hz, 2H), 3.90 – 3.77 (m, 3H), 3.76 – 3.59 (m, 3H), 3.38 (s, 3H), 3.26 – 3.17 (m, 1H), 3.14 – 3.06 (m, 2H), 2.60 – 2.53 (br s, 1H), 2.46 (s, 3H), 2.41 – 2.33 (br s, 1H), 2.10 – 2.01 (m, 1H), 2.00 – 1.90 (m, 2H), 1.89 – 1.70 (m, 6H), 1.69 – 1.40 (m, 21H), 1.25 (s, 1H), 1.18 (s, 9H), 1.05 (d, *J* = 6.7 Hz, 2H), 0.89 (s, 9H), 0.07 (s, 3H),

0.06 (s, 3H); **^{13}C NMR** (101 MHz, $CDCl_3$) δ 178.70, 156.77, 145.28, 136.71, 130.27, 128.10, 108.50, 85.80, 83.68, 81.80, 77.36, 76.75, 73.79, 73.50, 71.51, 64.51, 62.29, 58.25, 57.56, 51.12, 46.34, 44.54, 42.19, 41.61, 38.88, 35.82, 32.72, 32.65, 32.44, 28.63, 27.37, 26.82, 25.95, 25.94, 25.58, 21.81, 19.38, 18.23, -4.32, -4.81; **IR** (cast film, $CHCl_3$) *v* 2956.24, 2917.58, 2854.77, 1724.03, 1695.03; **HRMS (ESI-TOF)** *m/z*: $[M + NH_4]^+$ Calcd for $C_{52}H_{92}ClN_2O_{12}SSi$ 1031.5829; Found 1031.5832.

Synthesis of tetrahydropyran 434

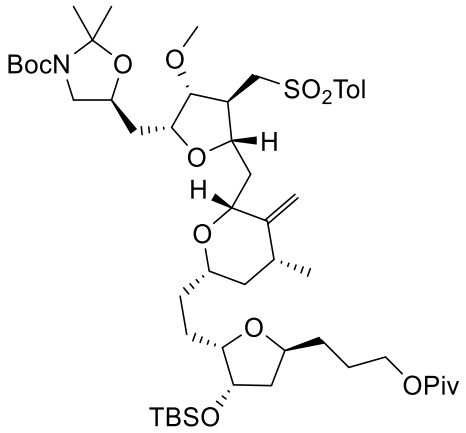

To a solution of alcohol alcohol **433** (60 mg, 0.067 mmol) in *t*-BuOAc (5.7 ml) at 0 °C were added 2,6-di-*tert*-butyl-4-methylpyridine (69 mg, 0.33 mmol) and $AgBF_4$ (39 mg, 0.20 mmol). The reaction flask was wrapped with aluminum foil and warmed to rt. After stirring 2 h at rt, the reaction mixture was treated with NH_4Cl (5 mL). The layers were separated, and the aqueous phase was extracted with EtOAc (2 x 5 mL). The combined organic phases were washed with brine (5 mL), dried (Na_2SO_4), filtered, and concentrated to provide a clear oil. The crude product **434** was used in the next step without further purification.

Synthesis of ketone 435

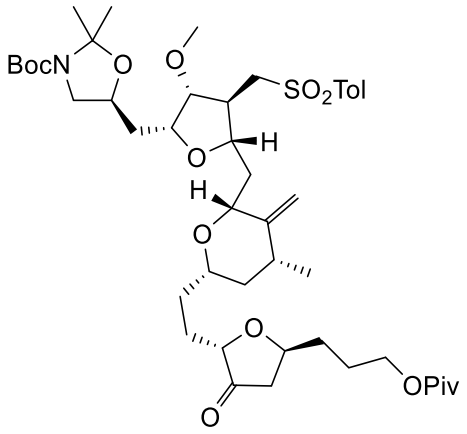

To a cold (0 °C) solution of compound **434** (56 mg, 0.065 mmol) in THF (0.2 mL) and pyridine (0.36 mL) was added HF-pyridine (70% in pyridine, 0.18 mL, 5 mmol). The resulting solution was stirred at room temperature for 15 hours. After this time, an aqueous solution of $NaHCO_3$ (0.5 mL) was added, the mixture was diluted with EtOAc (0.5 mL) and the phases were separated. The aqueous phase was extracted with EtOAc (0.5 ml x 3), and the combined organic phases were washed with water (1 mL) and brine (1 mL), dried ($MgSO_4$) and concentrated to provide a crude yellow oil that was directly used in the next step without further purification. The crude alcohol was diluted in CH_2Cl_2 (0.6 mL) and cooled to 0 °C. $NaHCO_3$ (28 mg, 0.32 mmol) in and DMP (28 mg, 0.071 mmol) were then added, and the mixture was stirred at room temperature for 1 hour. After this time, the reaction was quenched with $H_2O/Na_2S_2O_3$(aq)/NaHCO3(aq) = 1/1/1 (1 mL) and the resulting mixture was stirred for another 30 minutes. The mixture was extracted with CH_2Cl_2 (0.5 ml x 3), washed with brine, dried over anhydrous $MgSO_4$, and concentrated to provide a crude oil. Purification by flash chromatography (silica gel, hexanes-EtOAc 5:1) provided ketone **435** (34 mg, 70%) as a clear oil. **$[\alpha]^{20}_D$** – 2.0 (*c* 1.4, $CHCl_3$); **^{1}H NMR** (500 MHz, $CDCl_3$) δ 7.84 (d, *J* = 8.3 Hz, 2H), 7.42 (d, *J* = 8.0 Hz, 2H), 4.87 (s, 1H), 4.81 (s, 1H), 4.34 – 4.26 (m, 1H), 4.21 – 4.06 (m, 3H), 3.85 – 3.79 (m, 2H), 3.78 – 3.64 (m, 3H), 3.60 (br d, *J* = 9.8 Hz, 1H), 3.43 (s, 3H), 3.43 – 3.37 (m, 1H), 3.20 – 3.08 (m, 2H), 3.01 (dd, *J* = 14.5, 2.6 Hz, 1H), 2.61 – 2.51 (m, 2H), 2.48 (s, 3H), 2.25 – 2.08 (m, 3H), 2.00 (dt, *J* = 13.8, 6.3 Hz, 1H), 1.91 (ddd, *J* = 12.9, 9.3, 2.7 Hz, 1H), 1.85 – 1.54 (m, 10H), 1.53 – 1.46 (m, 15H), 1.22 (s, 9H), 1.09 (d, *J* = 6.3 Hz, 3H); **^{13}C NMR** (101 MHz, $CDCl_3$) δ 215.98, 178.47, 150.44, 144.97, 136.87, 130.09, 127.99, 104.97, 86.04, 81.02, 78.57, 77.99, 77.26, 76.11, 75.26, 74.65, 63.86, 60.35, 58.19, 57.51, 53.42, 50.85, 43.46, 42.65, 42.35,

38.73, 37.45, 36.64, 35.49, 31.99, 31.86, 31.43, 28.47, 27.20, 26.65, 24.90, 24.68, 21.62, 21.01, 17.88, 14.18; **IR** (cast film, $CHCl_3$) *v* 2959.93, 2923.02, 2872.69, 2349.30; 1762.16, 1725.26; **HRMS (ESI-TOF**) *m/z*: $[M + NH_4]^+$ Calcd for $C_{46}H_{75}N_2O_{12}S$ 879.5035; Found 879.5031.

Synthesis of alkene 420

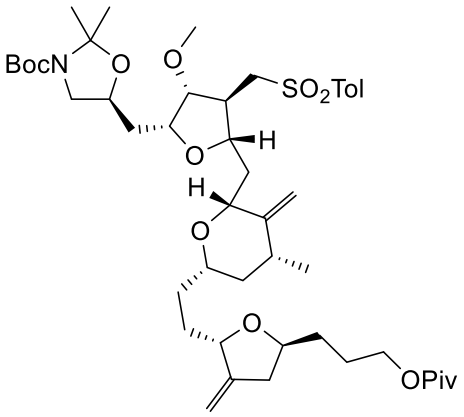

To a suspension of methyltriphenylphosphonium bromide (17 mg, 0.048 mmol) in dry THF (0.3 mL) was added *t*BuOK (48 µL of 1.0 M solution in THF, 0.048 mmol) at 0 °C. After the mixture was stirred for 30 minutes at the same temperature, a solution of ketone **435** (14 mg, 0.016 mmol) in dry THF (0.3 mL) was slowly added. After stirring for an additional 3 hours at room temperature, the resulting mixture was quenched with water (0.5 mL). The mixture was extracted with EtOAc (0.5 mL), washed with brine (0.5 mL), dried over anhydrous $MgSO_4$, and concentrated to provide the crude product as a yellow oil. Purification by flash chromatography (silica gel, hexanes-EtOAc 9:1) afforded the desired alkene **420** (9.5 mg, 70%). **$[\alpha]^{20}_D$** – 6.1 (*c* 0.7, $CHCl_3$); **^{1}H NMR** (500 MHz, $CDCl_3$) δ 7.83 (d, *J* = 8.3 Hz, 2H), 7.40 (d, *J* = 7.9 Hz, 2H), 4.90 (q, *J* = 2.1 Hz, 1H), 4.84 (s, 1H), 4.77 (s, 1H), 4.64 (q, *J* = 1.7 Hz, 1H), 4.24 (br s, 1H), 4.17 – 4.11 (m, 1H), 4.06 (td, *J* = 6.3, 4.8 Hz, 2H), 3.95 (p, *J* = 6.5 Hz, 1H), 3.87 (br s, 1H), 3.78 – 3.63 (m, 3H), 3.57 – 3.50 (m, 1H), 3.44 (s, 3H), 3.38 – 3.32 (m, 1H), 3.17 – 3.05 (m, 3H), 3.01 (br d, *J* = 14.2 Hz, 1H), 2.61 (dd, *J* = 15.5, 6.3 Hz, 1H), 2.58 – 2.50 (m, 1H), 2.48 (s, 3H), 2.46 (s, 3H), 2.25 – 2.06 (m, 3H), 2.03 – 1.95 (m, 1H), 1.89 – 1.82 (m, 1H), 1.76 – 1.70 (m, 2H), 1.66 – 1.49 (m, 9H), 1.48 – 1.43 (m, 15H), 1.18 (s, 9H), 1.06 (d, *J* = 6.2 Hz, 3H); **^{13}C NMR** (101 MHz, $CDCl_3$) δ 178.69, 151.39, 150.75, 145.19, 137.01, 130.26, 128.20, 115.47, 105.09, 105.02, 86.08, 81.16, 79.59, 79.57, 77.36, 76.91, 75.43, 64.38, 58.26, 57.68, 51.02, 43.60, 42.91, 38.91, 38.88, 37.64, 35.70, 31.99, 31.88, 31.76, 31.64, 29.84, 28.63, 27.36, 25.43, 21.77, 18.06;

IR (cast film, $CHCl_3$) *v* 2956.24, 2922.42, 2845.10, 1724.03; 1690.20, 1385.77; **HRMS (ESI-TOF)** *m/z*: $[M + NH_4]^+$ Calcd for $C_{47}H_{77}N_2O_{11}S$ 877.5243; Found 879.5238.

Synthesis of alcohol 370

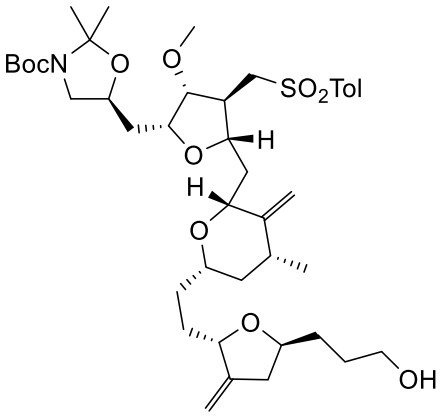

To a cold (–78 °C) solution of alkene **420** (9.5 mg, 0.011 mmol) in CH_2Cl_2 (0.2 mL) was added diisobutylaluminum hydride (1.00 M solution. in CH_2Cl_2, 22 µL, 0.022 mmol) and the reaction mixture was stirred for 5 hours. After this time, an aqueous solution of NH_4Cl (1.0 M, 15 mL) was added, the mixture was diluted with ether (0.5 mL) and the phases were separated. The aqueous phase was extracted with ether (2 × 0.5 mL), and the combined organic phases were washed with water (1 mL) and brine (1 mL), dried (Na_2SO_4), filtered, and concentrated to provide a crude oil. Purification of the crude product by flash chromatography (silica gel, hexanes-EtOAc 85:15) afforded alcohol **370** (8 mg, 90%) as a foamy solid. **^{1}H NMR** (500 MHz, $CDCl_3$) δ 7.83 (d, *J* = 8.3 Hz, 2H), 7.40 (d, *J* = 7.9 Hz, 2H), 4.91 (q, *J* = 2.0 Hz, 1H), 4.84 (br s, 1H), 4.77 (br s, 1H), 4.66 (q, *J* = 1.9 Hz, 1H), 4.33 – 4.26 (m, 1H), 4.20 – 4.09 (m, 1H), 3.97 (quint, *J* = 6.9 Hz, 1H), 3.86 (d, *J* = 3.0 Hz, 1H), 3.79 – 3.48 (m, 5H), 3.46 – 3.31 (m, 4H), 3.19 – 2.97 (m, 3H), 2.68 – 2.42 (m, 6H), 2.34 – 1.24 (m, 32H), 1.06 (d, *J* = 6.4 Hz, 3H). The ^{1}H NMR spectroscopic data of compound **370** matched that of Alphora's.

^{1}H NMR (500 MHz, $CDCl_3$) of alcohol 370

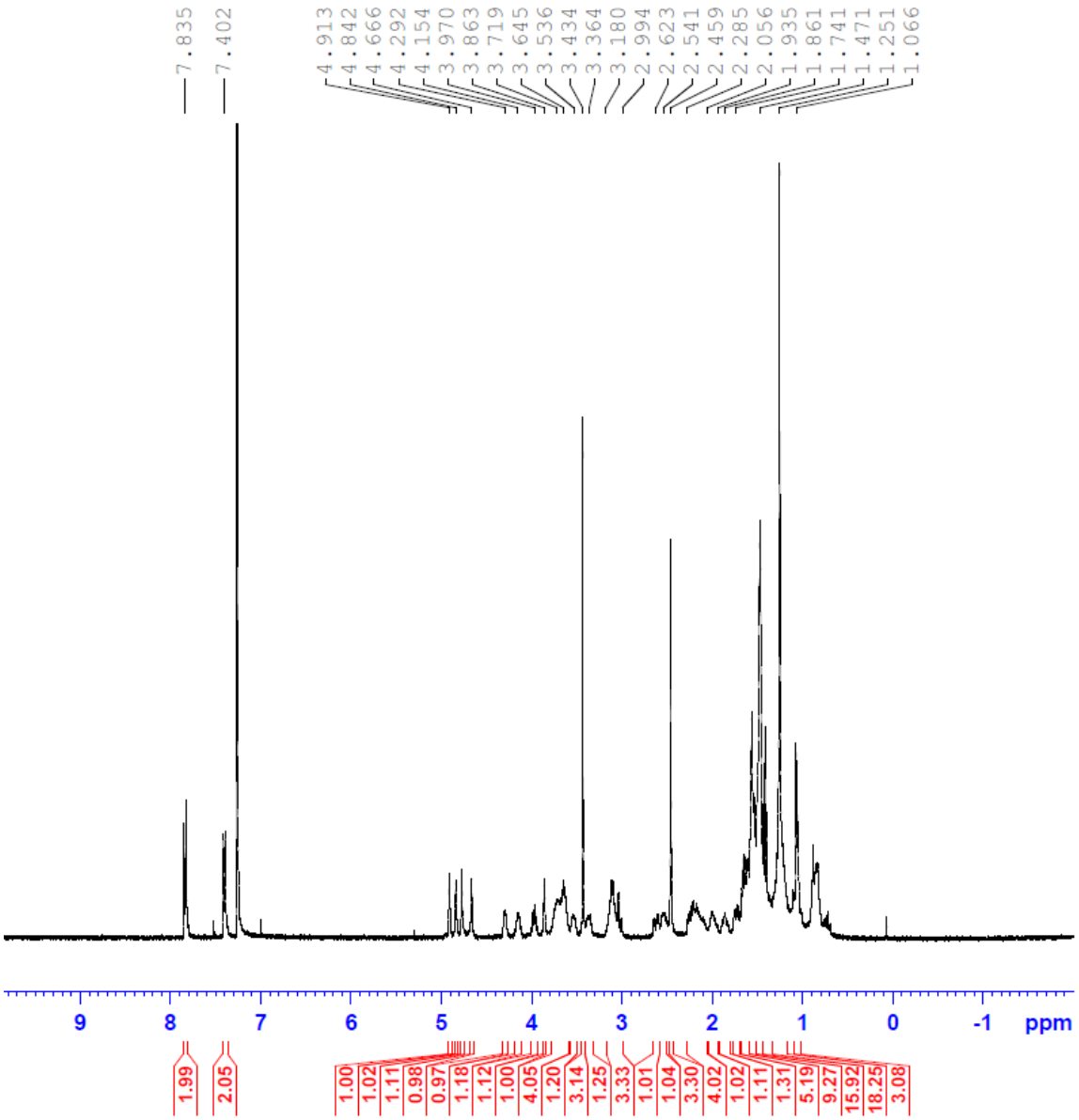

Chapter 4.

Formal Synthesis of the “Immucillins”

4.1. Introduction

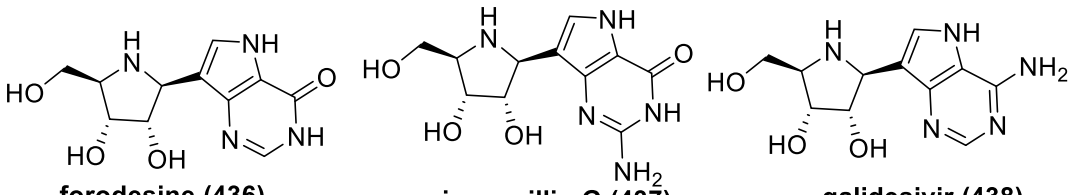

Figure 4.1. Key members of the “immucillin” family.

Transition state analogues (TSAs) are chemical compounds that resemble the transition-state (TS) of an enzyme-catalyzed reaction.[154] As enzymes have evolved to stabilize these high-energy transition states, TSAs can bind many times more tightly to a target enzyme than the natural substrate – up to 10^{10}- 10^{15} times.[155] Given the relevance of carbohydrate processing enzymes in numerous human diseases, TSA inhibitors have become attractive targets for the development of therapeutics. Most notably, the structure elucidation of the enzyme purine nucleoside phosphorylase (PNP) led to the discovery of various promising inhibitors known as the ”immucillins” (Figure 4.1). Among them, immucillin H (**436**), also known as forodesine, was approved in Japan in 2017 to treat peripheral T-cell lymphoma.[156] Immucillin A (galidesivir **438**), initially developed as a potential antibiotic against *Trichomonas vaginalis*, was found to be active against a broad range of viruses including the Ebola and Marburg filoviruses as well as the Yellow Fever and Zika flaviviruses.[157]

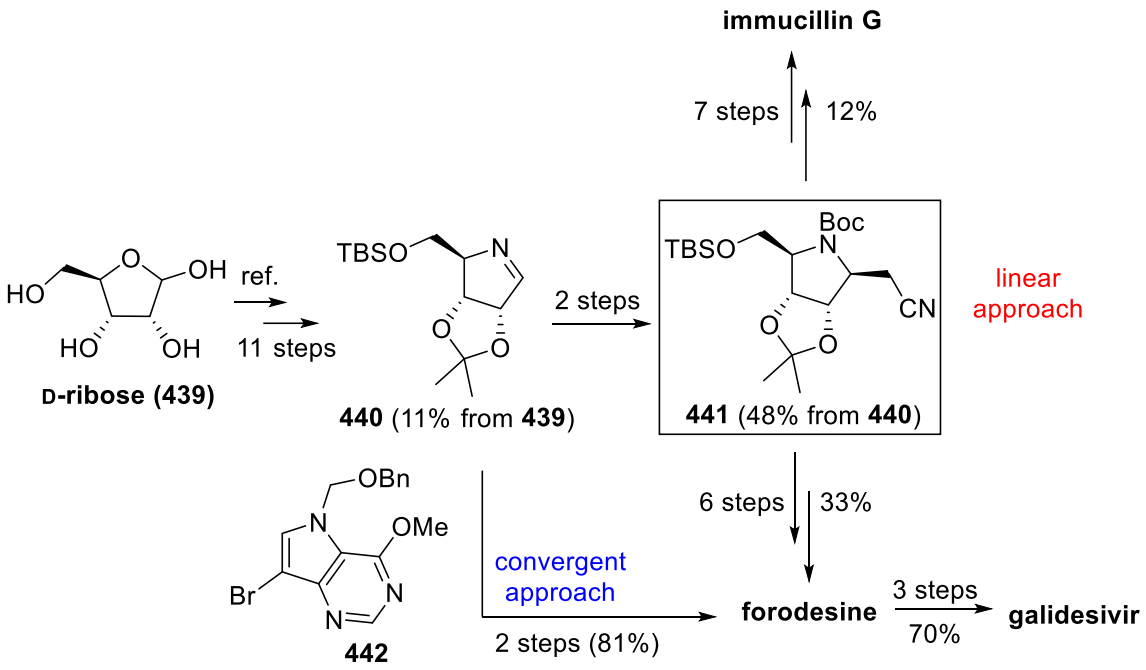

Scheme 4.1. Previous Syntheses of the "Immucillins".

Structurally, the "immucillins" are imino-C-nucleoside analogues. While much effort has been dedicated to the synthesis of polyhydroxylated pyrrolidine iminosugars, these processes are often lengthy and require the use of expensive chiral pool materials.[158] This reliance on naturally occurring carbohydrate starting materials also limits the accessible stereochemical and structural diversity. In fact, many imino-C-nucleoside analogues can be traced back to the imine **440** (Scheme 4.1).[159–161] For example, while the immunicillins were initially synthesized from D-gulonolactone,[160,162] an 11-step sequence was developed during scale-up campaigns in 2006 that initiates with a D-ribose **439** (Scheme 4.1).[163] The imine **440** is ultimately reacted with the anion derived from acetonitrile and, following Boc-protection, provides the common immucillin building block **441** in 2 additional steps. The latter material has been further elaborated into the valuable TSAs **436**, **437** and **438** (Figure 4.1) in 6 to 9 steps (Scheme 1.4).[160] Overall, this approach provided the PNP inhibitor **438** in 19 linear steps and 5% overall yield. In 2001, a more convergent route was developed based on the addition of a protected deazapurine **442** to the imine **440** (Scheme 4.1)[161] and thus, the overall length of the synthesis was considerably reduced.

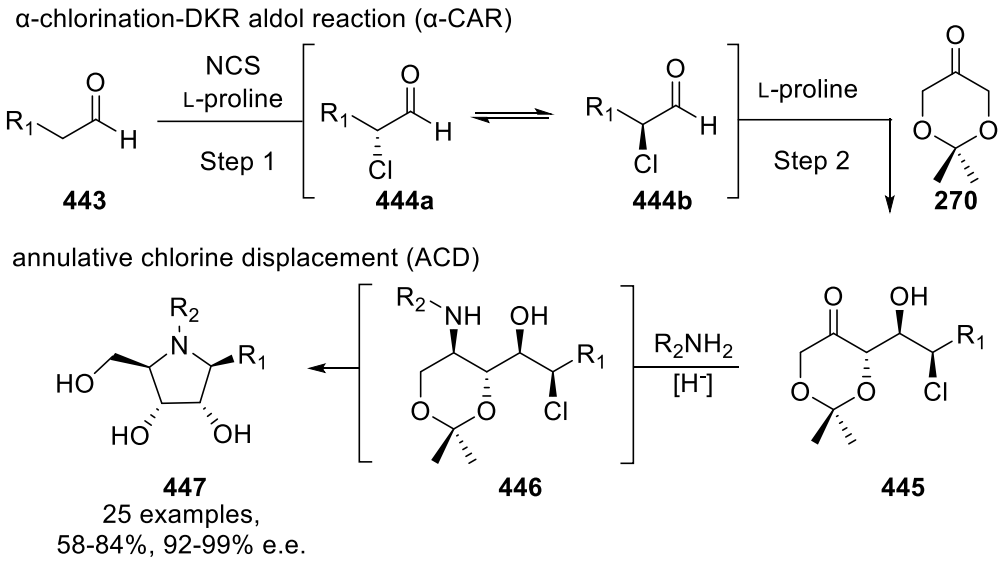

Scheme 4.2. General Platform to Access Imino-C-nucleoside Analogues.

Despite these improvements, challenges associated with the stereoselective construction of iminosugars continue to complicate drug discovery and development efforts. In an effort to address this challenge, in 2015 we reported a new platform for accessing iminosugars **447**.[164] This process relies on a tandem α-chlorination/aldol reaction of an aldehyde **443** with dioxanone **270** and a subsequent reductive amination/annulation sequence. Importantly, the second step of the tandem α-chlorination/aldol reaction was shown to involve a dynamic kinetic resolution (DKR)[120] and the chlorohydrins **445**, and ultimately iminosugars **447**, are produced in excellent diastereo- and enantioselectivity (Scheme 4.2). Considering the potential utility of this strategy for expediting the synthesis of imino-C-nucleosides, we envisioned the development of concise and stereoselective syntheses of the TSAs **436**, **437** and **438** (Figure 4.1).

4.2. Results and discussion

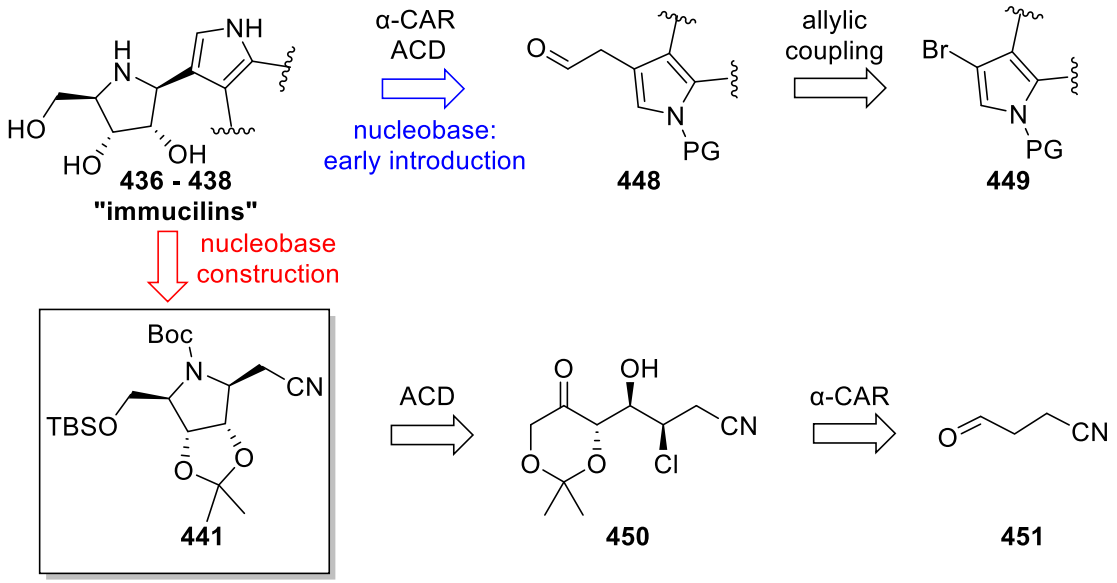

Scheme 4.3. Retrosyntheses Investigated.

We first explored a convergent approach that relies on the early introduction of an elaborated nucleobase acetaldehyde derivative **448** (Scheme 4.3). Most notably, we anticipated that the aldehyde function in **448** could result from an allylic coupling with the bromo analogue **449** followed by oxidative cleavage of the resulting olefin. Toward this goal, the synthesis of various β-pyrrole and β-deazapurine acetaldehydes was investigated. For example, the β-deazapurine acetaldehyde **456** was synthesized in 4 steps following procedures reported in the literature (Scheme 4.4).[165]

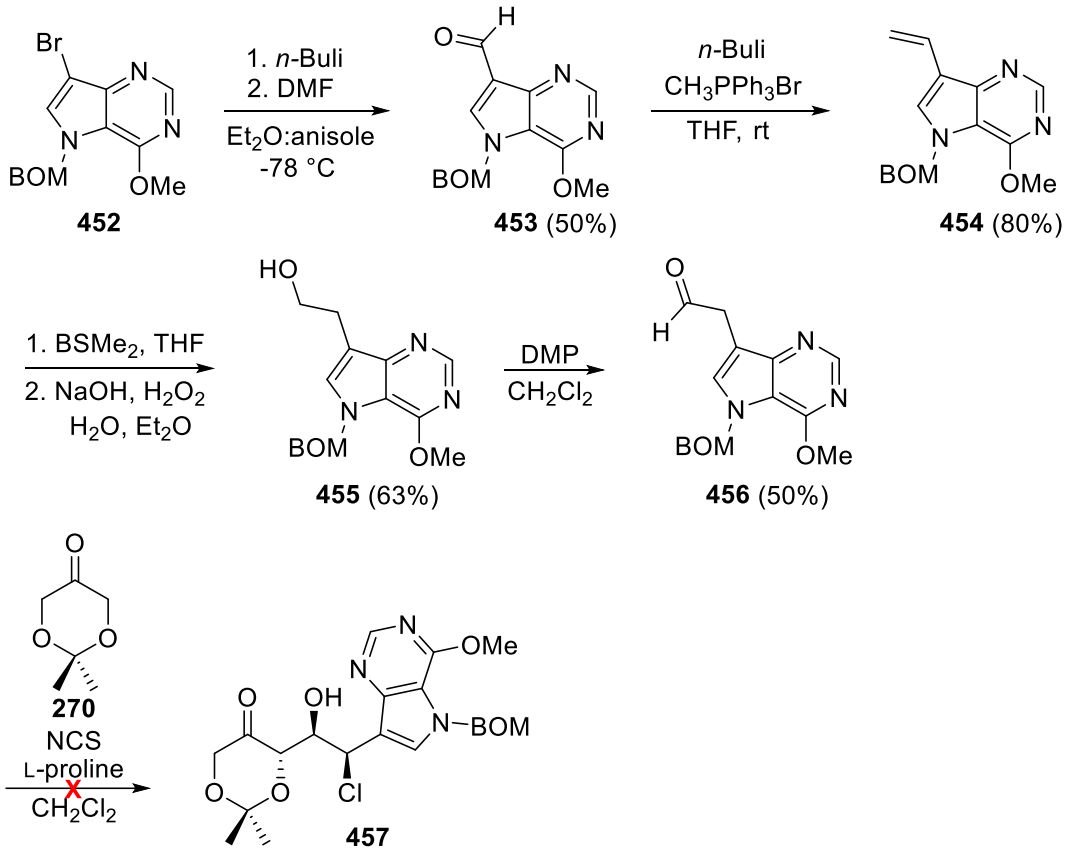

Scheme 4.4. Synthesis of the Acetaldehyde Derivative 456 and Subsequent Exploration of the α-Chlorination-DKR Aldol Reaction.

Here, lithium halogen exchange of the commercially available bromodeazapurine **452** with *n*-butyllithium and following reaction with DMF, provided the aldehyde **453** in 50% yield. Subsequently, Wittig reaction of aldehyde **453** with the ylide derived from methyltriphenylphosphonium bromide furnished the alkene **454** in excellent yield. Following Brown hydroboration and DMP oxidation then produced the target acetaldehyde derivative **456**. The latter material was then subjected to an α-chlorination-DKR aldol reaction with dioxanone **270** but, unfortunately, the reaction led to immediate decomposition of the aldehyde starting material **456**.

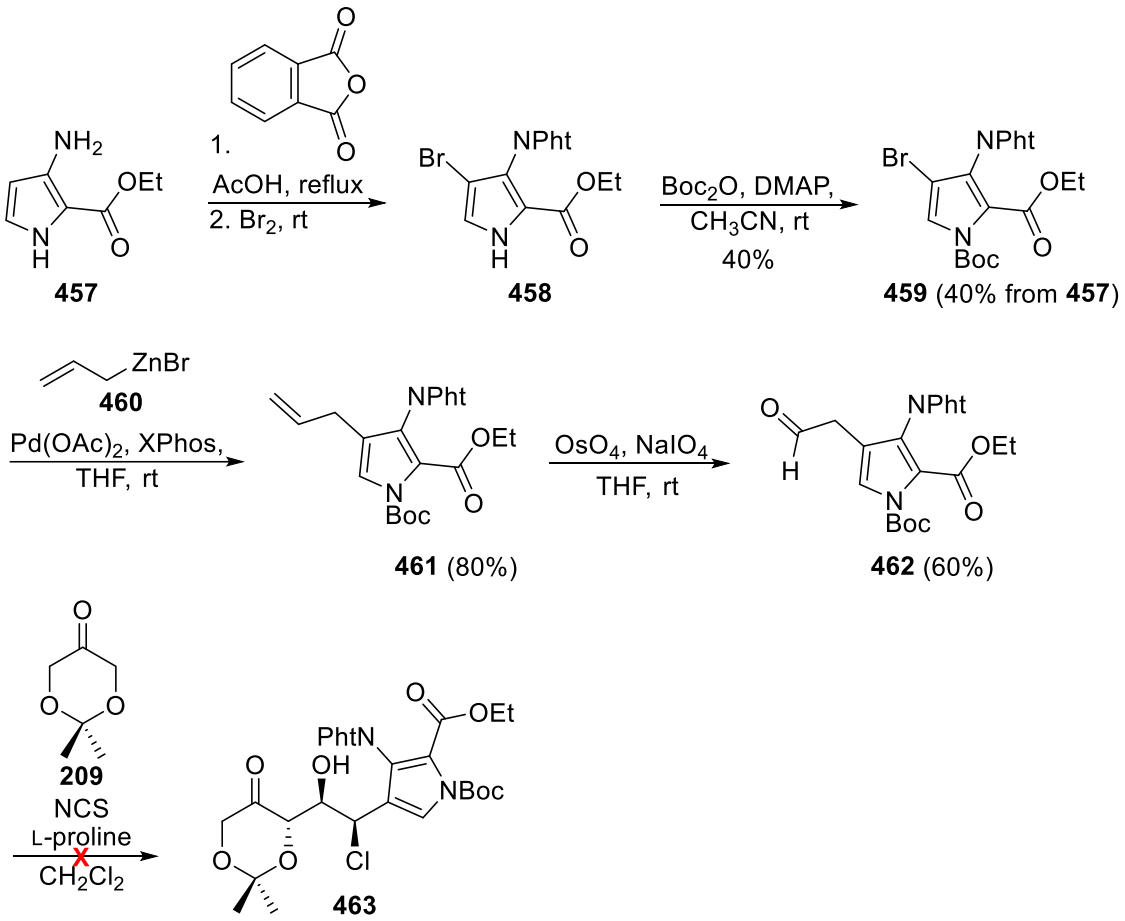

Scheme 4.5. Synthesis of the Acetaldehyde Derivative 462 and Subsequent Exploration of the α-Chlorination-DKR Aldol Reaction.

Following this disappointment, the β-pyrrole acetaldehyde **462** was synthesized from the commercially available pyrrole derivative **457** (Scheme 4.5). Here, protection of the amine **457** with a phthalimide and subsequent addition of bromine produced the bromopyrrole intermediate **458**. Boc-protection of the latter material then delivered the fully protected pyrrole **459** in 40% yield from **457**. To our delight, Negishi coupling[166] of the bromo derivative **459** with the organozincate **460** furnished the allylic product **461** in excellent yield. Subsequently, the olefin function in **461** was cleaved upon treatment with osmium tetroxide and sodium periodate, and the resulting aldehyde **462** was engaged in an α-chlorination-DKR aldol reaction with dioxanone **270**. Here, treatment of the β-pyrrole acetaldehyde **462** with L-proline and NCS promoted a dimerization of the pyrrole moiety and thus, addition of the dioxanone **270** led to undesired aldol products.

Given the unstable nature of the β-pyrrole and β-deazapurine acetaldehydes synthesized thus far, we elected to use the strategy reported by V. Schramm[160] and construct the nucleobase at a late stage in the synthesis (e.g., **441**, Scheme 4.1). Toward this goal, a succinct and stereoselective synthesis of the common immucillin building block **441** was developed (Scheme 4.6).

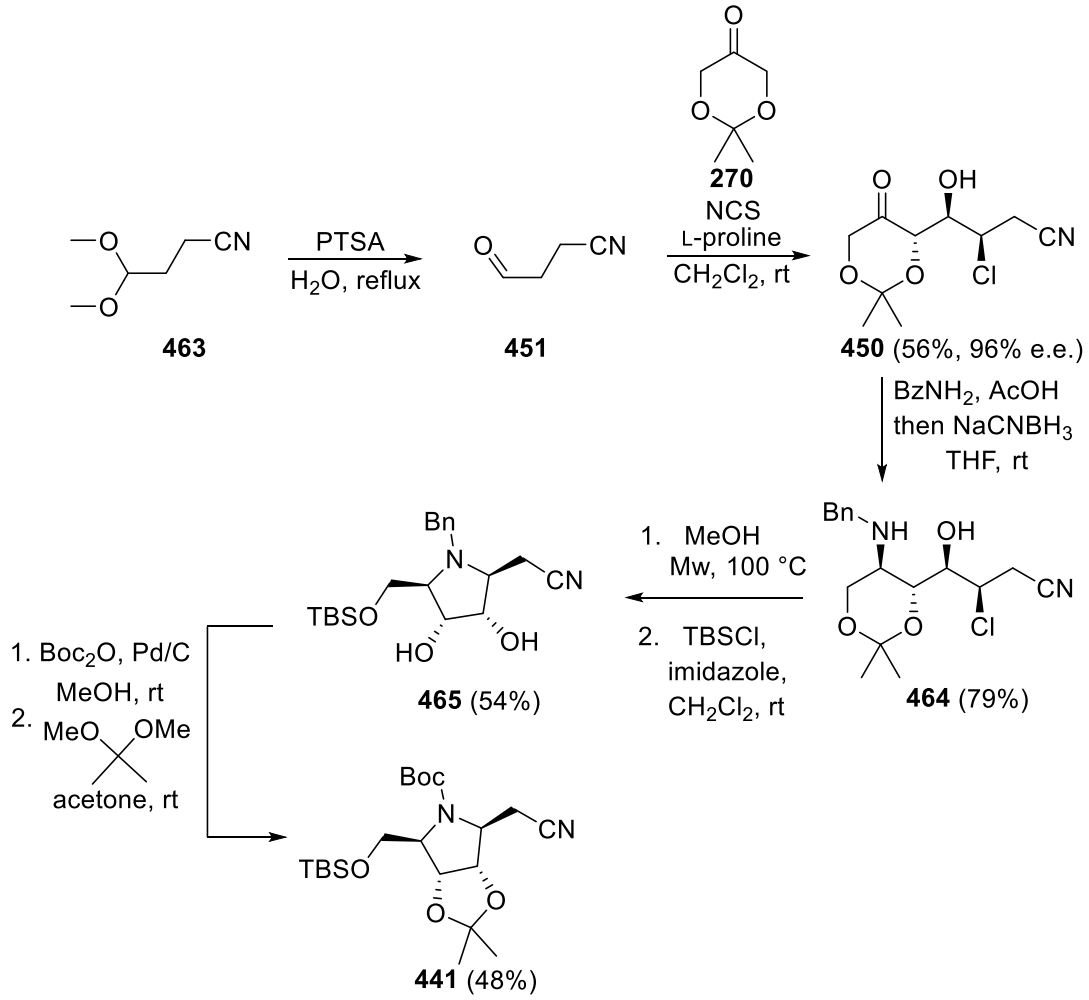

Scheme 4.6. Stereoselective Synthesis of the Common Immucillin Building Block 441.

Thus, as summarized in Scheme 4.6, deprotection of 4,4-dimethoxybutyronitrile **463** and a subsequent α-chlorination/aldol reaction with dioxanone **270**, provided the *syn*-chlorohydrin **450** in good yield and enantioselectivity. Ketone **450** was then smoothly converted to the corresponding amino chlorohydrin **464** by treatment with benzylamine

and sodium cyanoborohydride. Following thermal cyclization and TBS-protection, the iminosugar derivative **465** was produced in 54% yield. The latter material **465** was elaborated into the reported immucillin building block **441** through a one-pot benzyl removal/Boc-protection and a subsequent acetonide protection.

4.3. Conclusion

In summary, despite much effort, all pyrrole and deazapurine acetaldehyde analogues proved unstable with the exception of deazapurine **456** and pyrrole **462**. While these latter aldehydes could be prepared and isolated, subjection to α-chlorination reaction conditions led to immediate decomposition or undesired aldol reactions. Instead, use of the cyanoacetaldehyde **451**, readily available from cheap starting material, led to the development of a short, stereoselective synthesis of the common immucillin building block **441**. Notably, the length of the synthetic route was reduced by several steps, and the overall yield increased from 5% to 11%. This route may well prove to be more economic and flexible for the production of immucillin-like drug candidates.

4.4. Experimental

General considerations

All reactions were carried out with commercial solvents and reagents that were used as received. Flash chromatography was carried out with Geduran® Si60 silica gel (Merck). Concentration and removal of trace solvents was done via a Büchi rotary evaporator using dry ice/acetone condenser, and vacuum applied from an aspirator or Büchi V-500 pump. All reagents and starting materials were purchased from Sigma Aldrich, Alfa Aesar, TCI America, and/or Strem, and were used without further purification. All solvents were purchased from Sigma Aldrich, EMD, Anachemia, Caledon, Fisher, or ACP and used without further purification, unless otherwise specified.

Nuclear magnetic resonance (NMR) spectra were recorded using chloroform-d ($CDCl_3$) or acetonitrile-d_3 (CD_3CN). Signal positions (δ) are given in parts per million from tetramethylsilane (δ 0) and were measured relative to the signal of the solvent (^{1}H NMR: $CDCl_3$: δ 7.26, CD_3CN: δ 1.96; ^{13}C NMR: $CDCl_3$: δ 77.16, CD_3CN: δ 118.26). Coupling constants (*J* values) are given in Hertz (Hz) and are reported to the nearest 0.1 Hz. $_1$H

NMR spectral data are tabulated in the order: multiplicity (s, singlet; d, doublet; t, triplet; q, quartet; quint, quintet; m, multiplet), coupling constants, number of protons. NMR spectra were recorded on a Bruker Avance 600 equipped with a QNP or TCI cryoprobe (600 MHz), Bruker 500 (500 MHz), or Bruker 400 (400 MHz). Diastereoisomeric ratios (d.r.) are based on analysis of crude ^{1}H-NMR. High performance liquid chromatography (HPLC) analysis was performed on an Agilent 1100 HPLC, equipped with a variable wavelength UV-Vis detector. High-resolution mass spectra were performed on an Agilent 6210 TOF LC/MS, Bruker MaXis Impact TOF LC/MS, or Bruker micrOTOF-II LC mass spectrometer. Infrared (IR) spectra were recorded neat on a Perkin Elmer Spectrum Two FTIR spectrometer. Only selected, characteristic absorption data are provided for each compound. Optical rotation was measured on a Perkin-Elmer Polarimeter 341 at 589 nm.

The ^{1}H NMR spectroscopic analyses of the deazapurine intermediates **453**, **454**, **455** and **456** (Scheme 4.4) matched that reported in the literature.[165] Formation of the pyrrole derivatives **459**, **461** and **462** (Scheme 4.5) was confirmed by ^{1}H NMR and mass spectrometric analysis.

Synthesis of chlorohydrin 450

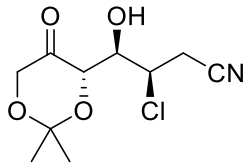

To a stirred solution of β-cyanopropionaldehyde dimethyl acetal **463** (1.0 g, 7.69 mmol) in water (7.9 mL), was added *p*-toluenesulfonic acid (1.6 mg, 0.01 mmol). The resulting mixture was heated at reflux for 2 hours. The water was removed under reduced pressure (bath <50 °C). The resulting mixture was dried ($MgSO_4$), filtered (CH_2Cl_2) and concentrated under reduced pressure. The crude aldehyde **451** was then added to a stirred suspension of *N*-chlorosuccinimide (1.1 g, 8.07 mmol) and L-proline (708 mg, 6.15 mmol) in CH_2Cl_2 (38.4 mL) at room temperature. 2,2-Dimethyl-1,3-dioxan-5-one **270** (0.10 mL, 8.07 mmol) was then added, and the resulting mixture was stirred for a total of 12 hours. The reaction mixture was then diluted with CH_2Cl_2 and the organic layer was removed and washed twice with water and once with brine. The organic layer was then dried ($MgSO_4$), concentrated under reduced pressure to provide a crude mixture (d.r.. =

2:1). Purification of the crude product by flash chromatography (silica gel, CH_2Cl_2-EtOAc 50:1) afforded chlorohydrin **450** (1.07 g, 96% e.e., 56% yield) as a crystalline solid.

Data for major diastereoisomer: **$[\alpha]^{20}_D$** -170.2 (*c* 1.0, $CHCl_3$); **^{1}H NMR** (400 MHz, $CDCl_3$) δ 4.44 (tt, *J* = 7.5, 1.6 Hz, 1H), 4.37 – 4.31 (m, 1H), 4.27 (d, *J* = 1.5 Hz, 1H), 4.09 (d, *J* = 17.7 Hz, 1H), 4.07 – 4.02 (m, 1H), 3.57 (dd, *J* = 2.9, 1.5 Hz, 1H), 2.98 (dd, *J* = 7.5, 1.7 Hz, 2H), 1.50 (s, 3H), 1.42 (s, 3H). **^{13}C NMR** (101 MHz, $CDCl_3$) δ 211.81, 116.56, 101.91, 72.48, 70.31, 66.44, 55.34, 23.93, 23.42, 23.38. **IR** (cast film, $CHCl_3$) *v* 3496.74, 2990.12, 2993.79, 2255.36, 1738.68; **HRMS (ESI-TOF)** *m/z*: $[M + NH_4]^+$ Calcd for $C_{10}H_{18}ClN_2O_4$ 265.0955; Found 265.0952.

Data for minor diastereoisomer: **$[\alpha]^{20}_D$** -57.1 (*c* 1.7, $CHCl_3$); ^{1}H NMR (400 MHz, $CDCl_3$) δ 4.56 – 4.49 (m, 2H), 4.29 (dd, *J* = 17.4, 1.5 Hz, 1H), 4.15 (td, *J* = 5.7, 3.5 Hz, 1H), 4.07 (d, *J* = 17.4 Hz, 1H), 3.22 (d, *J* = 3.8 Hz, 1H), 3.07 – 2.93 (m, 2H), 1.51 (s, 3H), 1.47 (s, 3H). **^{13}C NMR** (101 MHz, $CDCl_3$) δ 208.68, 116.46, 101.54, 73.96, 73.18, 67.03, 54.62, 24.03, 23.83, 23.69. **IR** (cast film, $CHCl_3$) *v* 3463.62, 2990.07, 2255.57, 1748.19; 1226.31; **HRMS (ESI-TOF)** *m/z*: $[M + NH_4]^+$ Calcd for $C_{10}H_{18}ClN_2O_4$ 265.0955; Found 265.0957.

*Determination of enantiomeric excess of **450***

A racemic mixture of **450** was prepared using the above procedure and L-:D-proline.

To a stirred solution of racemic **450** or optically enriched halohydrin **450** (1.0 equiv) in MeOH (0.15 M) was added sodium borohydride (1.5 equiv), and the resulting mixture was stirred at room temperature for 1 hour. The reaction mixture was then diluted with CH_2Cl_2 and washed with H_2O. The organic layer was removed, dried over $MgSO_4$, concentrated under reduced pressure, and the crude product was purified by flash chromatography. To a solution of purified diol in CH_2Cl_2 (0.10 M) was added triethylamine (6.0 equiv.), *p*-nitro benzoyl chloride (3.0 equiv.) and 4-dimethylaminopyridine (cat.) and left to stir for 1 hour. The reaction mixture was diluted with CH_2Cl_2 and washed with $NaHCO_3$. The organic layer was removed, dried over $MgSO_4$, concentrated under reduced pressure, and the crude product was purified by flash chromatography (silica gel, hexanes-EtOAc 8:2). The e.e. was then determined by chiral separation of the optically enriched diester and the racemic mixture using a CHIRALCEL-AD column; flow rate 1.0 mL/min; eluent: hexanes-EtOAc 70:30; detection at 260 nm; retention time = 5.61 min and 6.25 min (see chromatograms).

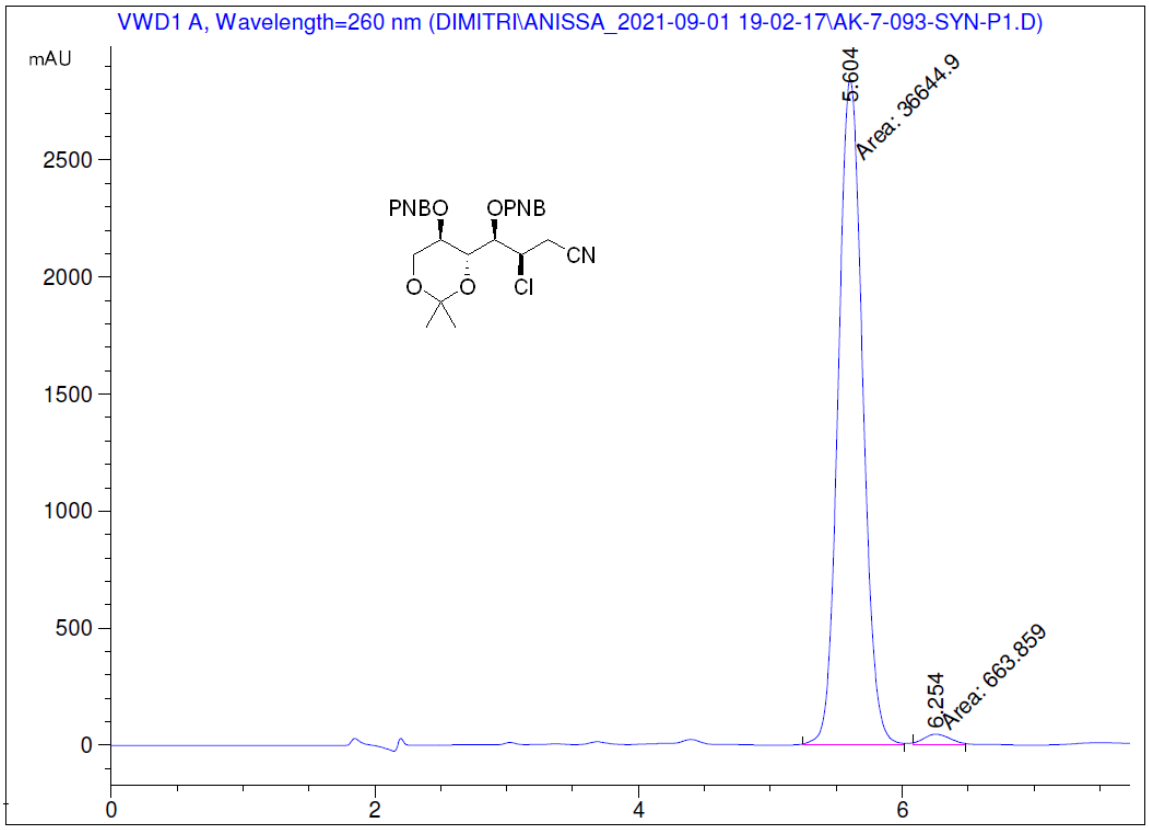

Synthesis of aminoalcohol 464

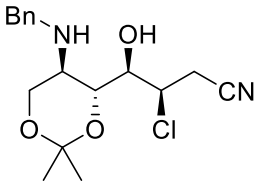

To a stirred solution of chlorohydrin **450** (148 mg, 0.60 mmol) in THF (5.9 mL) were added $BnNH_2$ (0.16 ml, 1.5 mmol) and glacial acetic acid (0.034 mL, 0.6 mmol), and the resulting mixture was stirred at 20 °C for 1 hour. $NaB(CN)H_3$ (94 mg, 1.5 mmol) was then added and the mixture was stirred for one additional hour. The reaction mixture was then diluted with CH_2Cl_2 (6 mL) and treated with water (6 mL). The layers were separated, and the organic layer was washed with brine, dried ($MgSO_4$) and concentrated under reduced pressure. Purification of the crude product by flash chromatography (silica gel, hexanes-EtOAc 8:2) afforded aminoalcohol **464** (175 mg, 86% yield) as a crystalline solid. **$[\alpha]^{20}_D$** -58.4 (*c* 2.2, $CHCl_3$); **^{1}H NMR** (500 MHz, $CDCl_3$) δ 7.42 – 7.16 (m, 6H), 4.43 (ddd, *J* = 8.2, 6.6, 1.6 Hz, 1H), 4.08 (dd, *J* = 11.5, 5.1 Hz, 1H), 3.91 – 3.82 (m, 2H), 3.77 (d, *J* = 12.6 Hz, 1H), 3.63 (dd, *J* = 10.0, 8.3 Hz, 1H), 3.55 (dd, *J* = 11.5, 9.5 Hz, 1H), 3.00 – 2.83 (m, 3H),

1.44 (s, 3H), 1.36 (s, 3H). **^{13}C NMR** (151 MHz, $CDCl_3$) δ 137.70, 129.86, 129.20, 128.90, 128.37, 128.01, 117.02, 99.27, 75.75, 69.60, 63.19, 56.05, 55.65, 50.87, 28.27, 23.57, 19.32. **IR** (cast film, $CHCl_3$) *v* 3285.37, 2996.83, 2926.37, 2855.92, 2366.08; **HRMS (ESI-TOF)** *m/z*: $[M + H]^+$ Calcd for $C_{17}H_{24}ClN_2O_3$ 339.1465; Found 339.1469.

Synthesis pyrrolidine 465

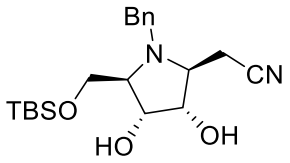

The chloroaminoalcohol **464** (175 mg, 0.52 mmol) was added to a microwave vial and dissolved in MeOH (5 mL). The vial was then sealed in a CEM Discover LabMate microwave reactor and the resulting mixture was heated at 100 °C for 30 minutes. Aqueous $NaHCO_3$. was added and MeOH was removed under reduced pressure. The resulting mixture was extracted with EtOAc (3x 3 mL) and the combined organic layers were washed with brine, dried ($MgSO_4$) and concentrated under reduced pressure. The crude product was diluted in CH_2Cl_2 (5 mL) and imidazole (46 mg, 0.67 mmol) and TBSCl (78 mg, 0.52 mmol) were successively added. After 1 hour, water (2 mL) was added and the phases were separated. The aqueous phase was extracted with CH_2Cl_2 (2 × 2 mL), and the combined organic phases were washed with water (1 mL) and brine (1 mL), dried ($MgSO_4$), filtered, and concentrated to provide a crude oil. Purification of the crude product by flash chromatography (silica gel, hexanes-EtOAc 8:2) afforded pyrrolidine **465** (106 mg, 54% yield) as an oil. **$[\alpha]^{20}_D$** -5.2 (*c* 1.0, $CHCl_3$); **^{1}H NMR** (400 MHz, $CDCl_3$) δ 4.12 (t, *J* = 4.8 Hz, 1H), 3.98 (t, *J* = 4.6 Hz, 1H), 3.90 – 3.79 (m, 2H), 3.50 (dd, *J* = 9.9, 4.7 Hz, 1H), 3.38 (dd, *J* = 9.9, 8.5 Hz, 1H), 3.06 (dt, *J* = 5.8, 4.1 Hz, 1H), 2.97 (dt, *J* = 8.5, 4.8 Hz, 1H), 2.64 (s, 2H), 2.37 (dd, *J* = 16.9, 3.8 Hz, 1H), 2.20 (dd, *J* = 16.9, 5.8 Hz, 1H), 0.85 (s, 9H), -0.01 (d, *J* = 5.0 Hz, 6H). **^{13}C NMR** (101 MHz, $CDCl_3$) δ 138.93, 129.08, 128.64, 128.42, 127.76, 127.29, 118.03, 77.36, 74.92, 74.66, 69.91, 65.84, 65.79, 59.85, 53.10, 26.02, 22.38, 18.33, -5.40. **IR** (cast film, $CHCl_3$) *v* 3429.80, 2951.41, 2932.08, 2859.60, 2342.55; **HRMS (ESI-TOF)** *m/z*: $[M + H]^+$ Calcd for $C_{20}H_{33}N_2O_3Si$ 377.2260; Found 377.2260.

Synthesis pyrrolidine 441

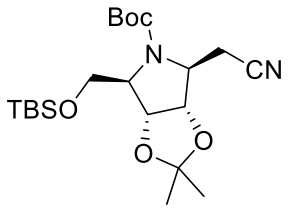

To a stirred solution of pyrrolidine **465** (50 mg, 0.13 mmol) in MeOH (0.6 mL) were added Boc_2O (61 mg, 0.27 mmol) and 10% Pd/C (4 mg). The resulting mixture was stirred under a H_2 atmosphere at 20 °C for 24 hours. The catalyst was removed by filtration over celite (MeOH) and the filtrate was concentrated in vacuo to provide a crude yellow oil. The mixture was diluted in acetone (0.4 mL) and 3,3-dimethoxypropane (50 mg, 0.13 mmol) and CSA (1.5 mg, $6.5*10^{-3}$ mmol) were successively added. After 1 hour, water (0.5 mL) and CH_2Cl_2 (1.5 mL) were added and the phases were separated. The aqueous phase was extracted with CH_2Cl_2 (2 × 1 mL), and the combined organic phases were washed with water (1 mL) and brine (1 mL), dried ($MgSO_4$), filtered, and concentrated to provide a crude oil. Purification of the crude product by flash chromatography (silica gel, hexanes-EtOAc 9:1) afforded pyrrolidine **441** (27 mg, 48% yield) as an oil. **$[\alpha]^{20}_D$** -30.1 (*c* 2.3, $CHCl_3$); **^{1}H NMR** (400 MHz, $CDCl_3$) δ 4.70 – 4.48 (m, 2H), 4.19 – 3.66 (m, 4H), 2.99 – 2.64 (m, 2H), 1.47 (d, *J* = 4.7 Hz, 9H), 1.45 (s, 3H), 1.33 (s, 3H), 0.90 (s, 9H), 0.08 (s, 3H), 0.07 (d, *J* = 1.8 Hz, 3H). **^{13}C NMR** (151 MHz, $CDCl_3$) δ 153.91, 153.59, 117.48, 117.38, 112.41, 112.37, 84.28, 83.19, 82.09, 81.34, 81.22, 80.98, 66.41, 66.08, 63.48, 63.12, 61.94, 61.66, 28.49, 28.44, 27.39, 27.38, 26.15, 25.37, 21.51, 20.73, 18.58, -5.28. **IR** (cast film, $CHCl_3$) *v* 2956.24, 2932.08, 2859.60, 1699.96, 1380.94; **HRMS (ESI-TOF)** *m/z*: $[M + H]^+$ Calcd for $C_{21}H_{39}N_2O_5Si$ 427.2628; Found 427.2624.

^{1}H NMR (400 MHz, $CDCl_3$) of compound 441:

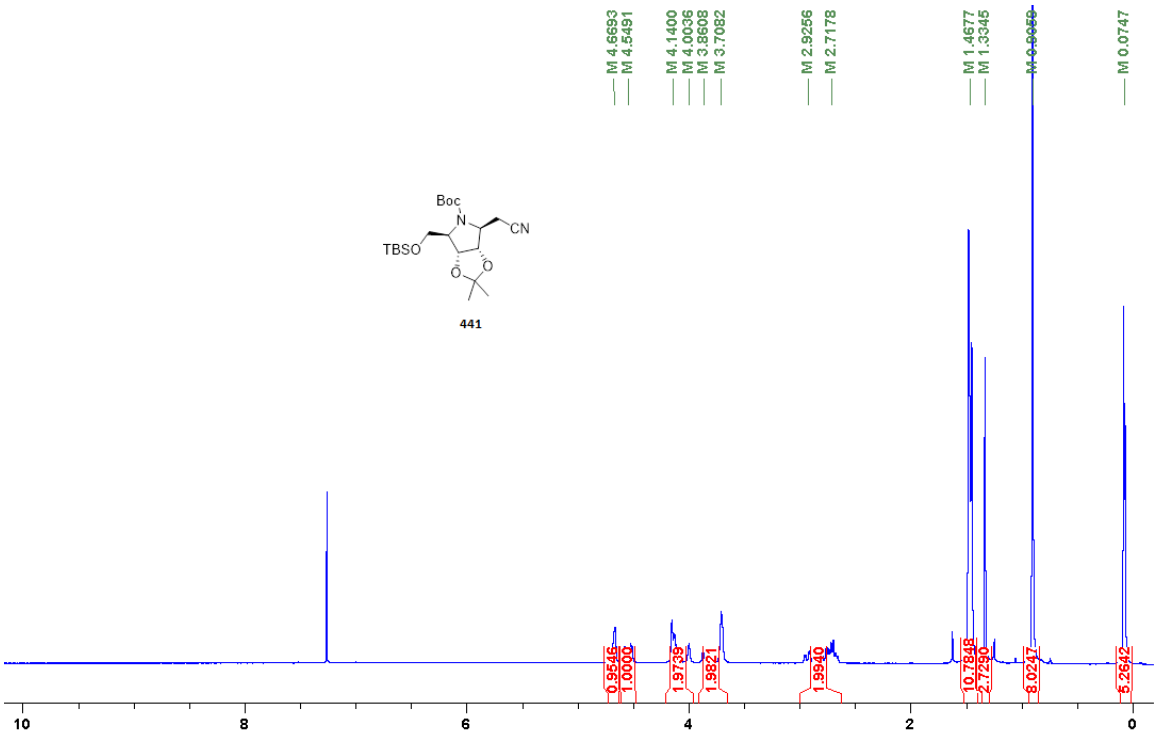

References

(1) Hanson, J. R. The Classes of Natural Product and Their Isolation. In *Natural Products*; **2003**, 1–34. https://doi.org/10.1039/9781847551535-00001.

(2) Atanasov, A. G.; Zotchev, S. B.; Dirsch, V. M.; Supuran, C. T. Natural Products in Drug Discovery: Advances and Opportunities. *Nat. Rev. Drug Discov.* **2021**, *20* (3), 200–216. https://doi.org/10.1038/s41573-020-00114-z.

(3) Ramoutsaki, I. A.; Askitopoulou, H.; Konsolaki, E. Pain Relief and Sedation in Roman Byzantine Texts: Mandragoras Officinarum, Hyoscyamos Niger and Atropa Belladonna. *Int. Congr. Ser.* **2002**, *1242*, 43–50. https://doi.org/10.1016/S0531-5131(02)00699-4.

(4) Tan, S. Y.; Tatsumura, Y. Alexander Fleming (1881–1955): Discoverer of Penicillin. *Singapore Med. J.* **2015**, *56* (7), 366–367. https://doi.org/10.11622/smedj.2015105.

(5) Shen, B. A New Golden Age of Natural Products Drug Discovery. *Cell* **2015**, *163* (6), 1297–1300. https://doi.org/10.1016/j.cell.2015.11.031.

(6) Newman, D. J.; Cragg, G. M. Natural Products as Sources of New Drugs over the Nearly Four Decades from 01/1981 to 09/2019. *J. Nat. Prod.* **2020**, *83* (3), 770–803. https://doi.org/10.1021/acs.jnatprod.9b01285.

(7) Bérdy, J. Thoughts and Facts about Antibiotics: Where We Are Now and Where We Are Heading. *J. Antibiot.* **2012**, *65* (8), 385–395. https://doi.org/10.1038/ja.2012.27.

(8) Ito, T.; Masubuchi, M. Dereplication of Microbial Extracts and Related Analytical Technologies. *J. Antibiot.* **2014**, *67* (5), 353–360. https://doi.org/10.1038/ja.2014.12.

(9) Harvey, A. Natural Products in Drug Discovery. *Drug Discov. Today* **2008**, *13* (19–20), 894–901. https://doi.org/10.1016/j.drudis.2008.07.004.

(10) La Clair, J. J. Natural Product Mode of Action (MOA) Studies: A Link between Natural and Synthetic Worlds. *Nat. Prod. Rep.* **2010**, *27* (7), 969. https://doi.org/10.1039/b909989c.

(11) Lachance, H.; Wetzel, S.; Kumar, K.; Waldmann, H. Charting, Navigating, and Populating Natural Product Chemical Space for Drug Discovery. *J. Med. Chem.* **2012**, *55* (13), 5989–6001. https://doi.org/10.1021/jm300288g.

(12) Nicolaou, K. C. *Classics in Total Synthesis I : Targets, Strategies*; VCH, **1996**, 2-3.

(13) Nicolaou, K. C.; Vourloumis, D.; Winssinger, N.; Baran, P. S. The Art and Science of Total Synthesis at the Dawn of the Twenty-First Century. *Angew. Chem. Int. Ed.* **2000**, *39*, 44-122.

(14) Nicolaou, K. C.; Rigol, S.; Yu, R. Total Synthesis Endeavors and Their Contributions to Science and Society: A Personal Account. *CCS Chem.* **2019**, *1*, 3–37. https://doi.org/10.31635/ccschem.019.20190006.

(15) Nicolaou, K. C.; Snyder, S. A. Chasing Molecules That Were Never There: Misassigned Natural Products and the Role of Chemical Synthesis in Modern Structure Elucidation. *Angew. Chem. Int. Ed.* **2005**, *44* (7), 1012–1044. https://doi.org/10.1002/anie.200460864.

(16) Paterson, I. CHEMISTRY: The Renaissance of Natural Products as Drug Candidates. *Science* **2005**, *310* (5747), 451–453. https://doi.org/10.1126/science.1116364.

(17) Tewari, D.; Rawat, P.; Singh, P. K. Adverse Drug Reactions of Anticancer Drugs Derived from Natural Sources. *Food Chem. Toxicol.* **2019**, *123*, 522–535. https://doi.org/10.1016/j.fct.2018.11.041.

(18) Gunasekera, S. P.; Gunasekera, M.; Longley, R. E.; Schulte, G. K. Discodermolide: A New Bioactive Polyhydroxylated Lactone from the Marine Sponge Discodermia Dissoluta. *J. Org. Chem.* **1990**, *55* (16), 4912–4915. https://doi.org/10.1021/jo00303a029.

(19) Longley, R. E.; Caddigan, D.; Harmody, D.; Gunasekera, M.; Gunasekera, S. P. Discodermolide--a New, Marine-Derived Immunosuppressive Compound. I. In Vitro Studies. *Transplantation* **1991**, *52* (4), 650–656. https://doi.org/10.1097/00007890-199110000-00014.

(20) Smith, A. B.; Sugasawa, K.; Atasoylu, O.; Yang, C.-P. H.; Horwitz, S. B. Design and Synthesis of (+)-Discodermolide–Paclitaxel Hybrids Leading to Enhanced Biological Activity. *J. Med. Chem.* **2011**, *54* (18), 6319–6327. https://doi.org/10.1021/jm200692n.

(21) Smith, A. B.; Kaufman, M. D.; Beauchamp, T. J.; LaMarche, M. J.; Arimoto, H. Gram-Scale Synthesis of (+)-Discodermolide. *Org. Lett.* **1999**, *1* (11), 1823–1826. https://doi.org/10.1021/ol9910870.

(22) Paterson, I.; Florence, G. J.; Gerlach, K.; Scott, J. P. Total Synthesis of the Antimicrotubule Agent (+)-Discodermolide Using Boron-Mediated Aldol Reactions of Chiral Ketones. *Angew. Chem. Int. Ed.* **2000**, *39* (2), 377–380. https://doi.org/10.1002/(SICI)1521-3773(20000117)39:2<377::AID-ANIE377>3.0.CO;2-E.

(23) Freemantle, M. Scaled-up Synthesis of Discodermolide. *C & E N* **2004**, *82(9)*, 33–35. https://doi.org/10.1021/CEN-V082N009.P033.

(24) Rinehart, K. L. Antitumor compounds from tunicates. *Med. Res. Rev.* **2000**, *20* (1), 1–27. https://doi.org/10.1002/(SICI)1098-1128(200001)20:1<1::AID-MED1>3.0.CO;2-A.

(25) Corey, E. J.; Gin, D. Y.; Kania, R. S. Enantioselective Total Synthesis of Ecteinascidin 743. *J. Am. Chem. Soc.* **1996**, *118* (38), 9202–9203. https://doi.org/10.1021/ja962480t.

(26) FDA Approves Yondelis for Soft Tissue Sarcoma Subtypes. *Oncol. Times* **2015**, *37* (22), 20. https://doi.org/10.1097/01.COT.0000475248.37309.e9.

(27) Thakare, R.; Dasgupta, A.; Chopra, S. Eravacycline for the Treatment of Patients with Bacterial Infections. *Drugs Today Barc. Spain 1998* **2018**, *54* (4), 245–254. https://doi.org/10.1358/dot.2018.54.4.2800623.

(28) Jukes, T. H. Some Historical Notes on Chlortetracycline. *Clin. Infect. Dis.* **1985**, *7* (5), 702–707. https://doi.org/10.1093/clinids/7.5.702.

(29) Rose, W. E.; Rybak, M. J. Tigecycline: First of a New Class of Antimicrobial Agents. *Pharmacotherapy* **2006**, *26* (8), 1099–1110. https://doi.org/10.1592/phco.26.8.1099.

(30) Conover, L. H.; Butler, K.; Johnston, J. D.; Korst, J. J.; Woodward, R. B. The Total Synthesis of 6-Demethyl-6-Deoxytetracycline. *J. Am. Chem. Soc.* **1962**, *84* (16), 3222–3224. https://doi.org/10.1021/ja00875a063.

(31) Muxfeldt, H. Syntheses in the Tetracycline Series. *Angew. Chem. Int. Ed. Engl.* **1962**, *1* (7), 372–381. https://doi.org/10.1002/anie.196203721.

(32) Muxfeldt, H.; Hardtmann, G.; Kathawala, F.; Vedejs, E.; Mooberry, J. B. Tetracyclines. VII. Total Synthesis of Dl-Terramycin. *J. Am. Chem. Soc.* **1968**, *90* (23), 6534–6536. https://doi.org/10.1021/ja01025a063.

(33) Wirmer, J.; Westhof, E. Molecular Contacts Between Antibiotics and the 30S Ribosomal Particle. In *Methods in Enzymology*; Elsevier, **2006**; *415*, 180–202. https://doi.org/10.1016/S0076-6879(06)15012-0.

(34) Charest, M. G.; Lerner, C. D.; Brubaker, J. D.; Siegel, D. R.; Myers, A. G. A Convergent Enantioselective Route to Structurally Diverse 6-Deoxytetracycline Antibiotics. *Science* **2005**, *308* (5720), 395–398. https://doi.org/10.1126/science.1109755.

(35) Charest, M. G.; Siegel, D. R.; Myers, A. G. Synthesis of (−)-Tetracycline. *J. Am. Chem. Soc.* **2005**, *127* (23), 8292–8293. https://doi.org/10.1021/ja052151d.

(36) Sun, C.; Wang, Q.; Brubaker, J. D.; Wright, P. M.; Lerner, C. D.; Noson, K.; Charest, M.; Siegel, D. R.; Wang, Y.-M.; Myers, A. G. A Robust Platform for the Synthesis of New Tetracycline Antibiotics. *J. Am. Chem. Soc.* **2008**, *130* (52), 17913–17927. https://doi.org/10.1021/ja806629e.

(37) Kummer, D. A.; Li, D.; Dion, A.; Myers, A. G. A Practical, Convergent Route to the Key Precursor to the Tetracycline Antibiotics. *Chem. Sci.* **2011**, *2* (9), 1710–1718. https://doi.org/10.1039/C1SC00303H.

(38) Wright, P. M.; Myers, A. G. Methodological Advances Permit the Stereocontrolled Construction of Diverse Fully Synthetic Tetracyclines Containing an All-Carbon Quaternary Center at Position C5a. *Tetrahedron* **2011**, *67* (51), 9853–9869. https://doi.org/10.1016/j.tet.2011.09.143.

(39) Xiao, X.-Y.; Hunt, D. K.; Zhou, J.; Clark, R. B.; Dunwoody, N.; Fyfe, C.; Grossman, T. H.; O'Brien, W. J.; Plamondon, L.; Rönn, M.; Sun, C.; Zhang, W.-Y.; Sutcliffe, J. A. Fluorocyclines. 1. 7-Fluoro-9-Pyrrolidinoacetamido-6-Demethyl-6-Deoxytetracycline: A Potent, Broad Spectrum Antibacterial Agent. *J. Med. Chem.* **2012**, *55* (2), 597–605. https://doi.org/10.1021/jm201465w.

(40) Clark, R. B.; Hunt, D. K.; He, M.; Achorn, C.; Chen, C.-L.; Deng, Y.; Fyfe, C.; Grossman, T. H.; Hogan, P. C.; O'Brien, W. J.; Plamondon, L.; Rönn, M.; Sutcliffe, J. A.; Zhu, Z.; Xiao, X.-Y. Fluorocyclines. 2. Optimization of the C-9 Side-Chain for Antibacterial Activity and Oral Efficacy. *J. Med. Chem.* **2012**, *55* (2), 606–622. https://doi.org/10.1021/jm201467r.

(41) Tetraphase Pharmaceuticals Announces FDA Approval of Xerava (eravacycline) for Complicated Intra-Abdominal Infections (cIAI) https://www.drugs.com/newdrugs/tetraphase-pharmaceuticals-announces-fda-approval-xerava-eravacycline-complicated-intra-abdominal-4811.html (accessed 2021 -08 -30).

(42) Yu, M. J.; Zheng, W.; Seletsky, B. M. From Micrograms to Grams: Scale-up Synthesis of Eribulin Mesylate. *Nat. Prod. Rep.* **2013**, *30* (9), 1158. https://doi.org/10.1039/c3np70051h.

(43) Caron, S.; Thomson, N. M. Pharmaceutical Process Chemistry: Evolution of a Contemporary Data-Rich Laboratory Environment. *J. Org. Chem.* **2015**, *80* (6), 2943–2958. https://doi.org/10.1021/jo502879m.

(44) Yee, N. K.; Farina, V.; Houpis, I. N.; Haddad, N.; Frutos, R. P.; Gallou, F.; Wang, X.; Wei, X.; Simpson, R. D.; Feng, X.; Fuchs, V.; Xu, Y.; Tan, J.; Zhang, L.; Xu, J.; Smith-Keenan, L. L.; Vitous, J.; Ridges, M. D.; Spinelli, E. M.; Johnson, M.; Donsbach, K.; Nicola, T.; Brenner, M.; Winter, E.; Kreye, P.; Samstag, W. Efficient Large-Scale Synthesis of BILN 2061, a Potent HCV Protease Inhibitor, by a Convergent Approach Based on Ring-Closing Metathesis. *J. Org. Chem.* **2006**, *71* (19), 7133–7145. https://doi.org/10.1021/jo060285j.

(45) Wei, X.; Shu, C.; Haddad, N.; Zeng, X.; Patel, N. D.; Tan, Z.; Liu, J.; Lee, H.; Shen, S.; Campbell, S.; Varsolona, R. J.; Busacca, C. A.; Hossain, A.; Yee, N. K.; Senanayake, C. H. A Highly Convergent and Efficient Synthesis of a Macrocyclic Hepatitis C Virus Protease Inhibitor BI 201302. *Org. Lett.* **2013**, *15* (5), 1016–1019. https://doi.org/10.1021/ol303498m.

(46) Paddon, C. J.; Keasling, J. D. Semi-Synthetic Artemisinin: A Model for the Use of Synthetic Biology in Pharmaceutical Development. *Nat. Rev. Microbiol.* **2014**, *12* (5), 355–367. https://doi.org/10.1038/nrmicro3240.

(47) Artemisinin Enterprise conference 2008. https://www.gov.uk/research-for-development-outputs/artemisinin-enterprise-conference-2008 (accessed 2021 -11 -23).

(48) Schmid, G.; Hofheinz, W. Total Synthesis of Qinghaosu. *J. Am. Chem. Soc.* **1983**, *105* (3), 624–625. https://doi.org/10.1021/ja00341a054.

(49) Zhu, C.; Cook, S. P. A Concise Synthesis of (+)-Artemisinin. *J. Am. Chem. Soc.* **2012**, *134* (33), 13577–13579. https://doi.org/10.1021/ja3061479.

(50) Kung, S. H.; Lund, S.; Murarka, A.; McPhee, D.; Paddon, C. J. Approaches and Recent Developments for the Commercial Production of Semi-Synthetic Artemisinin. *Front. Plant Sci.* **2018**, *9*, 87. https://doi.org/10.3389/fpls.2018.00087.

(51) Maier, M. E. Design and Synthesis of Analogues of Natural Products. *Org. Biomol. Chem.* **2015**, *13* (19), 5302–5343. https://doi.org/10.1039/C5OB00169B.

(52) Klar, U.; Hoffmann, J.; Giurescu, M. Sagopilone (ZK-EPO): From a Natural Product to a Fully Synthetic Clinical Development Candidate. *Expert Opin. Investig. Drugs* **2008**, *17* (11), 1735–1748. https://doi.org/10.1517/13543784.17.11.1735.

(53) Parr, M. D.; Waite, W. W.; Hansen, L. A.; McDaniel, P. A. Cost Comparison of Seven Antibiotic Combinations as Empiric Therapy in a Simulated Febrile Neutropenic Patient. *Am. J. Hosp. Pharm.* **1985**, *42* (11), 2484–2488.

(54) Siddiqui, M.; Rajkumar, S. V. The High Cost of Cancer Drugs and What We Can Do About It. *Mayo Clin. Proc.* **2012**, *87* (10), 935–943. https://doi.org/10.1016/j.mayocp.2012.07.007.

(55) Blay, J.-Y.; Schöffski, P.; Bauer, S.; Krarup-Hansen, A.; Benson, C.; D'Adamo, D. R.; Jia, Y.; Maki, R. G. Eribulin versus Dacarbazine in Patients with Leiomyosarcoma: Subgroup Analysis from a Phase 3, Open-Label, Randomised Study. *Br. J. Cancer* **2019**, *120* (11), 1026–1032. https://doi.org/10.1038/s41416-019-0462-1.

(56) Jackson, K. L.; Henderson, J. A.; Phillips, A. J. The Halichondrins and E7389. *Chem. Rev.* **2009**, *109* (7), 3044–3079. https://doi.org/10.1021/cr900016w.

(58) Yu, M. J.; Zheng, W.; Seletsky, B. M.; Littlefield, B. A.; Kishi, Y. Chapter 14 - Case History: Discovery of Eribulin (HALAVEN™), a Halichondrin B Analogue That Prolongs Overall Survival in Patients with Metastatic Breast Cancer. In *Annual Reports in Medicinal Chemistry*; Macor, J. E., Ed.; Academic Press, **2011**; *46*, 227–241. https://doi.org/10.1016/B978-0-12-386009-5.00013-8.

(58) Seletsky, B. M.; Wang, Y.; Hawkins, L. D.; Palme, M. H.; Habgood, G. J.; DiPietro, L. V.; Towle, M. J.; Salvato, K. A.; Wels, B. F.; Aalfs, K. K.; Kishi, Y.; Littlefield, B. A.; Yu, M. J. Structurally Simplified Macrolactone Analogues of Halichondrin B. *Bioorg. Med. Chem. Lett.* **2004**, *14* (22), 5547–5550. https://doi.org/10.1016/j.bmcl.2004.08.068.

(59) Littlefield, B. A.; Palme, M. H.; Jose, S.; Seletsky, B. M.; Towle, M. J.; Yu, M. J.; Zheng, W. Macrocyclic Analogs and Methods of Their Use and Preparation. US6214865B1, **2001**.

(60) Choi, H.; Demeke, D.; Kang, F.-A.; Kishi, Y.; Nakajima, K.; Nowak, P.; Wan, Z.-K.; Xie, C. Synthetic Studies on the Marine Natural Product Halichondrins. *Pure Appl. Chem.* **2003**, *75* (1), 1–17. https://doi.org/10.1351/pac200375010001.

(61) Katsuki, T.; Sharpless, K. B. The First Practical Method for Asymmetric Epoxidation. *J. Am. Chem. Soc.* **1980**, *102* (18), 5974–5976. https://doi.org/10.1021/ja00538a077.

(62) Stamos, D. P.; Kishi, Y. Synthetic Studies on Halichondrins: A Practical Synthesis of the C.1-C.13 Segment. *Tetrahedron Lett.* **1996**, *37* (48), 8643–8646. https://doi.org/10.1016/S0040-4039(96)01999-5.

(63) Chase, C.; Fang, F.; Lewis, B. M.; Wilkie, G. D.; Schnaderbeck, M.; Zhu, X. Process Development of Halaven®: Synthesis of the C1–C13 Fragment from D-(–)-Gulono-1,4-lactone. **2013**. https://doi.org/10.1055/S-0032-1317919.

(64) Austad, B. C.; Benayoud, F.; Calkins, T. L.; Campagna, S.; Chase, C. E.; Choi, H.; Christ, W.; Costanzo, R.; Cutter, J.; Endo, A.; Fang, F. G.; Hu, Y.; Lewis, B. M.; Lewis, M. D.; McKenna, S.; Noland, T. A.; Orr, J. D.; Pesant, M.; Schnaderbeck, M. J.; Wilkie, G. D.; Abe, T.; Asai, N.; Asai, Y.; Kayano, A.; Kimoto, Y.; Komatsu, Y.; Kubota, M.; Kuroda, H.; Mizuno, M.; Nakamura, T.; Omae, T.; Ozeki, N.; Suzuki, T.; Takigawa, T.; Watanabe, T.; Yoshizawa, K. Process Development of Halaven®: Synthesis of the C14–C35 Fragment via Iterative Nozaki–Hiyama–Kishi Reaction–Williamson Ether Cyclization. *Synlett* **2013**, *24* (03), 327–332. https://doi.org/10.1055/s-0032-1317920.

(65) Tokunaga, M.; Larrow, J. F.; Kakiuchi, F.; Jacobsen, E. N. Asymmetric Catalysis with Water: Efficient Kinetic Resolution of Terminal Epoxides by Means of Catalytic Hydrolysis. *Science* **1997**, *277* (5328), 936–938. https://doi.org/10.1126/science.277.5328.936.

(66) Bauer, A. Story of Eribulin Mesylate: Development of the Longest Drug Synthesis. In *Synthesis of Heterocycles in Contemporary Medicinal Chemistry* Topics in Heterocyclic Chemistry; **2016**, *44*, 209–270. https://doi.org/10.1007/7081_2016_201.

(67) Guo, H.; Dong, C.-G.; Kim, D.-S.; Urabe, D.; Wang, J.; Kim, J. T.; Liu, X.; Sasaki, T.; Kishi, Y. Toolbox Approach to the Search for Effective Ligands for Catalytic Asymmetric Cr-Mediated Coupling Reactions. *J. Am. Chem. Soc.* **2009**, *131* (42), 15387–15393. https://doi.org/10.1021/ja905843e.

(68) Liu, X.; Henderson, J. A.; Sasaki, T.; Kishi, Y. Dramatic Improvement in Catalyst Loadings and Molar Ratios of Coupling Partners for Ni/Cr-Mediated Coupling Reactions: Heterobimetallic Catalysts. *J. Am. Chem. Soc.* **2009**, *131* (46), 16678–16680. https://doi.org/10.1021/ja9079308.

(69) Liu, S.; Kim, J. T.; Dong, C.-G.; Kishi, Y. Catalytic Enantioselective Cr-Mediated Propargylation: Application to Halichondrin Synthesis. *Org. Lett.* **2009**, *11* (20), 4520–4523. https://doi.org/10.1021/ol9016595.

(70) Kim, D.-S.; Dong, C.-G.; Kim, J. T.; Guo, H.; Huang, J.; Tiseni, P. S.; Kishi, Y. New Syntheses of E7389 C14−C35 and Halichondrin C14−C38 Building Blocks: Double-Inversion Approach. *J. Am. Chem. Soc.* **2009**, *131* (43), 15636–15641. https://doi.org/10.1021/ja9058475.

(71) Belanger, F.; Chase, C. E.; Endo, A.; Fang, F. G.; Li, J.; Mathieu, S. R.; Wilcoxen, A. Z.; Zhang, H. Stereoselective Synthesis of the Halaven C14–C26 Fragment from D-Quinic Acid: Crystallization-Induced Diastereoselective Transformation of an α-Methyl Nitrile. *Angew. Chem. Int. Ed.* **2015**, *54* (17), 5108–5111. https://doi.org/10.1002/anie.201501143.

(72) Blanchette, M. A.; Choy, W.; Davis, J. T.; Essenfeld, A. P.; Masamune, S.; Roush, W. R.; Sakai, T. Horner-Wadsworth-Emmons Reaction: Use of Lithium Chloride and an Amine for Base-Sensitive Compounds. *Tetrahedron Lett.* **1984**, *25* (21), 2183–2186. https://doi.org/10.1016/S0040-4039(01)80205-7.

(73) Bernet, B.; Vasella, A. Carbocyclische Verbindungen Aus Monosacchariden. I. Umsetzungen in Der Glucosereihe. *Helv. Chim. Acta* **1979**, *62* (6), 1990–2016. https://doi.org/10.1002/hlca.19790620629.

(74) Corey, E. J.; Chaykovsky, M. Dimethyloxosulfonium Methylide ((CH3)2SOCH2) and Dimethylsulfonium Methylide ((CH3)2SCH2). Formation and Application to Organic Synthesis. *J. Am. Chem. Soc.* **1965**, *87* (6), 1353–1364. https://doi.org/10.1021/ja01084a034.

(75) Johnson, A. W.; LaCount, R. B. The Chemistry of Ylids. VI. Dimethylsulfonium Fluorenylide—A Synthesis of Epoxides1. *J. Am. Chem. Soc.* **1961**, *83* (2), 417–423. https://doi.org/10.1021/ja01463a040.

(76) Aggarwal, V. K.; Winn, C. L. Catalytic, Asymmetric Sulfur Ylide-Mediated Epoxidation of Carbonyl Compounds: Scope, Selectivity, and Applications in Synthesis. *Acc. Chem. Res.* **2004**, *37* (8), 611–620. https://doi.org/10.1021/ar030045f.

(77) Danishefsky, S. J.; Masters, J. J.; Young, W. B.; Link, J. T.; Snyder, L. B.; Magee, T. V.; Jung, D. K.; Isaacs, R. C. A.; Bornmann, W. G.; Alaimo, C. A.; Coburn, C. A.; Di Grandi, M. J. Total Synthesis of Baccatin III and Taxol. *J. Am. Chem. Soc.* **1996**, *118* (12), 2843–2859. https://doi.org/10.1021/ja952692a.

(78) Aggarwal, V. K.; Ford, J. G.; Fonquerna, S.; Adams, H.; Jones, R. V. H.; Fieldhouse, R. Catalytic Asymmetric Epoxidation of Aldehydes. Optimization, Mechanism, and Discovery of Stereoelectronic Control Involving a Combination of Anomeric and Cieplak Effects in Sulfur Ylide Epoxidations with Chiral 1,3-Oxathianes. *J. Am. Chem. Soc.* **1998**, *120* (33), 8328–8339. https://doi.org/10.1021/ja9812150.

(79) Akiyama, H.; Ohshima, K.; Fujimoto, T.; Yamamoto, I.; Iriye, R. Reactions of Cyclic Sulfur Ylides with Some Carbonyl Compounds. *Heteroat. Chem.* **2002**, *13* (3), 216–222. https://doi.org/10.1002/hc.10022.

(80) Britton, R.; Kang, B. α-Haloaldehydes: Versatile Building Blocks for Natural Product Synthesis. *Nat Prod Rep* **2013**, *30* (2), 227–236. https://doi.org/10.1039/C2NP20108A.

(81) Schroder, A. *Ber. Dtsch. Chem. Ges.* **1871**, *4*, 400.

(82) Martín, V. S.; Palazón, J. M. Stereocontrolled Synthesis of Chiral Nonracemic Halotetrahydropyrans. *Tetrahedron Lett.* **1992**, *33* (17), 2399–2402. https://doi.org/10.1016/S0040-4039(00)74222-5.

(83) Brochu, M. P.; Brown, S. P.; MacMillan, D. W. C. Direct and Enantioselective Organocatalytic α-Chlorination of Aldehydes. *J. Am. Chem. Soc.* **2004**, *126* (13), 4108–4109. https://doi.org/10.1021/ja049562z.

(84) Halland, N.; Alstrup Lie, M.; Kjærsgaard, A.; Marigo, M.; Schiøtt, B.; Jørgensen, K. A. Mechanistic Investigation of the 2,5-Diphenylpyrrolidine-Catalyzed Enantioselective α-Chlorination of Aldehydes. *Chem. – Eur. J.* **2005**, *11* (23), 7083–7090. https://doi.org/10.1002/chem.200500776.

(85) Amatore, M.; Beeson, T. D.; Brown, S. P.; MacMillan, D. W. C. Enantioselective Linchpin Catalysis by SOMO Catalysis: An Approach to the Asymmetric α-Chlorination of Aldehydes and Terminal Epoxide Formation. *Angew. Chem. Int. Ed.* **2009**, *48* (28), 5121–5124. https://doi.org/10.1002/anie.200901855.

(86) Cornforth, J. W.; Cornforth, R. H.; Mathew, K. K. A General Stereoselective Synthesis of Olefins. *J. Chem. Soc.* **1959**, *0*, 112–127. https://doi.org/10.1039/JR9590000112.

(87) Chérest, M.; Felkin, H.; Prudent, N. Torsional Strain Involving Partial Bonds. The Stereochemistry of the Lithium Aluminium Hydride Reduction of Some Simple Open-Chain Ketones. *Tetrahedron Lett.* **1968**, *9* (18), 2199–2204. https://doi.org/10.1016/S0040-4039(00)89719-1.

(88) Cee, V. J.; Cramer, C. J.; Evans, D. A. Theoretical Investigation of Enolborane Addition to α-Heteroatom-Substituted Aldehydes. Relevance of the Cornforth and Polar Felkin−Anh Models for Asymmetric Induction. *J. Am. Chem. Soc.* **2006**, *128* (9), 2920–2930. https://doi.org/10.1021/ja0555670.

(89) Bürgi, H. B.; Dunitz, J. D.; Lehn, J. M.; Wipff, G. Stereochemistry of Reaction Paths at Carbonyl Centres. *Tetrahedron* **1974**, *30* (12), 1563–1572. https://doi.org/10.1016/S0040-4020(01)90678-7.

(90) Winter, P.; Swatschek, J.; Willot, M.; Radtke, L.; Olbrisch, T.; Schäfer, A.; Christmann, M. Transforming Terpene-Derived Aldehydes into 1,2-Epoxides via Asymmetric α-Chlorination: Subsequent Epoxide Opening with Carbon Nucleophiles. *Chem. Commun.* **2011**, *47* (44), 12200. https://doi.org/10.1039/c1cc15173h.

(91) Kang, B.; Mowat, J.; Pinter, T.; Britton, R. Development of a Concise and General Enantioselective Approach to 2,5-Disubstituted-3-Hydroxytetrahydrofurans. *Org. Lett.* **2009**, *11* (8), 1717–1720. https://doi.org/10.1021/ol802711s.

(92) Halperin, S.; Kang, B.; Britton, R. Lithium Aldol Reactions of α-Chloroaldehydes Provide Versatile Building Blocks for Natural Product Synthesis. *Synthesis* **2011**, *2011* (12), 1946–1953. https://doi.org/10.1055/s-0030-1260032.

(93) Ye, L.; Cui, L.; Zhang, G.; Zhang, L. Alkynes as Equivalents of α-Diazo Ketones in Generating α-Oxo Metal Carbenes: A Gold-Catalyzed Expedient Synthesis of Dihydrofuran-3-Ones. *J. Am. Chem. Soc.* **2010**, *132* (10), 3258–3259. https://doi.org/10.1021/ja100041e.

(94) Halland, N.; Braunton, A.; Bachmann, S.; Marigo, M.; Jørgensen, K. A. Direct Organocatalytic Asymmetric α-Chlorination of Aldehydes. *J. Am. Chem. Soc.* **2004**, *126* (15), 4790–4791. https://doi.org/10.1021/ja049231m.

(95) Nahm, S.; Weinreb, S. M. N-Methoxy-n-Methylamides as Effective Acylating Agents. *Tetrahedron Lett.* **1981**, *22* (39), 3815–3818. https://doi.org/10.1016/S0040-4039(01)91316-4.

(96) Wessig, P.; Freyse, D.; Schuster, D.; Kelling, A. Fluorescent Dyes with Large Stokes Shifts Based on Benzo[1,2-d:4,5-d']Bis([1,3]Dithiole) ("S4-DBD Dyes"). *Eur. J. Org. Chem.* **2020**, *2020* (11), 1732–1744. https://doi.org/10.1002/ejoc.202000093.

(99) Mukaiyama, T.; Kobayashi, S. Tin(II) Enolates in the Aldol, Michael, and Related Reactions. In *Organic Reactions*; American Cancer Society, **2004**, 1–103. https://doi.org/10.1002/0471264180.or046.01.

(98) Sannes, K. A.; Brauman, J. I. 1,3-Hydrogen Rearrangements of Vibrationally Activated Enolate Ions in the Gas Phase. *J. Am. Chem. Soc.* **1995**, *117* (40), 10088–10092. https://doi.org/10.1021/ja00145a020.

(99) Cornish, C. A.; Warren, S. Synthesis of Single Isomers (E or Z) of Protected γ,δ-Unsaturated Ketones by the Horner-Wittig Reaction. *J. Chem. Soc. Perkin 1* **1985**, No. 0, 2585–2598. https://doi.org/10.1039/P19850002585.

(102) Brown Hydroboration. In *Comprehensive Organic Name Reactions and Reagents*; American Cancer Society, **2010**, 536–543. https://doi.org/10.1002/9780470638859.conrr118.

(103) Paterson, I.; Yeung, K.-S.; Smaill, J. B. ChemInform Abstract: The Horner-Wadsworth-Emmons Reaction in Natural Products Synthesis: Expedient Construction of Complex (*E*)-Enones Using Barium Hydroxide. *ChemInform* **1994**, *25* (25). https://doi.org/10.1002/chin.199425075.

(104) Haskel, A.; Keinan, E. Palladium-Catalyzed 1,4-Reduction (Conjugate Reduction). In *Handbook of Organopalladium Chemistry for Organic Synthesis*; John Wiley & Sons, Ltd, **2002**, 2767–2782. https://doi.org/10.1002/0471212466.ch127.

(103) Chen, X.-B.; Hu, Q.-P.; Yuan, Q.-J.; Ding, W.; Ren, J.; Zeng, B.-B. Simultaneous Dehalogenation and Hydrogenation Reduction of Halogen-Heteroaromatic Aldehydes. *Tetrahedron Lett.* **2012**, *53* (29), 3798–3801. https://doi.org/10.1016/j.tetlet.2012.05.054.

(106) Ferrier, G.; King, F. A New Platinum Catalyst for the Hydrogenation of Halonitroaromatics. *Johns. Matthey Technol. Rev.* **1983**, *27* (2), 72–77.

(107) Imamoto, T., Trost, B. M., Fleming, I. Reduction of Saturated Alkyl Halides to Alkanes. In *Comprehensive Organic Synthesis*; Pergamon: Oxford, **1991**, 793–809. https://doi.org/10.1016/B978-0-08-052349-1.00246-8.

(106) Ghosh, A. K.; Gong, G. Total Synthesis and Revision of C6 Stereochemistry of (+)-Amphidinolide W. *J. Org. Chem.* **2006**, *71* (3), 1085–1093. https://doi.org/10.1021/jo052181z.

(110) Ikeno, T.; Kimura, T.; Ohtsuka, Y.; Yamada, T. Selective 1,4-Reduction of a,b-Unsaturated Carbonyl Compounds by Combined Use of Bis(1,3-Diketonato)Cobalt(II) Complex and Diisobutylaluminum Hydride. *N. Y.* **1999**, *1*, 96-98. https://doi.org/10.1055/s-1999-2557

(108) Zeng, C.; Zhao, J.; Zhao, G. Enantioselective Divergent Total Syntheses of Fawcettimine-Type Lycopodium Alkaloids. *Tetrahedron* **2015**, *71* (1), 64–69. https://doi.org/10.1016/j.tet.2014.11.041.

(109) Deutsch, C.; Krause, N.; Lipshutz, B. H. CuH-Catalyzed Reactions. *Chem. Rev.* **2008**, *108* (8), 2916–2927. https://doi.org/10.1021/cr0684321.

(110) Paterson, I.; Fink, S. J.; Lee, L. Y. W.; Atkinson, S. J.; Blakey, S. B. Total Synthesis of Aplyronine C. *Org. Lett.* **2013**, *15* (12), 3118–3121. https://doi.org/10.1021/ol401327r.

(111) Baker, B. A.; Bošković, Ž. V.; Lipshutz, B. H. (BDP)CuH: A "Hot" Stryker's Reagent for Use in Achiral Conjugate Reductions. *Org. Lett.* **2008**, *10* (2), 289–292. https://doi.org/10.1021/ol702689v.

(112) Sass, D. C.; Heleno, V. C. G.; Cavalcante, S.; da Silva Barbosa, J.; Soares, A. C. F.; Constantino, M. G. Solvent Effect in Reactions Using Stryker's Reagent. *J. Org. Chem.* **2012**, *77* (20), 9374–9378. https://doi.org/10.1021/jo301595b.

(117) Kawai, Y.; Hayashi, M.; Tokitoh, N. Asymmetric Synthesis of α-Chiral Ketones by the Reduction of Enones with Baker's Yeast. **2001**, *12*, 3007-3011. https://doi.org/10.1016/s0957-4166(01)00537-7.

(114) Gololobov, Yu. G.; Nesmeyanov, A. N.; lysenko, V. P.; Boldeskul, I. E. Twenty-Five Years of Dimethylsulfoxonium Ethylide (Corey's Reagent). *Tetrahedron* **1987**, *43* (12), 2609–2651. https://doi.org/10.1016/S0040-4020(01)86869-1.

(115) Magnus, P.; Waring, M. J.; Scott, D. A. Conjugate Reduction of α,β-Unsaturated Ketones Using an MnIII Catalyst, Phenylsilane and Isopropyl Alcohol. *Tetrahedron Lett.* **2000**, *41* (50), 9731–9733. https://doi.org/10.1016/S0040-4039(00)01728-7.

(116) Zweig, J. E.; Kim, D. E.; Newhouse, T. R. Methods Utilizing First-Row Transition Metals in Natural Product Total Synthesis. *Chem. Rev.* **2017**, *117* (18), 11680–11752. https://doi.org/10.1021/acs.chemrev.6b00833.

(117) Hamilton, D. E.; Drago, R. S.; Zombeck, A. Mechanistic Studies on the Cobalt(II) Schiff Base Catalyzed Oxidation of Olefins by O2. *J. Am. Chem. Soc.* **1987**, *109* (2), 374–379. https://doi.org/10.1021/ja00236a014.

(118) Bifulco, G.; Dambruoso, P.; Gomez-Paloma, L.; Riccio, R. Determination of Relative Configuration in Organic Compounds by NMR Spectroscopy and Computational Methods. *Chem. Rev.* **2007**, *107* (9), 3744–3779. https://doi.org/10.1021/cr030733c.

(119) Hoye, T. R.; Jeffrey, C. S.; Shao, F. Mosher Ester Analysis for the Determination of Absolute Configuration of Stereogenic (Chiral) Carbinol Carbons. *Nat. Protoc.* **2007**, *2* (10), 2451–2458. https://doi.org/10.1038/nprot.2007.354.

(120) Bergeron-Brlek, M.; Teoh, T.; Britton, R. A Tandem Organocatalytic α-Chlorination–Aldol Reaction That Proceeds with Dynamic Kinetic Resolution: A Powerful Tool for Carbohydrate Synthesis. *Org. Lett.* **2013**, *15* (14), 3554–3557. https://doi.org/10.1021/ol401370b.

(121) Bahmanyar, S.; Houk, K. N.; Martin, H. J.; List, B. Quantum Mechanical Predictions of the Stereoselectivities of Proline-Catalyzed Asymmetric Intermolecular Aldol Reactions. *J. Am. Chem. Soc.* **2003**, *125* (9), 2475–2479. https://doi.org/10.1021/ja028812d.

(122) Panne, P.; Fox, J. M. Rh-Catalyzed Intermolecular Reactions of Alkynes with Alpha-Diazoesters That Possess Beta-Hydrogens: Ligand-Based Control over Divergent Pathways. *J. Am. Chem. Soc.* **2007**, *129* (1), 22–23. https://doi.org/10.1021/ja0660195.

(127) Byrom, N. T.; Grigg, R.; Kongkathip, B.; Reimer, G.; Wade, A. R. Palladium-Catalysed Synthesis of Endo- and Exo-Brevicomin and Related Di- and Tri-Oxabicyclo[x.2.1] Systems. *J. Chem. Soc. Perkin 1* **1984**, 1643–1653. https://doi.org/10.1039/p19840001643.

(124) Graham, T. H.; Horning, B. D.; MacMillan, D. W. C. The Preparation of (2r,5s)-2-t-Butyl-3,5-Dimethylimidazolidin-4-One. *Org. Synth.* **2011**, *88*, 42–53. https://doi.org/10.15227/orgsyn.088.0042.

(125) Chandankar, S. S.; Raghavan, S. Stereoselective Synthesis of the C1–C22 Carbon Framework of (−)-Amphidinolide K. *J. Org. Chem.* **2019**, *84* (15), 9584–9602. https://doi.org/10.1021/acs.joc.9b01248.

(126) Britten, T. K.; McLaughlin, M. G. Brønsted Acid Catalyzed Peterson Olefinations. *J. Org. Chem.* **2020**, *85* (2), 301–305. https://doi.org/10.1021/acs.joc.9b02489.

(127) VanRheenen, V.; Kelly, R. C.; Cha, D. Y. An Improved Catalytic OsO4 Oxidation of Olefins to Cis-1,2-Glycols Using Tertiary Amine Oxides as the Oxidant. *Tetrahedron Lett.* **1976**, *17* (23), 1973–1976. https://doi.org/10.1016/S0040-4039(00)78093-2.

(128) Sharma, G. V. M.; Punna, S.; Rajendra Prasad, T.; Radha Krishna, P.; Chorghade, M. S.; Ley, S. V. Stereoselective Syntheses of Pharmaceutically Relevant Chiral Tetrahydrofurans from (S)- and (R)-Glyceraldehyde Derivatives. *Tetrahedron Asymmetry* **2005**, *16* (6), 1113–1123. https://doi.org/10.1016/j.tetasy.2005.01.044.

(129) Mulzer, J.; Berger, M. Total Synthesis of the Boron-Containing Ion Carrier Antibiotic Macrodiolide Tartrolon B. *J. Org. Chem.* **2004**, *69* (3), 891–898. https://doi.org/10.1021/jo035391p.

(130) Schmidt, U.; Lieberknecht, A.; Kazmaier, U.; Griesser, H.; Jung, G.; Metzger, J. Amino Acids and Peptides; 75. Synthesis of Di- and Trihydroxyamino Acids - Construction of Lipophilic Tripalmitoyldihydroxy-α-Amino Acids. *Synthesis* **1991**, *1991* (01), 49–55. https://doi.org/10.1055/s-1991-26378.

(131) Hauser, C. R.; Walker, H. G. Condensation of Certain Esters by Means of Diethylaminomagnesium Bromide1,2. *J. Am. Chem. Soc.* **1947**, *69* (2), 295–297. https://doi.org/10.1021/ja01194a040.

(132) Liu, X.; Jiao, X.; Wu, Q.; Tian, C.; Li, R.; Xie, P. A Novel and Efficient Synthesis of Entecavir. *Tetrahedron Lett.* **2012**, *53* (29), 3805–3807. https://doi.org/10.1016/j.tetlet.2012.05.058.

(133) Nugent, W. A.; RajanBabu, T. V. Transition-Metal-Centered Radicals in Organic Synthesis. Titanium(III)-Induced Cyclization of Epoxy Olefins. *J. Am. Chem. Soc.* **1988**, *110* (25), 8561–8562. https://doi.org/10.1021/ja00233a051.

(134) RajanBabu, T. V.; Nugent, W. A. Intermolecular Addition of Epoxides to Activated Olefins: A New Reaction. *J. Am. Chem. Soc.* **1989**, *111* (12), 4525–4527. https://doi.org/10.1021/ja00194a073.

(135) Justicia, J.; Jiménez, T.; Morcillo, S. P.; Cuerva, J. M.; Oltra, J. E. Mixed Disproportionation versus Radical Trapping in Titanocene(III)-Promoted Epoxide Openings. *Tetrahedron* **2009**, *65* (52), 10837–10841. https://doi.org/10.1016/j.tet.2009.10.038.

(136) Dong, C.-G.; Henderson, J. A.; Kaburagi, Y.; Sasaki, T.; Kim, D.-S.; Kim, J. T.; Urabe, D.; Guo, H.; Kishi, Y. New Syntheses of E7389 C14−C35 and Halichondrin C14−C38 Building Blocks: Reductive Cyclization and Oxy-Michael Cyclization Approaches. *J. Am. Chem. Soc.* **2009**, *131* (43), 15642–15646. https://doi.org/10.1021/ja9058487.

(137) Ikawa, T.; Hattori, K.; Sajiki, H.; Hirota, K. Solvent-Modulated Pd/C-Catalyzed Deprotection of Silyl Ethers and Chemoselective Hydrogenation. *Tetrahedron* **2004**, *60* (32), 6901–6911. https://doi.org/10.1016/j.tet.2004.05.098.

(138) Trost, B. M.; Verhoeven, T. R. Cyclization Catalyzed by Palladium(0). Initial Studies and Macrolide Formation. *J. Am. Chem. Soc.* **1980**, *102* (14), 4743–4763. https://doi.org/10.1021/ja00534a030.

(139) Eurofins CDMO Alphora Inc. | API & DP Services https://www.eurofins.com/biopharma-services/cdmo/eurofins-alphora/ (accessed 2021 -09 -27).

(142) 5 Minutes with Dr Boris Gorin, Eurofins Alphora. *Scientific Update*, **2019**.

(143) Wouters, O. J.; McKee, M.; Luyten, J. Estimated Research and Development Investment Needed to Bring a New Medicine to Market, 2009-2018. **2020**, *323* (9), 844–853. https://doi.org/10.1001/jama.2020.1166.

(142) WTO | intellectual property (TRIPS) - agreement text - standards https://www.wto.org/english/docs_e/legal_e/27-trips_04c_e.htm (accessed 2021 -11 -23).

(143) Emcure launches world's first generic Eribulin for treatment of metastatic breast cancer https://www.biospectrumindia.com/news/43/13272/emcure-launches-worlds-first-generic-eribulin-for-treatment-of-metastatic-breast-cancer.html (accessed 2021 -09 -27).

(146) Souza, F. E. S.; Rudolph, A.; PAN, M.; Gorin, B.; NGOOI, T. K.; BEXRUD, J. A.; Orprecio, R.; RANGWALA, H. Synthetic Process for Preparation of Macrocyclic C1-Keto Analogs of Halichondrin b and Intermediates Useful Therein. WO2013142999A1, **2013**.

(145) Rudolph, A.; Alberico, D.; Jordan, R.; Pan, M.; Souza, F. E. S.; Gorin, B. Early Introduction of the Amino Group to the C27–C35 Building Block of Eribulin. *Tetrahedron Lett.* **2013**, *54* (51), 7059–7061. https://doi.org/10.1016/j.tetlet.2013.10.077.

(148) Austad, B.; Chase, C.; Fang, F. Intermediates for the Preparation of Halichondrin B, EP3587408, **2005**.

(147) He, M.; Beahm, B. J.; Bode, J. W. Chiral NHC-Catalyzed Oxodiene Diels−Alder Reactions with α-Chloroaldehyde Bisulfite Salts. *Org. Lett.* **2008**, *10* (17), 3817–3820. https://doi.org/10.1021/ol801502h.

(148) Pal, S.; Lucarini, F.; Ruggi, A.; Kilbinger, A. F. M. Functional Metathesis Catalyst Through Ring Closing Enyne Metathesis: One Pot Protocol for Living Heterotelechelic Polymers. *J. Am. Chem. Soc.* **2018**, *140* (9), 3181–3185. https://doi.org/10.1021/jacs.7b12805.

(149) Lee, J. H.; Li, Z.; Osawa, A.; Kishi, Y. Extension of Pd-Mediated One-Pot Ketone Synthesis to Macrocyclization: Application to a New Convergent Synthesis of Eribulin. *J. Am. Chem. Soc.* **2016**, *138* (50), 16248–16251. https://doi.org/10.1021/jacs.6b11663.

(150) Omura, K.; Swern, D. Oxidation of Alcohols by "Activated" Dimethyl Sulfoxide. a Preparative, Steric and Mechanistic Study. *Tetrahedron* **1978**, *34* (11), 1651–1660. https://doi.org/10.1016/0040-4020(78)80197-5.

(151) Jung, Y. C.; Yoon, C. H.; Turos, E.; Yoo, K. S.; Jung, K. W. Total Syntheses of (−)-α-Kainic Acid and (+)-α-Allokainic Acid via Stereoselective C−H Insertion and Efficient 3,4-Stereocontrol. *J. Org. Chem.* **2007**, *72* (26), 10114–10122. https://doi.org/10.1021/jo701988j.

(152) Musatov, D. M.; Kublitskii, V. S.; Malyshev, O. R.; Kurilov, D. V.; Vinogradov, M. G. Preparative Separation of Tetrahydrofurfurylamine Enantiomers. *Russ. J. Org. Chem.* **2007**, *43* (12), 1813. https://doi.org/10.1134/S1070428007120123.

(153) Crimmins, M. T.; Vanier, G. S. Enantioselective Total Synthesis of (+)-SCH 351448. *Org. Lett.* **2006**, *8* (13), 2887–2890. https://doi.org/10.1021/ol061073b.

(155) Richard B Silverman. *The Organic Chemistry of Drug Design and Drug Action*; Elsevier Academic Press, **2004**.

(155) Schramm, V. L. Immucillins as Antibiotics for T-Cell Proliferation and Malaria. *Nucleosides Nucleotides Nucleic Acids* **2004**, *23* (8–9), 1305–1311. https://doi.org/10.1081/NCN-200027564.

(156) Makita, S.; Maeshima, A. M.; Maruyama, D.; Izutsu, K.; Tobinai, K. Forodesine in the Treatment of Relapsed/Refractory Peripheral T-Cell Lymphoma: An Evidence-Based Review. *OncoTargets Ther.* **2018**, *11*, 2287–2293. https://doi.org/10.2147/OTT.S140756.

(157) Izawa, K.; Aceña, J. L.; Wang, J.; Soloshonok, V. A.; Liu, H. Small-Molecule Therapeutics for Ebola Virus (EBOV) Disease Treatment: Small-Molecule Anti-Ebola Virus Disease Therapeutics. *Eur. J. Org. Chem.* **2016**, *2016* (1), 8–16. https://doi.org/10.1002/ejoc.201501158.

(158) Hong, Z.; Liu, L.; Sugiyama, M.; Fu, Y.; Wong, C.-H. Concise Synthesis of Iminocyclitols via Petasis-Type Aminocyclization. *J. Am. Chem. Soc.* **2009**, *131* (24), 8352–8353. https://doi.org/10.1021/ja901656e.

(159) Evans, G. B.; Furneaux, R. H.; Hausler, H.; Larsen, J. S.; Tyler, P. C. Imino-C-Nucleoside Synthesis: Heteroaryl Lithium Carbanion Additions to a Carbohydrate Cyclic Imine and Nitrone. *J. Org. Chem.* **2004**, *69* (6), 2217–2220. https://doi.org/10.1021/jo035744k.

(160) Evans, G. B.; Furneaux, R. H.; Gainsford, G. J.; Schramm, V. L.; Tyler, P. C. Synthesis of Transition State Analogue Inhibitors for Purine Nucleoside Phosphorylase and N-Riboside Hydrolases. *Tetrahedron* **2000**, *56* (19), 3053–3062. https://doi.org/10.1016/S0040-4020(00)00194-0.

(161) Evans, G. B.; Furneaux, R. H.; Hutchison, T. L.; Kezar, H. S.; Morris, Philip E.; Schramm, V. L.; Tyler, P. C. Addition of Lithiated 9-Deazapurine Derivatives to a Carbohydrate Cyclic Imine: Convergent Synthesis of the Aza-C-Nucleoside Immucillins. *J. Org. Chem.* **2001**, *66* (17), 5723–5730. https://doi.org/10.1021/jo0155613.

(162) Fleet, G. W. J.; Son, J. C. Polyhydroxylated Pyrrolidines from Sugar Lactomes: Synthesis of 1,4-Dideoxy-1,4-Imino-d-Glucitol from d-Galactonolactone and Syntheses of 1,4-Dideoxy-1,4-Imino-d-Allitol, 1,4-Dideoxy-1,4-Imino-d-Ribitol, and (2s,3r,4s)-3,4-Dihydroxyproline from d-Gulonolactone. *Tetrahedron* **1988**, *44* (9), 2637–2647. https://doi.org/10.1016/S0040-4020(01)81716-6.

(163) Batra, H.; Moriarty, R. M.; Penmasta, R.; Sharma, V.; Stanciuc, G.; Staszewski, J. P.; Tuladhar, S. M.; Walsh, D. A.; Datla, S.; Krishnaswamy, S. A Concise, Efficient and Production-Scale Synthesis of a Protected L -Lyxonolactone Derivative: An Important Aldonolactone Core. *Org. Process Res. Dev.* **2006**, *10* (3), 484–486. https://doi.org/10.1021/op050222n.

(163) Bergeron-Brlek, M.; Meanwell, M.; Britton, R. Direct Synthesis of Imino-C-Nucleoside Analogues and Other Biologically Active Iminosugars. *Nat. Commun.* **2015**, *6* (1), 1–6. https://doi.org/10.1038/ncomms7903.

(164) Furneaux, R. H.; Schramm, V. L.; Tyler, P. C.; Evans, G. B. Inhibitors of Nucleoside Phosphorylases and Nucleosidases. EP1490373A4, **2009**.

(166) Manolikakes, G.; Schade, M. A.; Hernandez, C. M.; Mayr, H.; Knochel, P. Negishi Cross-Couplings of Unsaturated Halides Bearing Relatively Acidic Hydrogen Atoms with Organozinc Reagents. *Org. Lett.* **2008**, *10* (13), 2765–2768. https://doi.org/10.1021/ol8009013.

Appendix.

Design and Synthesis of Selective PRMT4 inhibitors

A collaboration between the Britton group, the Structural Genomics Consortium and Bayer has led to the design and synthesis of selective PRMT4 inhibitors. My contribution to this project has been the synthesis of the indole derivatives **12**, **13**, **14**, **15**, **28**, **29** and **30** (see manuscript).

Note: A full text version of *"Rational Design and Synthesis of Selective PRMT4 Inhibitors: A New Chemotype for Development of Cancer Therapeutics"* can be found at doi.org/10.1002/cmdc.202100018.